BIOLOGICAL TREATMENT OF HYPERSALINE PRODUCED WATER USING BIOFILM TECHNOLOGY

By

Abdullah Ismael Ibrahim

Submitted to the graduate degree program in the Department of Civil, Environmental and Architectural Engineering and the Graduate Faculty of the University of Kansas in partial fulfillment of the requirements for the degree of Doctor of Philosophy.

_____

Chairperson Prof. Dr. Edward F. Peltier

_____

Co-Chair Prof. Dr. Belinda S.M. Sturm

_____

Prof. Dr. Stephen J. Randtke

_____

Dr. Karen Peltier

_____

Dr. Reza Barati

Date Defended: March 9th, 2020

The Dissertation Committee for Abdullah Ismael Ibrahim

certifies that this is the approved version of the following dissertation:

BIOLOGICAL TREATMENT OF HYPERSALINE PRODUCED WATER USING BIOFILM TECHNOLOGY

_____

Chairperson Dr. Edward F. Peltier

_____

Co-Chair Prof. Dr. Belinda S.M. Sturm

Date Defended: March 9th, 2020

Abstract

Gas and oilfield produced water (PW) is associated with severe water quality issues, such as high salinity and high fractions of refractory organic matter. Sustainable management strategies for PW are a major challenge due to the high volume of wastewater generated and the toxicity of aqueous components, including dissolved organics. Biofilm-based biological treatment is a promising technique for removal of the biodegradable organic component of PW due to multiple performance advantages over conventional activated sludge systems, including smaller footprint, high settleability, and higher resistance against salinity and toxic compounds. Biofilm-based treatment also has the potential to degrade a broad range of organic compounds due to the presence of stratified redox zones within the same biofilm structure.

In this work, laboratory-scale sequencing batch reactors were constructed and used to assess the performance and viability of different biofilm-based biological treatment systems for produced water. First, the formation of aerobic granular sludge (AGS) under hypersaline conditions using both an enriched halophilic inoculum and an activated sludge culture was studied as a first step toward introducing biofilm technology to the field of hypersaline PW treatment. AGS formation could be achieved at hypersaline conditions up to 85 gL^{-1} NaCl) and was improved by the use of the enriched halophilic inoculum. Granule performance and stability were linked to the relative in production of extracellular polymeric substances (EPS) and alginate-like exopolysaccharides (ALE), but not to substitution of divalent cations in the EPS.

Second, two biofilm-based reactors, one containing AGS and the second containing a biofilm grown on activated carbon support material (Bio-GAC), were used to degrade a high-strength organic load consisting of a mixture of aromatic hydrocarbons (benzyl alcohol, o-cresol, and phenol) in a hypersaline synthetic produced water. The removal efficiency and production of secondary degradation by products were monitored and compared to the results from a

conventional activated sludge reactor. The Bio-GAC reactor achieved > 98% removal of influent organics with minimal export of catechol, a potentially toxic byproduct. The AGS reactor also showed high levels of organic degradation, but had more difficulty removing phenol. Both reactors outperformed the conventional activated sludge reactor (CAS) in terms of organic load removal. Sorption studies and X-ray photoelectron spectroscopy (XPS) analysis showed that Bio-GAC had rapid sorption and degradation of aromatics, while the AGS accumulated aromatics rapidly then degraded them more slowly.

Finally, the long-term performance of the two aerobic biofilm reactors (Bio-GAC and AGS) was compared to that of two anaerobic biofilm reactors with anaerobic biofilms grown 1) on an activated carbon support material (AnGAC) and 2) in an up-flow anaerobic sludge bed reactor (UASB) with respect to removal of influent organics and export of biomass. All four reactor designs achieved > 85% removal of influent aromatics after an extended conditioning time, with the aerobic systems outperforming the similar anaerobic designs. Biomass export was greater from the aerobic reactors, but all effluents would require treatment to remove solids. XPS showed differences in the structure of the biofilms formed under aerobic and anaerobic conditions. XPS technique is a powerful tool to monitor the fate of organic compounds within the biofilm and to observe the development of the biofilm itself.

The current study framed the application of biofilm-based technologies to remove toxic organic loads from hypersaline wastewater and overcome drawbacks associated with conventional biological treatment systems. Overall, the outcomes of this study can be manipulated beneficially to treat a wide variety of industrial wastewaters.

To my Parents, my lovely wife, and to the joy in life (my kids)

CONTENTS

FIGURES viii
TABLES x
NOMENCLATURE xi
ACKNOWLEDGEMENTS xiv
CHAPTER 1 1
INTRODUCTION 1
1.1. Biofilm-Based Biological Treatment Systems 2
1.2. Scope of Work 4
1.3. Intellectual Merit 5
1.4. Broader Impacts 5
CHAPTER 2 7
Produced water composition, treatment, reuse, and management strategies: A review 7
2.1. Introduction 7
2.2. Produced water composition 9
2.3. Environmental impact of produced water generation 13
2.4. Produced water treatment 15
2.5. Conclusions 20
CHAPTER 3 22
Experimental Setup and Operation Conditions 22
3.1. Reactor setup and operation 22
3.2. Analytical procedures 30
3.3. Volatility, biosorbtion, and biodegradation assessment 42
3.4. Aromatic compound detection 44
3.5. X-ray photoelectron spectroscopy analysis 49
3.6. Microbial community analysis 54
3.7. Statistical analysis 55
CHAPTER 4 57
Use of halophilic bacteria to improve aerobic granular sludge integrity in hypersaline wastewaters 57
4.1. Introduction 58
4.2. Materials and Methods 61
4.3. Results 65
4.4. Discussion 74
4.5. Summary 77

CHAPTER 5 78
Biodegradation of aromatic compounds under hypersaline conditions: Comparing aerobic biofilm reactors with conventional activated sludge 78
5.1. Introduction 78
5.2. Experimental Section 81
5.3. Results and discussion 84
5.4. Conclusions 100
CHAPTER 6 101
Long-term performance of aerobic versus anaerobic biofilm systems under hypersaline conditions and toxic organic load 101
6.1. Introduction 101
6.2. Materials and Methods 104
6.3. Results and discussion 107
6.4. Conclusions 116
CHAPETR 7 117
Major Findings, Implications and Proposed Future Work 117
7.1. Major Findings 117
7.2. Implications 120
7.3. Proposed Future Work 121
REFERENCES 123
Appendix A: Supplementary Information for Chapter 4 135
Appendix B: Supplementary Information for Chapter 5 141
Appendix C: Supplementary Information for Chapter 6 149
Appendix D: Agilent 7890B Gas Chromatograph (GC) Control Information 154

FIGURES

Figure 2-1: The fractions of HFF and FW to total PW in respect to time of production. 8
Figure 2-2: PW generated in Top Ten US States (bbl/ yr), data from Veil (2015). 10
Figure 2-3:Onshore PW disposal practices across U.S. (Clark and Veil 2009). 15
Figure 3-1: AGS formation reactors setup. 23
Figure 3-2: Bio-GAC, AGS, and CAS rectors. 25
Figure 3-3: Major phases of SBRs operations cycle. 26
Figure 3-4: Contact-aggregation strategy to enhance biofilm growth on GAC surface. 27
Figure 3-5: Quantification of growing DNA on GAC surface during startup period. 27
Figure 3-6: Anaerobic up-flow reactors; anaerobic granular activated carbon reactor (AnGAC) (lift) and anaerobic granular sludge reactor (UAGSR) (right) 29
Figure 3-7: Carbon source during startup and operating period. 31
Figure 3-8: Freundlich adsorption isotherm. 37
Figure 3-9: Breakthrough batch experiment reactors. 38
Figure 3-10: Breakthrough curves for mixture and individual aromatic compounds. 38
Figure 3-11: Batch experiment design flow diagram. 41
Figure 3-12: Preparation steps applied on collected samples prior to SEM observation. 43
Figure 3-13: Batch reactor setup to assess volatility, biosorption, and biodegradation. 44
Figure 3-14: Solid phase extraction steps. 45
Figure 3-15: Detected aromatic compounds by GC; Benzaldehyde (7.4 min), phenol (8.4 min), benzyl alcohol (8.9 min), o-cresol (9.5 min) and chlorodecane (12.8 min). 46
Figure 3-16: UV-Vis absorption spectra of samples with known catechol concentration: 0.1 mg/ l catechol (a), 0.25 mg/ l catechol (b), 0.3 mg/ l catechol (c), 0.75 mg/ l catechol (d) and 1.0 mg/ l catechol (e). 47
Figure 3-17: Catechol standard curve. 48
Figure 3-18: XPS instrument Model PHI 5000 VersaProbe II, Physical Electronics Inc. 51
Figure 3-19: AGS weight reduction during oven drying time. 51
Figure 3-20: XPS standard sample studs (left) and specified area on sample surface to retrieve targeted atoms (right). 52
Figure 3-21: Data acquisition and analysis using XPS technique. 53
Figure 4-1: MLVSS concentration for enriched halophilic and activated sludge culture along with study period 62
Figure 4-2: Average granule sizes (left) and aspect ratios (right) for reactors inoculated with an enriched halophilic culture or activated sludge at increasing salt concentrations. 67
Figure 4-3: Enriched halophilic AGS at (A) 40 g L^{-1} NaCl and (B) 85 g L^{-1} NaCl; activated sludge AGS at (C) 40 g L^{-1} NaCl and (D) 85 g L^{-1} NaCl. AGS, aerobic granular sludge. 67
Figure 4-4: (A) EPS production and (B) ALE production in reactors inoculated with an enriched halophilic culture or activated sludge. ‘‘*’’ Indicates a statistically significant difference ($p < 0.05$) in ALE production. EPS, extracellular polymeric substances;ALE, ... 69
Figure 4-5: Cation concentrations in the EPS of AGS formed from the activated sludge culture (top) and enriched halophilic culture (bottom). 70
Figure 4-6: Intracellular concentrations of calcium (filled symbols) and sodium (open symbols) in the halophilic and activated sludge reactors under hypersaline conditions. 71

Figure 4-7: Stacked bar plot showing taxa with relative abundance ‡0.1% at phylum level for inoculum (0 g L^{-1} NaCl) and at each saline concentration for (A) the reactor inoculated with an enriched halophilic culture and (B) the reactor inoculated with activated sludge. 73
Figure 5-1: Conceptual sketch of anticipated bioactivity within attached biofilm in Bio-GAC system. 80
Figure 5-2: Biosorption of aromatic compounds: Bio-GAC (a), AGS (b), and CAS (c). 87
Figure 5-3: Aromatic compounds biodegradation and intermediate derivatives generation over cycle time of SBRs..... 90
Figure 5-4: SEM observation showing the impact of carbon source changing on biofilm morphology. (a), (b), and (c) GAC fed with (AC), (AC, BA) & (AC, BA, OC and Ph) as carbon source respectively and (d), (e), and (f) AGS fed with (AC), (AC, BA) & (AC, BA, OC and Ph) as carbon source respectively too. 91
Figure 5-5: Activity of microorganisms in the three bioreactors measured as SOUR. The shaded area represents 95% confidence interval of observed means and the dashed lines show the mean values. 93
Figure 5-6: XPS scans of excited forms of carbon and oxygen. 96
Figure 5-7: Stacked bar plot showing taxa relative abundance of 0.1% at genus level for microbial community from AGS, CAS and Bio-GAC reactors. 99
Figure 6-1: Overall organic load removal. 109
Figure 6-2: Long term effluent MLSS from aerobic bioreactors. 111
Figure 6-3: Long-term effluent MLSS from anaerobic bioreactors..... 111
Figure 6-4: High-resolution C 1s spectra of (a) anaerobic biofilm integrated on GAC surface, (b) biofilm of anaerobic granular sludge, (c) aerobic biofilm integrated on GAC surface and (d) biofilm of aerobic granular sludge. 114

TABLES

Table 2-1: Inorganic elements / ions in produced water (Neff et al. 2011). 11
Table 2-2: Naturally occurring organic matter in PW (Neff et al. 2011). 12
Table 2-3:Common metals found in PW (Neff et al. 2011). 13
Table 2-4: Available biological techniques applied to treat PW. 20
Table 3-1: Final composition of brine solution used to mimic PW, including trace elements. 30
Table 3-2: The optimized biofilm detachment methods 34
Table 3-3: The optimized biofilm detachment methods. 35
Table 3-4: MDL calculations for benzyl alcohol, o-cresol, and phenol. 49
Table 4-1: Composition of reactor feed, including trace element composition. 63
We have employed XPS analysis to observe aromatic accumulation and degradation within the biofilm of Bio-GAC, AGS, and CAS cultures. Wide survey XPS spectra over the energy range of 0-1100 eV shows the presence of C, O, N, Na and Cl as major elements I nthe sample, with Na and Cl resulting from the high aqueous salinity (Figures B11 to B13).High-resolution scans from 282 to 290 eV were used to better identify the forms of carbon present in the samples. Peak fitting was used to classify the carbon into four forms; C-(C,H), C-(O,N), O-C-O, and COOR (Fang et al. 2018b, Yin et al. 2015) (Figure 5 a) . These peaks represent lipid side chains and/ or amino acids, alcoholic compounds or proteins, carboxylate or carbonyl groups, and carboxyl or esters, respectively. Additional studies also showed that carbon peak positions for AGS samples fed with acetate were located at different binding energies compared to AGS samples that fed with aromatic compounds (Tables 5-1 - 5-3).Table 5-1: Peak position, % content, O and N ratios with respect of C for Bio-GAC specimens. 93
Table 5-2: Peak position, % content, O and N ratios with respect of C for AGS specimens. 94
Table 5-3:Peak position, % content, O and N ratios with respect of C for CAS specimens. 94
Table 5-4: Impact of feast/ famine on carbon content for AGS, Bio-GAC and CAS. 96
Table 5-5: The ratio of carbon and oxygen functional groups to the total carbon. 97
Table 6-1: The ratio of functional groups to the total carbon. 113
Table 6-2: The ratio of functional groups to the total O 1s or N 1s. 113
Table 6-3: Observed specific substrate uptake rate in aerobic and anaerobic bioreactors. 116

NOMENCLATURE

AGS	Aerobic granular sludge
ALE	Alginate-like exopolysaccharides
AnGAC	Anaerobic biofilm/ GAC reactor
ANOVA	Analysis of variance
APHA	American Public Health Association
ASVs	Amplicon sequencing variants
ATCC	American Type Culture Collection
AuNPs	Gold nanoparticles
BA	Benzylalcohol
BAC	Biological activated carbon
Bio-GAC	Aerobic biofilm/ GAC reactor
BOD	Biological oxygen demand
BTEX	Benzene, toluene, ethylbenzene, and xylenes
CAS	Conventional activated sludge
COD	Chemical oxygen demand
DNA	Deoxyribonucleic acid
DO	Dissolved oxygen
DOC	Dissolved organic carbon
EPS	Extracellular polymeric substances
FTIR	Fourier-transform infrared
FW	Formation water
GAC	Granular activated carbon
GC	Gas Chromatograph
HF	Hydraulic fracturing
HRT	Hydraulic retention time
ICP-OES	Inductively coupled plasma – optical emission spectrometry
LB-EPS	Lightly bound EPS
MAFFT	Multiple sequence alignment
MBBR	Moving bed biological reactor
MCDCs	Microbial capacitive deionization cells

MCL	Maximum contaminant level
MDL	Method detection limit
MFCs	Microbial fuel cell
MLSS	Mixed liquor suspended solids
MLVSS	Mixed liquor volatile suspended solids
MPBA	4-mercaptophenylboronic acid
NIST	National Institute of Standard and Technology
NMDS	Nonmetric multidimentional scaling
NOM	Natural organic matter
NORMs	Naturally occurring radioactive materials
NPDES	National Pollutant Discharge Elimination System
OC	o-Cresol
OLR	Organic load rate
OTUs	Operational taxonomic units
OUR	Oxygen uptake rate
PAHs	Polycyclic aromatic hydrocarbons
PBS	Phosphate buffered saline
pCi	picoCuries
PCR	polymerase chain reaction
Ph	Phenol
POTWs	Publicly owned treatment works
PS	Polysaccharides
PTFE	Polytetrafluoroethylene
PW	Produced water
QIIME2	Quantitative Insights into Microbial Ecology 2
q_s	Specific substrate uptake rate batch experiment
RCF	Relative Centrifugal Force
RDP	Ribosomal Database Project
SABF	Submerged aerated biological filter
SBR	Sequencing batch reactors
SEM	Scanning electron microscopy
SIM	Selected ion monitoring mode

SOUR	Specific oxygen uptake rate
SPE	Solid phase extraction
SVI_5	Sludge volume index at 5 minutes
TB-EPS	Tightly bound EPS
TOC	Total organic carbon
UASB	Up-flow anaerobic sludge blanket reactor
XPS	X-ray photoelectron spectroscopy

ACKNOWLEDGEMENTS

I would like to thank my advisor, Prof. Dr. Edward Peltier and co advisor Prof. Dr. Belinda Sturm, with whom I had an excellent graduate education with many opportunities that helped form me develop? new research skills. I would also like to thank my coauthor on the paper that became a part of my dissertation, Mr. Yasawantha Hiripitiyage, who developed the research branch on microbial community analysis at the University of Kansas. I am grateful to Dr. Ray Carter who trained me on using Gas Chromatography at University of Kansas Environmental Engineering Labs, and Dr. Karen Peltier, who was previously working at University of Kansas, for her assistance in running ICP analysis. I am also grateful for Dr. Prem Singh Thapa-Chetri at Microscopy and Analytical Imaging laboratory who developed my skills in MultiPak software. Special thanks to Profs. Dr. Stephen Randtke and Dr. Reza Barati for their role in my PhD defense committee. I thank Dr. Justin Hutchison for allowing me to run some experiments in his Lab. Additionally, I would like to thank Amelia Wyndrum for her assistance in Lab work. I am also grateful for all of the students who contributed to my research in the laboratory.

Finally, I would like to acknowledge the National Science Foundation [Grant Numbers OIA-1632892 and CBET-1512667], the University of Kansas Strategic Initiative Program, and the Iraqi government grant program MOHESR program for funding this work.

CHAPTER 1

INTRODUCTION

The worldwide increasing demand of industry has stimulated increased production of wastewaters containing a variety of recalcitrant organic contaminants. To avoid negative environmental impacts from the hazardous waste stream, proper treatment is required before disposal (Salminikhas et al. 2016, Silva et al. 2019). In particular, gas and oilfield-produced water (PW), generated as a byproduct of oil and gas extraction, is associated with serious water quality issues, such as high salinity and high fractions of refractory organic matter. Developing a sustainable management strategy for PW is a big challenge due to the high volume of wastewater generated and the toxicity of existing dissolved organics. The most common practices for PW disposal are deep well injection and surface water discharge (Clark and Veil 2009, Guerra et al. 2011). However, these applications are associated with serious environmental issues, such as induced seismicity and contamination of surface and groundwater (Akyon 2017, Cozzarelli et al. 2017, Kondash and Vengosh 2015, Kondash et al. 2017).

Conventional activated sludge (CAS) treatment is the most common and cost-effective treatment process applied to remove organic load and nutrients from municipal wastewater (Corsino et al. 2019). However, the application of CAS to industrial wastewater treatment can be limited by the characteristics of these waters. High fractions of toxic organic compounds and the elevated salinity of some industrial streams results in a detrimental impact on metabolic activity of microorganisms in conventional biological treatment systems and hinder the CAS bioprocess (Campo and Bella 2019, Nadella et al. 2020, Zou et al. 2020). Consequently, the utilization of CAS can be very limited for salty wastewaters. Creating robust biological treatment systems that are cost-effective, environmentally friendly and able to achieve high performance under severe

water quality conditions has become a pressing research topic over the last decade (He et al. 2020b, Wu et al. 2020b).

1.1. Biofilm-Based Biological Treatment Systems

1.1.1. Aerobic Biofilm-Based Bioprocesses

Introducing biofilm-based biological treatment techniques to wastewater treatment systems has increased the resilience of biosystems against shocks and improved the performance of these systems significantly. Aerobic granular sludge (AGS), a biofilm-based biological treatment technique, is a new technology that has seen rapid growth due to multiple performance advantages over CAS. AGS is cited for having smaller footprint, high settleability, high resistance against shocks, the ability to retain slower growing microorganisms, and stratified redox zones, which enhance nutrient removal (He et al. 2020a, Meng et al. 2020). The main feature of AGS is that limited mass transfer of substances through the biofilm layers play a crucial role in protecting microorganisms against shocks. Recent studies have shown that AGS can be adapted to be utilized to treat high-salinity wastewater environments, such as those found in oil & gas wastewaters or canning and vegetable pickling waste (Ou et al. 2018a, Ozaki et al. 2015). Mass diffusion limitation through the biofilm improves the ability of AGS to withstand toxic and other potential shocks and makes it a promising technology for treatment of wastewaters containing both high salinity and toxic compounds. Nevertheless, the high toxicity of some dissolved organic matter and the overall ionic strength of some types of wastewater can influence the system performance and hinder AGS formation, or at least extend the acclimation period for biomass in order to function in harsh environments (Ou et al. 2018a, Ramos et al. 2015).

1.1.2. Anaerobic Biofilm-Based Bioprocesses

The main drawback associated with aerobic biological treatment techniques is the high dissolved oxygen demand, which increases the operational cost of these biosystems (Ekici 2017). Anaerobic biofilm-based biological treatment systems have been utilized to treat high-strength

wastewater (Chen et al. 2020b). Anaerobic microorganisms rely on different electron acceptors to conduct bioprocesses, and therefore do not incur the high costs of oxygen supply, reducing operational costs compared to aerobic systems (Yurtsever et al. 2020). The slow metabolic activity of anaerobic microorganisms also provides an advantage for anaerobic biological treatment systems with respect to shock resilience because it requires lower energy (Shoukat et al. 2019). Anaerobic processes have been applied successfully to remove toxic organic compounds from industrial wastewater and reported as cost-effective, especially considering bioenergy recovery potential and low produced sludge volume (Chen et al. 2020a, Genethliou et al. 2020, Kong et al. 2018, Yurtsever et al. 2020). The continuous up-flow anaerobic sludge blanket reactor (UASB) is commonly utilized to treat high-strength wastewater (Chen et al. 2020a). UASB is classified as high-rate anaerobic bioprocess that can retain high biomass content despite the upflow velocity (Li et al. 2020a). UASB have attracted much research attention since it was introduced to wastewater treatment in the 1970s because it has shown high resilience against high-strength organic load (Wu et al. 2020a). For that reason, UASB was utilized in the current study to treat toxic organic load under hypersaline conditions.

1.1.3. Hybrid Biofilm-GAC Based Bioprocesses

Granular activated carbon has been used extensively in post or tertiary treatment to improve water quality prior to reuse or discharge into the environment (Cozma et al. 2012, Paredes et al. 2018). Utilizing GAC as a moving-bed biofilm has also been reported to be an effective way to remove toxic organic load from pharmaceutical, textile and olive mill wastewater (Genethliou et al. 2020, Puyol et al. 2015, Wang et al. 2017b). Integration of GAC with a hybrid adsorptive biofilm to treat recalcitrant and toxic organic compounds incorporates both biological and physico-chemical processes to enhance contaminants removal (Pradhan et al. 2020). The high ratio of surface area to volume of GAC increases the adsorption rate of organic matter to the GAC surface. This reduces

the toxicity of these compounds and improves the overall biological treatment performance (Puyol et al. 2015). However, little work has been done previously to develop these hybrid systems for use with high salinity wastewaters. This work addresses the development of a hybrid aerobic biofilm/ GAC reactor (Bio-GAC) and anaerobic biofilm/ GAC reactor (AnGAC), both of which use GAC as a supportive medium for the growth of salt-tolerant biofilms.

1.2. Scope of Work

Coping with high salinity and mitigating the toxicity effects of some hydrocarbons were proposed to be the key factors for biological treatment of PW. Sequencing batch reactors (SBRs) were used in this study due to the low required footprint, ease of control, and favorable conditions for retaining floc-forming bacteria (Cetin et al. 2018). In this study, multiple reactor configurations were examined for treatment of a synthetic analogue for oil and gas produced waters. This wastewater contained both high salinity (85 g L^{-1} NaCl) and elevated concentrations of toxic aromatic hydrocarbons. The main experimental phases are included below:

1. Development of aerobic bacterial communities capable of granule formation under high salinity conditions.
2. Comparison of aerobic reactor performance (Bio-GAC, AGS and CAS).
3. Comparison of the long-term performance of anaerobic versus aerobic bioreactor systems (AnGAC and UASB versus Bio-AGC and AGS).

The first phase of this study was devoted entirely to compare AGS formation using activated sludge and halophilic inoculums under hypersaline conditions. To achieve the purpose of this phase, synthetic PW with the salinity range of <1 – 80 g NaCl L^{-1} was used to mimic real produced water. Acetate was utilized as the sole carbon source for this phase of study. The second phase of this study focused on the biodegradation of aromatic compounds, and byproduct formation, using three different aerobic reactor designs, AGS, Bio-GAC, as biofilm- based

biological treatment, and conventional activated sludge reactor. Phenol, benzyl alcohol and o-Cresol were utilized as the carbon source during this phase. In phase three, the performance of AGS and Bio-GAC, as aerobic biofilm-based reactors, compared to AnGAC and UASB, as anaerobic biofilm-reactors. The removal efficiency for influent organics and the viability of reactor biomass were examined to test the resilience of proposed treatment systems.

1.3. Intellectual Merit

The intellectual merit of this study is to investigate the most effective treatment strategies to remove organic load from high-salinity industrial wastewaters under harsh environment. The first hypothesis was that bioaugmentation of AGS with halophilic microorganisms can enhance granule formation and thus improve AGS stability and performance under hypersaline conditions. Microbial community adaptation and other key factors that play a crucial role on AGS formation under hypersaline conditions were investigated to test this hypothesis. The current study also hypothesized that diffusion through the biofilm has a unique role in mitigating some hydrocarbon toxicity. To test this hypothesis, the biodegradation efficiency of a mixture of aromatic compounds in sequencing batch reactors (SBRs) was assessed under hypersaline conditions (85000 mg L^{-1} as NaCl). The third hypothesis is that the adsorption of hydrocarbons on the GAC surface can mitigate toxicity and improve SBR performance. Finally, the fourth hypothesis proposed was that anaerobic biodegradation can also be applied to the treatment of produced water. The novelty of the current study is that it characterized the gown hybrid biofilm on GAC surface for first time in this field. It also introduced XPS analysis as a new approach to observe biosorption within the biofilm.

1.4. Broader Impacts

The broader impacts of this study will be to frame the application of biofilm-based technology to remove organic load from hypersaline wastewater and overcome drawbacks associated with

conventional biological treatment systems. The fossil fuel industry can get benefits from the results of this study to make better understanding of biofilm behavior under hypersaline conditions and thus improve SBRs performance. Furthermore, the research outcomes can be also manipulated beneficially in the field of reclamation and safe reuse of common industries around the world, such as cheese manufacturing, vegetable pickling, seafood canning, and pharmaceuticals. Since the current study has utilized synthetic PW as a model of industrial wastewater, the outcomes will provide vital information for produced water reclamation and reuse for different purposes. Furthermore, this research will bring to attention the manipulation of aerobic granular sludge and hybrid biofilm-granular activated carbon systems to overcome all conventional biological treatment systems drawbacks. This study suggests two different biological treatment systems that can be utilized beneficially to reduce the toxicity associated with some of hydrocarbon compounds, which could achieve safe reuse and disposal for treated wastewater.

CHAPTER 2

Produced water composition, treatment, reuse, and management strategies: A review

2.1. Introduction

The impacts of oil and gas development on water supplies include both increased water demand and the production of associated wastewater. Introducing advanced techniques to enhance oil and gas recovery, such as hydraulic fracturing (HF), intensified fresh surface and groundwater use (Barati and Liang 2014, Kondash and Vengosh 2015, Scanlon et al. 2016, Stringfellow et al. 2014). The required volume of water for HF depends on formation characteristics and the length of the drilled well. In general, HF water ranges from 10 m^3 to as much as 40×10^3 m^3 for each oil and gas well across the U.S. (Ikonnikova et al. 2017, Stringfellow et al. 2014, Walker et al. 2017). The increasing demand on water for HF activities could cause extreme water stress, especially for locations with arid climates (Kondash and Vengosh 2015, Walker et al. 2017).

The term "produced water (PW)" has been introduced to denote aqueous waste produced during oil and gas extraction processes (Orem et al. 2014, Scanlon et al. 2016). This type of wastewater is classified under two main categories: flowback water and formation water generated from the extraction processes (Abdel-Shafy et al. 2020, Cozzarelli et al. 2017, Scanlon et al. 2016). Flowback water represents the return of fluids added to develop the well, including hydraulic fracturing fluid. The volume and water quality of formation water depend on the characteristics of subsurface rock formation and the type of drilled well (Kondash et al. 2017, Walker et al. 2017). This type of PW is distinguished by higher salinity and a variety of organic and inorganic compounds when compared to HF fluid, as it is generated from released water stored in the oil-bearing formation (Al-Ghouti et al. 2019, Kondash et al. 2017). The fraction of FW in PW increases with time (Figure 2-1). Consequently, salinity increases and water quality decreases as oil and gas wells age (Kondash et al. 2017, Nie et al. 2020).

Management and treatment of produced water is also associated with challenges due to presence of toxic and recalcitrant substances that can impact water quality. HF fluid contains chemical additives and propping agents that increase the toxicity of flowback wastewater. Production of HF impacts receiving water resources and induces environmental issues associated with untreated PW disposal, reuse, and reinjection (Kondash and Vengosh 2015). These compounds could also inhibit microbial metabolism and thus limit biological treatment of PW (Gallegos et al. 2015, Ramos et al. 2015). The high ionic strength and presence of some hydrocarbons in PW inhibits dehydrogenase enzyme activity and carbon respiration processes for bacterial growth (Elias-Samlalsingh and Agard 2004, Oberoi and Philip 2017b, Stringfellow et al. 2014).

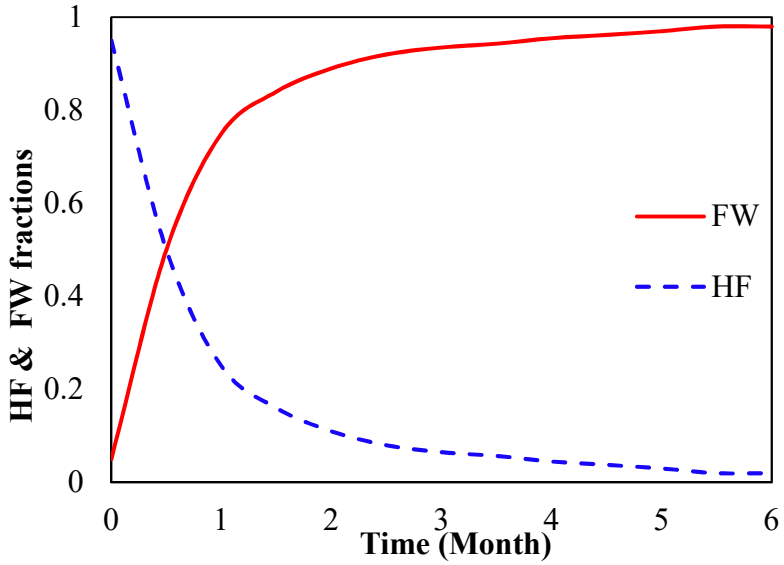

Figure 2-1: The fractions of HFF and FW to total PW in respect to time of production.

PW constitutes the largest volume of wastewater generated by the oil and gas extraction activities (Jimenez et al. 2018, Veil 2015). The global ratio of PW to extracted oil is around 3:1, but it is much higher in the U.S. (Abdel-Shafy et al. 2020, Veil 2015). The estimated worldwide PW volume is about 70 billion barrels per year, while approximately 20 billion barrels were

generated in the U.S. in 2012 (Figure 2-2), which represents 0.68% of total water uses across the country (Veil 2015). The quality of PW is significantly variable and changes substantially according to recovery stages and formation characteristics (Kondash et al. 2017, Tiedeman et al. 2016). Most of generated PW is considered as hypersaline wastewater due to total salt concentrations greater than 35 g L^{-1} (Benko and Drewes 2008, Jimenez et al. 2018, Sharghi et al. 2013). PW can also be enriched with hydrocarbon compounds from solubilized crude oil, such as n-alkanes, polycyclic aromatic hydrocarbons (PAHs), phenolic compounds and benzene, toluene, ethylbenzene, and xylenes (BTEX) (Ranck et al. 2005, Sharghi et al. 2013). In addition, multiple inorganic ions, such as magnesium, calcium, sodium, potassium and chloride are all typically present in concentrations up to hundreds of grams per liter (Sharghi et al. 2013). Other inorganic components can also be present, including carbonate, bicarbonate, sulfate and some metallic elements, such as strontium and barium (Li 2013). Naturally occurring radioactive materials (NORMs) can also be found in a wide range of concentrations (Zhang et al. 2014). Furthermore, additive chemicals used to improve HF fluid characteristics, many of which are toxic and recalcitrant (Butkovskyi et al. 2017), are also present, particularly in the early portion fraction of produced water returned from a well.

Increasing volumes of PW, along with high salinity, and toxic organic compounds are the main environmental issues associated with management, treatment, and disposal of PW (Jimenez et al. 2018, Li 2013, Pendashteh et al. 2012). Therefore, the objective of this review is first to highlight the potential PW resources, characteristics, environmental impact, then to highlight cost-effective method of treatment potential reuse.

2.2. **Produced water composition**

PW is a complex mixture of organic and inorganic compounds. The composition of PW is highly variable and depends substantially on chemical properties of bearing rocks, the type of

well (vertical/ horizontal), and the age of drilled well (Guerra et al. 2011, Li 2013). Therefore, PW comprises a variety of naturally occurring and artificially added compounds, such as inorganic compounds, dissolved organic compounds, metals and radioisotopes, and production chemicals. In this current review, we will focus on common properties that are used to characterize PW.

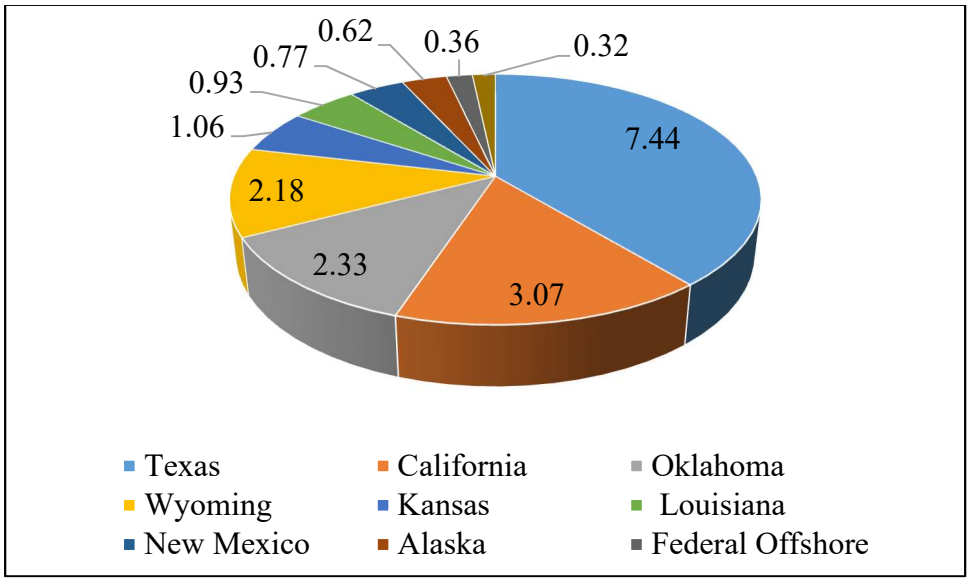

Figure 2-2: PW generated in Top Ten US States (bbl/ yr), data from Veil (2015).

2.1.1. Inorganic compounds

The inorganic composition of PW depends substantially on formation chemical characteristics and additives used to enhance production (Clark and Veil 2009, Guerra et al. 2011, Jimenez et al. 2018). The most common salt ions in PW are chloride and sodium, which range from a few milligrams per liter (mg L^{-1}) to hundreds of thousands of mg L^{-1} (Al-Ghouti et al. 2019). In addition, calcium, magnesium, barium, potassium, strontium, bromide, iodide, boron, lithium, sulfate and bicarbonate are present in PW at varying amount (Table 2-1). Sulfide can also be present in PW as a byproduct of sulfate biotransformation (Al-Ghouti et al. 2019, Horner et al. 2011). High concentrations of inorganic compounds in PW are a big challenge, as they increase the cost of treatment and limit reuse options.

Table 2-1: Inorganic elements / ions in produced water (Neff et al. 2011).

Element/ion	Seawater (mg L^{-1})	Produced water	
		Highest concentration (mg L^{-1})	Range of meanconcentrations (mg L^{-1})
Salinity	35000	-	<5,000–>300,000,000
Sodium	10760	120,000	23,000–57,300
Chloride	19353	270,000	46,100–141,000
Calcium	416	205,000	2,530–25,800
Magnesium	1294	26,000	530–4,300
Potassium	387	11,600	130–3,100
Sulfate	2712	8,400	210–1,170
Bromide	87	6,000	46–1,200
Strontium	0.008	4,500	7–1,000
Ammonium	-	3,300	23–300
Bicarbonate	142	3,600	77–560
Iodide	167	1,410	3–210
Boron	4.45	450	8–40
Carbonate	-	450	30–450
Lithium	0.17	400	3–50

2.1.2. **Dissolved organic compounds**

PW contains a miscellaneous collection of organic compounds, mostly composed of natural organic matter (NOM) and production chemicals (Butkovskyi et al. 2017, Li 2013, Orem et al. 2014). Usually the production chemicals are present only in the early flowback water from a new well, while NOM remain in PW throughout production (Orem et al. 2014). In addition, production chemicals tend to be more soluble in oil than in PW (Neff et al. 2011). Thus, we will focus on NOM only in this review. Characterization of PW with respect to NOM is a challenge due to complex nature of this type of wastewater (Wang et al. 2012). Therefore, the organic load of PW is reported in a variety of ways (Table2-2): as total organics (chemical or biological oxygen demand (COD or BOD), dissolved and total organic carbon (DOC and TOC), or oil and grease), by functional groups (organic acids, benzene, toluene, ethylbenzene, and xylene (BTEX), polycyclic aromatic hydrocarbons (PAHs), etc.) or sometimes as a list of individual organic compounds (Butkovskyi et al. 2017, Neff et al. 2011). The concentration and type of individual

component in NOM depend on several factors, such as type of hydrocarbon being extracted (i.e., natural gas or oil) and age of production (i.e., new well or old well) (Guerra et al. 2011). For instance, PW generated from natural gas extraction process has higher TOC and is enriched with aromatic compounds, while PW from oil wells is characterized by lower TOC and higher aliphatic content (Sirivedhin and Dallbauman 2004). Aqueous solubility of different compounds also affects the presence of NOM in PW. In general, NOM with lower molecular weight is more soluble in PW (Butkovskyi et al. 2017, Neff et al. 2011). The bioavailability of most of organic compounds is low and a large fraction of the NOM is biologically recalcitrant (Wang et al. 2012).

Table 2-2: Naturally occurring organic matter in PW (Neff et al. 2011).

Chemical Class	**Concentration, mg L^{-1}**
Total organic carbon	≤0.1 – >11,000
Total organic acids	≤0.001 – 10,000
Total saturated hydrocarbons	17 – 30
Total benzene, toluene, ethylbenzene, and xylenes (BTEX)	0.068 – 578
Total polycyclic aromatic hydrocarbons (PAH)	0.04 – 3.0
Total steranes / triterpenes	0.14 – 0.175
Ketones	1.0 – 2.0
Total phenols (primarily C_0-C_5 phenols)	0.4 – 23

2.1.3. **Metals and radioisotopes**

PW contains a variety of dissolved and particulate metals (Alley et al. 2011). The type and concentration of metals in PW mainly depends on characteristics of rock formation (Al-Ghouti et al. 2019, Benko and Drewes 2008, Kondash et al. 2017). The most common metals in PW are arsenic, barium, cadmium, chromium, copper, iron, lead, manganese, mercury, nickel, and zinc (Table 2-3) (Al-Ghouti et al. 2019, Guerra et al. 2011). The presence of metals in PW contributes to scale formation in production systems which increases the operation and maintenance costs (Hamed et al. 2015, Zhang et al. 2014).

Naturally occurring radioactive materials (NORMs) are also derived from subsurface formations. The alkaline earth metal radium-226/228 (Ra-226/ 228) is the most dominant NORM

in PW. Ra-226/228 is the main by-product of naturally decaying thorium-232 and uranium-238 (Akyon 2017, Rowan et al. 2011, Zhang et al. 2014). The activity of Ra-226/228 is in the range of 734 to 18000 pCi L^{-1}, which largely depends on the age of the reservoir (Akyon 2017), while the maximum contaminant level (MCL) for Ra-226/228 in drinking water is 5 pCi L^{-1} (Mathews et al. 2018). Radium has similar chemical properties to non-radioactive divalent cations, such as Ca^{+2}, Ba^{+2}, and Sr^{+2}. NORMs present in PW can pose serious health issues for mammals as they have the capability to substitute Ca^{2+} in bones, in addition to other issues radioactivity causes in humans and animals (Akyon 2017, Zhang et al. 2014). The presence of these constituents in PW has raised concerns due to their impact on treatment process, especially for biological treatment.

Table 2-3:Common metals found in PW (Neff et al. 2011).

Metal	**Concentration, µg L^{-1}**
Arsenic	0.5 - 90
Barium	301- 342,000
Cadmium	<0.05 - <10
Chromium	<0.1 - 34
Copper	<0.2 - 137
Iron	1,910 – 37,000
Lead	<0.1 - 45
Manganese	81 – 7,000
Mercury	<0.01 - <10
Nickel	<1.0 - 420
Zinc	<1 - 26000

2.3. **Environmental impact of produced water generation**

The rapid expansion of the fossil fuel industry greatly increased volumes of produced water, raising concerns about the environmental impact of generated PW. Direct disposal of PW into water resources releases a huge organic load along with toxic inorganic compounds and NORMs, which could overwhelm the water's capacity to dilute the pollution stream (Al-Ghouti et al. 2019, Cozzarelli et al. 2017, Zhang et al. 2014). Water scarcity in production sites could also cause a competition for water used for oil and gas extraction versus that required for other uses,

such as irrigational, agricultural, potable, livestock watering, recreational, and hydraulic fracturing (Gallegos et al. 2015, Osipi et al. 2018, Scanlon et al. 2016, Tiedeman et al. 2016).

Current management practices for produced water include deep well injection, surface water discharge under the National Pollutant Discharge Elimination System (NPDES), beneficial reuse, evaporation pits, and discharge to publicly owned treatment works (Clark and Veil 2009, Guerra et al. 2011). These applications can lead to serious environmental issues, including surface water and groundwater contamination, and induced seismicity (Akyon 2017, Cozzarelli et al. 2017, Kondash and Vengosh 2015, Kondash et al. 2017). Including toxic and refractory additives to stimulate hydrocarbon recovery during oil and gas extraction could also increase groundwater contamination (Rogers et al. 2017). Currently, gravity separation followed by deep well injection or discharge into the environment are the most common practices applied for PW disposal. Approximately one-quarter of the total generated PW across the US is managed by injection to Class II wells (Jimenez et al. 2018, Veil 2015).

The recent revolution in extraction techniques increased both the demand for water and generated PW volumes (Mohammad-Pajooh et al. 2018, Tiedeman et al. 2016, Walker et al. 2017). The largest fraction of onshore PW (92%) was injected into Class II wells in 1995 in U.S. while only 2% was reused for beneficial reuse (Figure 2-3). The main concern associated with PW injection is induced seismicity (Liden et al. 2018). In addition, several studies have shown that PW treated within publicly owned treatment works (POTWs) did not meet disposal requirements due to elevated concentration of bromide and organic disinfection byproduct (Hladik et al. 2014).

Therefore, management and reuse strategies are necessary to avoid adverse effects on surface and groundwater quality. There is also a persistent need to prevent or reduce earthquake activity due to deep well injections; various management scenarios have been suggested by

scientists to deal with increasing amount of PW (Abdel-Shafy et al. 2020, Liden et al. 2018, Nie et al. 2020). The current study presented the biological treatment as a cost-effective alternative to improve the quality of PW for safe reuse and disposal.

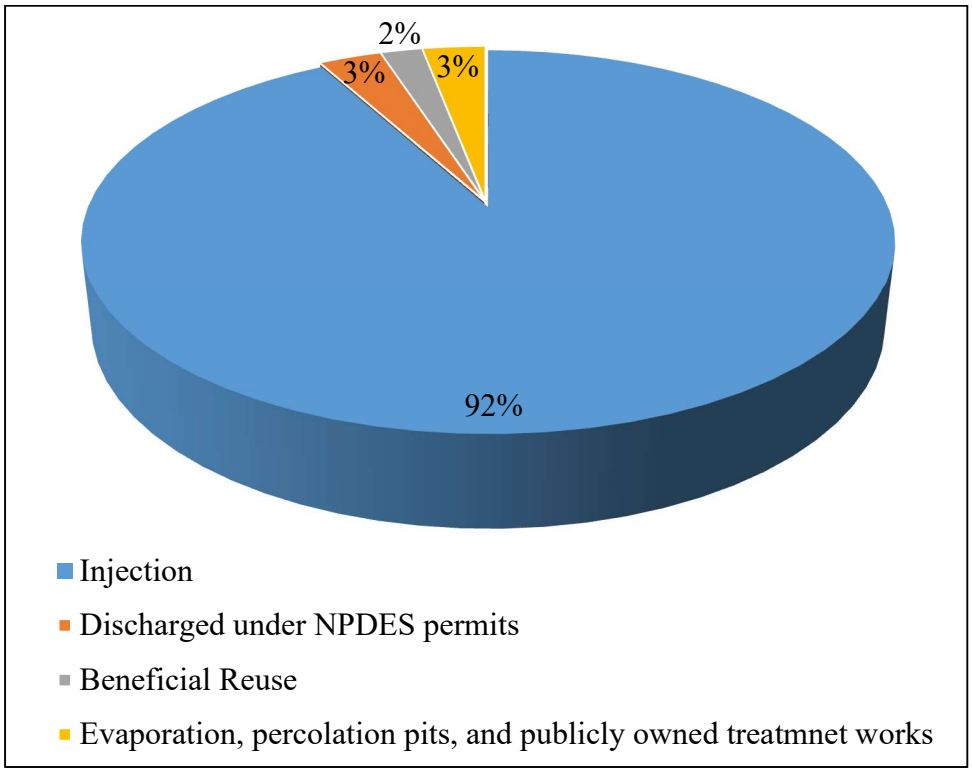

Figure 2-3:Onshore PW disposal practices across U.S. (Clark and Veil 2009).

2.4. **Produced water treatment**

Treatment and management strategies for PW disposal have become major research topics within the last decade (Li 2013, Sharghi and Bonakdarpour 2013, Walker et al. 2017). Environmental regulations and water scarcity have intensified the efforts to evaluate existing treatment systems with respect to both high salinity and organic load (Sudmalis et al. 2018).

2.4.1. **Physical treatment**

Numerous physical treatment methods have been considered since the last decade to treat PW (Abdel-Shafy et al. 2020). Membrane technology is one of the most commonly applied

methods to treat contaminated PW (Abdel-Shafy et al. 2020, Al-Ghouti et al. 2019, Osipi et al. 2018, Xu et al. 2018). Additionally, walnut shell media have been utilized as a cost-effective treatment to remove dissolved organic matter from PW (Zhang et al. 2019). Copolymers, zeolites, and resins have also been successfully utilized to reduce organic load in PW (Lu et al. 2019, Xu et al. 2018). Granular activated carbon has been widely used as a post or tertiary treatment to improve water quality prior to reuse or discharge into the environment (Cozma et al. 2012, Paredes et al. 2018). GAC has been used extensively to remove hydrocarbon compounds due to its high adsorption capacity, low cost, and non-toxic properties (Riley et al. 2018, Song et al. 2019).

Although the treatment of PW often targets organic load removal, desalination is another potential treatment especially in arid regions due to water scarcity and stricter environmental regulations (Osipi et al. 2018). Thermal and membrane processes are the most common physical treatments applied for secondary and tertiary recoveries of PW (Xu et al. 2018). Some other physical treatment processes such as electrodialysis and cyclones have been applied to reduce the salinity of PW as well (Ahmadun et al. 2009, Shaffer et al. 2013). However, physical treatment of PW is susceptible to fouling and scaling due to presence of organic compounds and scale-formers in treated water, which increases the cost of applying this technology to treat PW (Jimenez et al. 2018).

2.4.2. **Chemical treatment**

Chemical treatment is used as an upstream treatment, integrated with other downstream techniques, or rendering treatment (Al-Ghouti et al. 2019, Jimenez et al. 2018, Zhang et al. 2019). Chemical treatment can be applied mainly to remove suspended and colloidal particles, but it is ineffective to remove organic load unless strong oxidants and catalysts are employed (Abdel-Shafy et al. 2020, Al-Ghouti et al. 2019). Chemical precipitation, electrochemical processes, ion exchange, polymers, chemical oxidation, ozone, and the Fenton process are the most commonly

applied chemical treatments in oil and gas industry (Ahmadun et al. 2009, Jimenez et al. 2018). These chemical processes are usually associated with high costs (Al-Ghouti et al. 2019).

2.4.3. **Biological treatment**

Compared to other treatment methods, biological treatment is more attractive for organic removal from PW because it is relatively lower costs and environmentally friendly (Al-Ghouti et al. 2019, Nie et al. 2020). Numerous adapted microorganisms, such as bacteria, fungi, protozoa, and algae demonstrate the ability to achieve significant reduction in dissolved organic constituents present in PW (Al-Ghouti et al. 2019, Jimenez et al. 2018). Several biological techniques, such as conventional activated sludge, moving-bed biofilm reactors, membrane bioreactors and microbial fuel cells have been employed to harness microbes to achieve safe disposal or beneficial reuse of freshwater-based wastewater (Table 2-4) (Acharya et al. 2019, Al-Ghouti et al. 2019, Ding et al. 2020, Mohamed et al. 2020, Sambusiti et al. 2020). Other previous studies, however, have shown that most biological treatment systems demonstrated lower efficiency regarding organic load removal in PW compared to those applied on freshwater-based systems (Al-Ghouti et al. 2019, Campo and Bella 2019, Corsino et al. 2019). The primary limitation to biological treatment is extreme levels of salinity, which severely affects microbial metabolism, can cause cell lysis, and negatively influences the settling properties of sludge biomass. The other challenge associated with PW is the complex matrix of hydrocarbon compounds, which can increase the toxicity of NOM, thus limiting the performance of biological treatment (Butkovskyi et al. 2017, Corsino et al. 2017, Sudmalis et al. 2018). The presence of some individual toxic organic compounds poses an additional threat to conventional biological treatment systems (Sambusiti et al. 2020, Silva et al. 2019).

Recent studies have shown that biofilm techniques can be utilized as an alternative to conventional biological treatment systems to handle high-salinity wastewater environments, such

as those found in PW (Carrera et al. 2019a, Huang et al. 2019a, Ou et al. 2018b). Oberoi and Philip (2017a) have utilized moving bed biological reactor (MBBR) and submerged aerated biological filter (SABF) designs to treat wastewater contaminated with heterocyclic and homocyclic aromatic hydrocarbons, as well as phenolic compounds. These authors studied the effect of compound type, hydraulic retention time (HRT) and organic load rate (OLR) on removal efficiency, achieving up to90.4% and 85.8% removal of studied compounds in MBBR and SABF respectively. Corsino et al. (2015) compared the performance of aerobic granular sludge in acetate-based synthetic oily wastewater and a mixture of real and simulated slop with ratio of (20:80). The COD values of those two different wastes were approximately 900 and 1350 mg/ L respectively, while the amount of total petroleum hydrocarbons and aromatic hydrocarbons in real slop were much lower (6.8±1.5 and 1.18± 0.25 mg L^{-1} respectively). Shrestha et al. (2018) compared the performance of microbial fuel cells (MFCs) and microbial capacitive deionization cells (MCDCs) fed with Bakken shale produced water. The organic load removal efficiencies were 88% and 76% for MFCs and MCDCs respectively. However, MCDCs achieved up to 74% salinity removal compared to 38% in MFCs. This study also showed that higher impedance was enhanced by fouling under long-term operation for both treatment systems, which limits the application of microbial fuel cell techniques in the oil and gas industry. Zhang et al. (2018) have investigated the treatment of synthetic flowback water using aerobic granular sludge. Synthetic flowback water, with different salinity levels, was used to mimic real flowback water. The TOC removal efficient reached to 79% before it declined at 50 g L^{-1} salinity.

Hybrid physical/biological treatment systems have gained increasing attention, and have reported significant reductions in toxic compounds concentration (Pradhan et al. 2020, Warren 2019). The organic load can be removed within hybrid systems by a combination of physical and

biological conversion processes, which increases the capability of this system to withstand shocks much better than conventional treatment systems (Pradhan et al. 2020, Wang et al. 2019, Zhang et al. 2013). The most commonly utilized hybrid system is biological granular activated carbon (Bio-GAC) (Zhang et al. 2013). Florentino et al. (2019) observed the effect of using GAC on digestion of blackwater (the wastewater that contains high concentrations of organic matter and nutrients) and concluded that the addition of GAC to the digester enhanced methane production and that 86% of soluble COD in fed wastewater was removed by adsorption on GAC surface.

A combination of physical adsorption processes and biofilm growth on GAC surface is utilized in Bio-GAC to improve the biodegradation rate of organic matter (Florentino et al. 2019, Pramanik et al. 2015). The large surface area and high porosity of GAC plays a crucial role in enhancing biogrowth and in protecting colonized microbes against sloughing forces (Warren 2019). Pramanik et al. (2015) compared the impact of using biological activated carbon (BAC) and GAC (biogrowth inhibited in this reactor) on reducing microfiltration membrane fouling. The influent of both columns was biologically treated secondary effluent. Their study found that there was a significant improvement in flux when BAC prior to pass the wastewater through microfiltration membrane. Despite the high effluent water quality of biofilm and hybrid systems, the presence of recalcitrant and toxic dissolved organic compounds in PW, and the high salinity, can limit their performance unless adapted or halophilic microorganisms are utilized in these systems (Huang et al. 2019a, Nie et al. 2020, Ramos et al. 2015, Yusoff et al. 2019).

Table 2-4: Available biological techniques applied to treat PW.

Hydrocarbon Comps.	Conc. (mg/ L)	Bioprocess	Reference
Benzyl alcohol	54-108	Sequencing batch biofilm reactors	Mohan et al. 2009
Phenol	563	Continuous airlift reactor	Ramos et al. 2015
p-nitrophenol	350		
o-cresol	95		
Quinoline	100	Submerged aerated biological filter + Moving Bed Biological Reactor	Oberoi & Philip 2017
Pyridine	250		
Benzothiophene	20		
Benzofuran	20		
Naphthalene	20		
Benzene	100		
Toluene	5-104	Expanded granular sludge bed-anaerobic filter	Enright et al. 2007
Phenol	188-301	Vertical baffled bioreactor	Zou et al. 2018
Quinoline	129		
Phenol	5000	Extractive membrane bioreactor	Ren et al. 2017
Phenanthrene	200	Batch reactors	Mnif et al. 2017
Pyrene	500	Batch reactors	Qi et al. 2017
Naphthalene	500		
Phenanthrene	500		
Anthracene	500		

2.5. **Conclusions**

Increasing demands for water for various purposes, such as irrigation, livestock, recreational, and other uses, makes PW reclamation attractive. Current management practices for PW including deep well injection and surface water discharge also raise public concerns due to their impacts on receiving water bodies as well as induced seismicity. Water scarcity in some places increases pressure on available water resources and causes a competition for water used for oil and gas industry. All of these factors argue for increased treatment and recovery of PW.

The composition of PW is varied and substantially dependent on formation, extraction techniques, and hydrocarbons being extracted (oil or gas). In general, treatment and reuse is necessary to avoid adverse effects due to release of untreated PW. There are several available

treatment methods, but not all are viable and cost-effective. Conventional biological treatment has a good history of cost-effective treatment to remove organics from municipal wastewater. However, the high salinity and presence of toxic substances in PW limit applications of this technique in the oil and gas industry. Biofilm-based biological techniques are a reliable and promising alternative to conventional biological treatment. Hybrid biological treatment techniques can also be applied but require further investigation to verify their feasibility for full-scale applications.

CHAPTER 3

Experimental Setup and Operation Conditions

3.1. Reactor setup and operation

3.1.1. Operating conditions for aerobic granular sludge (AGS) reactors for start-up

Two identical 3.0 L bench-scale sequencing batch reactors (SBRs) were constructed with an internal diameter of 6.5 cm and an effective height of 88.5 cm (Figure 3-1); the volumetric exchange ratio was 50%. At steady state, reactors were operated with a 6-hour cycle comprised of four phases: 30 minutes anaerobic feeding through the settled sludge bed, 322 minutes aeration, 3 minutes settling, and 5 minutes decanting. In the initial formation period, the settling time was 10 minutes to retain small granules, with a corresponding reduction of the aeration time to 315 minutes. Beginning 37 days from cultivation, settling time was gradually reduced to 3 minutes over 20 days. The superficial up-flow air velocity was maintained at 1.1 cm s^{-1} throughout.

The first reactor was inoculated with an enriched halophilic culture obtained from a previous experiment that was conducted to enrich halophilic microorganisms. Prior to inoculation, this culture was pre-acclimated to the reactor feed solution (Table 1), with the NaCl concentration increased incrementally by 5 g L^{-1} on a biweekly basis from 0 to 40 g L^{-1}, for 120 days. The 5 most abundant genera were measured as a percentage of total detected genera. At time of inoculation into the SBR, the 5 most abundant genera in the enriched halophilic inoculum were *Halomonas* with a relative abundance of 59.2 ± 9.2%, followed by *Staphylococcus* (39.5 ± 11.3%), *Planktosalinus* (0.5 ± 0.1%), *Corynebacterium* (0.4 ± 0.1%), and *Marinobacter* (0.1 ± 0.05%) - all of which are known halophilic organisms. The second reactor was inoculated with activated sludge collected from the aeration tank of a municipal wastewater treatment plant in Lawrence, KS. The top 5 most abundant genera in the activated sludge culture were *Thiothrix* (2.9 ± 0.3%),

Bdellovibrio (2.7 ± 0.1%), *Planctomyces* (1.9 ± 0.1%), *Uncultured Xanthomonadaceae Family* (1.7 ± 0.1%), and *Hyphomicrobium* (1.6 ± 0.1%).

Figure 3-1: AGS formation reactors setup.

3.1.2. Operating conditions for aromatic compound biodegradation studies

Three identical bench scale SBRs (Figure 3-2), with a working volume of 3.0 L, were used in the current study. The first SBR was loaded with 125 g of Filtrasorb 400 granular activated carbon (manufactured by Calgon Carbon Co.) as the carrier medium and was inoculated with 2000 mg L^{-1} of AGS from the halophilic reactor from start-up (Section 3.1.1) to enhance biomass growth on its surface. The second and third reactors were each inoculated with 6000 mg L^{-1} MLVSS AGS from the halophilic reactor from start-up (Section 3.1.1). The settling time for the second and third SBRs was initially set to 30 min. to retain suspended growth in the reactor. After one month of

operation, the settling time was shortened to five minutes. Then all the suspended growth from the third reactor was collected as the activated sludge and the precipitated sludge was discarded as AGS. After the gravity separation of activated sludge from AGS was done, the settling time for activated sludge reactor was reset at 30 minutes again. Thus, the second reactor maintained aerobic granules, while the third reactor consisted of conventional suspended activated sludge (CAS).

The final operation cycle time for reactors 1 and 2 was 12 hours, comprising all SBR phases: anaerobic feeding for 30 minutes, aeration of 680 minutes, settling of 5 minutes, and decanting of 5 minutes (Figure 3-3). The CAS reactor (reactor 3) was operated with the same cycle time of the other SBRs except for the settling time, which was set to be 15 minutes, to retain activated sludge in the reactor. With that change of settling time, CAS reactor cycle time become: anaerobic feeding for 30 minutes, aeration of 670 minutes, settling of 15 minutes, and decanting of 5 minutes. All SBRs were supplied with air at a flow rate of 2.2-liter minute $^{-1}$, and the applied superficial up flow air velocity was 1.1 cm s^{-1}.

During initial operation, all reactors were fed with a synthetic produced water (PW) modeled after that reported in the existing literature (Pendashteh et al. 2012, Sharghi et al. 2014). The inorganic composition of synthetic PW in mM included: $CaCl_2.2H_2O$: 0.41; KCl: 26.8; $MgCl_2.6H_2O$: 0.25; $NaHCO_3$: 9.52; NH_4Cl: 16.1; KH_2PO_4: 0.73; Mg SO_4: 4.15. A trace element solution with mineral composition as shown in Table 3-1 was added at 0.2 ml per liter of final solution. The NaCl concentration was fixed at 85 g L^{-1} throughout the experiment to provide hypersaline conditions.

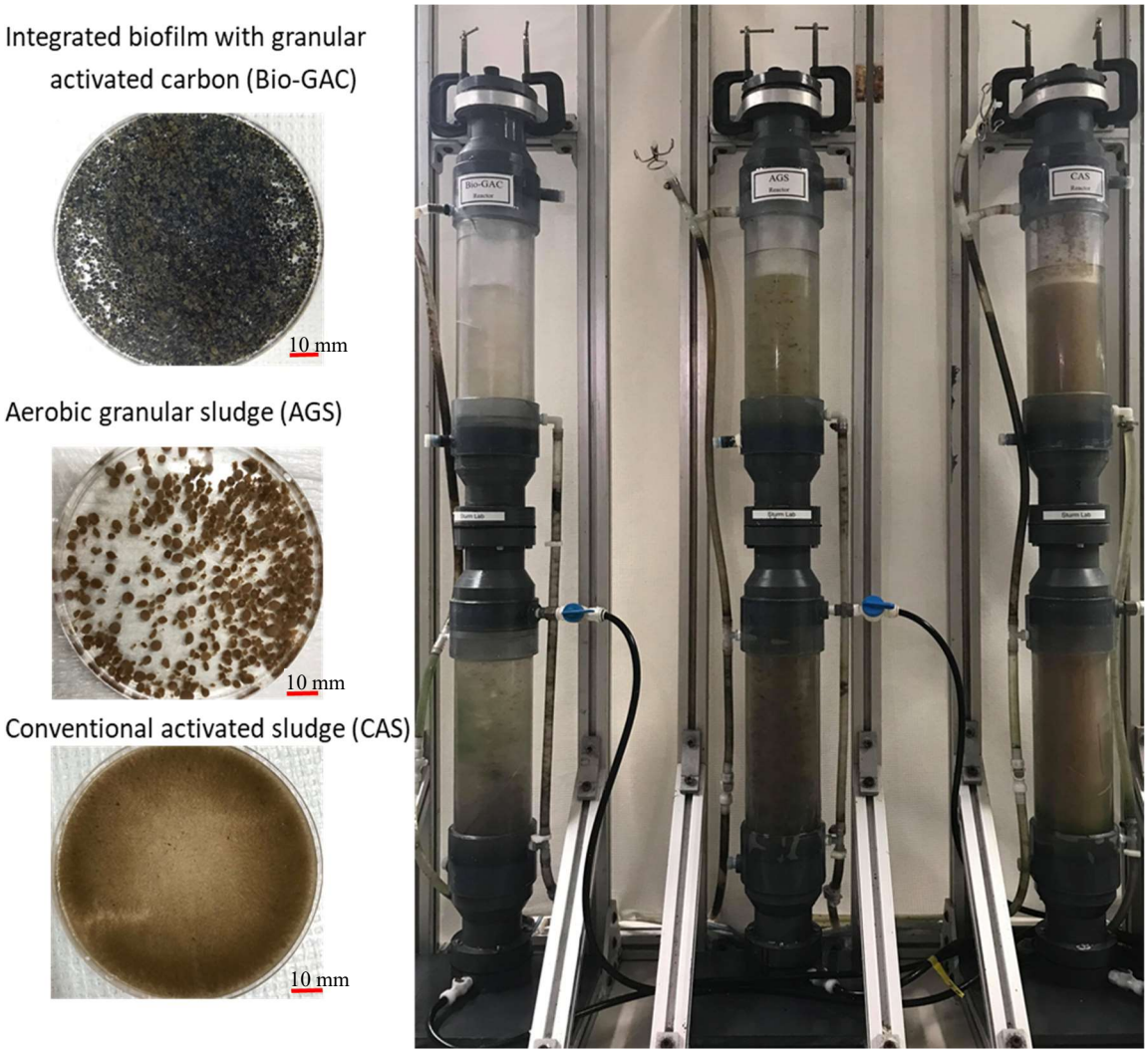

Figure 3-2: Bio-GAC, AGS, and CAS rectors.

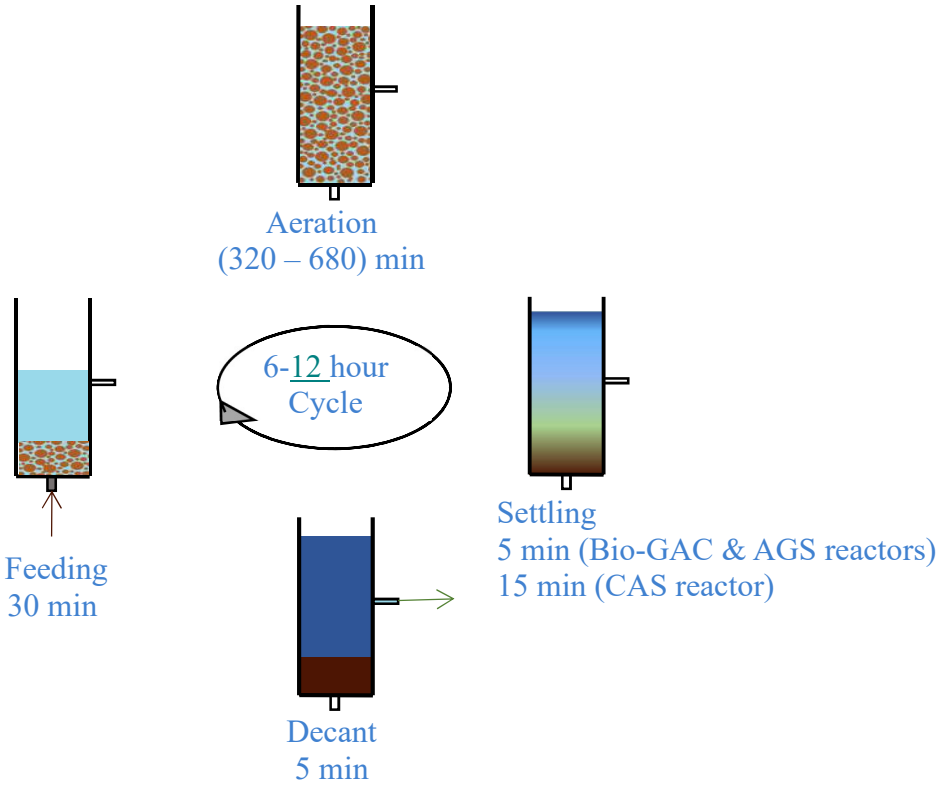

Figure 3-3: Major phases of SBRs operations cycle.

3.1.3. Stimulated biofilm growth on GAC surface

The contact-aggregation strategy suggested by Zhou et al (2015) was applied in this study to stimulate biofilm formation on GAC surface (Figure 3-4). The main idea behind this strategy is that the coexistence of AGS in Bio-GAC reactor during start-up period enhances biofilm growth initiation on GAC surface. During the startup period, the SBR was inoculated with a mixture of 125 g GAC and 2000 mg L^{-1} of AGS acclimated to hypersaline conditions and fed with 1350 mg L^{-1} acetate as the sole carbon source. The development of biofilm on the GAC surface was monitored during the startup period through quantification of deoxyribonucleic acid (DNA) (as described in section 3.6.1). The collected Bio-GAC samples were rinsed by PBS solution three times prior to DNA extraction process to ensure that all AGS and suspended growth were washed out and the taken samples represent grown biofilm on GAC surface only. After 60 days of inoculation, the amount of quantified DNA reached 6 µg of DNA per gram of GAC (Figure 3-5).

At this point, the AGS was washed out by gravity separation, and only GAC remained in the system.

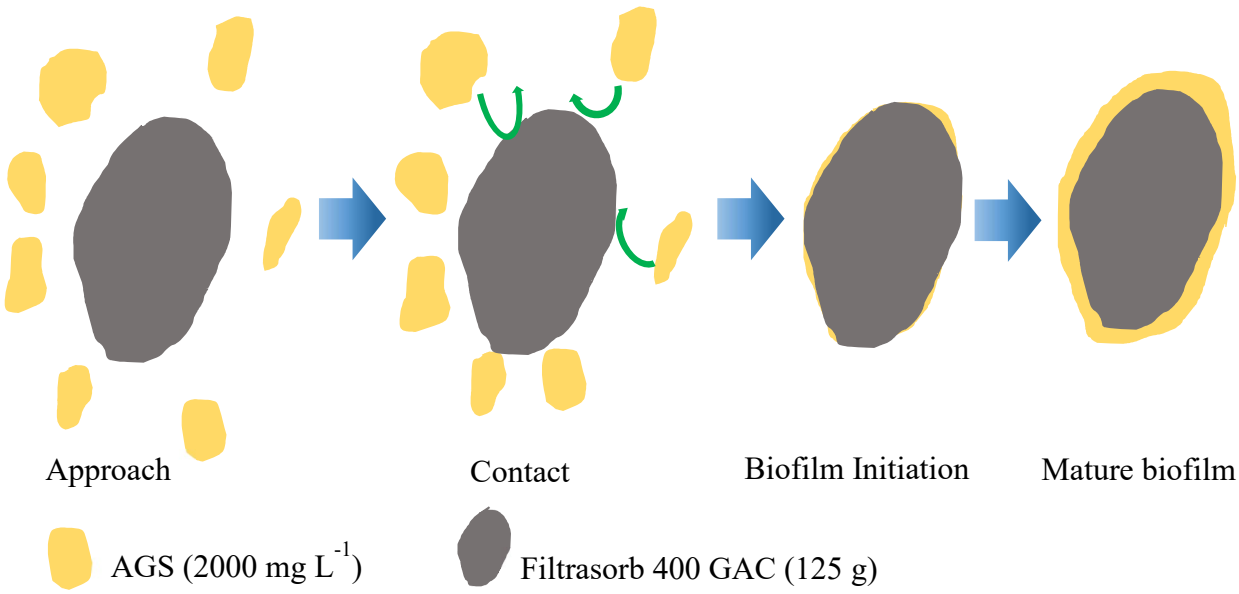

Figure 3-4: Contact-aggregation strategy to enhance biofilm growth on GAC surface.

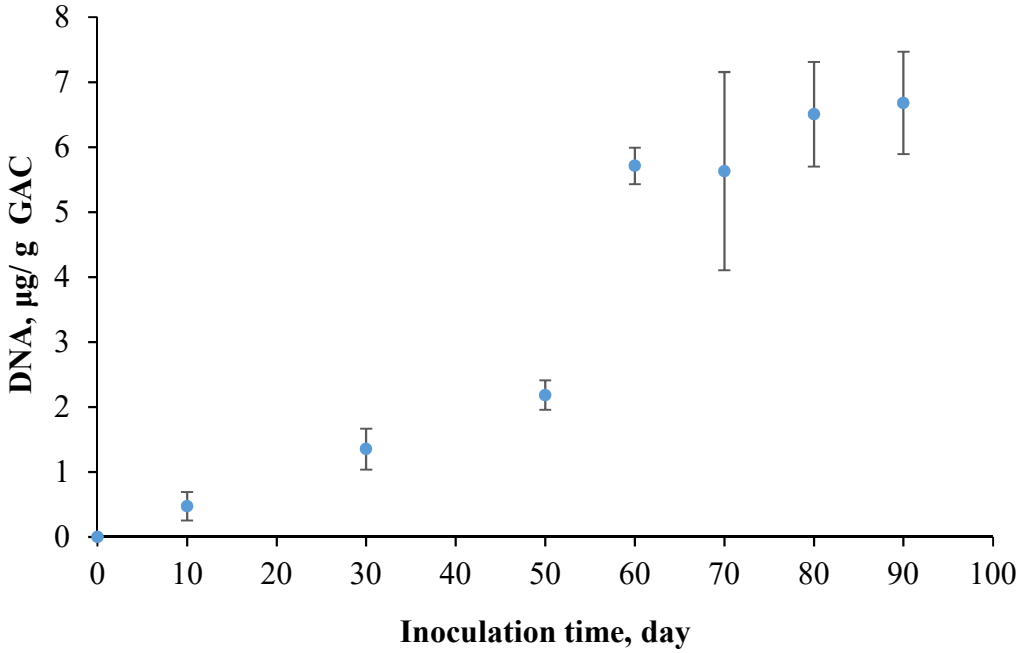

Figure 3-5: Quantification of growing DNA on GAC surface during startup period.

3.1.4. Anaerobic up-flow reactors

Two 4.1-L up-flow anaerobic reactors were operated to investigate the anaerobic process performance under both hypersaline conditions and high aromatic compound loads (Figure 3-6). All reactor dimensions were the same as described in section (3.1.1). The up-flow anaerobic sludge bed reactor (UASB) was seeded for the first time with 6000 mg L^{-1} of anaerobic granular sludge brought from an UASB at operating Water Pollution Control Facility, in the City of Cedar Rapids, IA. The anaerobic granular activated carbon reactor (AnGAC) was loaded with a mixture of Filtrasorb 400 GAC from Calgon Carbon Co., PA. AnGAC also was inoculated with anaerobic granular sludge from the City of Cedar Rapids, IA to enhance biofilm growth. After the biofilm growth on GAC surface was observed using DNA extraction approach, all anaerobic granular sludge was washed out and AnGAC retained in the system. Both reactors were initially operated to study the anaerobic biodegradation of a mixture of toluene and glucose under different salinity levels (Warren 2019). For the current study, both anaerobic reactors were operated to investigate their ability to remove a mixture of aromatic compounds. The salinity of synthetic PW was increased incrementally over 80 days from 30 g L^{-1} at the end of the previous experiment to 85 g L^{-1} (as NaCl) and the carbon source switched from acetate as the sole carbon source to a mixture of aromatic compounds (benzyl alcohol, o-cresol and phenol with concentration of 100, 100 and 250 mg L^{-1}) during the same period of time. The hydraulic retention time for both reactors was maintained at 24 h, and temperature set at 35 ± 1 °C.

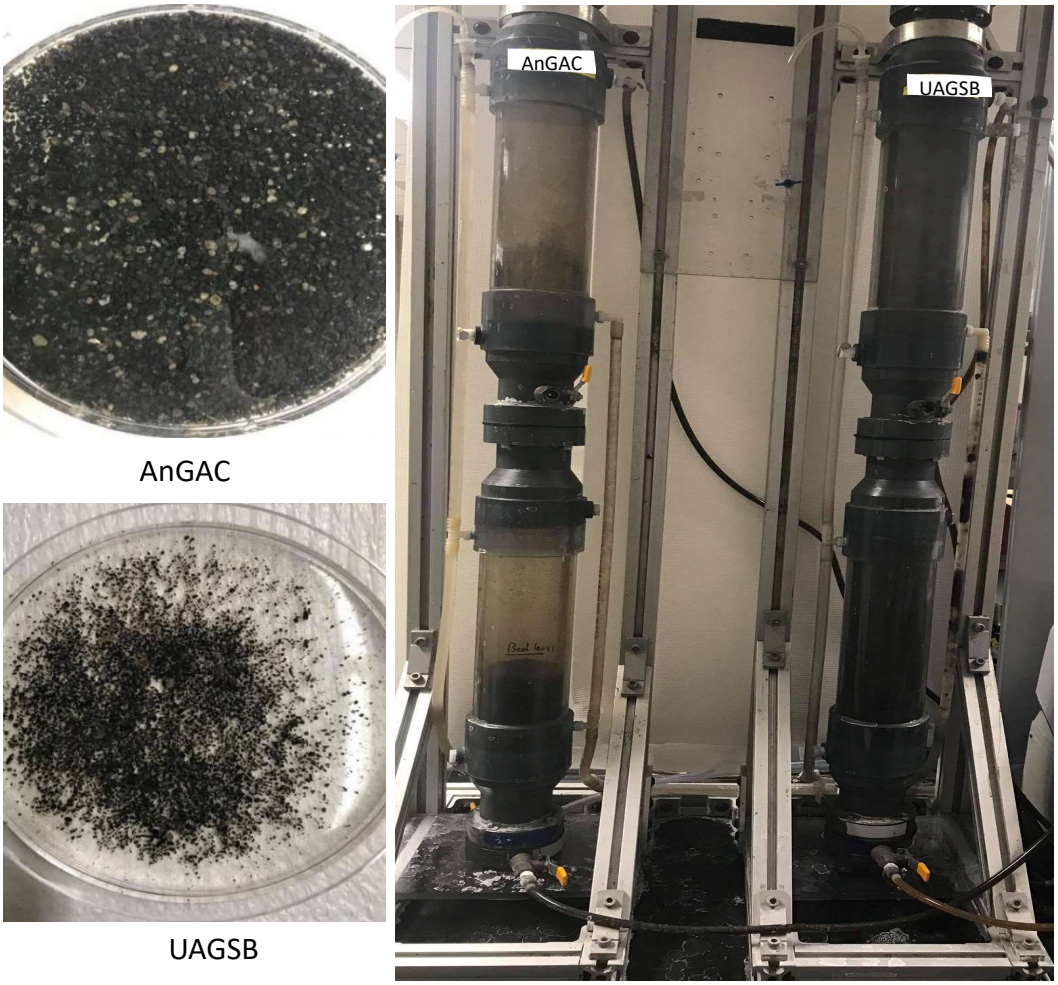

Figure 3-6: Anaerobic up-flow reactors; anaerobic granular activated carbon reactor (AnGAC) (lift) and anaerobic granular sludge reactor (UAGSR) (right).

3.1.5. Synthetic PW composition

3.1.5.1.Acetate based PW

A hypersaline, synthetic produced water modified from previously published PW recipes (Pendashteh et al. 2012, Sharghi et al. 2014) was used as the basis for the reactor influent during these experiments (Table 3-1). Acetate was used as the sole carbon source for the first experiment, with an organic load of approximately 1350 mg COD L^{-1}. The C/N/P molar ratio was adjusted to approximately 100/10/1 by adding NH_4Cl and KH_2PO_4, and a trace element solution was added at 0.2 ml per liter of final solution (Li et al. 2017, Vishniac and

Santer 1957). The NaCl content was increased stepwise over time from 0 g L-1 to 85 g L-1 to adjust salinity.

Table 3-1: Final composition of brine solution used to mimic PW, including trace elements.

Compound	Concentration (mM)	Compound	Concentration (µM)
NaCl	0-1283	$FeCl_3.6H_2O$	11.1
$CaCl_2.2H_2O$	0.41	H_3BO_3	4.85
KCl	26.8	$CuSO_4.5H_2O$	0.24
$MgCl_2.6H_2O$	0.25	KI	0.36
$NaHCO_3$	9.52	$MnCl_2.4H_2O$	1.21
NH_4Cl	16.1	$Na_2MoO_4.2H_2O$	0.50
KH_2PO_4	0.73	$ZnSO_4.7H_2O$	0.83
Mg SO_4	4.15	$CoCl_2.6H_2O$	1.26

3.1.5.2. Aromatic compounds in synthetic PW

A mixture of benzyl alcohol, o-cresol, and phenol was utilized as the carbon source for the three SBRs in the aromatic degradation experiments. Following a 90 day (phase I start-up period) with acetate as the sole carbon source, 20% of the influent acetate was replaced by 100 mg L^{-1} of benzyl alcohol. Then, beginning at 120 days (phase II start-up period), o-cresol was added in a similar manner. 100 mg L^{-1} of o-cresol was added to the influent wastewater and acetate was simultaneously reduced to maintain a constant COD (1200 mg L^{-1}). After 150 days of operation, the remaining acetate was substituted gradually with 250 mg L^{-1} of phenol as shown in Figure 3-7.

3.2. Analytical procedures

Mixed liquor suspended solids (MLSS), mixed liquor volatile suspended solids (MLVSS), and sludge volume index at 5 minutes (SVI_5), were quantified based on Standard Methods (APHA 2005).Other measurements were carried out according to specific procedures as explained below.

3.2.1. Chemical oxygen demand

The COD measurement was used to estimate the total EPS that extracted from MLSS samples in current experimental work. The principles of the COD test are that the organic matter is oxidized by potassium dichromate under acidic conditions using silver sulfate as a catalyst. This

produces an equivalent measure for the required oxygen to oxidize the same amount of organic matter in wastewater. The high chloride content in hypersaline wastewater causes an interference with silver sulfate to form silver chloride and reacts with dichromate to form chromic acid, which could lead to overestimation of COD. To avoid this interference, the chloride content was reduced in wastewater samples prior to conducting the COD test by adding $HgSO_4$ in the molar ratio of 20:1 ($HgSO_4$: Cl^-) to precipitate $HgCl_2$, according to the method proposed by Vyrides and Stuckey (2009).

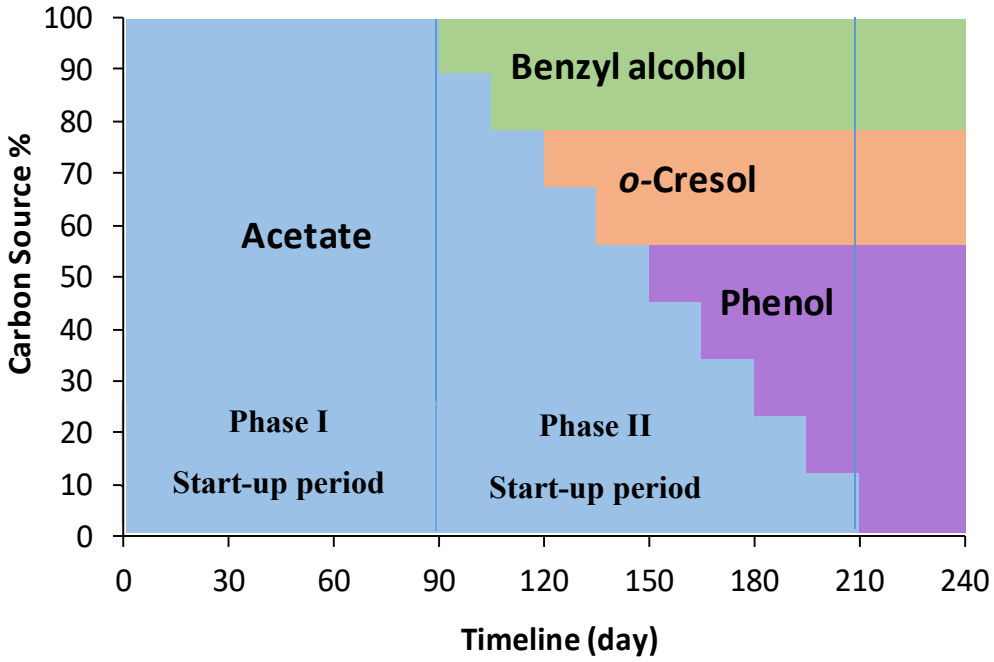

Figure 3-7: Carbon source during startup and operating period.

3.2.2. Extracellular polymeric substances extraction

A significant amount of extracellular polymeric substances (EPS) is expressed by microorganisms to form AGS. EPS is predominantly comprised of proteins and polysaccharides with smaller amounts of nucleic acids, lipids, and humic substances (Felz et al. 2016a). Moreover, EPS can be divided into two groups, tightly-bound (TB-EPS) and loosely-bound (LB-EPS) EPS. These two groups play significantly different roles in the sludge properties. The high fraction of

LB-EPS deteriorates cell adhesion and weaken AGS structure while high TB-EPS content is reported to associate with strong AGS structure and improve sludge settleability and dewaterability (Li and Yang 2007).

EPS was extracted using the heat method suggested by Li and Yang (2007) with some modifications. Representative samples were collected to have volatile suspended solid (VSS) mass between 0.1 and 0.15 g per sample. Then the samples were centrifuged at 4,000 g for 20 minutes at 4°C. The supernatant was discarded and the pellet resuspended into 30 mL of pre heated phosphate buffered saline (PBS) solution (60 °C). The sludge mixture was vortexed for 1 min in a high-speed vortex (3000 rpm), and, immediately centrifuged at 8,000 g for 10 min at 4°C. The supernatant collected from this step was designated as the LB-EPS. The remaining pellet was resuspended again in 30 mL PBS solution and digested in a water bath at 60°C for 30 minutes. The sample was then centrifuged at 10,000 g for 10 minutes at 4°C. The supernatant was collected as the TB-EPS and the pellet stored for further analysis. LB-EPS and TB-EPS were stored at -20 °C to be tested later.

3.2.3. Sludge and EPS digestion for selected anions and cations measurement

The biomass pellet remaining after the TB-EPS extraction step was collected and stored at -20 °C then digested to determine intracellular cation concentrations. A temperature-controlled microwave assisted digestion procedure based on Özsoy (2006) was used to extract selected cations (Ca^{+2}, Mg^{+2}, Na^{+}) from sludge samples. About 0.35 ± 0.1 g of biomass was mixed with 6 mL of nitric acid and 2 mL of hydrochloric acid and added to an Anton Paar Multiwave PRO microwave digestion unit. The mixture was heated to 170 ˚C over 10 minutes, and then held at that temperature for an additional 10 minutes, followed by 17 minutes heating at 70 ˚C. Digested samples were diluted to 100 mL with deionized water, filtered through a 0.45 µm PTFE filter, and stored at 4°C to be analyzed later.

The same microwave assisted digestion procedure was applied on extracted EPS samples. All samples were diluted with Milli Q water at a ratio of 1:10 and mixed with 2 mL of nitric acid and 0.5 mL of hydrochloric acid to make a final volume of 22.5 mL. Then, the digested EPS was filtered through a PTFE 0.45 µm syringe filter and stored at 4 ˚C. The concentration of selected cations in digested sludge and EPS samples was detected using inductively coupled plasma – optical emission spectrometry (ICP-OES, PerkinElmer, Optima 2000 DV).

3.2.4. Alginate-like exopolysaccharides extraction

Alginate-like exopolysaccharides (ALE) are considered the dominant exopolysaccharides in AGS and play a crucial role in establishing hydrogel properties of AGS, which improve AGS formation under harsh conditions (Lin et al. 2013a). The ALE fraction of the TB-EPS was isolated according to the method proposed by Felz et al. (2016a) as the sodium form of ALE. For ALE extraction, the collected pellet after the LB-EPS extraction step was resuspended in 50 mL of MQ containing 0.25 g Na_2CO_3 anhydrous, covered with aluminum foil to avoid evaporation and heated in a water bath to 80 ˚C with continuous stirring at 400 rpm for 35 min. Then the mixture was centrifuged at 400 g and 4 ˚C for 20 min. The supernatant was then collected in a dialysis bag with a 3500 Da molecular weight cutoff and let stir in 900 mL of Milli Q water for 12 hours. After 12 hours, the Milli Q was replaced with fresh solution to enhance the effect of the dialysis. After 24 h dialyzation, the acidic form of ALE was obtained by adjusting the pH of the dialyzed extract to 2.2 ± 0.05 using 1 M HCl. After adjusting the pH, the extract was transferred into a 50 mL centrifugation tube and centrifuged at 4000 g and 4 ˚C for 20 min. After the supernatant was discarded, the gel-like pellet was collected and exposed to a pH 8.5 solution (using 0.5 M NaOH) to obtain the sodium form of ALE. The extracted ALE was quantified by a phenol-sulfuric acid assay using sodium alginate as a standard (Dubois et al. 1956).

3.2.5. EPS extraction from biofilm on GAC

Three methods for biofilm detachment were examined in this study: grinding in a mortar and pestle, sonication at 25 W for a specific time range using a Branson Digita Sonifier (Model SSE-1) equipped with a 1/8" microtip, and bead beating for 2 hours at 30°C, 200 rpm, and three different bead to GAC ratios (Table 3-2). The presence of soluble DNA was used as an indicator of cell lysis, so the optimum method is the one that achieves maximum EPS production with minimum detected DNA. Grinding for two minutes and sonication for two minutes had the highest EPS production compared to other detachment methods (2.1 mg EPS/ g GAC). The application of these two methods also did not cause a significant increase in detected DNA. Therefore, the suggested method is to grind the sample in a mortar and pestle for 2 minutes, followed by sonication at 25 W for 2 minutes as well. This developed method was applied on all studied samples as an optimum detachment method prior to EPS extraction procedure. EPS extraction from detached biofilm was carried out according to the heat method described by Li and Yang (2007).

Table 3-2: The optimized biofilm detachment methods

Method description	Method ID	Time/ ratio	DNA, ng/ g GAC	EPS, mg/ g GAC
Grinding in a mortar and pestle	G_1	1 min.	3.5 ± 0.5	0.60 ± 0.11
	G_2	2 min.	4.1 ± 0.3	1.04 ± 0.04
	G_3	3 min.	6.0 ± 0.4	1.08 ± 0.03
Sonication @ 25 W for diff. times	S_1	1 min.	5.1 ± 0.3	1.05 ± 0.07
	S_2	2 min.	5.8 ± 0.2	1.16 ± 0.05
	S_3	3 min.	60.4 ± 4.5	1.47 ± 0.03
Bead beating 2 h @ 30 °C, 200 rpm, Bead: GAC	B_1	0.5:1	75.2 ± 8.6	0.45 ± 0.04
	B_2	1 to 1	56.6 ± 7.4	0.50 ± 0.02
	B_3	2 to 1	74.8 ± 9.2	0.62 ± 0.08
Grinding in a mortar and pestle for 2 min. followed by sonication @ 25 W for 2 min.	G_2S_2	2 min.	5.9 ± 0.4	2.10 ± 0.03

3.2.6. MLVSS quantification in GAC samples

The assessment of mixed liqueur volatile suspended solids in GAC samples is an unconventional test because of losses in GAC itself due to burning at 550 °C. Consequently, there will be over estimation in MLVSS values unless this loss is accounted for. Ten samples of fresh GAC were used to standardize the losses due to burning (Table 3-3). GAC samples were rinsed gently three times with tap water to wash out dust and very small particles that could be burned out on the furnace. Then, a specific amount of GAC was transferred to a known weight metal dish and put in the drying oven at 105 °C overnight. The dried GAC samples were weighed after cooling and then burned at 550 °C for 15 minutes. The final weight was measured to assess the losses in GAC samples due to burning according to equation 3-1. The average losses and standard deviation of tested samples were 4.1 % and 0.36 % respectively. Based on this finding, a 4.1 % loss was considered for the GAC when the MLVSS content was measured for all GAC samples.

$$Lossess\ due\ to\ burning\ \% = \left(\frac{\text{Dry weight} - \text{Burned weight}}{\text{Dry weight}}\right) \times 100 \ldots\ldots\ldots\ldots\ldots\ Eq.(3-1)$$

Table 3-3: The optimized biofilm detachment methods.

Sample #	Dish Wt., g	Dish+ Dry Wt., g	Dish+ Burned Wt., g	Losses %
1	1.004	5.6046	5.4179	4.06
2	1.0206	6.3557	6.1071	4.66
3	0.9956	5.2014	5.0433	3.76
4	1.0354	5.3893	5.1871	4.64
5	1.005	5.3261	5.1389	4.33
6	1.0375	4.8028	4.6329	4.51
7	1.0065	4.7737	4.6373	3.62
8	1.0174	5.3008	5.1348	3.88
9	1.0014	6.0263	5.8212	4.08
10	1.0393	5.5952	5.4203	3.84
Average % =				4.14
Standard deviation =				0.36

3.2.7. GAC adsorption capacity and related isotherms

To determine the aromatic compounds adsorptive capacity of Filtrasorb 400 GAC, an isotherm study was conducted. Four sets of sealed 250 mL batch reactors were filled with 100-1000 mg of GAC, and 1000 mg L^{-1} of either benzyl alcohol, o-cresol, or phenol dissolved in the same synthetic PW that used to feed SBRs. All samples were allowed to shake at 150 rpm for 24 hours at 21±1 °C. A control reactor with no GAC was used to account for aromatic losses due to volatilization or sorption to the reactor surface. Samples from each reactor were filtered through 0.45 μm glass-fiber filters and analyzed to determine aqueous phase aromatic concentrations, with the mass of adsorbed compound determined by difference. The Freundlich model (Eq 3-2 and 3-3) was the best fit to the resulting isotherms (Figure 3-8).

$$log\ q_e = \log K + \frac{1}{n}\log C \ldots\ldots\ldots\ldots\ldots\ Eq.(3-2)$$

$$q_e = \frac{x}{m} \ldots\ldots\ldots\ldots\ldots\ldots\ldots\ldots\ldots\ldots\ldots\ldots eq.(3-3)$$

Where:

x = mass of adsorbate (mg).

m = mass of adsorbent (g)

q_e = maximum adsorption capacity (mg. g^{-1})

K = a constant that indicates the relative adsorption capacity of the adsorbent ($mg^{1-(1/n)}\ L^{1/n}\ g^{-1}$).

n = a constant indicating the intensity of the adsorption.

C = equilibrium concentration of adsorbate in solution (mg L^{-1}).

Breakthrough curves for GAC treating mixed and/ or individual compounds were also determined by batch experiments. The purpose of this experiment was to estimate the maximum loading of aromatic compounds that can be adsorbed on GAC surface before it is exhausted. Three sets of sealed 160 mL batch reactors were inoculated with 1 ± 0.1 g GAC (Figure 3-9). The control reactor, which had no added GAC, was also used to account for any losses in aromatic compounds concentration during the experiment. All four reactors were filled with synthetic PW containing a mixture of aromatic compounds as benzyl alcohol, o-cresol, and phenol with concentration of 100,

100, and 250 mg L^{-1}. The same procedure was applied on batch reactors containing the same amount of fresh GAC and fed with a single compound of studied aromatics in concentration of 450 mg L^{-1} of each individual compound. All reactors were shaken at 150 rpm and 21±1 °C for 24 h then 10 mL aqueous samples were taken and the rest of the solution was replaced with fresh synthetic wastewater. All taken samples filtered immediately through 0.45 µm glass-fiber filters and analyzed to determine aqueous phase aromatic concentrations. This experiment was stopped when the detected concentration of aromatic compounds was equal to the feed concentration. Figure (3-10) demonstrates the breakthrough time for the mixture and individual aromatic compounds. It is observed that the GAC samples were saturated with benzyl alcohol faster than other aromatic compounds. The observed adsorption capacities were 566, 530.5, 441.3 and 589.5 mg g^{-1} for the mixture, phenol, benzyl alcohol and o-cresol respectively.

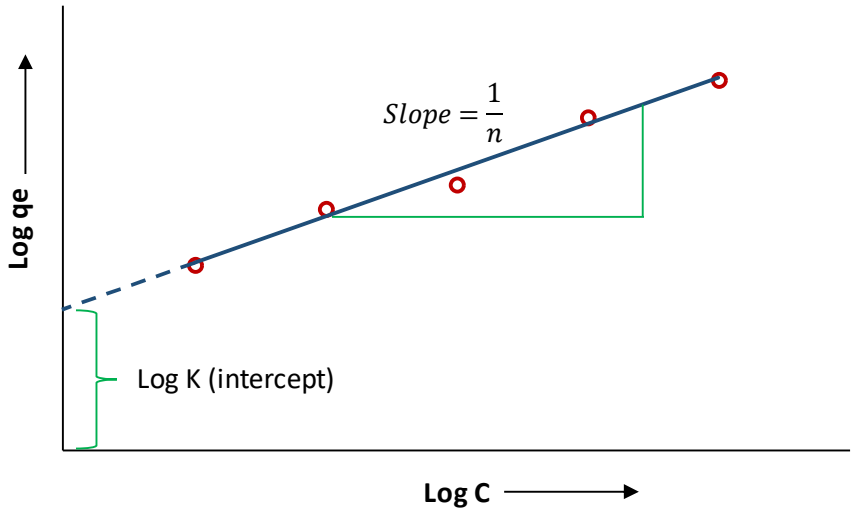

Figure 3-8: Freundlich adsorption isotherm.

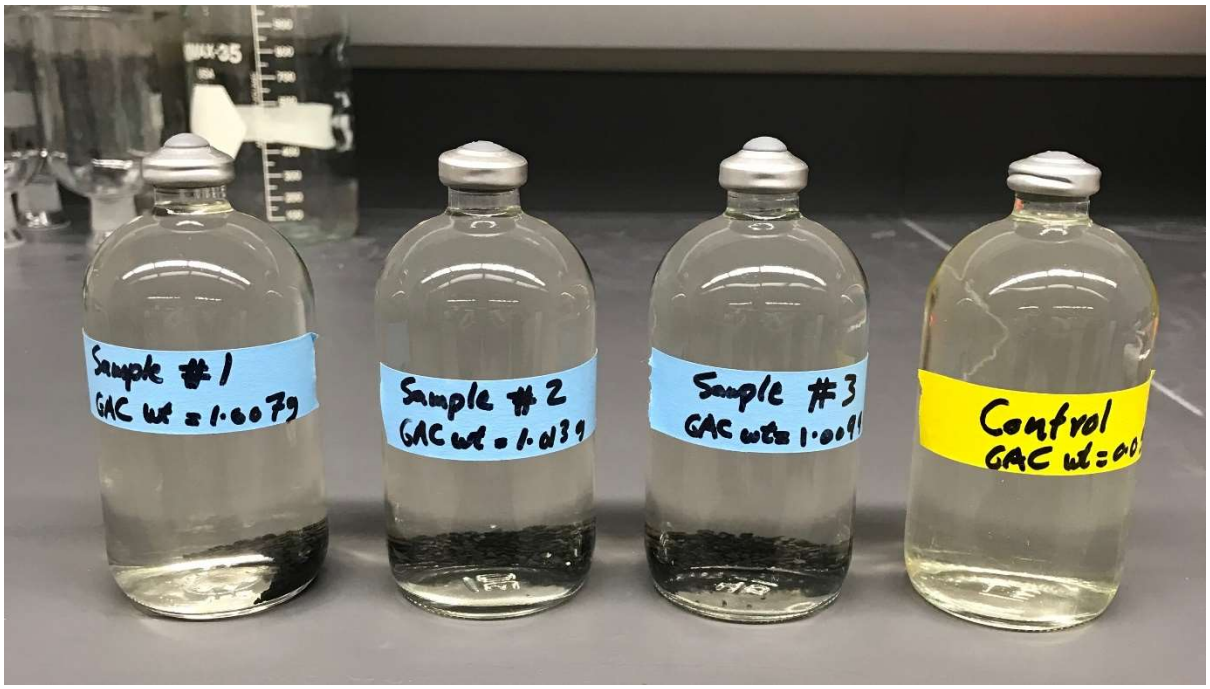

Figure 3-9: Breakthrough batch experiment reactors.

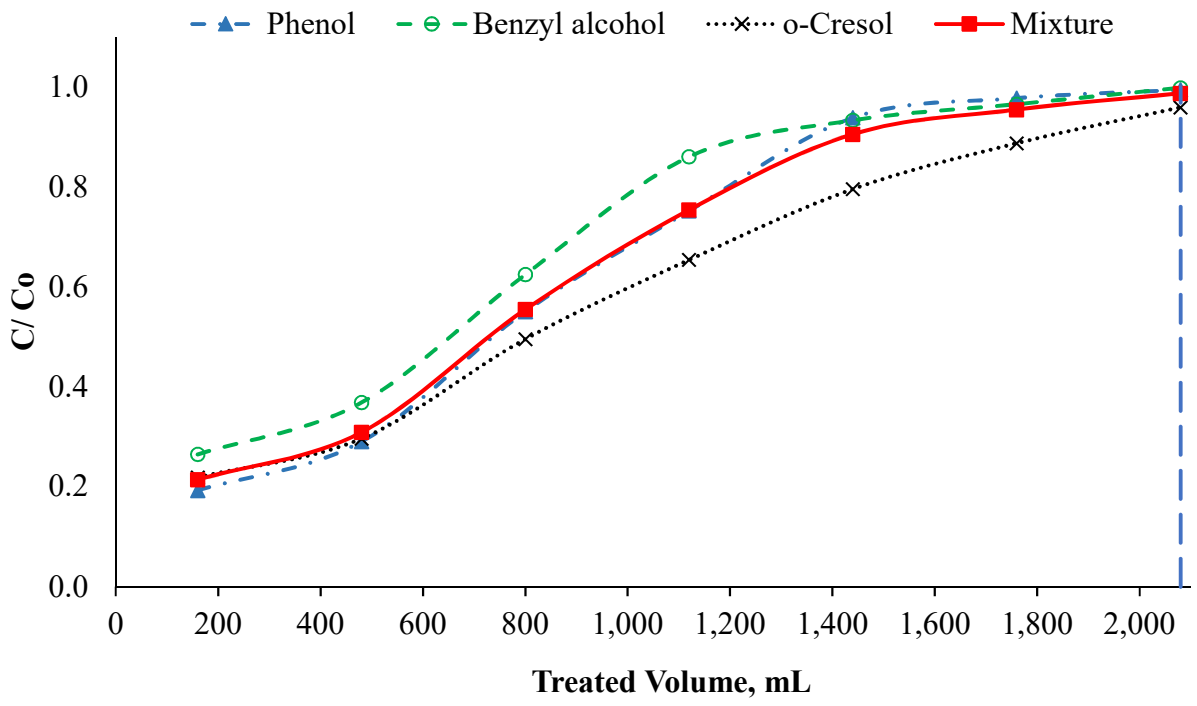

Figure 3-10: Breakthrough curves for mixture and individual aromatic compounds.

3.2.8. Specific oxygen uptake rate

Specific oxygen uptake rate (SOUR) was utilized to observe the impact of aromatic compounds on the activity of microorganisms based on oxygen consumption. A synthetic brine solution was prepared with either a mixture of benzyl alcohol, o-cresol, and phenol with concentrations of 100, 100, 250 mg L^{-1} respectively, or with each individual aromatic compound at a concentration of 450 mg L^{-1}, was used as the carbon source in this experiment. The SOUR experiment was conducted according to Standard Methods (APHA 2005). AGS, Bio-GAC, or CAS samples were aerated for 30 min prior to the test. The brine solution was also aerated to increase dissolved oxygen (DO) level in solution. An airtight 300 mL bottle was filled with wastewater then inoculated with a known amount of biomass. The DO probe was inserted into the bottle, and the DO level was monitored over 15 min or until no change was detected in the DO level. The collected data was used to plot DO versus time. Oxygen uptake rate (OUR) was calculated as the slope of the linear part of the DO reduction curve. Afterward, SOUR was calculated using the measured sample VSS according to equation (3-4).

$$SOUR\left(\frac{mg\ O_2}{g\ VSS\ h}\right) = \frac{measured\ OUR\left(\frac{mg}{L}\cdot\frac{1}{h}\right)}{VSS\ (g)} \dots\dots\dots\dots\dots\dots\dots\ Eq.(3-4)$$

Where:

SOUR= specific oxygen uptake rate.

OUR= oxygen uptake rate.

VSS= volatile suspended solids

3.2.9. Specific substrate uptake rate

In order to evaluate the resilience of biomass from the aerobic and anaerobic processes under high concentrations of aromatic compounds, comparative batch cultivations were carried out under controlled operation conditions. Aerobic batch reactors were allowed headspace for aeration, while anaerobic batch reactors were sealed without headspace to avoid interruption of

anaerobic conditions via surface aeration. Four separate batch tests, one for each reactor, were performed to assess the specific substrate uptake rate from four separate carbon sources. Each batch test consisted of four bottles containing 160 mL of synthetic PW, dosed with 450 mg L^{-1} of either benzyl alcohol, o-cresol, phenol, or a mixture of all of these compounds as depicted schematically in Figure (3-11). The mixture of the compounds was comprised of 250, 100 and 100 mg L^{-1} of phenol, benzyl alcohol and o-cresol, respectively, to represent the load of the bench scale reactors. For the sludge-based reactors, each test was inoculated with 3000 mg L^{-1} of AGS (as MLVSS) to mimic the same food to microorganism ratio in the AGS bench-scale reactor. For the GAC-based reactors, each test was loaded with 6.5 g of GAC, to simulate the same ratio of GAC weight to reactor volume as the Bio-GAC bench-scale reactor.

All batch reactors were allowed to shake at 150 rpm for 24 hours. The aerobic batch sets were shaken at 21 ± 1˚C, and the aerobic batch reactors were shaken at 35 ± 1˚C. Representative samples from each reactor were collected hourly for 18 hours, filtered through 0.45 µm glass-fiber filters, extracted using SPE method and analyzed using GC to determine aqueous phase aromatic concentrations. The mass of biodegraded compounds was determined from the differences between the initial and residual concentrations. The specific substrate uptake rate for each compound and for each type of biomass was calculated by applying Eq. (3-5).

$$\frac{dM_s}{dt} = q_s M_x \dots\dots\dots\dots\dots (3-5)$$

Where:

dMs: Biodegraded substances (mg L^{-1}).

dt: Biodegradation time (h).

qs: Specific substrate uptake rate (mg h^{-1} g^{-1} MLVSS).

Mx: Biomass concentration (g L^{-1} as MLVSS).

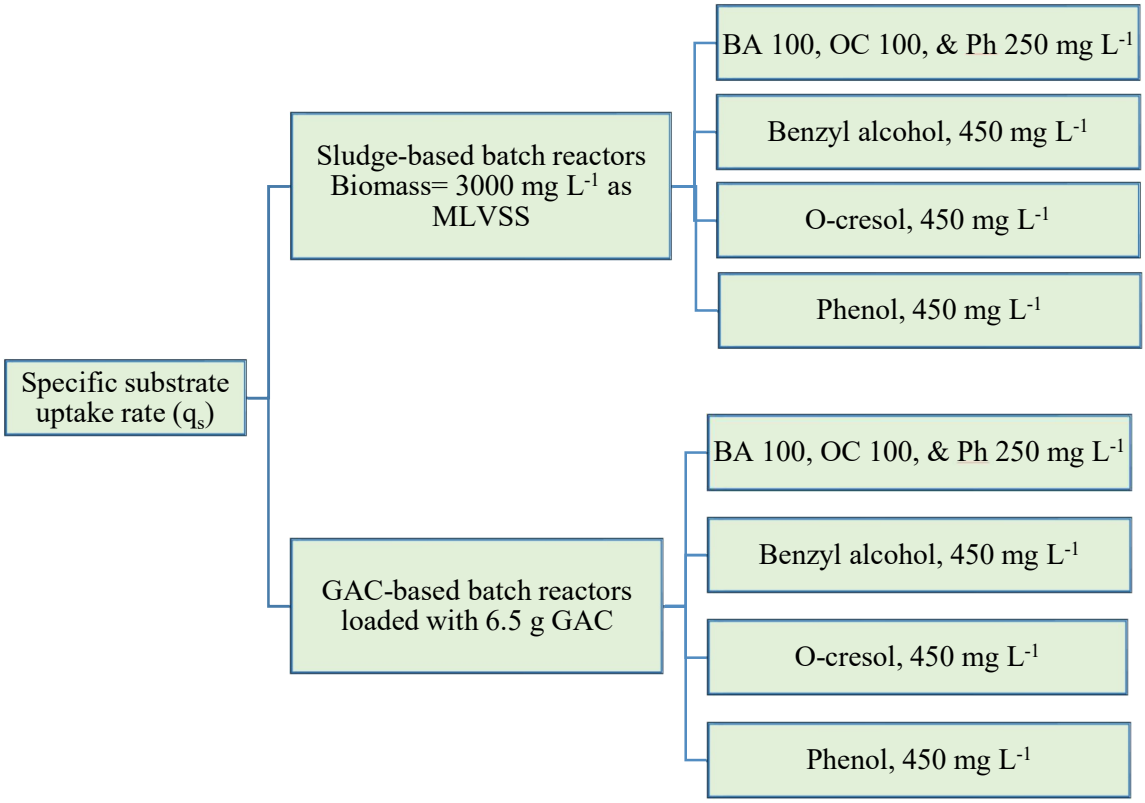

Figure 3-11: Batch experiment design flow diagram.

3.2.10. Microscopic observation

3.2.10.1. Image analysis

Image analysis was applied on AGS samples in order to monitor AGS morphology in terms of mean size, aspect ratio, and the distribution of granules size during the study period. This analysis is important because it gives a quick assessment for the impact of salinity or any other treatment on AGS structure. A stereomicroscope (Fisher Scientific) was used to visualize granules twice a week during AGS formation experiment. The average granule diameter and aspect ratio were analyzed using Fiji image software (https://imagej.net/Fiji).

3.2.10.2. Scanning electron microscopy analysis

The impact of substitution of acetate as the sole carbon source by a mixture of aromatic compounds on biofilm morphology was assessed visually using scanning electron microscopy (SEM) analysis. Representative samples from the AGS and Bio-GAC reactors during the aromatic

degradation experiments were collected after each aromatic compound had been introduced into the treatment system. Fixation and wash steps were applied on collected samples according to a procedure proposed by Bassin et al. (2012) and Dernburg (2012) with some modification. Collected samples were fixed overnight with 4% paraformaldehyde in PBS solution at 4 °C. Three gentle washing steps, 10 min duration for each step, were performed with PBS solution followed by three steps post fixation with osmium tetroxide 1% in cacodylate 0.1 M, 10 min for each step. Then, samples were dehydrated gradually (10 min for each step) using stepwise increased ethanol solutions (10%, 30%, 50%, 70%, 90%, and 100%). Hexamethyldisilazane reagent was used to remove liquids from samples instead of critical point drying in this study. The dehydrated samples were immersed in hexamethyldisilazane solution for 20 min as depicted in Figure 3-12. Finally, fixed and dried samples were coated with 10 μm of gold powder using an EMS150R S compact rotary sputter coater and mounted on studs, then loaded to FEI VERSA 3D dualbeam field emission/ low vacuum scanning electron microscopy at the University of Kansas/ the Microscopy and Analytical Imaging Research Resource Core Laboratory (MAI) , Lawrence, KS.

3.3. Volatility, biosorbtion, and biodegradation assessment

The volatility, biosorption, and biodegradation of each of the aromatic compounds in contact with aerobic halophilic granules were investigated using three sets of batch reactors (Figure 3-13). These reactors were filled with 2 liters of PW containing either benzyl alcohol, o-cresol, or phenol as the only carbon source and injected with air at a rate of 2.2 Liters per minute. The first reactor contained only the aromatic solution without adding any microorganisms, to account for compound losses through volatilization. The second set of reactors was inoculated with inactivated or fixed microorganisms to assess aromatic compound biosorption on the reactor biomass. A fixation protocol adapted from the SILVA FISH procedure was applied to preserve biofilm morphology and to stop all microbial biotic activity (Dernburg 2012). Representative samples were

taken from Bio-GAC, AGS, and CAS reactors individually, fixed, and then washed three time gently with PBS solution prior to the batch experiment. The third set of reactors was inoculated with active biomass with the same mass concentration as the inactivated reactors. The purpose of running this batch reactor is to assess the biodegradation of the selected aromatic compounds.

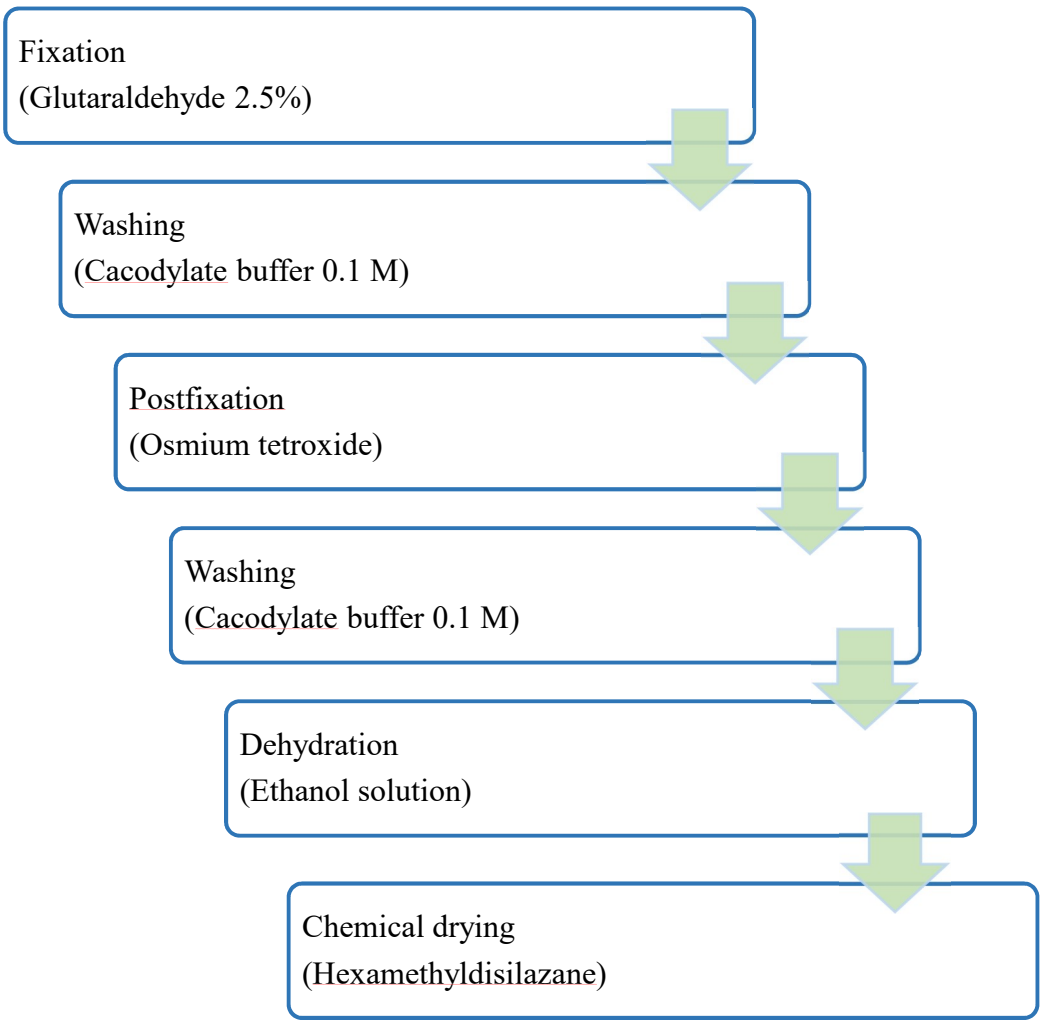

Figure 3-12: Preparation steps applied on collected samples prior to SEM observation.

Figure 3-13: Batch reactor setup to assess volatility, biosorption, and biodegradation.

3.4. Aromatic compound detection

3.4.1. Solid phase extraction for aromatic compounds

Bond Elut Jr Plexa, 200 mg cartridges were used to extract aromatic compounds from wastewater samples according to the procedure suggested by Kovács et al. (2011). SPE cartridges were conditioned with 5 mL of each of acetone followed with 5 mL methanol and, then washed with 5 mL MilliQ water prior to the elution step (Figure 3-14). The cartridges were never allowed to run dry during the conditioning process. 100 mL of diluted sample was passed through the cartridge at a maximum rate of 3 drops/ second. Following this step, the cartridge was dried with air for at least 2 min. 5 mL of acidified acetone with acetic acid (1:100) was then used to elute samples. The collected samples were spiked with 50 µL of 600 mg L^{-1} chlorodecane solution prior to inject into an Agilent 7890B Gas Chromatograph (GC) for analysis. The following parameters were manipulated to run the GC: column type Agilent 19091S-433UI, initial temperature setpoint 40 ˚C, and max temperature 300 ˚C. Selected ion monitoring mode (SIM) was used for quantitative

purposes. All other applied parameters are shown in Appendix B. Benzaldehyde, phenol, benzyl alcohol and o-Cresol peaks appeared at 7.4, 8.4, 8.9 and 9.5 minute. The internal standard (chlorodecane) peak appeared at 12.8 minute (Figure 3-15).

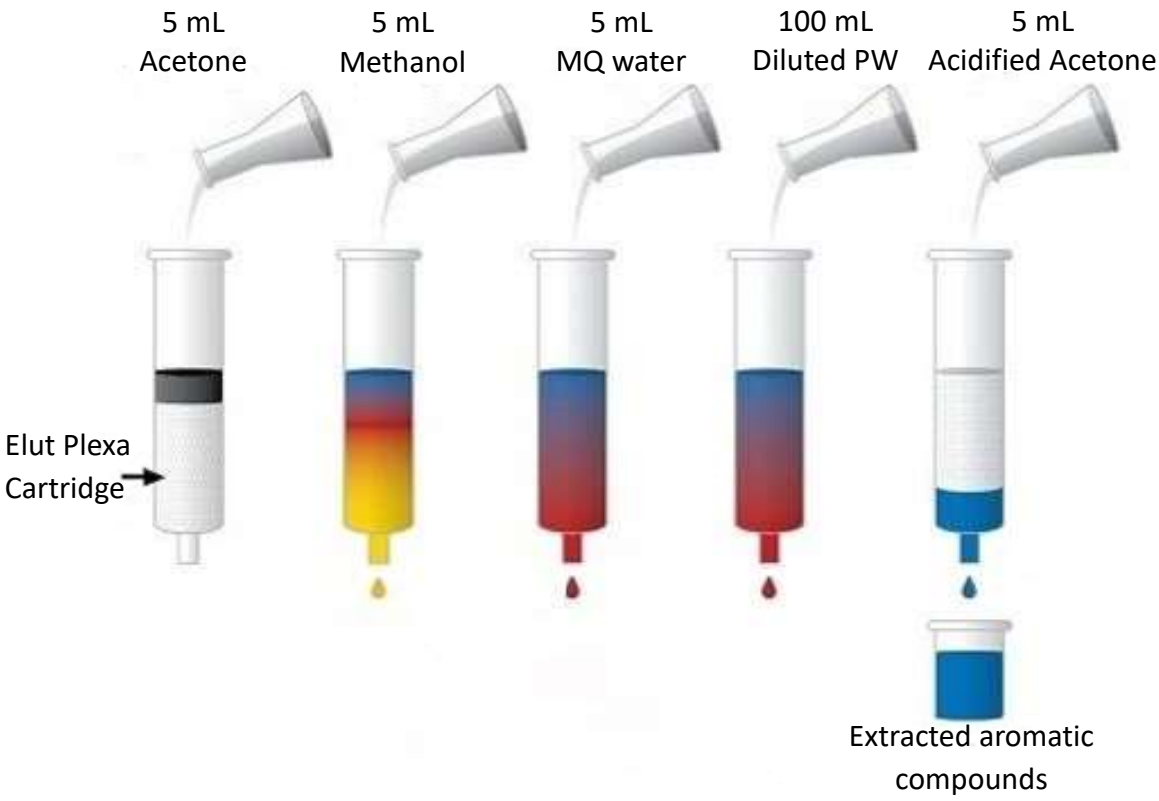

Figure 3-14: Solid phase extraction steps.

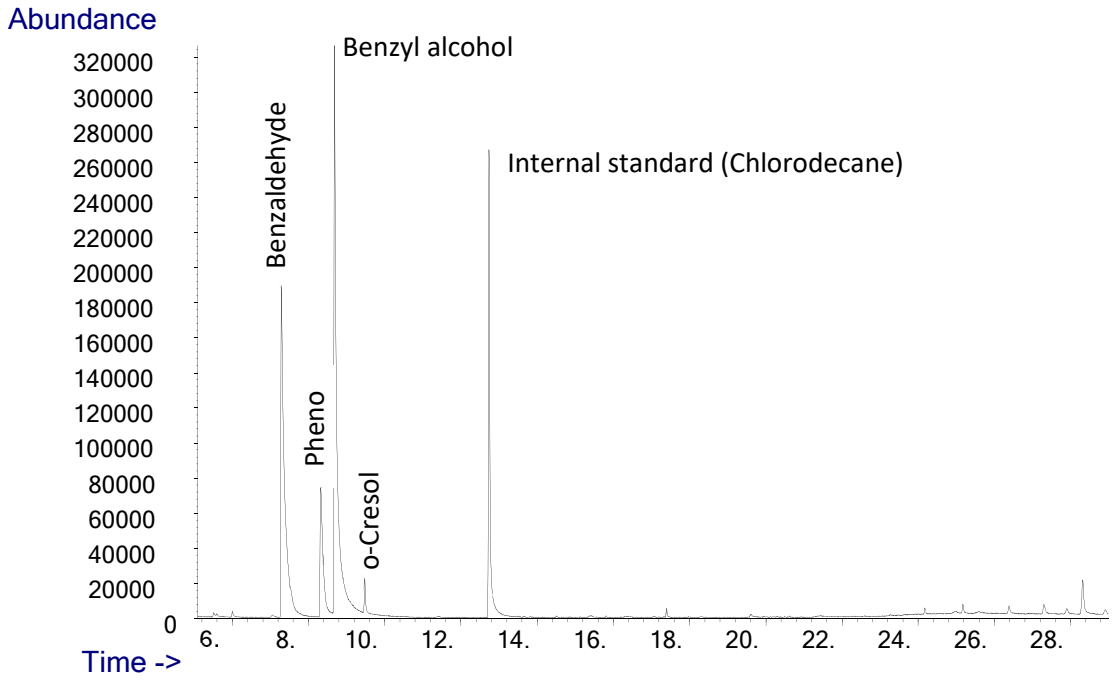

Figure 3-15: Detected aromatic compounds by GC; Benzaldehyde (7.4 min), phenol (8.4 min), benzyl alcohol (8.9 min), o-cresol (9.5 min) and chlorodecane (12.8 min).

3.4.2. Colorimetric method for catechol detection

A gold nanoparticles (AuNPs) based colorimetric method was used in current research to quantified catechol in synthetic PW. This method was proposed for the first time by Keshvari and Bahram (2017). This method relies on the fact that the presence of 4-mercaptophenylboronic acid (MPBA) in aqueous solution enhances AuNPs aggregation, which give blue color for solution. As the catechol concentration increases in solution, the color of solution changes from blue to wine red because the presence of catechol alters the interaction between MPBA and AuNPs and thus lightens AuNPs aggregation. Manufacturer synthesized 20 nm AuNPs and (MPBA) were purchased from Fisher Scientific™. A Shimadzu UV–Visible spectrophotometer model UV-1650PC was used to collect UV-Vis absorption spectra for selected samples. Initial tests showed that the elevated chloride concentration can cause interference with the catechol detection test. Therefore, all tested samples were passed through Dionex™ OnGuard™ II Ag/H 2.5 cc cartridges

to reduce chloride content prior to catechol quantification. The concentration of catechol in solution was then assessed by calculating the ratio of absorbance value at 525 nm to that at 725 nm as shown in Figure (3-16). Five concentrations (0, 0.25, 0.5, 0.75 and 1 mg L^{-1}) of catechol were selected to plot a catechol standard curve as shown in Figure 3-17.

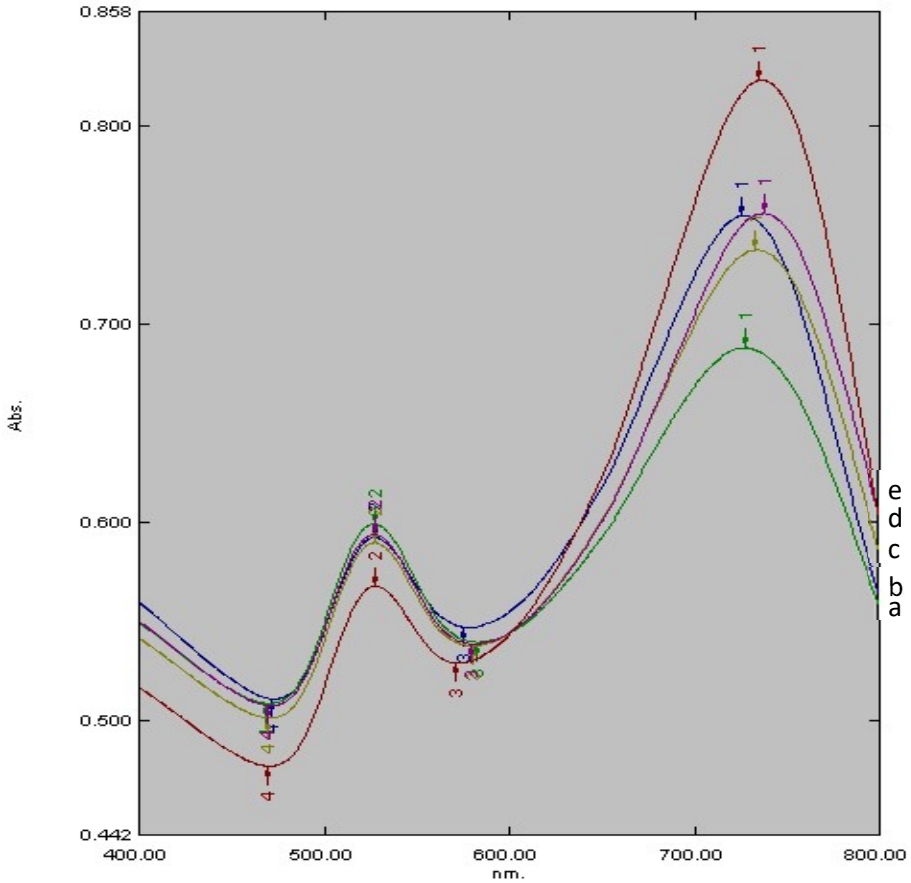

Figure 3-16: UV-Vis absorption spectra of samples with known catechol concentration: 0.1 mg/ l catechol (a), 0.25 mg/ l catechol (b), 0.3 mg/ l catechol (c), 0.75 mg/ l catechol (d) and 1.0 mg/ l catechol (e).

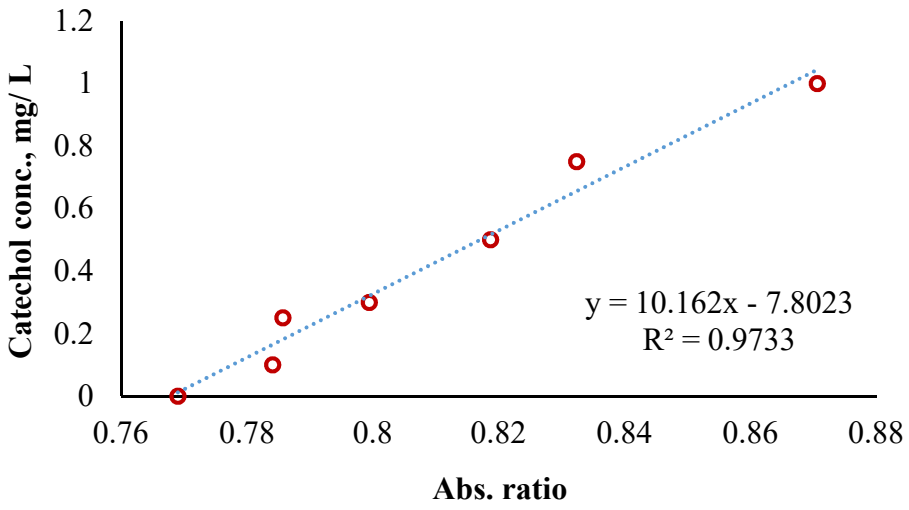

Figure 3-17: Catechol standard curve.

3.4.3. Extraction method detection limit

The SPE method detection limit (MDL) was estimated based on the method suggested by USEPA (2016) for all studied aromatic compounds. Ten samples of known concentration for each compound were analyzed using the GC and the acquired data was used to calculate the MDL according to equation (3-6). The analysis showed that the MDL were 0.28, 0.19, and 0.34 and 0.3 mg L^{-1} for benzyl alcohol, o-cresol, phenol and benzaldehyde respectively. All calculation details are shown in Table (3-4).

$$MDL = t_{(n-1,1-\alpha=0.99)}S_s \ldots\ldots\ldots\ldots\ldots Eq.(3-6)$$

Where:

MDL= the method detection limit.

$t_{(n-1,\ 1-\alpha=0.99)}$= the Student's t-value with n-1 degree of freedom and a single-tailed 99th percentile *t* statistic.

S_s= standard deviation for tested samples.

Table 3-4: MDL calculations for benzyl alcohol, o-cresol, and phenol.

Sample No.	Benzyl alcohol, mg L^{-1}	o-Cresol, mg L^{-1}	Phenol, mg L^{-1}	Benzaldehyde, mg L^{-1}
1	1.07	0.83	1.05	1.25
2	1.00	1.00	1.07	1.15
3	1.08	0.96	1.18	1.23
4	0.91	1.05	0.87	1.35
5	1.03	1.07	1.11	1.20
6	0.83	1.06	0.85	0.98
7	1.09	0.96	1.05	1.15
8	0.95	0.99	0.88	1.10
9	1.16	1.06	1.12	1.25
10	0.88	1.03	0.83	1.35
Std Dev. (*S*)=	0.10	0.07	0.12	0.11
n=	10	10	10	10
d.f.=	9	9	9	9
α=	0.01	0.01	0.01	0.01
t=	2.821	2.821	2.821	2.821
MDL	0.28	0.19	0.34	0.30

3.5. X-ray photoelectron spectroscopy analysis

X-ray photoelectron spectroscopy (XPS) was used in this research to observe aromatic compounds biosorption on, and loss from, the biomass (Figure 3-18) during the aerobic and anaerobic biodegradation studies. Samples collected from the SBRs were dried under low temperature (30 °C) to avoid aromatic compounds evaporation. Drying of the AGS samples required about 5 hours (Figure 3-19), while less time was needed for the Bio-GAC and CAS samples. The same drying procedure was also applied on anaerobic samples from AnGAC and UASB reactors. Dried samples were mounted on XPS standard sample studs using double-sided tape (Figure 3-20). X-ray photoelectron spectroscopy (PHI 5000 VersaProbe II, Physical Electronics Inc.) was conducted at ultrahigh vacuum (1x10-9 bar, with a monochromated Alk X-ray source used to observe on the composition of the biofilm. The charge compensation was achieved with a combination of electron and argon ion flood guns. The X-ray beam size was 100 μm and and the data acquisition was achieved by specify approximately 400×400 μm area upon

sample surface to retrieve targeted atoms (Figure 3-20). According to that setting, each data point on the survey spectra curve is an average of 16 data point. Survey spectra were recorded with pass energy (PE) of 117 eV, step size 1 eV and dwell time 20 ms, whereas high-energy resolution spectra were recorded with PE of 23.5eV, step size 0.1 eV and dwell time 20ms. Auto-z (i.e., automated height adjustment to the highest intensity) was performed before each measurement to find the analyzer's focal point. The number of average sweeps of each of the elements was adjusted to 5-30 sweeps to obtain the optimal signal-to-noise ratio.

The XPS instrument is equipped with an electron energy analyzer unit to analyze the kinetic energy of excited atoms as shown in Figure 3-21. The acquired data were used to plot broad survey scans for all detected atoms on the surface of sample. Multipak and CasaXPS software tools were utilized in the current study for carbon, oxygen and nitrogen peaks curve fitting of the high-resolution scans. The binding energies were calibrated by assigning the C1s, O1s, and N1s peaks for carbon, oxygen, and nitrogen atoms respectively, at 284.6, 5321.3, 399.4 eV respectively. The acquired data was analyzed using either the built in library or the National Institute of Standard and Technology (NIST) library (https://srdata.nist.gov) in order to create chemical state maps for each atom of interest.

Figure 3-18: XPS instrument Model PHI 5000 VersaProbe II, Physical Electronics Inc.

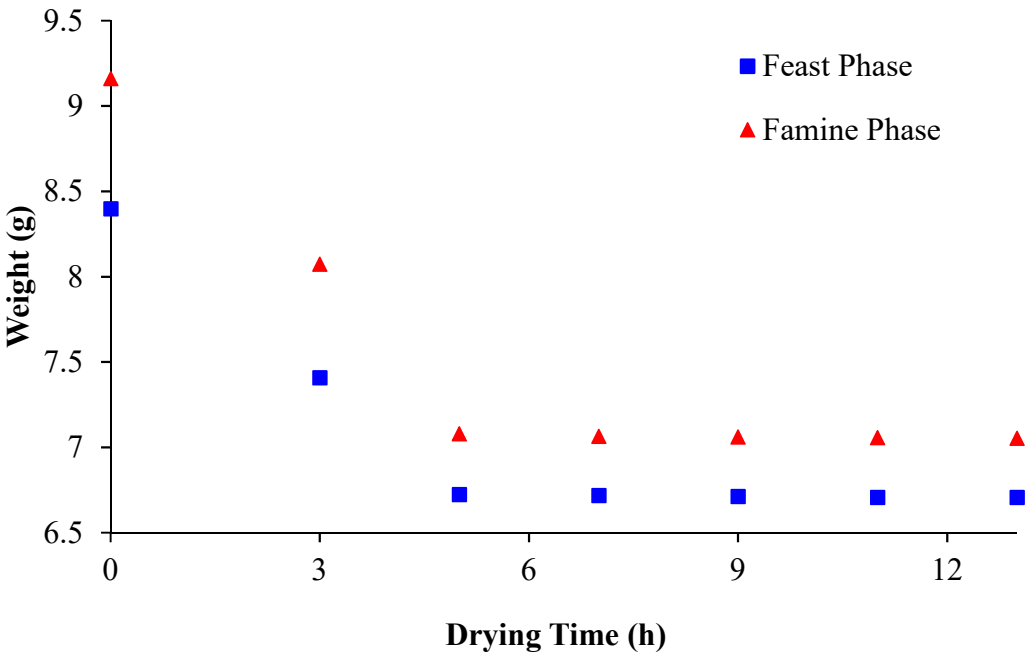

Figure 3-19: AGS weight reduction during oven drying time.

Figure 3-20: XPS standard sample studs (left) and specified area on sample surface to retrieve targeted atoms (right).

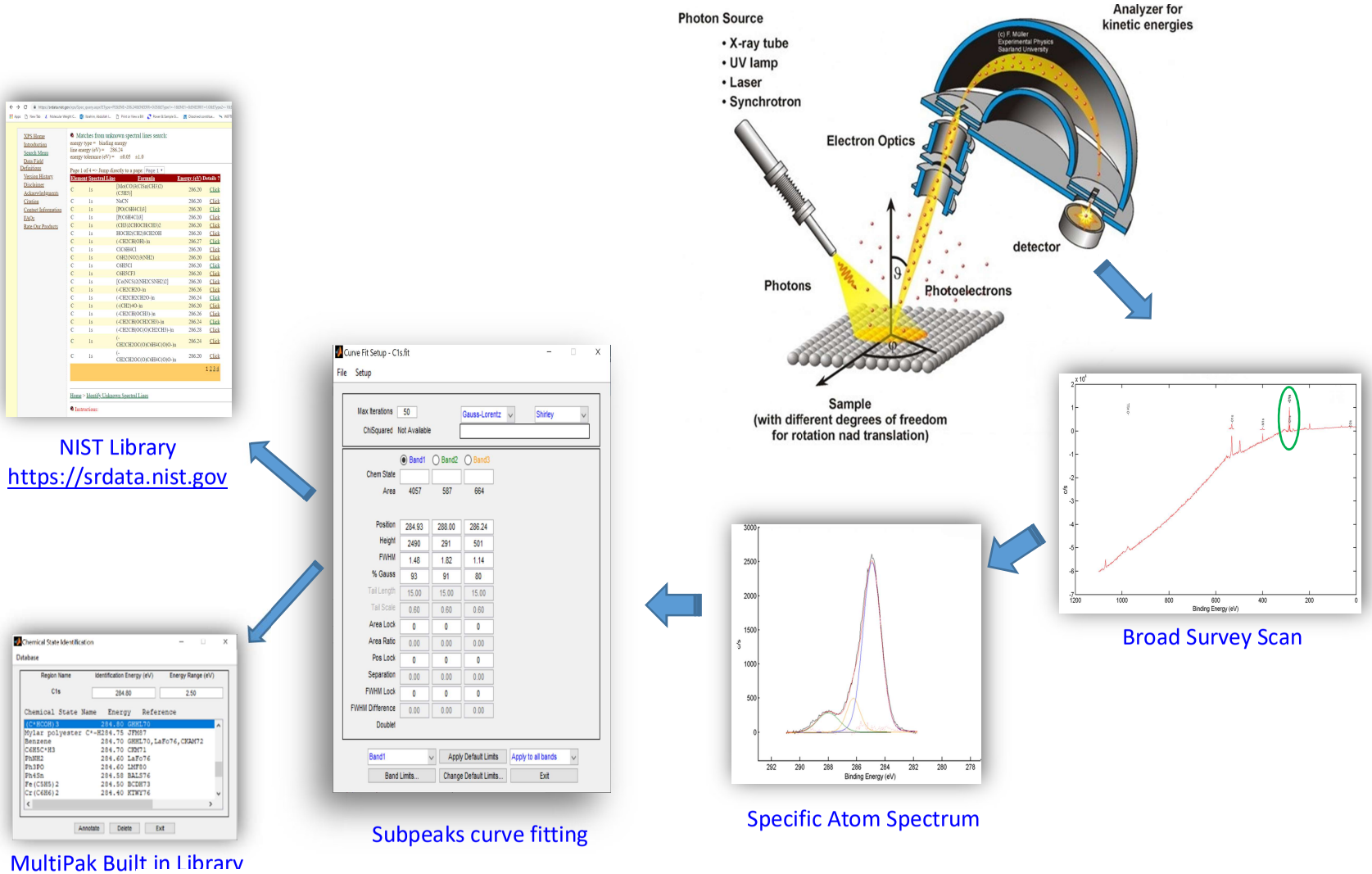

Figure 3-21: Data acquisition and analysis using XPS technique.

3.6. Microbial community analysis

3.6.1. Sample collection and DNA extraction

Representative samples were collected in triplicate and put in 2 mL sterile microcentrifuge tubes. The samples were centrifuged at 10,000 g for 3 minutes. The centrifugation steps were repeated three times for each sample, the supernatant was discarded after each run, and the pellet resuspended with PBS. Then, the collected pellets were stored at –20 °C. At the time of inoculation, duplicate samples of each inoculum were collected and stored in 2 mL sterile centrifuge tubes at -80 ˚C until DNA extraction was performed. Upon inoculation, granule samples were collected twice at every stepwise increase in saline concentration for both reactors. In preparation for storage, granule samples were transferred to 2mL sterile centrifuge tubes using aseptic technique. The tubes were then centrifuged at 10,000 RCF for 5 minutes and the supernatant was discarded. The tubes containing the granule pellets were then stored at -80 ˚C until DNA extraction was performed. DNA extraction was performed using the Qiagen DNeasy PowerSoil Kit, (Germantown, MD) according to the manufacturer's protocol. Then, the extracted DNA was quantified with Qubit 2.0 Fluorometer according to manufacturer protocol using a Qubit dsDNA HS Assay Kit.

3.6.2. 16S rRNA gene amplification and Illumina targeted gene sequencing

The polymerase chain reaction (PCR) was performed to amplify the V4 hypervariable region of the 16S rRNA gene using primers 515F-Y (Parada et al., 2016) and 806R-Y (Caporaso et al. 2011). All PCR reactions were performed with Q5 high fidelity DNA polymerase (New England Biolabs, Ipswich, MA) on an Eppendorf Mastercycler gradient thermal cycler (Eppendorf, Hamburg, Germany). The PCR conditions consisted of an initial denaturation step at 98◦C for 30 seconds, followed by 22 cycles of 98◦C for 10 seconds, 50◦C for 30 seconds, and 72◦C for 30 seconds while ending with a final extension step at 72◦C for 5 minutes. Fragment size of the PCR product was confirmed through gel electrophoresis. PCR products were purified using

AmpureXP beads and dual indexed libraries were prepared using the Illumina Nextera® XT v2 indices (Illumina, San Diego, CA) following Illumina's 16S Metagenomic Sequencing Library Preparation protocol. The prepared libraries were pooled and sequenced as a paired-end 300 cycle sequence run on an Illumina MiSeq sequencer (Illumina, San Diego, CA) at the University of Kansas Genome Sequencing Core, Lawrence, KS.

Illumina sequence data was analyzed by the Center for Microbial Metagenomic Community Analysis at the University of Kansas, Lawrence, KS. The raw reads were processed using the Quantitative Insights into Microbial Ecology2 (QIIME2 v2019.4) (Bolyen et al. 2019). Raw sequence data was first demultiplexed and assigned into individual samples using the QIIME2 demux plugin. A total of 4,784,382 reads were demultiplexed into 42 individual samples. Reads per sample (library size) ranged from 86,514 to 146,943, with a mean of 113,914. The resulting reads were denoised, dereplicated into amplicon sequencing variants (ASVs) and filtered for chimeras using DADA2 (Callahan et al. 2016) plugin found in QIIME2. Sequences representative of the ASVs were aligned using multiple sequence alignment (MAFFT) software version 7 (Katoh and Standley 2013). A phylogenetic tree was constructed from the aligned data using FastTree2 (Price et al. 2010). Taxonomic assignment of the ASV's were carried out using the naïve Bayesian classifier implemented in the QIIME2 taxonomy plugin. Prior to classification, the classifier was trained using reference reads matching the primer target sequence extracted from the SILVA132 SSU (Quast et al. 2013, Yilmaz et al. 2013) reference database.

3.7. Statistical analysis

The normality of data distribution and homoscedasticity (equality of variances) were assessed for all data sets prior to applying statistical analysis. For all tested data sets, It was observed that they had a normal distribution with non-significant differences in variances. Minitab

17 (Minitab 17 Statistical Software, 2010) and R version 3.4 (R Core Team, http://www.r-project.org/) were used to perform statistical analysis in current study. The effect of high salinity on AGS formation in activated sludge versus enriched halophilic culture was assessed using the Two-Sample t-Test. The differences between group means were considered statistically significant when $p < 0.05$ (95% confidence interval). Relative abundances at different taxonomic levels were calculated for each sample using the R package phyloseq (McMurdie and Holmes 2013). Faith's Phylogenetic Diversity (Faith 1992) and Shannon Index for richness and evenness, respectively, were calculated using R packages phyloseq (McMurdie and Holmes 2013) and Picante (Kembel et al. 2010). Differential abundance testing was performed using R package DESeq2 (Love et al. 2014). Nonmetric multidimensional scaling (NMDS) analysis was performed using R package vegan (Oksanen et al. 2017) Pairwise comparisons of sequence data were performed using R package RVAideMemoire (Hervé 2017). All figures representing biocommunity analysis were generated using R package ggplot2 (Wickham 2016) while other figures were generated using MS Excel. Analysis of variance (ANOVA) test was performed to test the statistical differences among reactors when their performance was compared to each other. The error bars represent either standard deviation or 95% confidence intervals, as indicated whenever they reported.

CHAPTER 4

Use of halophilic bacteria to improve aerobic granular sludge integrity in hypersaline wastewaters

This chapter is a peer-reviewed journal article in *Environmental Engineering Science* shown in its entirety with the Supporting Information in Appendix A.

Reproduced with permission from: Abdullah Ibrahim, Yasawantha Hiripitiyage, Edward Peltier, and Belinda S. M. Sturm (2020). Use of halophilic bacteria to improve aerobic granular sludge integrity in hypersaline wastewater. *Environmental Engineering Science:* doi: 10.1089/ees.2019.0349.

Abstract

Aerobic granular sludge reactors are often limited in their ability to treat high-salinity wastewaters. In this study, the performance of an aerobic granular sludge reactor inoculated with an enriched halophilic culture was compared to one seeded with activated sludge at salt concentrations ranging from < 1 g NaCl L^{-1} to 85 g NaCl L^{-1}. While the activated sludge inoculated reactor initially formed larger granules, the halophile inoculated reactor better retained granule structure at hypersaline conditions (> 40 g NaCl L^{-1}), with average granule diameters between 0.8 and 1 mm, approximately double the size of those in the activated sludge reactor. The halophilic reactor also produced significantly higher amounts of both total extracellular polymeric substances and alginate-like exopolysaccharides (ALE) under hypersaline conditions. The halophilic inoculum also retained lower concentrations of intracellular Na^+ (100 mg/g MLVSS versus 125 mg/g MLVSS in the activated sludge reactor) at 85 g L^{-1} NaCl. In contrast, both cultures exhibited the same behavior with respect to Na^+ substitution for divalent cations in extracted extracellular polymeric substances. Illumina 16S targeted gene sequencing data analysis showed that the population of both reactors converged towards halophile-dominated systems, primarily by bacteria

belonging to the phyla *Proteobacteria* and *Bacteroidetes*, at hypersaline conditions. This represented a substantial decrease in diversity for the activated sludge reactor compared to the initial inoculum, but a slight increase for the halophile inoculated reactor. Despite the similarity in community structure, the differences in granule formation and stability indicate that adding halophilic organisms in the initial inoculum produces better granules under hypersaline conditions.

4.1. Introduction

High salinity wastewaters from industries (tanning, food processing, oil and gas production) and coastal communities present special challenges for biological treatment, as conventional activated sludge processes have limited ability to perform in these harsh environments (Corsino et al. 2018, Lefebvre and Moletta 2006, Salminikhas et al. 2016). Aerobic granular sludge (AGS) is a biofilm technology that has seen rapid growth for municipal and industrial wastewater treatment within the last decade (Ahmadun et al. 2009, Pronk et al. 2014). The formation of granules improves the settleability of the microbial biomass, while also improving its ability to withstand shocks due to fluctuations in wastewater composition and protecting slower-growing microorganisms from high pollutant concentrations (Gao et al. 2011, Taheri et al. 2012). These properties make AGS a promising technology for treating industrial wastewaters. However, maintaining the structure of aerobic sludge granules becomes more difficult as the salinity increases. Multiple studies using bacteria derived from domestic wastewater treatment and related sources have noted severe degradation in granule structure and activity as salt concentrations reach 20 to 50 g L^{-1} (Corsino et al. 2017, Pronk et al. 2014, Ramos et al. 2015, Taheri et al. 2012, Wang et al. 2017a). Some success has been reported using individual salt-tolerant microorganisms to treat high-salinity wastewaters (Abou-Elela et al. 2010, Castillo-Carvajal et al. 2014), but these systems are often sensitive to disruptions resulting from changes in wastewater composition (Cui et al. 2016). More recently, Huang et al. (2019b) successfully used

a mixture of salt-tolerant and halophilic species obtained from estuarine sediments to develop halophilic granules to remove ammonia and chemical oxygen demand (COD) from wastewater at 30 g L^{-1} salinity.

A key component to granular stability is the production of extracellular polymeric substances (EPS), which bind organisms together and help protect cells from environmental conditions (Capodici et al. 2015, Deng et al. 2016). Salt stress can result in changes in the quantity and quality of EPS production in AGS systems (Corsino et al. 2017, Taheri et al. 2012, Wang et al. 2017a). For example, Corsino et al. (2017) observed increases in the fraction of 'not-bound' EPS and a reduction in EPS protein content above 50 g L^{-1} NaCl. Alginate-like exopolysaccharides (ALE) are predominantly comprised both of mannuronic and guluronic acids (Li et al. 2017) and are classified as one of the most abundant exopolysaccharides in AGS (Lin et al. 2013b). It has been reported that the presence of ALE can increase AGS stability because it has strong mechanical properties and a high affinity for some divalent cations, such as Ca^{2+} and Mg^{2+}. In addition, ALE has the ability to embed some components, such as proteins and lipids, which enhance AGS aggregation (Li et al. 2017, Lin et al. 2010).

High concentrations of aqueous sodium, which occur in most high-salinity wastewaters, can impact both individual organism viability and AGS stability. It has been suggested that divalent cations, primarily Ca^{2+} and Mg^{2+}, play an important role in bioflocculation by bridging negatively charged sites on cell surfaces and by binding biopolymers to each other (Kara et al. 2008). Substitution of monovalent Na^{+} and K^{+} for divalent cations in the EPS matrix has been shown to negatively impact granule formation and activated sludge settleability (Fang et al. 2018a, Higgins and Novak 1997, Ismail et al. 2010, Li and Yang 2007).

More recently, investigators have developed AGS systems with some tolerance for high salinity wastewaters (Bassin et al. 2011, Pronk et al. 2014, Taheri et al. 2012). Ou et al. (2018a) investigated the effect of 0 to 9% w/v NaCl on AGS formation and the bacterial community in lab-scale reactors. As the salt content increased to 9%, halophilic bacteria became abundant in the reactors. However, removal efficiency (as chemical oxygen demand) declined to 50% at 9% salt content. In addition, Wang et al. (2017c) studied adaption strategies to reduce the effect of salinity on AGS formation and nutrient removal, with higher levels of dissolved oxygen improving AGS formation as the NaCl content increased to 15 g L^{-1}. Li et al. (2017) studied AGS granulation in mixtures of saline synthetic sewage with seawater, and observed stronger granular structure, with more ALE production, as the salinity increased due to higher seawater content. This result was attributed to the difference between real seawater and synthetic salt solutions, particularly the presence of a wider range of metal cations. While studies of AGS systems using halophilic bacteria are rare, Huang et al. (2019b) used selective settling pressure to form aerobic halophilic granules in a sequencing batch reactor (SBR) at a salt concentration of 30 g L^{-1}. EPS production was observed to increase with higher organic loading rates. The protein content of EPS was correlated with increasing granule size, while ALE was found only in mature granules.

Based on these results, the use of AGS for remediation of high-salinity wastewaters may be improved using halophilic organisms that are adapted to function in these environments. This study investigates the effectiveness of bioaugmentation with a halophilic bacteria culture on the development of stable aerobic granules under hypersaline conditions. Two sequencing batch reactors (SBRs) were operated – one with activated sludge and one with an enriched halophilic community as the inoculum. Granule size, integrity and composition (including EPS and ALE production and divalent cation content) were examined in both systems as salt concentrations

gradually increased from < 1 to 85 g L^{-1} to provide insight on adaptations that improve granule stability under high salinity conditions. Insight on reactor community changes were provided through 16S targeted gene sequencing of the samples obtained during hypersaline operation.

4.2. Materials and Methods

4.2.1. Experimental setup and operation conditions

Two identical 3.0 L bench-scale SBRs were operated with an internal diameter of 6.5 cm and an effective height of 88.5 cm; the volumetric exchange ratio was 50%. The superficial up-flow air velocity was maintained at 1.1 cm s^{-1}. Initially, reactors were operated with a 6 hour cycle comprised of four phases: 30 minutes anaerobic feeding through the settled sludge bed, 315 minutes aeration, 10 minutes settling, and 5 minutes decanting. Fine bioflocs started to appear in both reactors after 14 days of operation, with stable granules (diameter > 0.2 mm) appearing after 37 days of operation. At this point, settling time was gradually reduced to 3 minutes and the aeration time increased to 322 minutes over a 20-day period. These time parameters were then used throughout the experiment. Once mature granules appeared (after 37 days of operation), the sodium chloride content was increased stepwise over time from <1 to 85 g NaCl L^{-1}. After each increase in influent salt concentration, the reactors were maintained at that new concentration until the MLVSS concentration and COD removal stabilized, a process that typically took 7 to 10 days (Figure 4-1). Once the reactor reached stable operation, the salt concentration was increased again. Throughout the experiment, sludge retention time (SRT) in both reactors was maintained at approximately 28-30 days, depending on the mass of sludge withdrawn for measurements. The temperature was maintained at 21±1 °C, while the pH of the influent wastewater was adjusted to 7.2 ± 0.1 by addition of 1 M HCl or 1 M NaOH.

A hypersaline feed solution (Table 1) was modified from previously published recipes for high-salinity oil and gas synthetic wastewater, or produced water (Pendashteh et al. 2012, Sharghi

et al. 2014). The C/N/P ratio was adjusted to approximately 100/10/1 by adding NH_4Cl and KH_2PO_4, and a trace element solution was added at 0.2 ml per liter of final solution (Li et al. 2017) . The NaCl content was increased stepwise over time from <1 to 85 g L^{-1} using a commercially available salt compound which our analysis confirmed to be 95-98% pure NaCl. Acetate was used as the sole carbon source with an organic load of 1350 mg COD L^{-1}. For the first reactor, a halophilic biomass culture obtained from a previous experiment was grown in marine salts medium (ATCC medium no. 1487) for 15 days to select for halophilic organisms. 50 mL of this material was then used to inoculate the reactor. The second reactor was inoculated with activated sludge collected from the aeration tank of a municipal wastewater treatment plant in Lawrence, KS, USA.

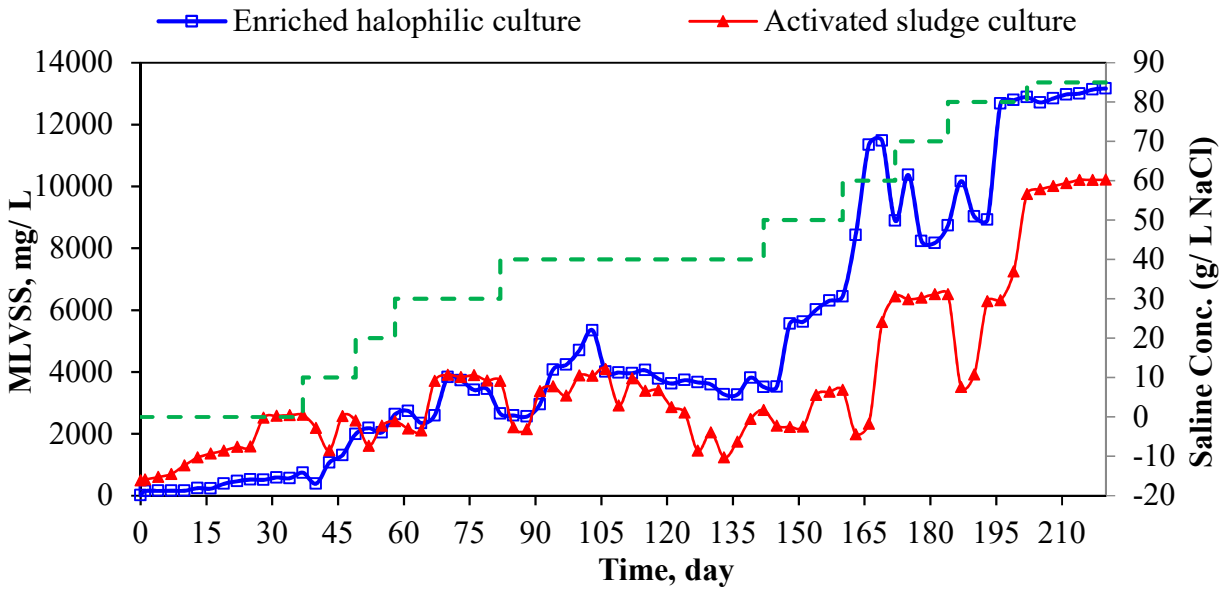

Figure 4-1: MLVSS concentration for enriched halophilic and activated sludge culture along with study period.

Table 4-1: Composition of reactor feed, including trace element composition.

Compound	Concentration (mM)	Compound	Concentration (µM)
NaCl	0-1,283	$FeCl_3.6H_2O$	11.1
$CaCl_2.2H_2O$	0.41	H_3BO_3	4.85
KCl	26.8	$CuSO_4.5H_2O$	0.24
$MgCl_2.6H_2O$	0.25	KI	0.36
$NaHCO_3$	9.52	$MnCl_2.4H_2O$	1.21
NH_4Cl	16.1	$Na_2MoO_4.2H_2O$	0.50
KH_2PO_4	0.73	$ZnSO_4.7H_2O$	0.83
Mg SO_4	4.15	$CoCl_2.6H_2O$	1.26
$NaCH_3COO$	39.0		

4.2.2. Analytical *procedures*

Mixed liquor suspended solids (MLSS), volatile suspended solids (MLVSS), and sludge volume index at 5 minutes (SVI_5), were quantified based on Standard Methods (APHA 2005). A stereomicroscope (Fisher Scientific) was used to capture granule images twice a week during the experiment. The average granule diameter and aspect ratio, defined here as the ratio of longitudinal to latitudinal diameter of the granular sludge particle, were analyzed using Fiji image software (https://imagej.net/Fiji). Since the chloride content was elevated in these samples, COD was determined according to the method proposed by Vyrides and Stuckey (2009), which accounts for chloride interference.

Extraction of loosely- and tightly-bound EPS (LB- EPS and TB- EPS) was carried out using the heat method described by Li and Yang (2007), and quantified as COD. During the extraction process, samples were centrifuged twice, with the supernatant discarded each time and the biomass pellet re-suspended into 30 mL of phosphate buffered saline (PBS) solution pre-heated at 60 ºC. After a third centrifugation step, the biomass pellet remaining in the centrifuge tube after the TB-EPS extraction was stored and was later digested to determine intracellular cation concentrations. The alginate-like extracellular (ALE) fraction of the EPS was isolated according to the method proposed by Felz et al. (2016b) as the sodium form of ALE, then quantified by a phenol-sulfuric

acid assay using sodium alginate as a standard (Dubois et al. 1956). ALE extraction began only once both reactors had reached 40 g L^{-1} NaCl, and was carried out throughout the hypersaline range.

A temperature-controlled microwave assisted digestion procedure based on Özsoy (2006) was used to extract cations (Ca^{2+}, Mg^{2+}, Na^{+}, K^{+}) from EPS and biomass samples. Diluted samples of extracted EPS were mixed with 2 ml of nitric acid and 0.5 ml of hydrochloric acid to make a final volume of 22.5 mL. The solution was heated to 170 ˚C over 10 minutes, and then held at that temperature for an additional 10 minutes, followed by 17 minutes heating at 70 ˚C. For intracellular cation analysis, about 0.35 ± 0.1 g of biomass left after TB-EPS extraction was mixed with 6 ml of nitric acid and 2 ml of hydrochloric acid, and then the same microwave-assisted digestion procedure was applied. Digested samples were diluted to 100 mL with deionized water and filtered through a 0.45 µm filter, then analyzed by inductively coupled plasma – optical emission spectrometry (ICP-OES, PerkinElmer, Optima 2000 DV) to determine Ca^{2+}, Mg^{2+}, K^{+} and Na^{+} concentrations.

4.2.3. Microbial community analysis

4.2.3.1. DNA extraction

DNA was extracted from duplicate mixed liquor samples collected at inoculation and at every stepwise increase in NaCl concentration from 40 g L^{-1} on in both reactors. The extracted DNA was used to generate amplicons with primers targeting the V4 hypervariable region of the 16S rRNA gene (Caporaso et al. 2011). Illumina NGS libraries were prepared from the amplicons and finally sequenced on an Illumina MiSeq sequencer at the Integrated Genomic Facility at Kansas State University, Manhattan, KS. A detailed description of the DNA extraction, amplicon generation, and Illumina library preparation is available in the supplemental information.

4.2.3.2.Sequence data analysis

Illumina sequence data was analysed by the Center for Microbial Metagenomic Community Analysis at the University of Kansas, Lawrence, KS. The raw reads were filtered for quality and sorted into operational taxonomic units (OTUs) using the Quantitative Insights into Microbial Ecology2 software suite (QIIME2 v2017.12) (Caporaso et al. 2010).

4.2.4. Statistical analysis

Duplicate samples were taken for all measurements. All plots of reactor data show mean values for the relevant data, with error bars representing two standard deviations from this mean. Differences in mean values between reactors or between different operating conditions were analyzed for statistical significance using a two-sample student's *t*-test at 95% confidence (*p* value $\leq$ 0.05). T-test and Pearson's correlation analysis were performed using Minitab 17 (Minitab 17 Statistical Software, 2010). R version 3.4 (R Core Team, http://www.r-project.org/) was employed to run statistical analysis related to microbiome community data.

4.3. Results

MLVSS concentrations in the halophilic reactor were initially lower than in the activated sludge reactor, but reached comparable levels at 20 g L^{-1} NaCl (Figure 4-1). Above 40 g L^{-1}, the halophilic reactor MLVSS continued to increase, and was consistently between 10,000 and 13,000 mg L^{-1} by the end of the study, with MLVSS/MLSS ratios around 0.78. By contrast, the biomass content in the activated sludge reactor dropped to below 4,000 mg L^{-1} when the salt concentration was increased to 40 g L^{-1} NaCl. Under hypersaline conditions, activated sludge reactor biomass was always lower than that in the enriched halophile reactor, although concentrations did begin to increase again after 165 days (70 g L^{-1} NaCl). MLVSS/MLSS ratios were similar in both reactors, at 0.76-0.78. COD removal was initially lower in the enriched halophile reactor, possibly due to the low-salinity environment, but increased as NaCl was added, and remained above 90% under hypersaline conditions (Table A1). COD removal in the activated-sludge reactor varied between

80 and 90% throughout the experiment. Although the reactors had different solid contents, statistical analysis showed no significant differences ($p > 0.05$) in SVI_5 between reactors.

4.3.1. Aerobic granular sludge formation

Granule sizes in both reactors were very similar during the startup period (Figure 4-2). The average granule diameter in the activated sludge reactor was higher during the lower salinity stage (10 to 40 g L^{-1}). This better granulation corresponded with a dark yellow appearance and a solid, smooth surface (Figure 4-3). By contrast, the halophile-inoculated granules had a light-yellow appearance and a rougher granule surface. Under hypersaline conditions (40 to 85 g L^{-1}), average granule size in the activated sludge reactor declined from 1.25 ± 0.2 mm to 0.4 ± 0.1 mm as salinity increased, and the aspect ratio decreased to 0.52 (Figure 4-2). By contrast, the granule size in the halophilic reactor decreased only slightly (from 1.05 ± 0.2 mm to 0.95 ± 0.4 mm) and maintained an aspect ratio of 0.60. Statistical analysis showed that there was a significant difference ($p < 0.05$) between granule sizes in the two reactors during hypersaline operation ($\geq$ 40 g L^{-1}), but not during operation at lower salinity. At higher salinity levels, the external shape of the halophile-inoculated granules also appeared more solid (Figure 4-3).

4.3.2. EPS production and composition

EPS extracted at the end of the aeration cycle (measured as mg of COD) was normalized to MLVSS concentration (Figure 4-4a). EPS production was relatively stable in the halophile-inoculated reactor, with a small decrease in production relative to total biomass at 80 to 85 g L^{-1}. In the activated sludge reactor, EPS production increased through the low salinity range, but decreased rapidly between 35 and 45 g L^{-1} NaCl. It then remained relatively consistent at approximately 400 mg g^{-1} MLVSS throughout the hypersaline range. Tightly bound EPS accounted for approximately two thirds of the total EPS, on average, in both reactors (Figures A1

and A2). No consistent impact of salinity on the relative amounts of tightly and loosely bound EPS was observed.

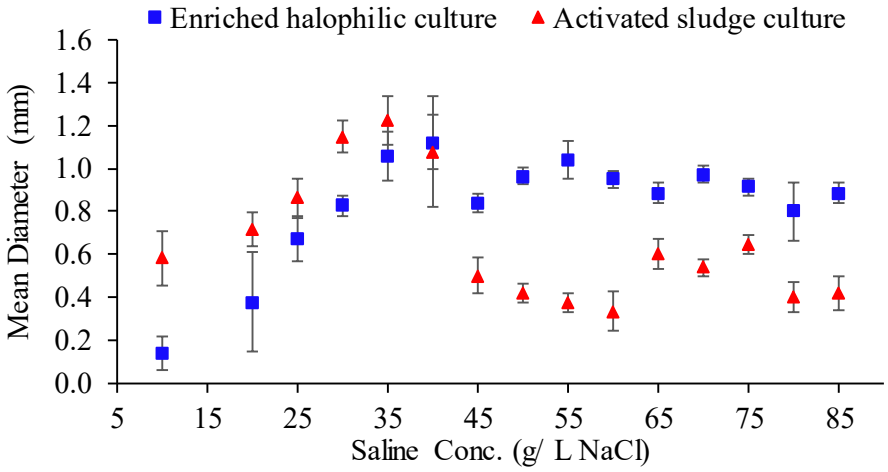

NaCl, g L^{-1}	Halophilic Inoculum	Activated Sludge
0	0.67	0.68
20	0.73	0.71
40	0.73	0.71
60	0.75	0.57
85	0.60	0.52

Figure 4-2: Average granule sizes (left) and aspect ratios (right) for reactors inoculated with an enriched halophilic culture or activated sludge at increasing salt concentrations.

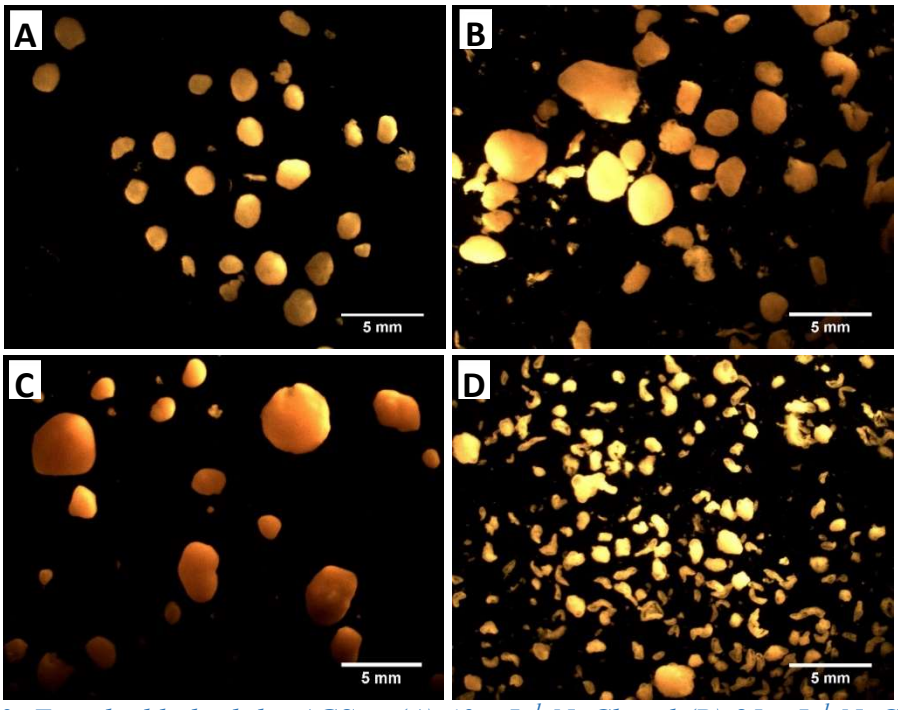

Figure 4-3: Enriched halophilic AGS at (A) 40 g L^{-1} NaCl and (B) 85 g L^{-1} NaCl; activated sludge AGS at (C) 40 g L^{-1} NaCl and (D) 85 g L^{-1} NaCl. AGS, aerobic granular sludge.

ALE concentrations under hypersaline conditions (40- 85 g L^{-1} NaCl) ranged from 81-161 mg g^{-1} MLVSS and 116-171 mg g^{-1} MLVSS in the activated sludge and halophilic reactor,

respectively. These concentrations are in the upper range of reported ALE concentrations for aerobic granular reactors under saline conditions (Huang et al. 2019b, Li et al. 2017, Meng et al. 2019, Wang et al. 2017c). ALE production in the activated sludge reactor was lower than in the halophilic reactor, except at the highest salinity, and showed greater fluctuations as salinity increased (Figure 4-4b). The difference in mean ALE concentration across the hypersaline range (40 – 80 g NaCl L^{-1}) between the two reactors was statistically significant at 95% confidence, which mirrors the trends in total EPS (Figure 4-4a) over the same range. However, the difference in ALE production was non-significant once the salinity increased to 85 g L^{-1}. Higher concentrations of EPS and ALE corresponded to the larger, and more consistent, granule sizes observed in the halophilic reactor under hypersaline conditions. Pearson's correlation analysis also showed that SVI_5 values were positively correlated with ALE production in both cultures ($r= 0.91$, $p= 0.001$ for the enriched halophilic culture and $r= 0.71$, $p= 0.033$ for the activated sludge culture), further emphasizing the link between ALE production and granule structure.

The EPS cation content was dominated by Na^+ in both systems throughout the experiment, but there were notable differences in divalent cation concentrations based on both inoculant and total salinity (Figure 4-5). Below 40 g L^{-1} NaCl, both Ca^{2+} and Mg^{2+} were present at higher concentrations in EPS from the halophile-inoculated reactor, while the Na^+ concentration was 25 to 30% lower. Above 40 g L^{-1}, divalent cation concentrations in EPS decreased to below 2 mg g^{-1} MLVSS in both reactors. While both reactors saw an increase in the sodium content of EPS under these same conditions, Na^+ continued to be present at higher concentrations in the activated-sludge reactor EPS, with a maximum concentration of 130 mg Na^+ g^{-1} MLVSS, compared to 100 mg Na^+ g^{-1} MLVSS in the halophile-inoculated EPS.

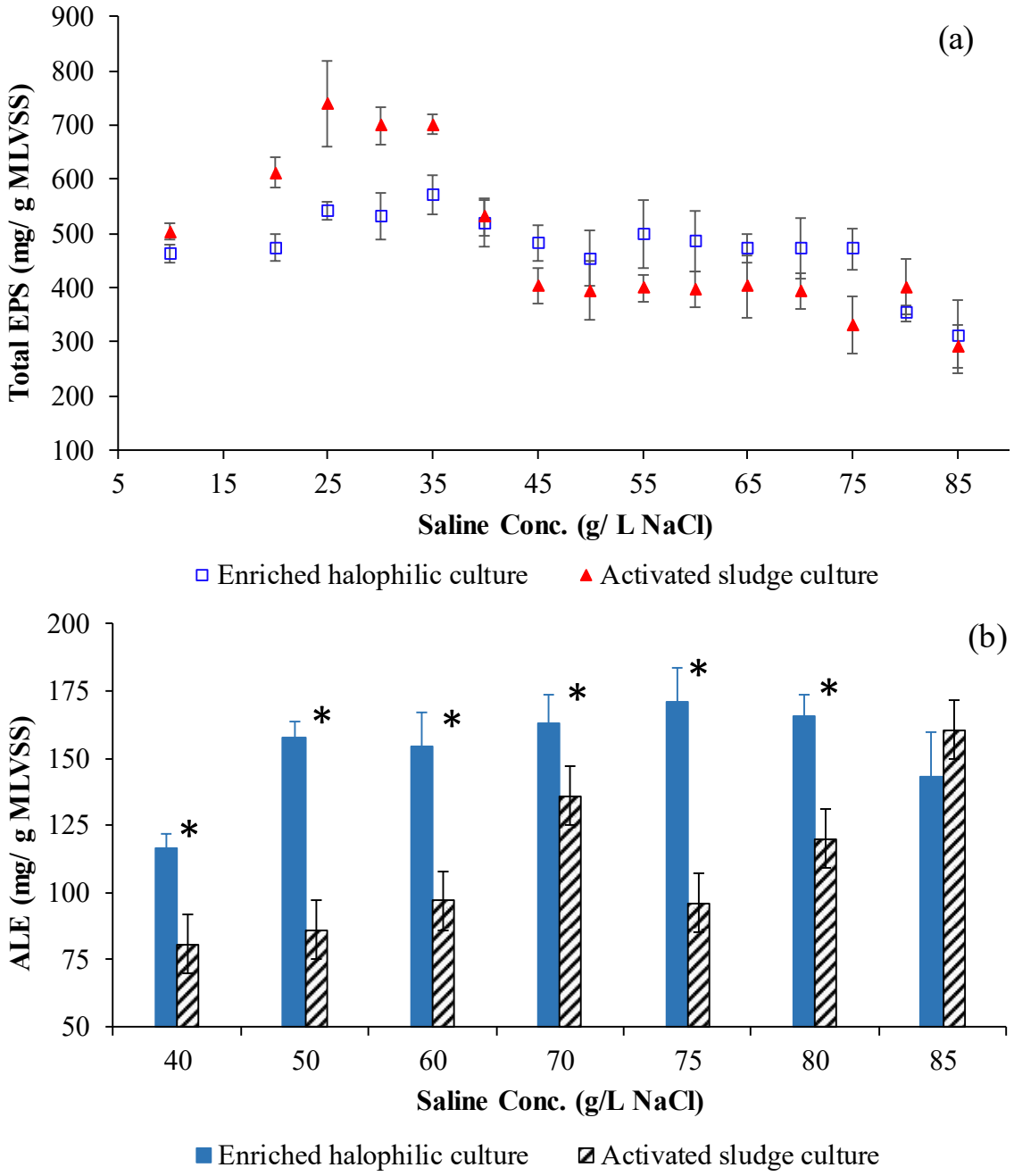

Figure 4-4: (A) EPS production and (B) ALE production in reactors inoculated with an enriched halophilic culture or activated sludge. '''' Indicates a statistically significant difference ($p < 0.05$) in ALE production. EPS, extracellular polymeric substances;ALE,*

The differences in cation concentrations between the halophilic and activated-sludge reactors were compared using a two-sample *t*-test, which showed significant differences at 95% confidence for Ca^{2+} and Na^{+} (*p* values of 0.035 and 0.00, respectively), while Mg^{2+} was just above

the threshold for significance at 95% confidence (p = 0.057). K^+ followed a similar trend to the divalent cations in the enriched halophilic reactor, decreasing in the EPS as the bulk sodium concentration increased from 10 to 40 g L^{-1} NaCl (Figure A1). In the activated sludge reactor, EPS-associated K^+ was initially present at lower concentrations, but rose slightly as the bulk Na^+ concentration increased.

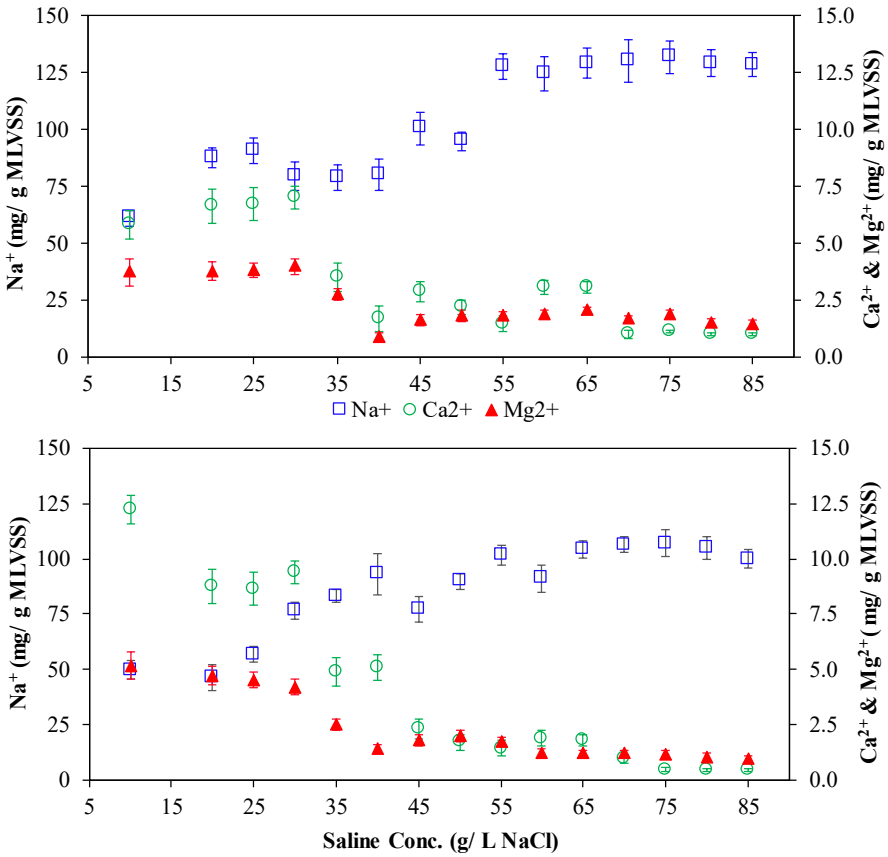

Figure 4-5: Cation concentrations in the EPS of AGS formed from the activated sludge culture (top) and enriched halophilic culture (bottom).

4.3.3. Intracellular cations

Intracellular calcium concentrations in the activated sludge reactor decreased with increasing addition of NaCl to the reactor, while intracellular Na^+ declined with increasing salinity from 45 to 60 g L^{-1} , and then recovered, reaching approximately the same concentration at 85 g L^{-1} NaCl as at 45 g L^{-1} (Figure 6). Intracellular calcium concentrations in the halophilic reactor were generally below 10 mg g^{-1} MLVSS at hypersaline conditions. Sodium concentrations were

higher, averaging 46.8 ± 3.7 mg g^{-1} MLVSS, but both Ca^{2+} and Na^{+} were unaffected by changes in salinity. At all salinities, intracellular Ca^{2+} and Na^{+} concentrations in the halophilic reactor were substantially lower than corresponding values in the activated sludge reactor, pointing to a consistently different response to high external salt levels between the two microbial communities. Intracellular potassium concentrations were 35-40 mg g^{-1} MLVSS in both reactors and showed no consistent trend with increasing salinity. (Figure A3)

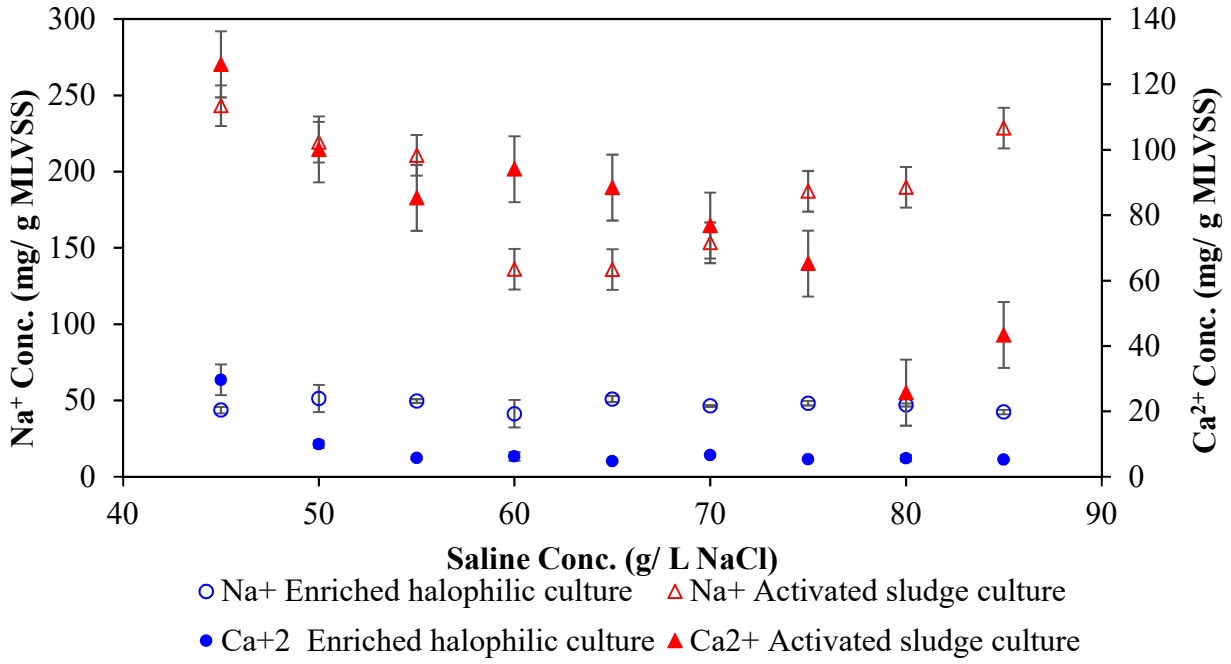

Figure 4-6: Intracellular concentrations of calcium (filled symbols) and sodium (open symbols) in the halophilic and activated sludge reactors under hypersaline conditions.

4.3.4. Microbial community structure

At inoculation, the enriched halophilic culture was comprised of 9 phyla across all samples; 7 of these phyla contained relative abundances greater than 0.1% although two phyla, *Proteobacteria* and *Firmicutes*, were much more prevalent than the others (Figure 7). The 5 most abundant genera in the enriched halophilic inoculum were *Halomonas* with a relative abundance of 59.2 ± 9.2%, followed by *Staphylococcus* (39.5 ± 11.3%), *Planktosalinus* (0.5 ± 0.1%), *Corynebacterium* (0.4 ± 0.1%), and *Marinobacter* (0.1 ± 0.05%), all of which are known to contain

halophilic organisms (Figure A4). The activated sludge inoculum was much more diverse, being comprised of 37 phyla; 19 with relative abundances greater than 0.1%. *Proteobacteria*, however, was the most abundant phylum in this inoculum as well. The five most abundant genera classified in the activated sludge culture were *Thiothrix* (with a relative abundance of 2.9 ± 0.3%), followed by *Bdellovibrio* (2.7 ± 0.1%), *Planctomyces* (1.9 ± 0.1%), *Uncultured Xanthomonadaceae Family* (1.7 ± 0.1%), and *Hyphomicrobium* (1.6 ± 0.1%)) (Figure A4). The halophilic genera *Halomonas (0.22* ± 0.02)*, Haloferula (0.003* ± 0.001)*,* and *Planktosalinus (0.04* ± 0.01) were also detected in in the activated sludge inoculum, albeit at very low abundance levels.

The increase in salinity from 0 – 40 L^{-1} in the activated sludge inoculated reactor resulted in a microbial community shift favoring halophilic organisms. The resulting community structure of both reactors was relatively consistent across the hypersaline range of 40 to 85 g L^{-1}. At the phylum level, both reactors were dominated by *Proteobacteria*, followed by *Bacteroidetes* and then *Actinobacteria* (Figure 7). At the genus level, *Halomonas* had a mean relative abundance of 23.2 ± 2.1% across all tested salinities in the halophile-inoculated reactor. *Halomonas* was also selected as the most common genus in the activated sludge-inoculated reactor, with a final mean relative abundance of 25.2 ± 6.1%. Core microbiome analysis, which identifies the organisms that are present in at least 90% of the samples, showed that 14 taxa were responsible for 75% of the relative abundance in both systems between 40 g L^{-1} NaCl and 85 g L^{-1} NaCl (Figure A5). Identifiable core genera in both reactors included *Aequorivita, Azoarcus, Corynebacterium, Marinicella, Marinobacter, Nitratireductor, Pelagibacterium, Planktosalinus, Stappia,* and *Wenzhouxiangella,* which are all known halophilic genera.

The convergence of bacterial communities between the two reactors represented a substantial decrease in the diversity from the activated sludge inoculum, but an increase in diversity for the

halophile-inoculated system. Faith's phylogenetic diversity analysis (Figure A6) revealed that the activated sludge inoculum diversity, at 76.4 ± 4.8, was significantly higher than the enriched halophilic culture inoculum value of 2.6 ± 1.7 ($p < 0.05$). At 40 g L^{-1}, the activated sludge reactor was significantly less diverse with a Faith's diversity index of 17.9 ± 5.7, while the diversity index in the halophile-inoculated reactor increased to 7.8 ± 0.2. By 45 g L^{-1}, the activated sludge reactor had a diversity index of 8.3 ± 1.0, and the halophile-inoculated reactor had a diversity index of 10.3 ± 0.5. No significant change in richness was observed in either reactor as salinity increased beyond this point.

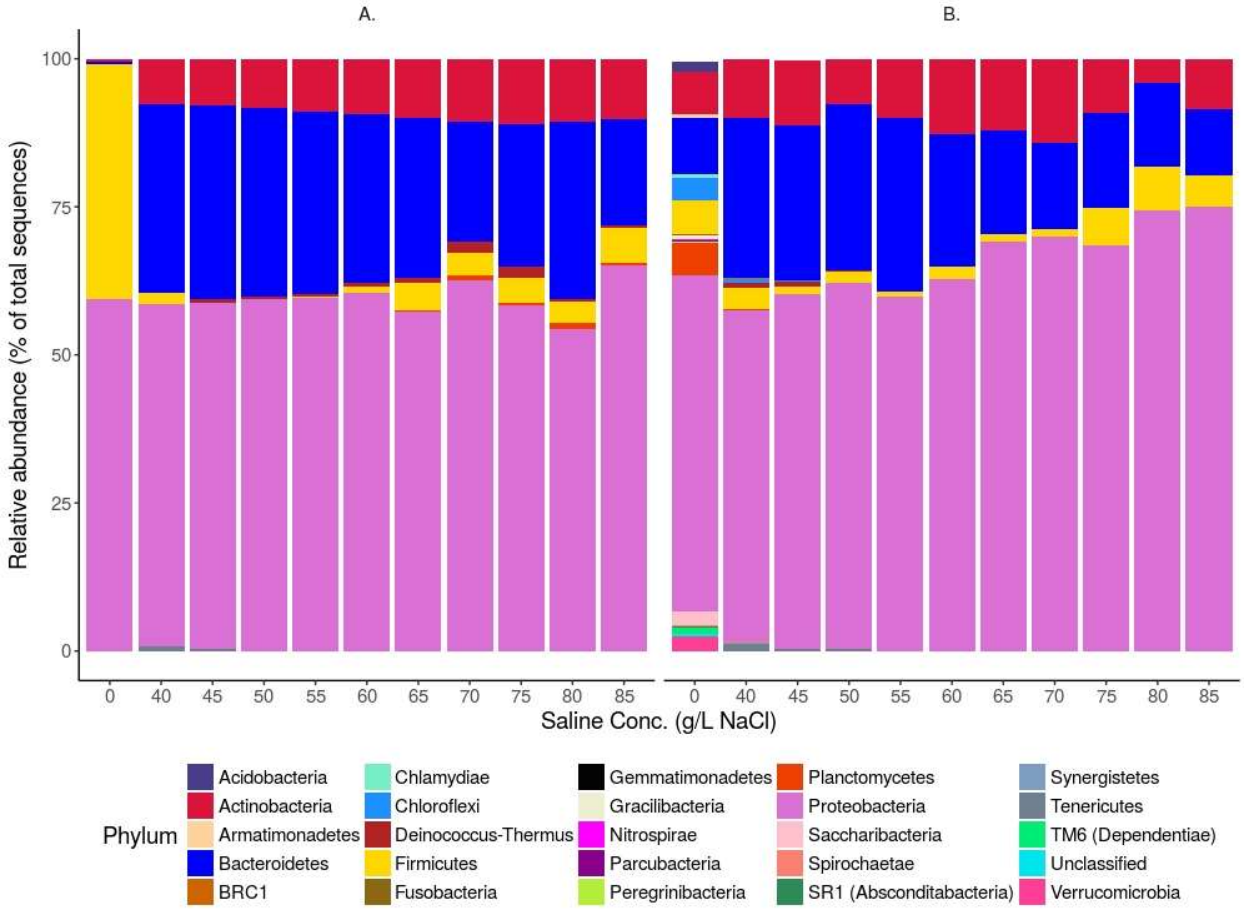

Figure 4-7: Stacked bar plot showing taxa with relative abundance ‡0.1% at phylum level for inoculum (0 g L^{-1} NaCl) and at each saline concentration for (A) the reactor inoculated with an enriched halophilic culture and (B) the reactor inoculated with activated sludge.

4.4. **Discussion**

Despite the observed similarity in community structure, only the halophile-inoculated reactor was able to retain larger granules at hypersaline conditions ($\geq$ 40 g NaCl L^{-1}). Several previous studies have shown that AGS formation using organisms from domestic wastewater decreases as the salinity increases above 15-30 g NaCl L^{-1} (Corsino et al. 2017, Pronk et al. 2014, Wang et al. 2017a), which is consistent with results reported here for the activated sludge reactor from 40 to 70 g L^{-1} NaCl . The maintenance of stable granules in the halophile-amended reactor at up to 85 g L^{-1} NaCl, by contrast, represents a higher level of salinity tolerance than was observed in most previous studies. (Ou et al. (2018a) were also able to maintain stable granules up to 9% salinity, and noted that their system was also dominated by moderate halophiles.) Overall, there was a strong correlation between EPS and granule size in both reactors ($p < 0.05$). This finding is in agreement with previous studies (Corsino et al. 2017, McSwain et al. 2005, Ramos et al. 2015, Wang et al. 2017a, Wang et al. 2017c) that emphasize the role of EPS in AGS formation. Secretion of EPS protects embedded microorganisms from external shocks (Xu et al. 2020). Halophilic organisms may be more capable of maintaining EPS production even in the face of increased bulk salinity, thus producing the more stable granules observed in the halophile-amended reactor at hypersaline conditions.

ALE can also play a crucial role in maintaining AGS structure due to the presence of a polysaccharide network that maintain AGS elasticity and high affinity to cations, which strengthen the AGS structure (Li et al. 2017, Lin et al. 2010, Pishgar et al. 2020). ALE production in the enriched halophilic culture was consistently higher over the salinity range of 40 – 80 g NaCl L^{-1}. Statistical analysis showed that this difference was statistically significant at 95% confidence. Other studies have reported that increased ALE production with high salinity may help cope with high osmotic pressure and sodium toxicity (Meng et al. 2019, Wan et al. 2014). The higher

concentrations of ALE present in the halophilic reactor may therefore be another sign that these organisms are better able to adapt to salt stress in ways that maintain granule integrity. It is interesting to note that, at 85 g L^{-1} NaCl, where MLVSS concentrations increase significantly in the activated sludge reactor, ALE production in the two reactors was not statistically different.

The three dominant phyla present in both reactors at hypersaline conditions (*Proteobacteria*, *Bacteroidetes* and *Actinobacteria*) are identical to those reported by Huang et al. (2019b) for an SBR operated at 30 g L^{-1} NaCl, although the current study also has *Firmicutes* present (at lower abundance) in both reactors. This finding is also in agreement with previous studies that reported *Proteobacteria* as one of the bacterial lineages in a marine biocommunity (Ou et al. 2018a, Zhang et al. 2016) In addition, ALE production was correlated with *Proteobacteria* in both reactors. These results strongly suggest that microbes in the phylum *Proteobacteria* are an important component to halophilic granule formation, possibly as a major contributor to ALE production. However, the current study also found a negative correlation between *Proteobacteria* and total EPS production in both reactors.

Pearson's correlation analysis further showed that there was a negative correlation between ALE and phylum *Bacteroidetes* in both reactors. Thomas et al. (2011) observed that organisms in the phylum *Bacteroidetes* were the main contributor to polysaccharides and protein degradation while Zhang et al. (2016) reported that this phylum played a main role in the biodegradation of organic matter. There was also a negative correlation between salt content above 60 g L^{-1} NaCl and *Bacteroidetes*. This finding indicates that granule structure could benefit at higher salinities from *Bacteroidetes* inhibition resulting in higher ALE content. However, *Bacteroidetes* had a positive correlation with total EPS production. As with the similar (but opposite) correlations between *Proteobacteria*, ALE and EPS, these results suggest a complicated relationship between

the microbial community composition and granule stability. Statistical analysis of community results at the genus level did not produce any significant correlations to EPS or ALE production in either reactor. While it is possible that granule integrity may be linked to the presence of individual halophilic species, rather than the presence of halophiles more generally, such an analysis is beyond the scope of this work.

Relatively few previous studies have reported Na^+ concentrations in the EPS matrix under high salinity conditions. Both Kara et al. (2008) and Fang et al. (2018a) reported that sodium concentrations in the sludge matrix increased with increasing concentration in the wastewater. Kara et al. (2008) measured Na^+ concentrations of 23-115 mg g^{-1} sludge as the bulk NaCl content increased from 10 to 460 mg L^{-1}.Despite the higher bulk salt concentrations, the current values for the activated sludge reactor are similar (13-130 mg g^{-1} sludge), but higher in the halophilic reactor (19-425 mg g^{-1} sludge), particularly under hypersaline conditions. Fang et al. (2018a) reported accumulation of 100 mg Na^+ g^{-1} EPS at bulk NaCl concentrations of 30 g L^{-1}. Normalizing the Na^+ concentrations reported in Figure 5 to EPS production by dividing by total EPS concentration (Figure 4a) shows that Na^+ accumulation in the EPS was higher in both reactors in the current study, with 322 and 440 mg Na^+ g^{-1} EPS in the activated sludge and halophilic reactors, respectively, at 85 g L^{-1} NaCl. As the solution NaCl concentration increased from 10 to 85 g L^{-1} in the current study, Na^+ concentrations in the EPS approximately doubled in both reactors (Figure 5), which suggests there may be a maximum capacity of the EPS for cation accumulation. However, this experiment did not observe a correlation between sodium substitution for divalent cations in the EPS and granule integrity. The decrease in $Ca^{2+}$and Mg^{2+} EPS concentrations in the activated sludge reactor began well before the salinity (40 g L^{-1}) where granule size began to decay. Additionally, the halophilic reactor showed the same trends with respect to divalent cation

concentration, but without the decrease in granule size. Thus, there is no indication that divalent cation replacement by Na^+ necessarily leads to AGS fragmentation.

The halophilic reactor did accumulate less intracellular Na^+ and Ca^{2+} under hypersaline conditions. Individual organisms within the granule structure may address increased osmotic pressure caused by high salinity through selective accumulation of intracellular cations (Ca^{2+}, Mg^{2+}, Na^+ and K^+) (Hänelt and Müller 2013, Wan et al. 2014). Wang et al. (2017a) also observed an increase in K^+ concentration in granules, and corresponding decrease in Na^+, that was attributed to the actions of K^+/Na^+ and Na^+/H^+ pumps. In the current study, however, no increase was observed in intracellular K^+ with higher salinity. Wan et al. (2014) reported that intracellular Ca^{2+} can be regulated by Na^+/ Ca^{2+} membrane exchange. However, the current study did not address whether better exclusion of sodium from the cells is due to an active response to the high salinity conditions, or a function of existing differences in microbial populations between the two reactors. Either way, this result provides an avenue for further exploration in assessing how granule structures adapt to high salinity wastewater environments.

4.5. **Summary**

Community analysis showed that the population of both reactors converged towards a halophile-dominated system, but the differences in granule size and integrity indicate a positive effect of inoculating with halophilic organisms. Most notably, bioaugmentation with halophilic organisms resulted in much less sensitivity of EPS and ALE production to salinity, particularly at hypersaline conditions. Additionally, intracellular cation concentrations were much lower in the halophile-amended system throughout the hypersaline range. Sodium substitution for divalent cations in the EPS, by contrast, occurred to a similar extent in both reactors and did not correspond to changes in granule integrity.

CHAPTER 5

Biodegradation of aromatic compounds under hypersaline conditions: Comparing aerobic biofilm reactors with conventional activated sludge

5.1. Introduction

The increasing demand for fossil fuels has stimulated the generation of oil and gas wastewater, or produced water (PW) (Jimenez et al. 2018, Scanlon et al. 2016). Most existing management strategies for PW, i.e. deep well injection and surface water discharge, can cause serious issues for the environment, such as inducing seismicity, water contamination, etc. (Clark and Veil 2009, Guerra et al. 2011). The water quality of PW depends substantially on geographical features, age of production well, type of well, and extraction technique (Al-Ghouti et al. 2019).PW contains a variety of organic compounds, including natural occurring organic matter and production chemicals (Butkovskyi et al. 2017, Li 2013, Orem et al. 2014). The most predominant organic component commonly found in PW include oil and grease, organic acids, and benzene, toluene, ethylbenzene, and xylenes (BTEX) (Al-Kaabi et al. 2019). The presence of refractory organic compounds limits options for cost-effective treatment (Nie et al. 2020).

Biological treatment has become a standard approach for removing organics from wastewater due to its economic and sustainability advantages over physico-chemical processes and the ability to remove a wide range of contaminants and associated intermediate byproducts. (Acharya et al. 2019, Ren et al. 2017, Silva et al. 2019, Sudmalis et al. 2018, Wang et al. 2018b). However, the presence of refractory and toxic organic compounds in PW can pose a tremendous threat to biological treatment systems, particularly when biodegradation pathways result in the production of secondary byproducts with higher toxicity than the parent compounds, such as catechol production during the aerobic biodegradation of benzyl alcohol and phenol (Kim and Ihm 2011, Ramos et al. 2015). Microorganisms may be more sensitive to mixtures of toxic compounds than to the compounds individually (Boyd et al. 1997, Schmidt et al. 2005). The high salinity of

many produced waters provides an additional source of stress on biological treatment components (Nie et al. 2020). For these reasons, implementation of conventional activated sludge (CAS) for petroleum wastewater treatment is typically unreliable s (Felz et al. 2020, Gao et al. 2020).

Biofilm techniques have shown promise as an alternative treatment approach to CAS systems that provide additional protection against toxic and shock loadings to the embedded microorganisms (Wang et al. 2018a, Yusoff et al. 2018, Zhao et al. 2019). Substrates mass-diffusion transport through biofilm improves the ability of microorganisms to withstand toxic and other potential shocks (Corsino et al. 2015, He et al. 2020a, Ofman et al. 2020). Aerobic granular sludge (AGS), as a self-immobilized biofilm technique, is a new technology that has seen rapid growth for municipal and industrial wastewater treatment within the last decade (Wu et al. 2020b). The granule structure controls the flux of organic compounds to the biomass and helps to retain slower growing microorganisms, resulting in a robust system with multiple potential biodegradation pathways (Corsino et al. 2017, Fang et al. 2018b, Li et al. 2017, Ou et al. 2018a, Ramos et al. 2015).

Hybrid biofilm techniques have also been applied recently to further improve the performance of self-immobilized systems (Wang et al. 2018b). The use of hybrid biofilm techniques, including integration of granular activated carbon (GAC) as an adsorptive biofilm surface (Bio-GAC), can further improve treatment performance by incorporating both biological and physico-chemical processes to remove organics (Wang et al. 2018b, Zhang et al. 2013). The high adsorption capacity of GAC can act as a short-term sink for organic compounds (Figure 5-1). reducing toxicity and protecting against toxic shocks (Puyol et al. 2015). Over time, the biodegradation of refractory organic compounds is achieved due to close proximity of the attached biomass to adsorbed organic matter and nutrients (Puyol et al. 2015, Wang et al. 2018b). The Bio-

GAC design can also reduce the amount of GAC required compared to packed biofilm reactors and improve the settling properties of the biomass (Loukidou and Zouboulis 2001, Wang et al. 2018a, Wang et al. 2018b).

The current study examined the use of biofilm based aerobic reactor designs to improve the biodegradation of aromatic hydrocarbons in a high-salinity, produced water environment. A mixture of benzyl alcohol and o-cresol (daughter products of toluene biodegradation) along with phenol were supplied as the carbon source. These compounds are representative of the most commonly found aromatic compounds in produced water. Two different biofilm techniques, AGS and Bio-GAC, were compared with a CAS reactor for their ability to remove influent aromatics and prevent the formation of toxic by-products. Batch studies and X-ray photoelectron spectroscopy (XPS) were used to further examine the sorption and biodegradation processes involved in aromatic removal in the two biofilm reactor configurations.

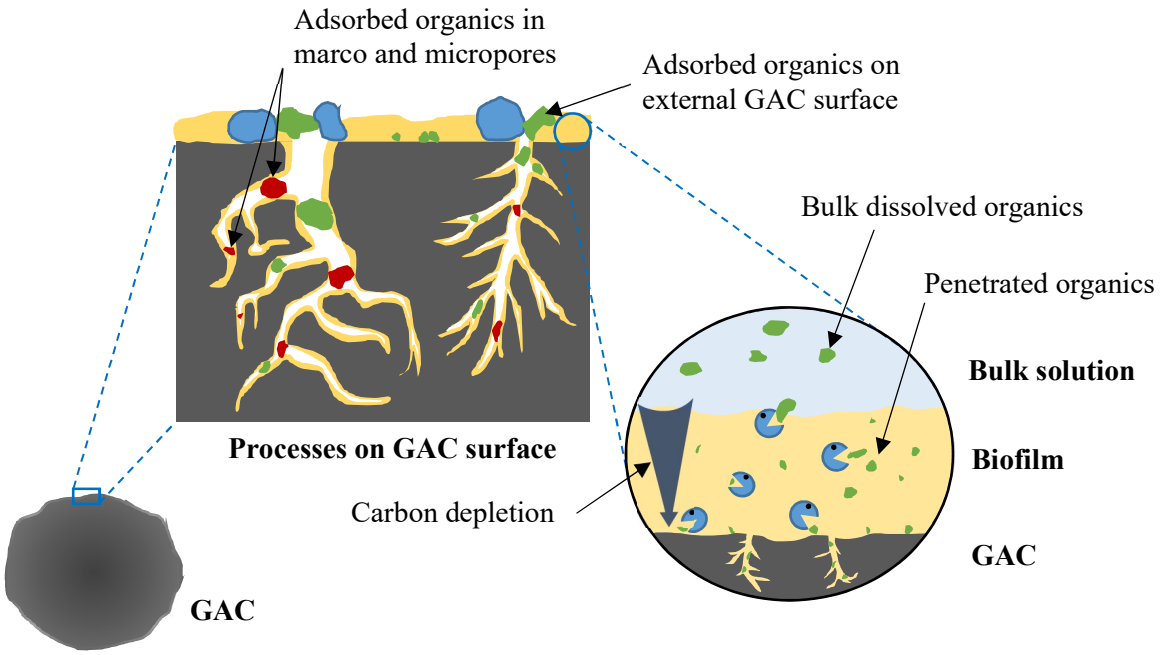

Figure 5-1: Conceptual sketch of anticipated bioactivity within attached biofilm in Bio-GAC system.

5.2. Experimental Section

5.2.1. Experimental Setup

Three identical aerobic bench scale sequencing batch reactors (SBRs) were used in this study. Each SBR had a working volume of 3.0 L, inner diameter of 65 mm, height of 885 mm, and volume exchange ratio of 50%. Fine bubble diffusers were installed at the bottom of each reactor to provide the required oxygen demand for maintaining aerobic process. The cycle time for the AGS and Bio-GAC reactors was 12 h, comprised of 30 min anaerobic feeding, 680 min aeration, 5 min settling, and 5 min decanting. The CAS reactor was operated with the same 12 hour cycle, but had 665 minutes of aeration and 15 minutes settling to retain activated sludge in the reactor. The temperature for all SBRs was maintained at 21± 1 °C.

The AGS and CAS reactors were inoculated with 6000 mg L^{-1} of aerobic granular sludge and activated sludge, respectively. Both inoculums had been previously adapted to a high-salinity environment (85 g L^{-1} NaCl) as described in our previous experiment, and consisted primarily of halophilic organisms. The Bio-GAC reactor was inoculated with a mixture of 125 g of Filtrasorb 400 GAC and 6000 mg L^{-1} of the same above-mentioned AGS. All SBRs were fed with a synthetic brine solution that was described in our previous experiment, using a NaCl concentration of 85 g L^{-1}. During the startup period, acetate was used as the sole carbon source at a concentration of 1350 mg COD L^{-1}.

The development of biofilm on the GAC surface was monitored during the startup period through quantification of DNA on the GAC surface resulting from biogrowth (Figure B1). The collected Bio-GAC samples were rinsed by PBS solution three times prior to DNA extraction process to ensure that all AGS and suspended growth were washed out and taken samples represent grown biofilm on GAC surface only. After 60 days of inoculation, the remaining AGS was washed out by gravity separation, leaving only biofilm-coated GAC in the SBR.

Based on extracted DNA from biofilm on GAC surface, the reactors had reached steady-state operation after 90 days of operation (i.e., the amount of extracted DNA was consistent after 90 days of operation). Beginning at day 90, benzyl alcohol was substituted for a portion of the acetate in the influent feed, increasing to a final concentration of 100 mg L^{-1}. This was followed by addition of o-cresol and then phenol to final concentrations of 100 and 250 mg L^{-1}, respectively, following the schedule in Figure B2. As aromatic compounds were added, the acetate concentration was reduced to maintain a consistent COD addition to the reactors. By day 210 the carbon source for each reactor consisted entirely of the benzyl alcohol, o-Cresol, and phenol mixture at 100, 100 and 250 mg L^{-1}, respectively.

5.2.2. Batch Studies

The biosorption, biodegradation, and volatility of the individual aromatic compounds were investigated for each biomass configuration using small batch reactors over a 12-hour period corresponding to a single cycle for the SBRs. Each batch reactor was filled with 2 liters of the synthetic brine solution containing either benzyl alcohol, o-cresol, or phenol as the only carbon source and injected with air at a rate of 2.2 liter per minute. For each aromatic compound, a control reactor to assess potential losses from volatilization was carried out using an aerated batch reactor with no biomass present. Biosorption and biodegradation studies were carried out using acclimated biomass from the AGS, Bio-GAC or CAS reactor that had been previously adapted to the aromatic carbon feed. For biosorption studies, the biomass material was treated with 4% paraformaldehyde in PBS solution at 4 °C to inactivate the organisms (Dernburg 2012). Biodegradation studies were carried out in an identical manner using active biomass.

5.2.3. Analytical methods

Aromatic compounds were extracted from wastewater samples using a solid-phase extraction method based on Kovács et al. (2011). 100 mL of diluted sample was loaded to Bond

Elut Jr. Plexa 200 mg cartridges and 5 mL of acidified acetone with 1% acetic acid were used to elute the samples. Collected samples were spiked with 50 μL of 600 mg L^{-1} chlorodecane solution prior to injection into an Agilent 7890B Gas Chromatograph (GC) for analysis using a Agilent 19011S-433UI column. Selected ion monitoring mode (SIM) was used to quantify identified peaks.Catechol was assessed according to the method of Keshvari and Bahram (2017) (Keshvari and Bahram 2017) using aggregation of 20 nm gold nanoparticles to quantify the concentration of catechol present. To avoid chloride interference, all the samples were passed through Dionex™ OnGuard™ II Ag/H 2.5 cc cartridges prior to catechol quantification.

Characterization of biofilm growth in the AGS and Bio-GAC reactors was performed by scanning electronic microscopy (SEM). Representative samples were collected from reactors one week after changing the carbon source. Paraformaldehyde 4% in PBS solution was applied overnight on all samples to inactivate the biomass, followed by washing ans post-treatment according to the procedure proposed by Bassin et al. (2012). The fixed samples were dried with hexamethyldisilazane reagent for 20 min and then mounted on SEM studs. Selected samples were coated with 10 μm of gold powder with EMS150R S compact rotary sputter coater. SEM analysis was performed by FEI VERSA 3D dualbeam field emission/ low vacuum scanning electron microscopy.

X-ray photoelectron spectroscopy (XPS) (PHI 5000 VersaProbe II, Physical Electronics Inc.) was employed to observe accumulation and breakdown of benzyl alcohol, o-Cresol, and phenol in the biomass of each reactor. About 1 g of biomass from each reactor was added to 50 mL of solution containing the same mixture of aromatic compounds as the final reactor feed for one hour with continued aeration. Biomass samples were collected at the end of this hour (“feast phase” samples) for XPS analysis. Additional biomass samples from the reactor were put in aerated

PW with no added carbon source for 24 h ("famine phase" samples) prior to collection. All feast and famine phase samples were dried at 30 °C overnight then mounted on XPS standard sample studs using double-sided tape. The X-ray beam size was 100 μm and survey spectra were recorded with pass energy (PE) of 117 eV step size 1 eV and dwell time 20 ms, whereas high-energy resolution spectra were recorded with PE of 23.5eV, step size 0.1 eV and dwell time 20ms. The collected data was analyzed using a Multipak and CasaXPS software tools. The binding energies were calibrated using the C_{1s} and O_{1s} peaks for carbon and oxygen respectively at 284.6 and 532.3.

5.2.4. Microbial community analysis

Illumina MiSeq 16S targeted gene sequencing was carried out on representative samples collected in duplicate to characterize the microbial community in each reactor at different stages of the experiment. Sequence data was processed using the Quantitative Insights into Microbial Ecology2 (QIIME2 v2019.4) (Bolyen et al. 2019). A detailed description of the methods used for sample collection, DNA extraction, library preparation and sequence data analysis details are explained in section (3.6.2).

5.2.5. Statistical analysis

One-way analysis of variance (Scheuner et al.) was employed to run the statistical analysis for the data acquired from all SBRs. The gained microbiome data was analyzed by R version 3.4 (R Core Team, http://www.r-project.org/). A 5% level of statistical significant was used throughout. Mean data points were used to plot figures in this paper and the error bars represent 95% confidence intervals.

5.3. Results and discussion

5.3.1. Batch experiment

Volatile losses due to aeration were negligible for all compounds (Figure B3). The inactivated AGS and CAS biomass showed similar patterns of biosorption, with most loss of compounds from solution occurring in the first hour of contact time (Figure 5-2). The AGS reactor

had greater biosorption of o-Cresol and phenol than CAS ($p < 0.05$), but benzyl alcohol results were similar. In both cases, o-Cresol showed the least sorption (less than 50% loss in AGS, less than 25% loss in CAS). The Bio-GAC material had the highest levels of biosorption of all three compounds, with less than 20% of each compound remaining in solution after 12 hours of contact time (Figure 5-2 a). Again, o-Cresol had the least removal from solution. The continuous reduction in aromatic concentration in Bio-GAC reactor might be attributed to a slower sorption/diffusion process into the GAC, or it could indicate that the fixation process was inactive for the biofilm fixation on the GAC. The possible scenario in this case is that the adsorption of paraformaldehyde on GAC surface could mitigate its toxicity and helped some of microorganism to survive this toxic shock. Thus, some of bioactivities were taken place in fixed Bio-GAC biofilm.

The biodegradation batch experiment showed that the all three aromatic compounds were removed entirely in Bio-GAC batch reactor after three hours of contact with active biomass (Figure 5-2). The integrated biological and physico-chemical processes on GAC surface might contributed to this fast removal of organic load. The AGS batch reactor achieved > 99 % benzyl alcohol removal after 5 hours of operation and approximately 93.6 % and 94.4 % of phenol and o-Cresol were removed by the end of 12-hour cycle time. The performance of batch CAS reactor was the lowest among all run reactors. Approximately 99 %, 87.7 % and 89.2 % of benzyl alcohol, phenol and o-Cresol were removed in batch CAS reactor. Although the microbial communities in AGS and CAS reactors were similar, the performance of them were significantly different. This observation showed that the existed biofilm in AGS system played a crucial role to improve bioreactor performance in terms of aromatic compounds removal.

5.3.2. Biodegradation in the sequencing-batch reactors

The performance of all three reactors was consistent over 30 days after the phase II startup period. Bio-GAC reactor showed high performance in terms of aromatic compounds removal,

approximately 99 % of parent aromatic compounds (benzyl alcohol, phenol and o-Cresol) were removed. The concentration of catechol, a bioproduct of phenol and benzyl alcohol biodegradation, in effluent was approximately 0.4 ± 0.1 mg L^{-1}. The AGS reactor achieved > 99 % , 90 % and 92 % removal of benzyl alcohol, o-Cresol and phenol respectively. The concentration of catechol decreased from 0.9 ± 0.1 to 0.4 ± 0.1 mg L^{-1}. The CAS reactor removed > 99 % of influent benzyl alcohol while it had much lower removal for phenol and o-Cresol, 62.8 ± 5.9 to 73.6 ± 5.6 mg L^{-1} respectively. The concentration of catechol in the effluent was much higher than other reactors, 2.4 ± 0.6 mg L^{-1}. ANOVA analysis showed that there were significant differences among the three reactors in terms of aromatic compounds removal and catechol generation.

Biofilm based SBRs (i.e., AGS and Bio-GAC) showed excellent removal of all three influent aromatic compounds over a single cycle (Figure 5-3). In the Bio-GAC reactor, rapid sorption resulted in maximum concentrations of 14, 15 and 82 mg L^{-1} for benzyl alcohol, o-cresol and phenol, respectively at 0.5 hours, the end of the feed portion of the cycle. Within 4 hours, all three compounds were not detectable in the aqueous phase. The AGS reactor had higher peak concentrations of all three compounds, particularly phenol (150 mg L^{-1}). Only benzyl alcohol was completely removed from the aqueosu phase dbefore the end of the SBR cycle, while o-cresol and phenol showed 94% and 89% removal, respectively. The CAS reactor had much lower removal for phenol (58%), but achieved 93% and 89% removal for benzyl alcohol and o-cresol, respectively. The high phenol concentration in the CAS reactor at time zero is consistent with substantial carryover from the previous cycle. ANOVA analysis showed that removal effecieny for for all three compounds in CAS reactor was signifiantly lower than that in the Bio-GAC and AGS reactor. The perfromance of the Bio-GAC and AGS reactors was staistical similar in terms of benzyl alcohol and o-cresol removal,but phenol removal was significantly higher in the Bio-

GAC reactor. . The development of biofilm in these biosystems protected the embedded microorganisms and enhanced biodegradation of aromatic compounds (Yusoff et al. 2018). In addition, the faster biodegradation process in Bio-GAC SBR can be contributed to integrated biological and physico-chemical processes on GAC surface (Zhang et al. 2013).

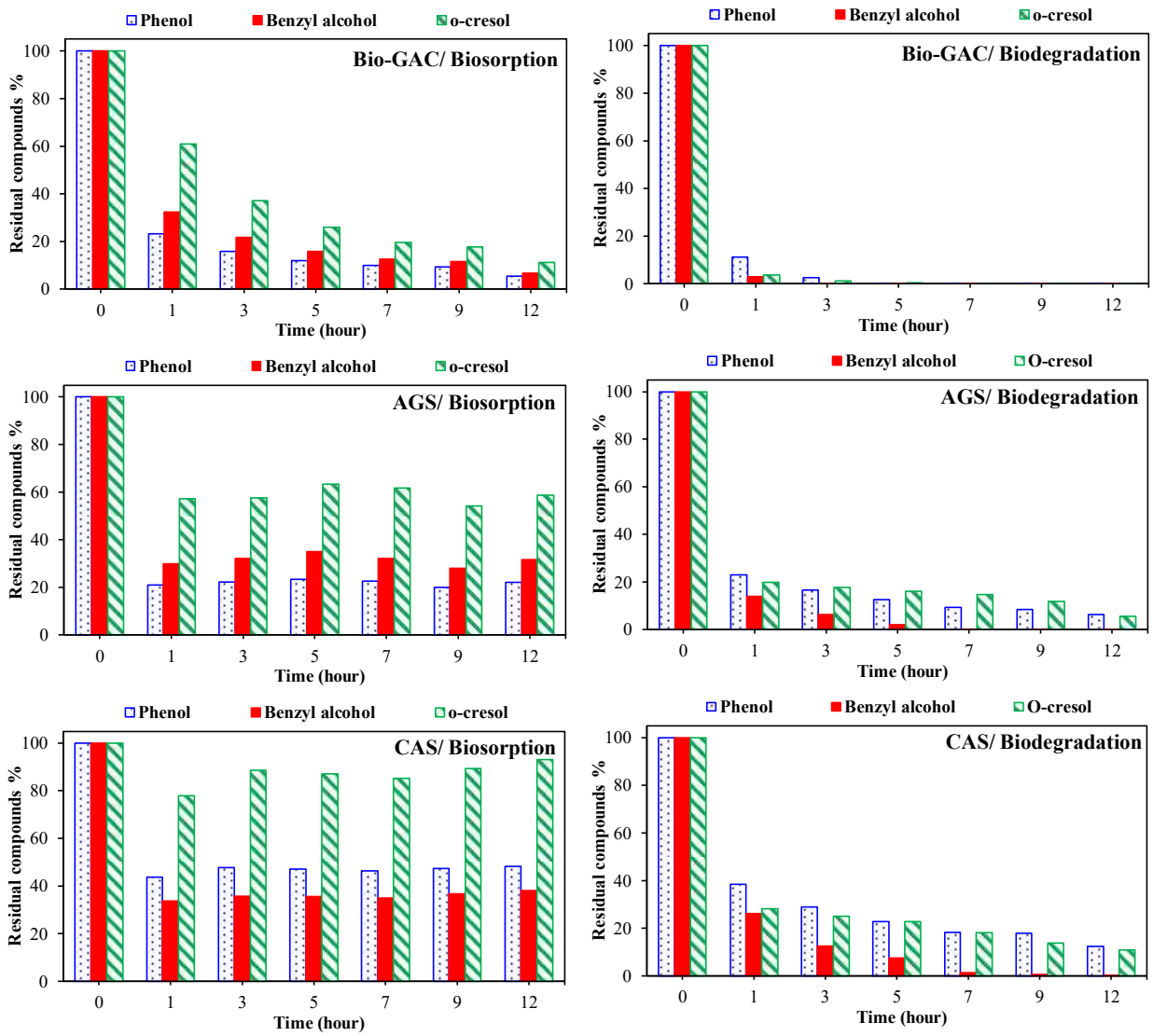

Figure 5-2: Biosorption of aromatic compounds: Bio-GAC (a), AGS (b), and CAS (c).

Catechol and benzaldehyde were observed as putative metabolic intermediates of phenol and benzyl alcohol degradation (Figure 5-3). The maximum benzaldehyde concentration in solution was 24.1 mg L^{-1} and 28.1 mg L^{-1} in AGS and CAS reactor respectively, with peak

concentrations occurring 1 hour into the reactor cycle. Benzaldehye was not detected in the Bio-GAC reactor. Catechol was detected in all three reactors at maximum concentrations of 9.1, 6.2 and 4.6 mg L^{-1} for Bio-GAC, AGS and CAS respectively. Catechol concentrations in the Bio-GAC and AGS reactor increased over the first half of the cycle time but decreased to < 5 mg L^{-1} in hours 11 to 12, which indicates that catechol could be utilized as a carbon source by these microbial populations. Catechol formation is also further direct evidence of biodegradation occurring in the Bio-GAC reactor, rather than sorption and accumulation of the influent aromatics on the activated carbon. Catechol concentrations in the CAS reactor never exceeded 5 mg L^{-1}, but were more consistent throughout the whole cycle. The generation of these intermediate byproducts is attributed to previously described aerobic metabolic processes for benzyl alcohol and phenol. (Pugh et al. 2015, Zou et al. 2018). The byproduct derivatives were generated simultaneously with the reduction of mother compounds, which confirms the proposed biodegradation pathways (Figure B4). Overall, the performance of biofilm systems was higher than conventional activated sludge both for removal of influent aromatic compounds and for their derivatives. This finding is in agreement with previous studies (Kondash et al. 2017, Oberoi and Philip 2017a, Yusoff et al. 2019).

5.3.3. Biofilm morphology

SEM images were used to monitor biofilm development in the Bio-GAC and AGS reactors as aromatic compounds were added to the system. At the end of the startup period, the Bio-GAC reactor showed substantial biofilm growth on the activated carbon surface, but major gaps and breaks in the biofilm were also visible (Figure 5-4 a and c). The substitution of aromatic compounds for acetate had a detrimental impact on biofilm morphology in both reactors (Figure 5-4). The biofilm density of biofilm was much less uniform, with big holes were observed in both systems by the end of startup period (Figure B5). SEM imaging also revealed that significant

differences between Bio-GAC and AGS biofilm were observed in terms of texture of biofilm and type of bacterial growth. The developed biofilm on GAC surface during the startup period comprised cocci bacteria only (Figure B6), while AGS biofilm contained both strip-like and rod shape bacteria entangled together (Figure B7). The different biofilm formation conditions could select for different microbial community (Yusoff et al. 2019). AGS biofilm is developing by coiling while the biofilm in Bio-GAC is formed by adhesion to carrier media (Xu et al. 2020). The similar findings were observed by previous studies (Asri et al. 2018, Dai et al. 2019). As the study went on, both cultures could establish homogenous biofilm. The appearance of mature biofilm in Bio-GAC was smooth and comprised a mixture of short-rod-like and string-like biogrowth (Figure B8) while the appearance of mature biofilm in AGS reactor was colonized and dominated by short-rod-like biogrowth (Figure B9).The mature biofilm after 240 days showed complete biofilm coverage of the activated carbon surface (Figure B10). Despite the differences in composition, both reactors were able to establish strong biofilm structures after they adapted to the presence of aromatic compounds. This strong biofilm structure can protect individual microorganisms against toxic impacts of the influent aromatics while keeping them available as a carbon source (through sorption in the case of Bio-GAC, or slow diffusion into the AGS granules). These factors likely are responsible for the higher performance of biofilm-based reactors compared to CAS.

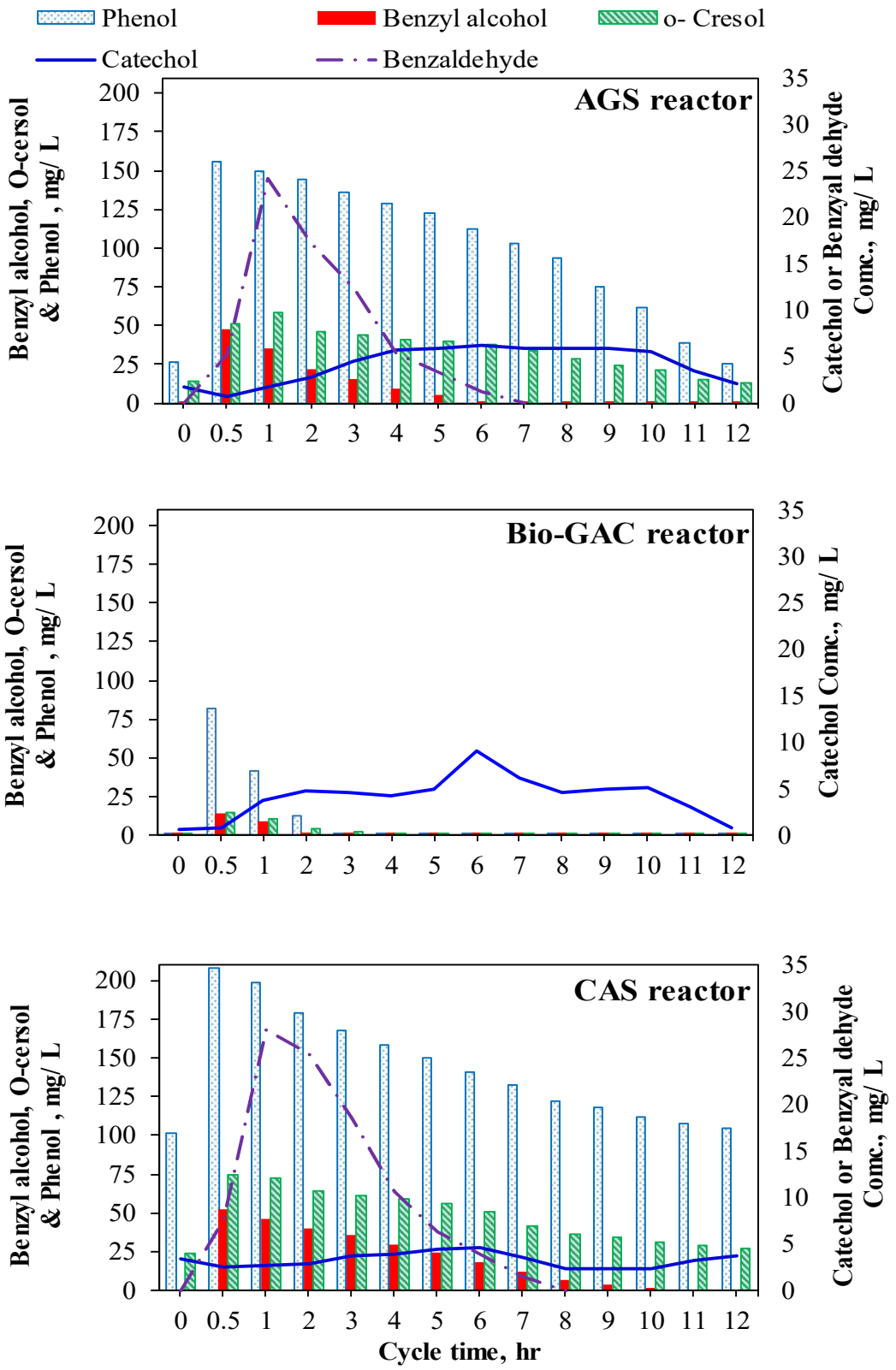

Figure 5-3: Aromatic compounds biodegradation and intermediate derivatives generation over cycle time of SBRs.

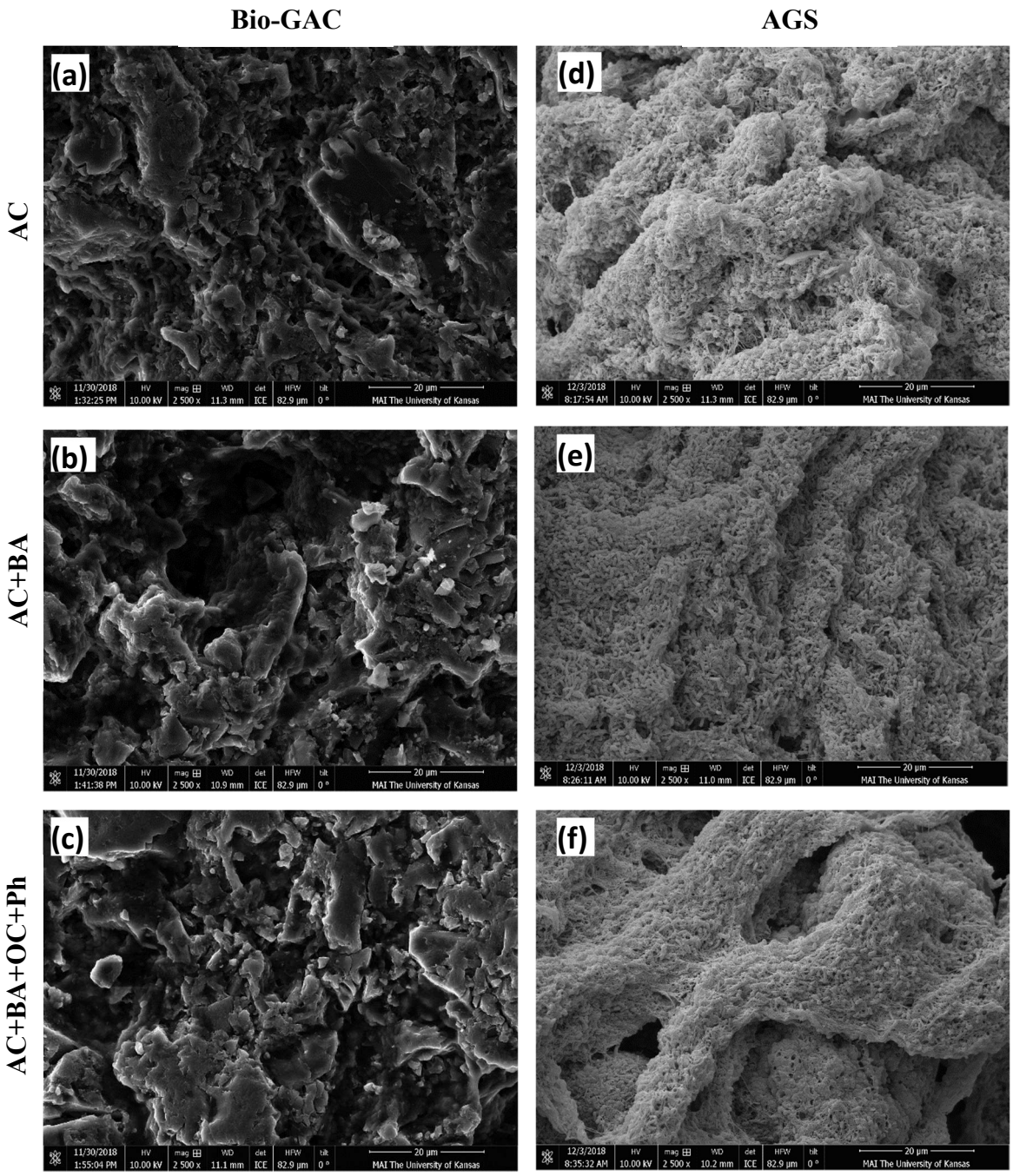

Figure 5-4: SEM observation showing the impact of carbon source changing on biofilm morphology. (a), (b), and (c) GAC fed with (AC), (AC, BA) & (AC, BA, OC and Ph) as carbon source respectively and (d), (e), and (f) AGS fed with (AC), (AC, BA) & (AC, BA, OC and Ph) as carbon source respectively too.

5.3.4. Biofilm activity

The specific oxygen uptake rate (SOUR) was measured at different points during the experiment to assess the impact of each new aromatic compound on microbial activity. During the

startup phase, with acetate as the sole carbon source, the CAS reactor showed the highest activity (45±1.4 mg O_2 g^{-1} MLVSS-h), while the AGS reactor had the lowest activity under the same conditions (Figure 4). When benzyl alcohol was added, the SOUR for the CAS reactor dropped to 10 mg O_2 g^{-1} MLVSS-h, and continued to decrease as o-cresol and phenol were added. Biomass activity in the Bio-GAC and AGS reactors was less affected by the change in carbon composition. The lowest SOUR values for both reactors were recorded when o-cresol was added to the system, but were unaffected by the substitution of phenol for the remaining acetate. ANOVA analysis revealed that the activity of biomass in Bio-GAC, AGS and CAS was significantly different ($p < 0.05$) when all three reactors were compared while differences between the Bio-GAC and AGS reactors were not significant ($p > 0.05$). These results are consistent with the lower level of aromatic removal observed in the CAS reactor, and further indicate that both of the biofilm reactors provide better environments for aromatic biodegradation.

The integrated biological and physico-chemical processes could have played a crucial role to mitigate the toxicity of aromatic compounds in Bio-GAC reactor, which boosted the activity of biomass in that system (Xu et al. 2020, Yusoff et al. 2019). Although the microbial communities in CAS and AGS reactors were similar as shown in Figure 7, the activity of biomass in AGS reactor was significantly different ($p< 0.05$). The main merit of biofilm in AGS bioreactor is that to control substances diffusion through AGS structure and protect the embedded microorganisms against shocks (Gao et al. 2020, He et al. 2020a, Xu et al. 2020).

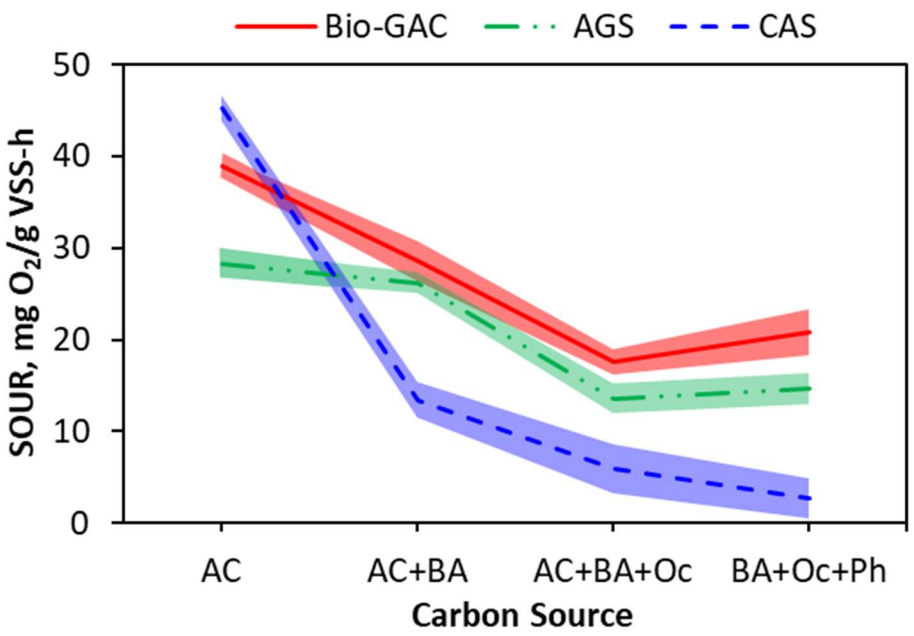

Figure 5-5: Activity of microorganisms in the three bioreactors measured as SOUR. The shaded area represents 95% confidence interval of observed means and the dashed lines show the mean values.

5.3.5. Observation of biosorption and biodegradation by XPS analysis

We have employed XPS analysis to observe aromatic accumulation and degradation within the biofilm of Bio-GAC, AGS, and CAS cultures. Wide survey XPS spectra over the energy range of 0-1100 eV shows the presence of C, O, N, Na and Cl as major elements in the sample, with Na and Cl resulting from the high aqueous salinity (Figures B11 to B13). High-resolution scans from 282 to 290 eV were used to better identify the forms of carbon present in the samples. Peak fitting was used to classify the carbon into four forms; C-(C,H), C-(O,N), O-C-O, and COOR, based on previously published approaches (Fang et al. 2018b, Yin et al. 2015) (Figure 5 a). These peaks represent lipid side chains and/ or amino acids, alcoholic compounds or proteins, carboxylate or carbonyl groups, and carboxyl or esters, respectively.

The oxygen peak resolved into two sub peaks for all analyzed samples (Figure 5-6 b). The peak located at 531.5 ± 0.4 represents C=O oxygen forms, such as carboxylate, carbonyl, and ester

groups. The second peak appeared at 532.5 ± 0.4. This peak is attributed to C-OH(C-O-C), which represents alcoholic compounds and/ or acetal groups (Fang et al. 2018b, Yin et al. 2015).

Table 5-1: Peak position, % content, O and N ratios with respect of C for Bio-GAC specimens.

	Aromatic fed		Famine phase		Fresh GAC		
Element	**Peak (eV)**	**Content %**	**Peak (eV)**	**Content %**	**Peak (eV)**	**Content %**	**Assignment**
C_{1s}	284.97 ± 0.2	48.12 ± 2.1	284.16 ± 0.10	37.46 ± 1.8	283.4 ± 0.1	27.8 ± 1.8	C-(C,H)
C_{1s}	285.64 ± 0.5	37.13 ± 3.2	285.02 ± 0.19	22.48 ± 1.6	283.6 ± 0.1	29.8 ± 2.6	C-(O, N)
C_{1s}	286.80 ± 0.7	10.96 ± 2.2	285.83 ± 0.1	16.7 ± 1.8	284.9 ± 0.2	22.5 ± 1.1	C=O,O-C-O
C_{1s}	287.76 ± 0.2	13.79 ± 1.7	287.39 ± 0.11	23.35 ± 0.5	287.7 ± 0.2	19.9 ± 1.9	COOR
O_{1s}	531.60 ± 0.2	54.84 ± 1.6	530.75 ± 0.06	48.78 ± 1.25	531.3 ± 0.1	28.2 ± 1.4	C=O
O_{1s}	532.98 ± 0.2	35.79 ± 2	532.12 ± 0.07	36.17 ± 2	533.2 ± 0.2	11.4 ± 1.8	O-(C,H)
N_{1s}	400.10 ± 0.2	21.71 ± 1.9	397.53 ± 0.22	1.12 ± 0.5			N_{nonpr}
N_{1s}	401.31 ± 0.4	3.6 ± 1.5	399.33 ± 0.1	25.29 ± 1.3			N_{pr}
O/C		90.63 ± 3.1		84.95 ± 2.7		39.55 ± 3.5	
N/C		7.13 ± 3.2		26.42 ± 1.6			

Table 5-2: Peak position, % content, O and N ratios with respect of C for AGS specimens.

	Aromatic fed		Famine phase		Acetate fed		
Element	**Peak (eV)**	**Content %**	**Peak (eV)**	**Content %**	**Peak (eV)**	**Content %**	**Assignment**
C_{1s}	284.25 ± 0.3	49.24 ± 1.8	284.55 ± 0.3	36.35 ± 1.3	284.02 ± 0.1	31.32 ± 2.1	C-(C,H)
C_{1s}	284.66 ± 0.4	4.96 ± 0.5	285.52 ± 0.7	2.61 ± 0.2	284.84 ± 0.1	3.19 ± 1.1	C-(O, N)
C_{1s}	286.21 ± 0.5	29.80 ± 0.8	286.52 ± 0.7	36.27 ± 1.1	285.77 ± 0.2	29.84 ± 2.1	C=O,O-C-O
C_{1s}	288.07 ± 0.6	16.12 ± 1.1	288.35 ± 0.9	24.76 ± 1.2	287.44 ± 0.1	34.04 ± 3.1	COOR
O_{1s}	531.27 ± 0.7	14.22 ± 0.9	531.66 ± 0.7	47.78 ± 2.5	530.74 ±0.2	56.26 ± 3.6	C=O
O_{1s}	532.61 ± 0.6	57.75 ± 1.3	533.18 ± 0.9	10.03 ± 0.5	532.20 ± 0.1	18.27 ± 1.8	O-(C,H)
N_{1s}	399.41 ± 0.2	10.13 ± 0.5	399.38 ± 0.1	20.36 ± 1.2	397.57 ± 0.7	0.36 ± 0.2	N_{nonpr}
N_{1s}	401.03 ± 0.7	0.81 ± 0.5	400.70 ± 0.1	1.21 ± 0.5	399.29 ± 0.2	15.12 ± 1.3	N_{pr}
O/C		72 ± 1.8		57.81 ± 1.8		74.53 ± 3.2	
N/C		11 ± 2.1		21.56 ± 1.2		15.38 ± 1.6	

The mass fractions of carbon in the samples that collected from all SBRs under feast and famine phases were calculated as a percent of the total area under carbon, oxygen and nitrogen then compared with each other to observe the reduction in carbon content (Table 5-4). Under feast conditions, the AGS biomass has the highest carbon content of the three samples. Under famine

conditions, the carbon content in the AGS samples decreased by 5%, while the carbon content of the other two samples changed by less than 1% (Table 5-4).

Table 5-3:Peak position, % content, O and N ratios with respect of C for CAS specimens.

	Aromatic fed		Famine phase		
Element	**Peak (eV)**	**Content %**	**Peak (eV)**	**Content %**	**Assignment**
C_{1s}	284.40 ± 0.2	37.5 ± 1.4	284.27 ± 0.1	41.2 ± 3.8	C-(C,H)
C_{1s}	285.48 ± 0.1	24.87 ± 1.3	285.31 ± 0.2	13.69 ± 2.5	C-(O, N)
C_{1s}	286.62 ± 0.6	13.3 ± 1.4	285.95 ± 0.1	20.7 ± 1.3	C=O,O-C-O
C_{1s}	287.67 ± 0.1	24.3 ± 2.2	287.34 ± 0.1	24.38 ± 2.4	COOR
O_{1s}	531.19 ± 0.3	45.78 ± 1.2	530.71 ± 0.1	33.1 ± 2.3	C=O
O_{1s}	532.48 ± 0.3	30.84 ± 1.4	532.1 ± 0.1	46.23 ± 3.2	O-(C,H)
N_{1s}	398.62 ± 0.8	7.68 ± 2.2	399.36 ± 0.1	17.8 ± 2.4	N_{nonpr}
N_{1s}	399.62 ± 0.2	14.76 ± 1.6	400.26 ± 0.3	3.87 ± 1.7	N_{pr}
O/C		76.6 ± 2.5		79.25 ± 2.3	
N/C		22.45 ± 3.2		21.7± 1.9	

The AGS samples also had a significantly lower ratio of oxygen to carbon in the biomass than the other two reactors in both the feast phase (O/C molar ratio of 72 ± 1.8 % for AGS, vs 90.63± 3.1 % for Bio-GAC and 76.6 ± 12.5 % for CAS) and famine phase (57.81 ± 1.8 % vs 84.95 ± 2.7 % for Bio-GAC and 79.25 ± 2.3 % for CAS). The ratio of oxygen to carbon in the AGS sample was also more affected by the change from feast to famine conditions (Figure B14).

The distribution of carbon between the identified functional groups were also affected by operational phase (Table 5-2). The C-(O,N) fraction, which includes alcoholic compounds, was reduced significantly in all three samples from feast to famine phase, with much smaller changes for CAS than the other samples. At the same time, the fraction of C-(C,H) increased from feast to famine phase for all three conditions, 14 ± 2 %, 47 ± 2 % and 19 ± 1 % to 41 ± 2 %, 56 ± 3 % and 38 ± 4 % for Bio-GAC, AGS and CAS samples respectively. These changes are consistent with accumulation of the influent aromatic compounds in the biofilm during feast phase followed by

biodegradation during famine phase, which has also been observed in other studies (Wang et al. 2018c, Yusoff et al. 2019). Additional studies also showed that carbon peak positions for AGS samples fed with acetate were located at different binding energies compared to AGS samples that fed with aromatic compounds (Tables 5-1 - 5-3). Peak locations also shifted as the operation conditions have changed from feast to famine phase (Figure B12) and (Tables 5-1 to 5-3). The shifting of peaks' locations suggests that some oxidation and assimilation/ dissimilation reduction activities on adsorbed aromatic compound took place within the biofilm during feast and famine phases (Li et al. 2019, Luo et al. 2020).

Table 5-4: Impact of feast/ famine on carbon content for AGS, Bio-GAC and CAS.

	Carbon content %				
Biofilm type	**Feast**	**STD**	**Famine**	**STD**	**Carbon reduction %**
Bio-GAC	65.07	1.72	64.72	0.33	-0.4
AGS	73.36	2.23	68.38	2.77	-5
CAS	68.44	1.09	68.12	0.91	-0.3

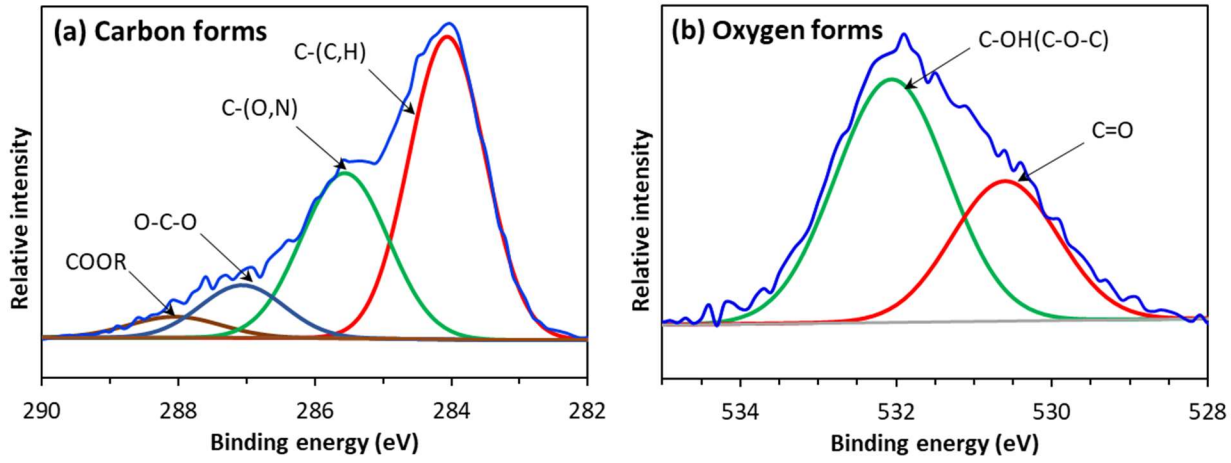

Figure 5-6: XPS scans of excited forms of carbon and oxygen.

The XPS analysis is consistent with the results of the batch biosorption and biodegradation studies and the reactor cycle profile. The AGS reactor, which has rapid biosorption but slower biodegradation (based on Figure 5-3), shows the most difference between feast and famine phases,

as the influent compounds (all containing C-OH functional groups) are taken up into the biomass then broken down over a longer period. The Bio-GAC reactor, which has both rapid sorption and high levels of microbial activity, breaks down the aromatics more quickly. This results in changes in the carbon distribution between feast and functional phases, but less difference in total carbon content. The carbon composition of the CAS reactor, which has the lowest level of biosorption and biodegradation, is least affected by the transition from feast to famine conditions. Overall, these results confirm the advantages previously reported for biofilm-based systems studies (Corsino et al. 2019, Dai et al. 2019, Puyol et al. 2015, Zhao et al. 2019).

Table 5-5: The ratio of carbon and oxygen functional groups to the total carbon.

Biosystem	Phase	Carbon functional groups/ Total carbon			Oxygen functional groups/ Total carbon)		
		C-(C,H)	C-(O, N)	C=O,O-C-O	COOR	C=O	O-(C,H)
Bio-GAC	Feast phase	14 ± 2	38 ± 3	20 ± 2	27 ± 2	55 ± 2	40 ±1
	Famine phase	41 ± 2	20 ± 2	22 ± 2	28 ± 1	49 ± 1	36 ± 1
AGS	Feast phase	47± 2	36± 2	12± 2	5 ± 1	14 ± 1	58 ± 1
	Famine phase	56 ± 3	16 ± 1	15 ± 1	12 ± 1	48 ± 3	10 ± 1
CAS	Feast phase	19 ± 1	38 ± 2	27± 1	16 ± 2	46 ± 1	32 ± 1
	Famine phase	38 ± 4	32 ± 3	15 ± 1	16 ± 2	33 ± 2	35 ± 3

5.3.6. Microbial Community Structure

Relative abundance data obtained from Illumina 16S targeted gene sequencing showed that the microbial communities in the acetate fed AGS, Bio-GAC, and CAS reactors were dominated by *Proteobacteria, Bacteroidetes, Actinobacteria,* and *Firmicutes* with relative abundance of 86.9

± 8 %, 9.2 ± 5.6 %, 1.7 ± 1.3 % and 0.8 ± 0.3 % respectively. The microbial structure of all reactors shifted slightly as the carbon source switched from acetate to aromatic compounds, with relative abundances of 91.4 ± 5 %, 6.7 ± 4 %, 0.51 ± 0.1 % and 0.97 ± 1.1 % respectively, for the same four phyla. At the genus level, *Halomonas* had the highest relative abundant in all reactors under initial conditions, at 56.4 ± 1.2 %, 61.2 ± 1.1 % and 58.1 ± 0.95 % for Bio-GAC, AGS and CAS respectively. *Marinobacter* was the next highest genus in Bio-GAC but had a much smaller presence in the other two systems. As the aromatic compounds replace acetate in the reactor feed, *Marinobacter* species became dominant in the Bio-GAC reactor. *Marinobacter*, *Halomonas* and *Marinicella* represented 97 % of the detected genera in Bio-GAC reactor at the end of the experiment. In the AGS and CAS reactors, by contrast, *Halomonas* continued to be the most common genera, although the addition of phenol was accompanied by a substantial increase in the *Marinobacter* component of both systems. These two genera accounted for ~ 75% of the total abundance in both reactors under final conditions, with no other genera above 4% contribution.

The microbiome analysis revealed that the microbial community has shifted in all reactors as the carbon source changed from acetate to a mixture of aromatic compounds (Figure 5-7). The selection for *Marinobacter* over other halophilic genera in the Bio-GAC reactor may be due to the known surface properties of *Marinobacter*, such as hydrophobicity and adhesion phenomenon, that make it adhere more strongly to GAC surface (Consuegra et al. 2020, Guo et al. 2019). The high performance of Bio-GAC can be attributed to presence of *Marinobacter* has also been shown to achieve high levels of aromatic compounds biodegration, consistent with the better performance of the Bio-GAC reactor (Appolinario et al. 2019). The microbial community analysis also showed that the introducing phenol to the recipe of wastewater was selected for *Marinobacter* in all reactors (Figure 5-7). The relative abundance of *Marinobacter* increased from 44 %, 6 % and 3 %

to 77 %, 26 % and 27 for Bio-GAC, AGS and CAS cultures respectively. This finding indicates that phenol is one of favorable biodegraded substances for *Marinobacter.* The zeta potential of *Halomonas* surface is lower than that of *Marinobacter*, which reduces the electrosatic repulsion among *Halomonas* cells. This could be related to the continued abundance of *Halomonas* genus in AGS reactor, with the lower zeta potential producing a more compacted floc structure (Consuegra et al. 2020). *Marinicella* is classified as a denitrifying genus (Villemur et al. 2019), and the deep crevices in GAC can provide a suitable anoxic environment for it. This may explain the high relative abundance of *Marinicella* in Bio-GAC reactor compared to other SBRs.

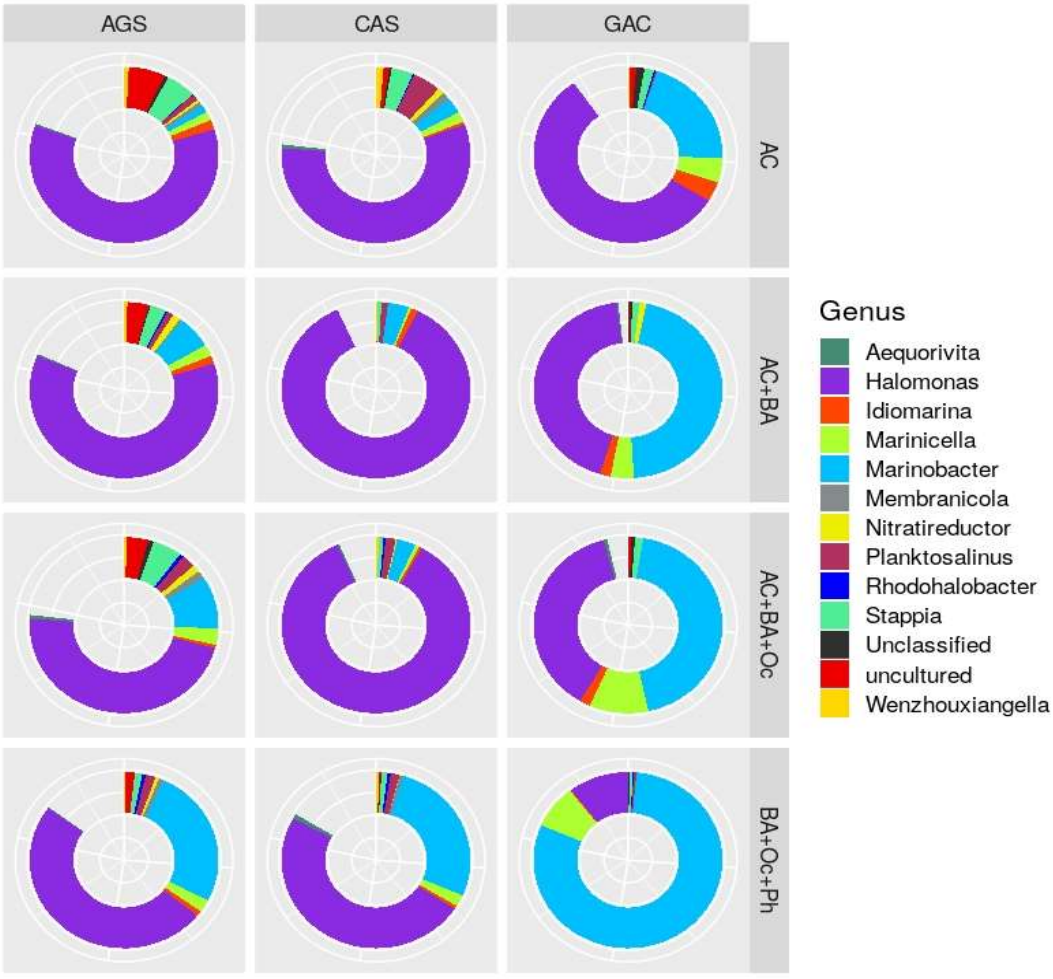

Figure 5-7: Stacked bar plot showing taxa relative abundance of 0.1% at genus level for microbial community from AGS, CAS and Bio-GAC reactors.

5.4. Conclusions

In this study, the performance of two different biofilm-based reactors was compared to conventional activated sludge system. The capacity of biofilm to accumulate organic matter was observed by running batch experiment and XPS analysis. Biofilm-based reactors achieved the higher adsorption capacity compared CAS flocs. The integrated results from batch experiment and XPS analysis showed that the high adsorption capacity was associated with high removal efficiency. The detected intermediate derivative compounds suggest that the approach that used by microorganisms was to adsorb then biodegrade organic matter, or both processes can happen simultaneously. SEM observation showed that the biofilm morphology was impacted by changing the carbon source, but both reactors (bio-GAC and AGS) could acclimate and establish strong biofilm structure after the startup period was finished. The microbiome analysis proved that the biocommunity structure is a function of carbon source and operation conditions. Finally, Bio-GAC reactor is a promising alternative to conventional biological treatment systems because it had the highest performance among all reactors in terms of biosorption and biodegradation of the selected aromatic compounds.

CHAPTER 6

Long-term performance of aerobic versus anaerobic biofilm systems under hypersaline conditions and toxic organic load

6.1. Introduction

Oilfield-produced water (PW) is a toxic wastewater due to the presence of a mixture of hydrocarbon compounds and production chemicals (Ibrahim et al. 2020b, Nadella et al. 2020, Silva et al. 2020). Existing management strategies, such as surface water discharge and deep well injection have created serious environmental concerns (Nadella et al. 2020, Warren 2019). A major factor limiting treatment options is the high salinity found in many produced waters (Yousefi et al. 2019), which can reduce the effectiveness of both biological and chemical processes for removing organic constituents.

Biological treatment is commonly applied as a cost-effective treatment option to remove organic load from wastewater (Nie et al. 2020). Both the toxicity and high salinity of PW pose tremendous challenges to the use of conventional activated sludge systems (CAS) for treatment of petroleum wastewaters (Huang et al. 2017, Zhang et al. 2018, Zou et al. 2020). Biofilm-based biological treatment systems, however, have gained attention as sustainable, cost-effective, and more environmentally friendly alternatives to CAS (Asri et al. 2018). Biofilm formation plays a vital role in controlling substrate permeation and retaining slow growing bacteria in a treatment system, which improves the ability of biomass to withstand toxicity and other potential shocks (Mancini et al. 2017, Tang et al. 2020).

Aerobic biofilm-based treatment systems are the most commonly applied processes to treat industrial wastewater due to their smaller footprint, high rate of biological activity and good resilience against shocks (Felz et al. 2020, He et al. 2020b, Pishgar et al. 2020). The major drawback associated with aerobic biological treatment is the relatively high aeration cost, which can reach to 70% of total operation cost (Ekici 2017). Biofilm-based biological treatment

techniques, such as aerobic granular sludge (AGS), can mitigate the cost of aeration significantly (Xue et al. 2017, Zhang et al. 2020). For instance, the biodegradation of 0.43 mmol L^{-1} of phenol to CO_2 requires 2.97 mmol L^{-1} of dissolved oxygen, which is difficult to achieve even if pure oxygen is injected into wastewater. With manipulation of biofilm-based biological treatment, complete transformation of phenolic compounds could be achieved due to the multiple redox zones within the biofilm structure without a high efficiency aeration system (Han et al. 2020). AGS, as an application of biofilm-based treatment systems, has particular advantages in treating strong wastewater (Felz et al. 2020, Liu et al. 2020b). The stratified multiple redox zones that form within the AGS structure enhance utilization of multiple electron acceptors, such as oxygen, nitrate and sulfate simultaneously and thus achieve high *in situ* electron donor biodegradation rate (Han et al. 2020, He et al. 2020a, Li et al. 2020b). Utilization of granular activated carbon (GAC) as carrier media in hybrid biological treatment system provides another approach to promote biomass growth within the GAC reactor (Tang et al. 2020). Integrating physico-chemical processes on the GAC surface with biomass activity in this hybrid system improves the resilience of biofilm-based treatment system against shocks and mitigates the cost of using the GAC because it reduces the amount of needed GAC to 10% of packed bed columns (Hussain et al. 2015, Paredes et al. 2018, Tang et al. 2020). In addition to the role of biofilm in toxic compound mitigation, the adsorption of hydrocarbons on GAC surface can enhance microorganisms' tolerance against toxic substances, and improves overall biosystem performance (Pradhan et al. 2020).

Anaerobic biological processes have also been utilized to treat high-strength wastewater from agricultural and industrial sources, as well as domestic sewage sludge (Chen et al. 2020b). The interest in applying anaerobic processes to handle toxic substances have increased recently due to many advantages of these systems, such as cost-effective, bioenergy recovery, low biomass

yield and elimination of greenhouse gas emissions (Chen et al. 2020a, Genethliou et al. 2020, Kong et al. 2018). Genethliou et al. (2020) utilized an anaerobic upflow packed bed reactor to achieve 95% organic load removal efficiency under thermophilic conditions from olive mill wastewater containing phenolic compounds. Chen et al. (2020b) investigated glutamate-rich wastewater biodegradation pathways using a lab scale up-low anaerobic sludge blanket reactor (UASB) under various hydraulic retention times (HRT). This study showed that the optimum HRT was in the range of 4.5-6 h and the glutamate-rich wastewater was biodegraded in UASB reactor by at least three biodegradation pathways. Yurtsever et al. (2020) showed that an anaerobic membrane bioreactor (AnMBR) could achieve 90% removal efficiency of chemical oxygen demand from real textile wastewater.

Although these results show the potential of anaerobic treatment systems to successfully treat wastewater, the slower biodegradation rates compared to aerobic biological treatment systems result in a larger footprint and potentially higher capital costs for these units (Tisler and Zwiener 2019).

The previous chapter examined the short-term performance of two aerobic biofilm reactors used to biodegrade a mixture of aromatic hydrocarbons under hypersaline conditions representative of the salinities found in many produced waters. The current experimental work was designed to compare the performance of these aerobic biofilm processes with similar reactor designs utilizing anaerobic biological processes over longer treatment period. As with the previous experiment, the designs utilized both a biomass-only and a hybrid system where biofilm growth occurred on the surface of granular activated carbon. Organic load removal efficiency, effluent wastewater characteristics and the resilience to increased loading of toxic compounds was compared for all four reactor designs during operation under hypersaline conditions to assess the

feasibility of the different approaches to treatment of high-salinity wastewaters with potentially toxic organic loads.

6.2. Materials and Methods

6.2.1. Reactors configuration and operational conditions

All reactors were operated under hypersaline conditions using a mixture of aromatic as the sole carbon source. Benzyl alcohol, o-cresol and phenol, with concentration of 100, 100 and 250 mg L^{-1} respectively, were selected to represent the organic load in synthetic PW. Two identical 3.0-L bench-scale sequencing batch reactors (SBRs) were utilized for aerobic biodegradation of the selected aromatic compounds. The first aerobic SBR was inoculated with 6000 mg MLVSS L^{-1} AGS (as mixed liquor volatile suspended solids (MLVSS)) previously acclimated to hypersaline conditions ((Ibrahim et al. 2020a)). The second aerobic SBR was loaded with 125 g of Filtrasorb 400 GAC (Calgon Carbon Co., Pittsburgh, PA) as a carrier media to enhance biogrowth. This reactor was inoculated with 2000 mg L^{-1} of the same acclimated AGS to enhance biogrowth on GAC surface. After 60 days of inoculation, all suspended growth and AGS were washed out and the only remaining biomass was present as a film on the activated carbon (Bio-GAC reactor).. The cycle time for both aerobic systems was 12 h, consisting of30 min anaerobic feeding, 680 min aeration, 5 min settling, and 5 min decanting. The volume exchange ratio was 50% to achieve a target hydraulic residence time (HRT) of 24 h. The temperature was maintained at 21± 1 °C. Further description of the startup and initial operation of these reactors is reported in the previous chapter.

The anaerobic systems consisted of two 4.1-L bench scale reactors. The first anaerobic reactor was seeded with 6000 mg L^{-1} of anaerobic granular sludge from a reactor at the Cedar Rapids, IA Water Pollution Control Facility, and operated as an upflow anaerobic sludge bed (UASB) reactor. The second anaerobic reactor was loaded with a mixture of Filtrasorb 400 GAC

(540 g L^{-1}) from Calgon Carbon Co., PA, and inoculated with 6000 mg MLVSS L^{-1} of anaerobic granular sludge to enhance biofilm growth. After biofilm growth on the GAC surface was observe, the anaerobic granular sludge was washed out and only 170 g of biofilm-coated Filtrasorb 400 GAC was retained in the system, resulting in a hybrid Anaerobic GAC reactor (AnGAC). Prior to this experiment, the biomass in both anaerobic systems had been fed a mixture of 1340 mg L^{-1} of glucose and 10 mg L^{-1} toluene in synthetic PW with a salinity of 3% as NaCl (Warren 2019). Over an 80 day period, the carbon source was switched to a mixture of aromatic compounds and the salinity increased to 85 g L^{-1} (as NaCl) in both reactors (Figure C1). Both anaerobic reactors were operated under continuous flow mode with a HRT of 24 h, upflow velocity of 0.035 cm s^{-1}, and temperature of 35± 1 °C. Variable-speed peristaltic pumps (Cole-Primer model 7524, Masterflex® L/S model no. 07528-10) were used to control wastewater pumping, recycling and waste.

6.2.2. XPS analysis

Biofilm characterization for carbon content in representative samples from bench scale aerobic and anaerobic reactors was observed using X-ray photoelectron spectroscopy (XPS) instrument type PHI 5000 VersaProbe II, Physical Electronics Inc. Selected samples were collected and dried at 30 °C overnight then mounted on XPS standard sample studs using double-sided tape. Data acquisition was achieved using the following parameters: pass energy (PE) of 117 eV, step size 1 eV and dwell time 20 ms. High-energy resolution spectra were then collected using a PE of 23.5 eV with step size 0.1 eV and dwell time 20 ms. Binding energy for carbon atoms was calibrated using the C_{1s} at peak of 284.6. The collected data was analyzed using Multipak software tools.

6.2.3. Aromatic compounds extraction

Solid-phase extraction using Bond Elut Jr Plexa cartridges with bed mass of 200 mg was used to extract the selected aromatic compounds from wastewater based on the procedure

suggested by Kovács et al. (2011). (Kovács et al. 2011). Three steps of conditioning with 5 mL of each of acetone, methanol and MilliQ water were applied respectively, prior to passing 5 mL of wastewater sample through the cartridge. The sample was then eluted with 5 mL of acidified acetone (1% glacial acetic acid). Benzyl alcohol, o-cresol, phenol and benzaldehyde concentrations in the eluent were quantified by Agilent 7890B Gas Chromatograph (GC). The overall removal efficiency in each reactor was calculated according to Eq. (1).

$$Overall\ Removal\ Efficiency = \frac{\sum_{i=1}^{n} E_i \times C_i}{C_t} \ldots\ldots\ldots\ldots\ldots\ (6-1)$$

Where:

E_i: Removal efficiency of individual aromatic compounds (%).

C_i: Initial concentration of individual aromatic compounds (mg L^{-1}).

C_t: Summation of initial concentration for all aromatic compounds (mg L^{-1}).

6.2.4. Specific substrate uptake rate batch experiment

Four separate batch tests, one for each reactor, were performed to assess the specific substrate uptake rate from high concentrations of different carbon sources to test the resilience of the different systems Aerobic batch reactors were allowed headspace for aeration, while anaerobic batch reactors were sealed without headspace to avoid interrupting anaerobic conditions via surface aeration.. Each batch test consisted of four bottles containing 160 mL of synthetic PW, dosed with 450 mg L^{-1} of either benzyl alcohol, o-cresol, phenol, or a mixture of all of these compounds. The mixture of the compounds was comprised of 250, 100 and 100 mg L^{-1} of phenol, benzyl alcohol and o-cresol respectively, to represent the applied load on the bench scale reactors. The granular sludge batch reactors contained biomass transferred from the DBR reactors at an MLVSS concentration of 4500 ± 100 mg L^{-1} and 3800±100 mg L^{-1} for AGS and UASB respectively. For the GAC-based reactors, each test set was loaded with 6.5 g of GAC, to provide the same ratio of GAC weight to reactor volume as the hybrid Bio-GAC reactors. The MLVSS

concentration in batch reactors were. The MLVSS for GAC based batch tests were calculated as 350±30 mg $g^{-1}$and 280 ± 20 mg g^{-1} in the Bio-GAC and AnGAC systems, respectively.

All batch tests were allowed to shake at 150 rpm for 24 hours. The aerobic batch sets were shaken at 21 ± 1˚C, and the aerobic batch sets were shaken at 35 ± 1˚C. Representative samples from each reactor were collected hourly for 18 hours, filtered through 0.45 µm glass-fiber filters, extracted by the SPE method described above and analyzed to determine aqueous phase aromatic concentrations. The mass of biodegraded compounds was determined from the differences between initial and residual concentration. The specific substrate uptake rate for each compound and for each type of biomass was calculated by applying Eq. (6-2).

$$\frac{dM_s}{dt} = q_s M_x \dots\dots\dots\dots\dots (6-2)$$

Where:

dM_s: Biodegraded substances (mg L^{-1}).

d_t: Biodegradation time (h).

q_s: Specific substrate uptake rate (mg h^{-1} g^{-1} MLVSS).

M_x: Biomass concentration (g L^{-1} as MLVSS).

6.2.5. Statistical Analysis

One-way analysis of variance (ANOVA) was performed to analyze differences in the obtained data, with a significance level of 95% (p value = 0.05).. Mean data points were used to plot figures in this paper and the error bars represent 95% confidence intervals.

6.3. Results and discussion

6.3.1. Long-term reactors performance

6.3.1.1. Overall removal efficiency

Over the 100-day experiment, the aerobic Bio-GAC reactor showed the highest removal of influent aromatic compounds. Removal efficiency in this reactor was 95 % at the first day of operation, increasing to > 98 % at times ≥ 28 days. The AGS bioreactor had a lower initial removal efficiency (90%) that increased to 95% by the end of the experiment.

The removal efficiencies in both anaerobic bioreactors were lower than those in the aerobic systems. The reduction in aromatic compound content was 84% and 85.7% at the beginning of the acclimation period in the AnGAC and UASB reactors, respectively. The removal efficiency improved by 9% after 50 days of operation in the AnGAC reactor, achieving comparable levels of removal as the AGS reactor for the second half of the experiment. The UASB reactor reached 90% removal after 50 days, at which time its performance was comparable to the AnGAC and AGS reactors. However, no further increases in removal efficiency were achieved in this reactor, resulting in the lowest removal efficiency at 100 days.

Overall, the performance of Bio-GAC reactor was significantly greater than the other reactors for entire experiment (Figure 6-1). The high performance of this reactor can be attributed to integrated adsorption/ biodegradation removal mechanism (Pramanik et al. 2015). ANOVA analysis also showed significant differences in aromatic compounds removal efficiency when comparing the AGS reactor to the anaerobic reactors for the first 20 days (P<0.05). However, differences in aromatic removal between the two anaerobic reactors and the AGS reactor were not significant for the rest of the study time (P= 0.253). These findings are supported by previous studies that reported aerobic biological processes are faster than anaerobic biodegradation processes (Jimenez et al. 2018, Wu et al. 2020b). In the absence of dissolved oxygen under anaerobic conditions, some carbon atoms–associated with organic substrates serve as electron acceptors, while the rest act as electron donors, which require higher oxidation-reaction potential. As a result, high energy is required for metabolic processes via anaerobic biodegradation. Thus, anaerobic biodegradation is slower, achieving complete oxidation of organic compounds at a lower rate than aerobic biodegradation, when performance is compared at the same lower energy inputs (Aziz et al. 2019, Kadića et al. 2019, Nagarajan et al. 2019).

Throughout the experiment, the aerobic Bio-GAC reactor showed better removal of influent organics that the other reactors. The high performance of Bio-GAC reactor can be attributed to the combination of GAC sorptive capacity and biomass activity within the reactor (Liu et al. 2020c, Pradhan et al. 2020, Wang et al. 2019). The same trend was observed in AnGAC reactor as shown in Figure (6-1). Although the same operation conditions were applied on anaerobic reactors, the performance of AnGAC was higher over the whole operation period which reveals the role of adsorption capacity of GAC. However, the performance of AnGAC rector is significantly lower than the performance of aerobic Bio-GAC (P<0.05) as aerobic processes are generally faster than anaerobic processes (Aziz et al. 2019, Shoukat et al. 2019).

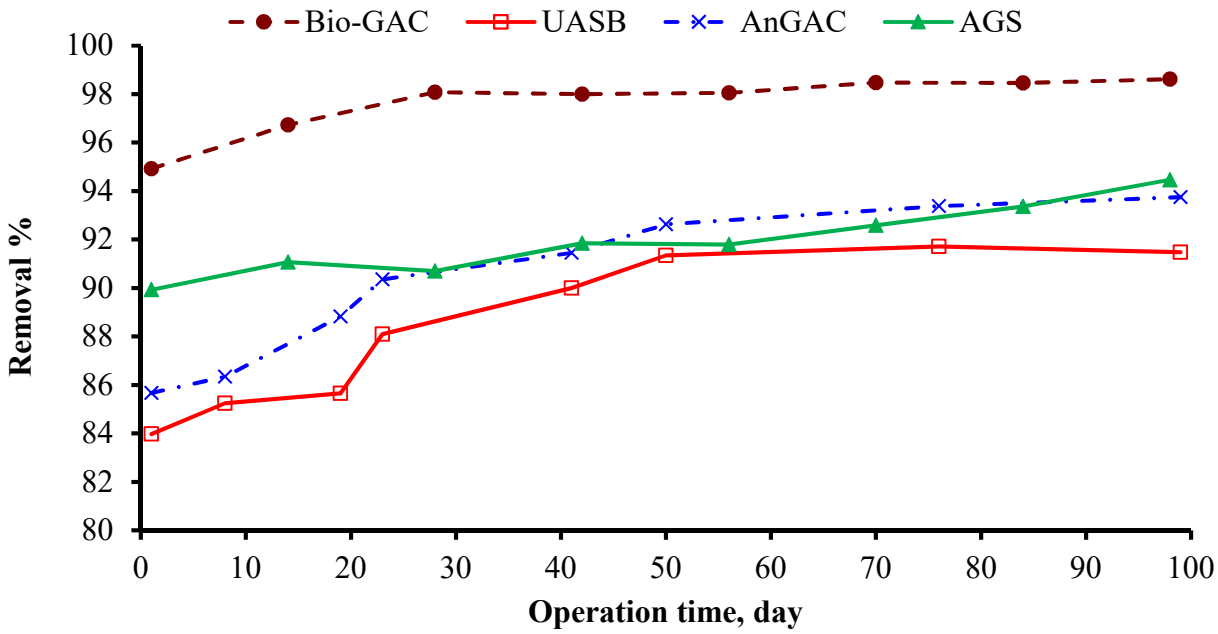

Figure 6-1: Overall organic load removal.

6.3.1.2. **Effluent suspended solids**

Figures 6-2 and 6-3 show the effluent MLSS concentrations from the aerobic reactors, (Bio-GAC and AGS) and anaerobic reactors (AnGAC and UASB), respectively. The effluent MLSS from aerobic reactors were in the ranges from 120±6 mg L^{-1} to 468±40 mg L^{-1} and from 96±23 mg L^{-1} to 356±45 mg L^{-1} for Bio-GAC and AGS reactor respectively, while it was lower

for anaerobic reactors, from 182±6 mg L^{-1} to 238±2 mg L^{-1} and from 182±4 mg L^{-1} to 221±4 mg L^{-1} for AnGAC and UASB reactor respectively. ANOVA analysis revealed that effluent MLSS values from the aerobic reactors were not significantly different, (p=0.298), while the effluent MLSS from AnGAC was significantly higher than the effluent MLSS from UASB reactor ($p < 0.05$). While biofilm sloughing is expected to be taking place over time due to continued biomass production, which contributes to effluent SS, these effluent MLSS values are high for SBR operation. The main reason for the higher biomass export from the aerobic reactions is likely the shear forces generated by the applied upflow air velocity (1.1 cm s^{-1}), which could apply an overwhelming pressure on biofilm that increases erosion. The applied upflow velocity within the anaerobic reactors via recirculation was 0.073 cm s^{-1}, which is approximately 1/15 of the superficial upflow velocity applied to the aerobic systems. It has been reported that operation conditions, such as the applied shear stress on biofilm is the main drive of detachment force (Liu et al. 2020a, Long et al. 2019). It is also worth noting the concentration of effluent SS of the Bio-GAC reactor was high (> 400 mg L^{-1}) due to GAC abrasion at the beginning of operation period (Figure 6-2). High salinity wastewaters have also been linked to increased effluent SS from AGS reactors by Carrera et al. (2019b), who observed effluent SS increasing from 200±60 mg L^{-1} to 1170±130 mg L^{-1} when salinity increased from 5.48±059 to 13.45 ± 0.51 g NaCl L^{-1}.

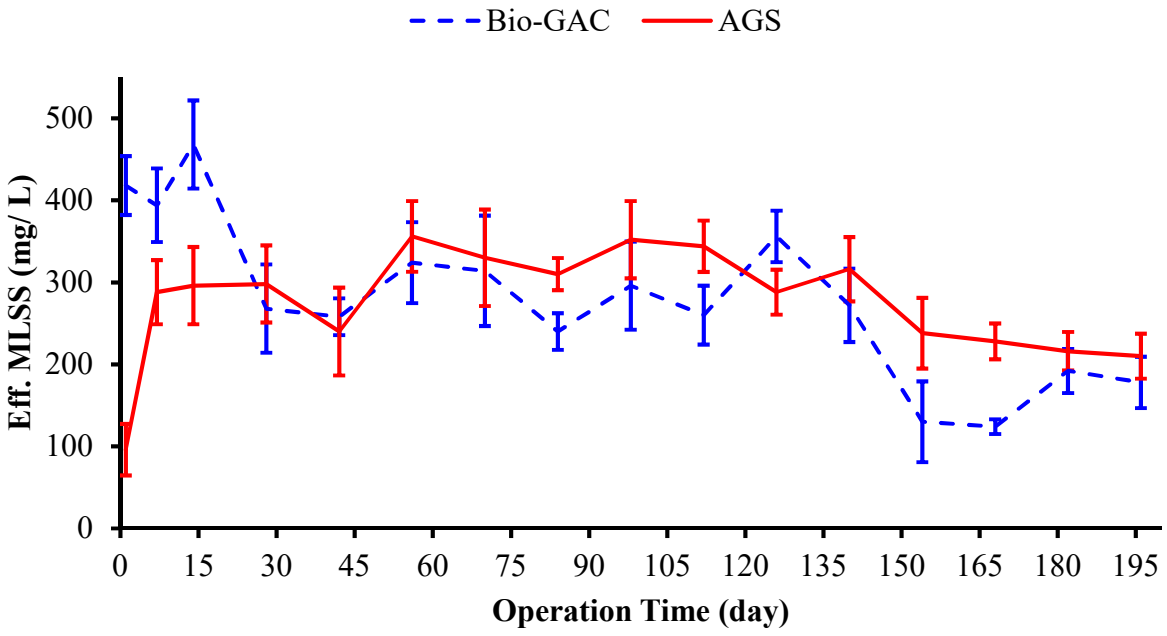

Figure 6-2: Long term effluent MLSS from aerobic bioreactors.

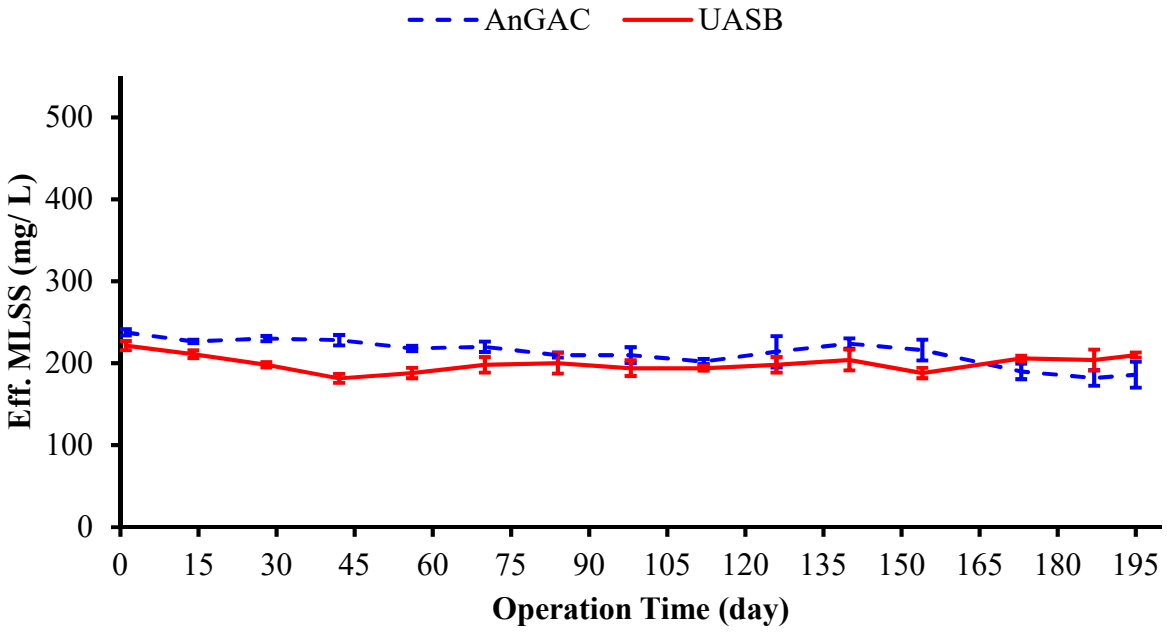

Figure 6-3: Long-term effluent MLSS from anaerobic bioreactors.

6.3.2. XPS analysis

The atomic composition of biomass was observed using high resolution XPS spectra analysis. The current study focused on the content of carbon, oxygen and nitrogen on the surface

of biofilm from the aerobic and anaerobic reactors in terms of C 1s, O 1s and N 1s spectra (Figures C2 to C5). The primary excited carbon forms were C-(C/H), C-OH, C=O and O-C=O (Figure 6-4). The XPS observation revealed that C-(C/H) peak had the highest ratio to the total carbon in all reactors. C-(C/H) functional groups made up 51 ± 2.5 % and 52 ± 2.5 % of total carbon in AnGAC and UASB respectively, but only 44 ± 0.5 % and 43±1 of carbon in aerobic Bio-GAC and AGS respectively (Table 1). The C-(C/H) functional group has been reported to represent amino acids or side chains of lipids and may be responsible for the hydrophobicity of the sludge surface (Fang et al. 2018b, Yin et al. 2015). The higher C-(C/H) content in anaerobic is consistent with the lower effluent SS(Hou et al. 2015, Huang et al. 2018). This finding indicates that C-(C/H) functional group played a crucial role in reducing the concentration of effluent SS from anaerobic reactors. In contrast, the C-OH functional group, which has been reported as a hydrophilic component (Huang et al. 2018), was significantly higher in the aerobic biofilm (Table 2). The relatively higher percentage of C-OH can be another reason to elevate the concentration of effluent MLSS of aerobic reactors. The ratio of C=O and O-C=O functional groups were roughly similar in the aerobic and anaerobic reactors.

XPS spectra of O 1s consisted of two peaks as shown in Figure (C6). The first O 1s peak, attributed to the C=O functional group (carbonyl, carboxylate, or ester groups), is located approximately at a binding energy of 531.9 eV. The second peak, located at 533.8 eV, corresponds to O-(C,H), which is assigned to polysaccharides (PS), alcohol, hemiacetal or acetal groups. The percentage of C=O functional groups were higher in the anaerobic samples, at 76 ± 3.3 % and 82 ± 1.8 % for AnGAC and UASB respectively (Table 3). In contrast, the percentage of C=O functional groups for Bio-GAC and AGS was 63 ± 4.7 % and 65 ± 2.5 % respectively, with correspondingly higher fraction of O-(C,H) functional groups. Higher polysaccharide production in aerobic biomass or a

more stable equilibrium between polysaccharide production and consumption could explain these findings. This finding is supported by previous studies that reported that aeration mode had a direct impact on the presence of PS in biomass (He et al. 2018, Rollemberg et al. 2020).

The N element was excited in two peaks (Figure C7). The first peak, located at 399.2 eV, is assigned for non-protonated nitrogen (N_{nonpr}) and represents amines and amides. The second nitrogen peak appeared at a binding energy of 400.1 eV, and is attributed to protonated amines (N_{pr}), predominantly from amino acids and amino sugars (Fang et al. 2018b, Yin et al. 2015). AnGAC, UASB and Bio-GAC reactors all had similar N profiles while the AGS was distinct from the other three (Table 6-2).. The presence of N_{pr} functional groups enhance bioaggregation and increases biofilm resilience against detachment due to it is hydrophobic properties (Fang et al. 2018b). The major finding of XPS analysis is that the aerobic biofilm is enriched with PS while the anaerobic biofilm was characterized by high fraction of amino acids or side chains of lipids. The output of this analysis can be used to interpret the relatively high effluent SS from aerobic reactors.

Table 6-1: The ratio of functional groups to the total carbon.

	The ratio of functional group to total carbon %			
Reactor	**C-(C/H)**	**C-OH**	**C=O**	**O-C=O**
AnGAC	51 ± 2.5	27 ± 0.3	12 ± 1.4	11 ± 1.2
UASB	52 ± 2.5	21 ± 6	13 ± 0.9	15 ± 0.85
Bio-GAC	44 ± 0.5	31 ± 0.2	13 ± 1.3	12 ± 1.4
AGS	43 ± 1	33 ± 1	11 ± 0.8	13 ± 0.7

Table 6-2: The ratio of functional groups to the total O 1s or N 1s.

	The ratio of functional groups to total nitrogen/ oxygen			
Reactor	**N_{nonpr}**	**N_{pr}**	**C=O**	**O-(C,H)**
AnGAC	77 ± 0.5	23 ± 0.5	76 ± 3.3	24 ± 3.3
UASB	76 ± 0.5	24 ± 0.5	82 ± 1.8	18 ± 1.8
Bio-GAC	78 ± 0.8	21 ± 0.8	63 ± 4.7	37 ± 4.7
AGS	82 ± 3.1	18 ± 3.1	65 ± 2.5	35 ± 2.5

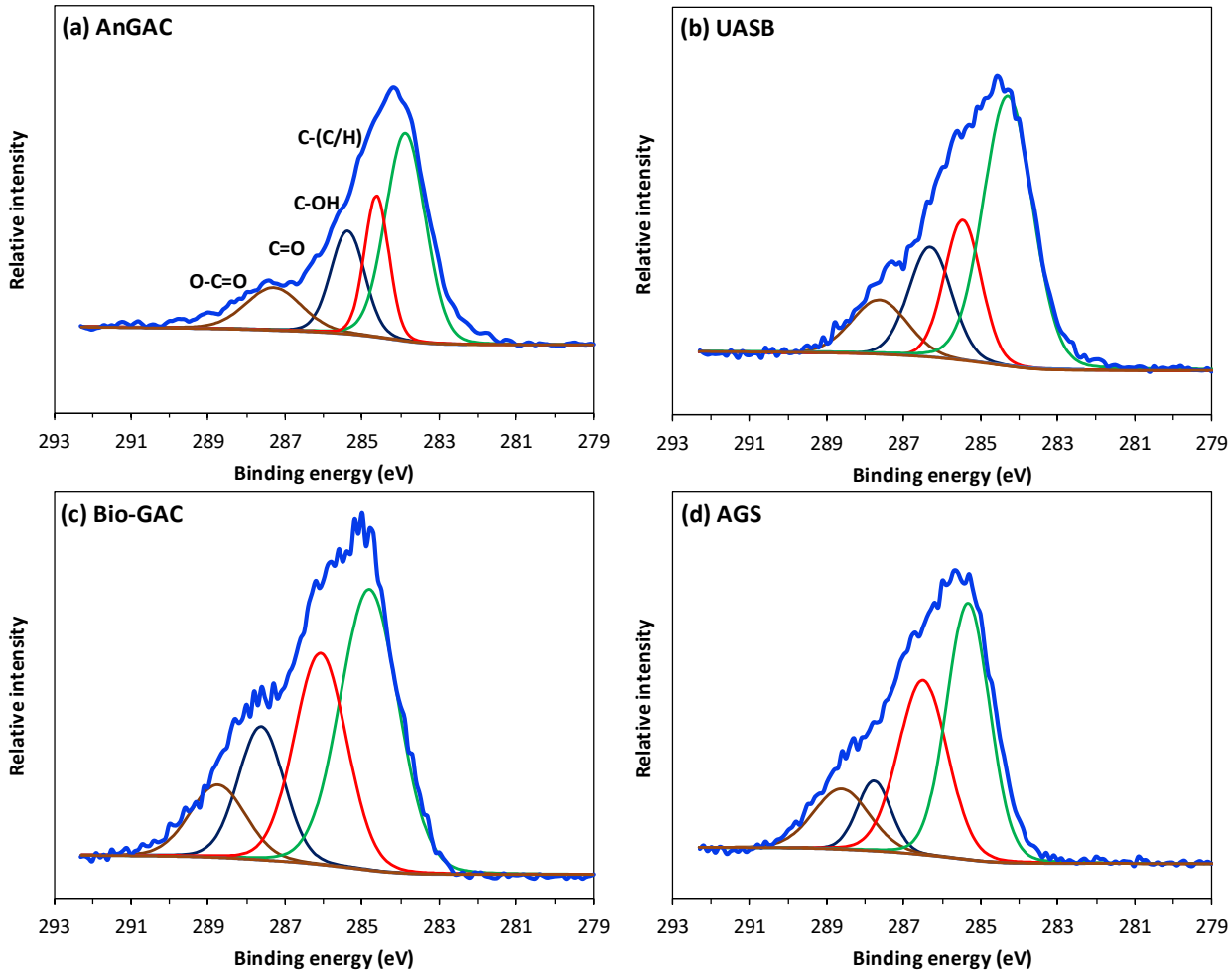

Figure 6-4: High-resolution C 1s spectra of (a) anaerobic biofilm integrated on GAC surface, (b) biofilm of anaerobic granular sludge, (c) aerobic biofilm integrated on GAC surface and (d) biofilm of aerobic granular sludge.

6.3.3. Resilience and shocks loading

Specific substrate uptake rate (q_s) was employed in the current study to assess the resilience of biomass against the presence of high concentrations of aromatic compounds. Overall results demonstrated that the aerobic systems showed greater resilience against elevated concentrations of aromatic compounds (Table 6-3). Moreover, q_s values for granule-based biosystems (i.e. UASB and AGS) are higher than those for GAC-based systems even while the overall organic load reduction in GAC-based systems were significantly higher (Figure C8). This may be due to the

fact that biomass concentration in AnGAC and Bio-GAC were much higher than in the UASB and AGS systems. When the substrate uptake rate was normalized to biomass concentration (as MLVSS) to calculate q_s, the produced values became much lower for GAC-based systems. The results also revealed that, in general, the anaerobic biodegradation process of all studied aromatic compounds was slower than aerobic biodegradation (Figures C9). This can be attributed to the fact that anaerobic bioprocesses are usually slower than aerobic bioprocesses (Aziz et al. 2019, Shoukat et al. 2019).

According to the obtained q_s, the performance of microorganisms with a mixture of aromatic substrates was better than with only one substrate (Table 6-3 and Figures C4 & C5). A long acclimation period (> 120 days) for biodegradation of a mixture of aromatic compounds could explain this behavior. Additionally, due to this long acclimation period, system performance with this mixture would be expected to be higher. Furthermore, the mixture of substrates increases the chance for some toxic and recalcitrant compounds to be degraded by cometabolic processes (Jesus et al. 2016). The results showed that the order of studied aromatic compounds in terms of specific substrate uptake rate was benzyl alcohol, o-cresol and then phenol (Table 6-3). Phenol is reported as an inhibitory substance and the biodegradation of it is sensitive to bulk solution pH (Genethliou et al. 2020, Silva et al. 2019). O-cresol has been reported to show high resistance against biodegradation due to the presence of a methyl group attached to benzene ring (Singh et al. 2020), while benzyl alcohol is readily biodegradable organic compound due to the presence of an active hydroxyl group within its structure (Wang et al. 2014).

Table 6-3: Observed specific substrate uptake rate in aerobic and anaerobic bioreactors.

	Specific substrate uptake rate (mg h^{-1} g^{-1} MLVSS)			
Reactor	**Ph**	**BA**	**Oc**	**Mixture**
AnGAC	1.6	2.1	1.9	1.6
UASB	5.8	8.3	7.7	5.8
Bio-GAC	1.9	2.8	2.3	2.6
AGS	6.2	8.8	8.3	8.3

6.4. Conclusions

In this study, we have investigated the performance of four different biological treatment systems (two aerobic versus two anaerobic) and compared them to each other in terms of efficiency of organic load removal, effluent suspended solids and resilience against toxic shocks. From the studied parameters, we concluded that removal efficiency in the aerobic Bio-GAC system was significantly higher than those of the other systems. Removal efficiency in the AGS system was comparable to the anaerobic systems. Effluent MLSS from aerobic systems fluctuated and was higher than that of anaerobic systems. According to XPS analysis, the proportion of hydrophobic functional groups was higher in anaerobic systems while the proportion of hydrophilic functional groups were higher in aerobic systems, which could explain the lower effluent MLSS in aerobic systems. The resilience of aerobic biofilm system against toxicity of aromatic compounds was higher compared to the anaerobic systems as shown through specific substrate uptake rate. From these results, we conclude that the aerobic biofilm systems (Bio-GAC and AGS) showed the most promise to provide a reliable alternative to the CAS systems in use today.

CHAPETR 7

Major Findings, Implications and Proposed Future Work

7.1. Major Findings

This study was completed in three major phases. During the first phase, AGS formation under hypersaline conditions using both an enriched halophilic inoculum and an activated sludge culture was assessed through monitoring of biomass production, COD removal, granule morphology, EPS production and microbial community structure. The major findings of this part of the study are as follows:

- The MLVSS concentration in the halophilic reactor was initially lower than in the activated sludge reactor, but it was much higher under hypersaline conditions (>85 g NaCl L^{-1}). However, the ratio of MLVSS/MLSS was around 0.76-0.78 for both cultures.
- COD removal was lower in the enriched halophile reactor under relatively low-salinity environment (<20 g NaCl L^{-1}) but increased significantly under hypersaline conditions.
- The average granule diameter in the activated sludge reactor was higher during the lower salinity stage (10 to 40 g L^{-1}) but decreased significantly during hypersaline operation ($\geq$ 40 g L^{-1}).
- EPS production was relatively stable as salinity increased in the enriched halophilic reactor, with a small decrease in production relative to total biomass at 80 to 85 g NaCl L^{-1}. However, it decreased significantly between 35 and 45 g NaCl L^{-1} and then remained relatively consistent throughout the hypersaline range. Tightly bound EPS accounted for approximately two thirds of the total EPS, on average, in both reactors. No consistent impact of salinity on the relative amounts of tightly and loosely bound EPS was observed.
- ALE production in the activated sludge reactor was lower than in the halophilic reactor across the hypersaline range (40 – 80 g NaCl L^{-1}). However, non-significant differences in ALE

production were observed as the salinity increased to 85 g L^{-1}. Pearson's correlation analysis showed that ALE production was positively correlated to SVI_5 values in both cultures, which emphasizes the role of ALE production in granule integrity.

- Na^+ dominated the EPS cation content in both cultures throughout the experiment, but Ca^{2+} and Mg^{2+} concentrations were higher in EPS of halophilic culture.
- Intracellular Ca^{2+} and Na^+ concentrations in the halophilic reactor were substantially lower than corresponding values in the activated sludge reactor while there were non-significant differences observed regarding to intracellular potassium concentrations in both cultures.
- The microbial community analysis showed that although the reactors were inoculated with different cultures at the beginning of study time, the hypersaline conditions selected for halophilic microorganisms in both biosystems.

Use of enriched halophilic inoculum resulted in better granule formation under high salinity conditions. Higher production of EPS and ALE under these conditions may explain the ability to keep granule integrity as salinity increased.

In the second phase of the study, two biofilm-based systems seeded with the hypersaline-adapted organisms developed in phase 1 were used to biodegrade a mixture of aromatic hydrocarbon compounds. The performance of the biofilm-based AGS and Bio-GAC systems was compared to that of a CAS system. The major findings of this phase of study are listed below:

- The batch experiment revealed that the biosorption took place within the biofilm of Bio-GAC and AGS. It also showed that the biosorption in Bio-GAC system was irreversible while it fluctuated in the AGS system and was weak in CAS system. Overall, the biosorption of selected aromatic compounds was in order of benzyl alcohol > phenol > o-cresol. The volatile losses due to aeration were negligible for all compounds.

- The biosorption is the main feature of biofilm-based systems that controls toxic compounds diffusion, elevates biosystem performance against toxic substances, and thus improves the overall performance of AGS and Bio-GAC compared to CAS treatment.

  The overall removal efficiency of biosystems was >99%, 93% and 73% for Bio-GAC, AGS and CAS reactors. The intermediate metabolic derivatives catechol and benzaldehyde were observed in all reactors as evidence for aerobic biodegradation of selected aromatic compounds. The Bio-GAC reactor achieved complete removal of the influent aromatics and had the lowest levels of catechol at the end of the 12-hour reaction cycle. While the AGS reactor achieved better removal than the CAS reactor, it did not achieve complete removal of phenol.
- Significant differences between Bio-GAC and AGS biofilm were observed in terms of texture of biofilm and type of bacterial growth. AGS biofilm predominantly consisted of string-like bacteria while GAC surface comprised cocci bacteria only.
- XPS analysis confirmed that the alcoholic compounds were captured by biofilm of AGS and Bio-GAC during feast phase and then utilized during famine phase as a carbon source.
- The microbiome analysis showed that the microbial community was similar for all SBRs at the beginning of the study period. After addition of the aromatic hydrocarbons, the *Marinobacter* content of all three reactors increased, with *Marionobacter* becoming the dominant genus in the Bio-GAC system.
- This part of study showed that Bio-GAC had the highest performance among all operated reactors. XPS analysis is a powerful tool to observe biosorption of organic matter on biofilm structure.

The last part of this study was to compare the long-term performance of four different types of biofilm-based biosystems. The performance of two aerobic biosystems (Bio-GAC and AGS) versus another two anaerobic biosystems (AnGAC and UASB) was investigated. The main findings of this phase of the study are:

- ANOVA analysis showed that there were significant differences in aromatic compounds removal efficiency when comparing the aerobic reactors to the anaerobic reactors while there were non-significant differences between anaerobic reactors when they were compared to each other.
- The effluent MLSS from aerobic reactors was consistently higher than values of anaerobic MLSS, likely due to higher solid production by aerobic process versus anaerobic and the high shear velocity imparted by the aeration process.
- The XPS spectra analysis showed that the fraction of observed hydrophobic functional groups in anaerobic reactors was higher than in aerobic reactors, which enhances compressibility and settleability of sludge in anaerobic reactors. In contrast, the fraction of hydrophilic component in aerobic reactors was higher than in anaerobic reactors.
- The aerobic treatment systems showed greater resilience against high concentration of aromatic compounds. The current study also showed that the anaerobic biodegradation process of aromatic compounds was slower than aerobic biodegradation.
- Finally, this part of study concluded that aerobic biofilm-based technique can be applied successfully to remove organic load under hypersaline conditions.

7.2. Implications

The main implication of the current study is the biofilm-based biological treatment is a reliable alternative to the CAS systems to treat hypersaline wastewater. Bio-GAC and AGS, as biofilm-based biological systems, showed high resilience against organic shocks. The anaerobic

biofilm-based systems (AnGAC and UASB) also can be applied to improve effluent characteristics in terms of effluent SS, but they required longer processing time, which make them suitable for low stream wastewater. The outcomes of the current study can be also applied to deal with high-strength industrial wastewater, such as oil and gas produced water, pharmaceuticals, vegetable pickling, pulp and paper mill wastewater. The current study introduced XPS technique as a powerful tool to investigate biosorption of the selected aromatic compounds on biofilm, and it was beneficial to employ it this study to make better understand of biofilm behavior under both hypersaline conditions and toxic organic load.

7.3. Proposed Future Work

The current study hypothesizes that the limited mass transfer of toxic organic substances through the biofilm mitigates their toxicity and improves overall biological treatment system. In this study, the performance of aerobic, anaerobic granular sludge and conventional activated sludge biological systems was evaluated under hypersaline conditions and high-strength organic load. Further research is necessary to extend the knowledge of biofilm-based biological treatment systems, to better understand the treatment mechanism and to optimize treatment approaches. Therefore, the future work below is proposed:

- Since the inorganic constituents of PW vary widely and can impact the structure of biofilm, it is necessary to investigate the impact of divalent and multivalent cations and their ratio to monovalent cations on the performance of biological treatment system.
- The coexistence of sludge flocs within biofilm-based reactors is inevitable. The presence of sludge flocs in treatment system can increase the competition for food (carbon source), which could negatively impact the performance of biofilm-based treatment system. In contrast, the coexistence of this type of biomass can improve the performance of treatment system because the substrate diffusion limitation through flocs is less than through compacted or aggregated

biofilm. Therefore, it is recommended to study the impact of the presence of sludge flocs on the performance of treatment systems.

- Investigate the reliability of using XPS technique to observe biofilm characteristics compared to other instrumental analysis techniques, such as surface-enhanced Raman and FTIR spectroscopy.
- Study the feasibility of applying intermittent aeration mode to enhance the performance of biosystems and mitigate the aeration cost.
- There is a lack of studies that attempt to observe biological organic load removal kinetics of halophilic biomass especially for Bio-GAC treatment systems. Therefore, it is worthwhile to investigate metabolic kinetics of marine biomass under harsh conditions.

REFERENCES

Abdel-Shafy, H.I., Mansour, M.S.M. and El-Toony, M.M. (2020) Integrated treatment for oil free petroleum produced water using novel resin composite followed by microfiltration. Separation and Purification Technology 234, 116058.

Abou-Elela, S.I., Kamel, M.M. and Fawzy, M.E. (2010) Biological treatment of saline wastewater using a salt-tolerant microorganism. Desalination 250(1), 1-5.

Acharya, K., Werner, D., Dolfing, J., Meynet, P., Shamas Tabraiz, Baluja, M.Q., Petropoulos, E., Mrozik, W. and Davenport, R.J. (2019) The experimental determination of reliable biodegradation rates for mono-aromatics towards evaluating QSBR models. Water Research 160, 278-287.

Ahmadun, F.l.-R., Pendashteh, A., Abdullah, L.C., Biak, D.R.A., Madaeni, S.S. and Abidin, Z.Z. (2009) Review of technologies for oil and gas produced water treatment. Journal of Hazardous Materials 170, 530-551.

Akyon, B. (2017) Biological treatment of hydraulic fracturing produced water, University of Pittsburgh, ProQuest.

Al-Ghouti, M.A., Al-Kaabi, M.A., Ashfaq, M.Y. and Da'na, D.A. (2019) Produced water characteristics, treatment and reuse: A review. Journal of Water Process Engineering 28, 222-239.

Al-Kaabi, M.A., Al-Ghouti, M.A., Ashfaq, M.Y.M., Ahmed, T. and Zouari, N. (2019) An integrated approach for produced water treatment using microemulsions modified activated carbon. Journal of Water Process Engineering 31, 100830.

Alley, B., Beebe, A., Jr., J.R. and Castle, J.W. (2011) Chemical and physical characterization of produced waters from conventional and unconventional fossil fuel resources. Chemosphere 85, 74-82.

APHA (2005) Standard Methods for the Examination of Water and Wastewater, 21 ed., American Public Health Association, Washington, DC, USA.

Appolinario, L.R., Tschoeke, D., Paixao, R.V.S., Venas, T.a., Calegario, G., Leomil, L., Silva, B.S., Thompson, C.C. and Thompson, F.L. (2019) Metagenomics sheds light on the metabolic repertoire of oil-biodegrading microbes of the South Atlantic Ocean. 249, 295-304.

Asri, M., Elabed, S., Koraichi, S.I. and Ghachtouli, N.E. (2018) Handbook of Environmental Materials Management. (eds), I.H.C. (ed), Springer, Cham.

Aziz, A., Basheer, F., Sengar, A., Irfanullah, Khan, S.U. and Farooqi, I.H. (2019) Biological wastewater treatment (anaerobic-aerobic) technologies for safe discharge of treated slaughterhouse and meat processing wastewater. Science of the Total Environment 686, 681-708.

Barati, R. and Liang, J.-T. (2014) A Review of Fracturing Fluid Systems Used For Hydraulic Fracturing of Oil and Gas Wells. Journal of Applied Polymer 131(16), 40735 (40731-40711).

Bassin, J.P., Kleerebezem, R., Rosado, A.S., Loosdrecht, M.C.M.v. and Dezotti, M. (2012) Effect of Different Operational Conditions on Biofilm Development, Nitrification, and Nitrifying Microbial Population in Moving-Bed Biofilm Reactors

environmnetal Science and Technology 46, 1546-1555.

Bassin, J.P., Pronk, M., Muyzer, G., Kleerebezem, R., Dezotti, M. and Loosdrecht, M.C.M.v. (2011) Effect of Elevated Salt Concentrations on the Aerobic Granular Sludge Process: Linking Microbial Activity with Microbial Community Structure. Applied & Environmental Microbiology 77(22), 7942–7953.

Benko, K.L. and Drewes, J.E. (2008) Produced Water in the Western United States: Geographical Distribution, Occurrence, and Composition. Environmental Engineering Science 25(2), 239-246.

Bolyen, E., Rideout, J.R., Dillon, M.R., Bokulich, N.A., Abnet, C.C., Al-Ghalith, G.A., Alexander, H., Alm, E.J., Arumugam, M. and Asnicar, F. (2019) Reproducible, interactive, scalable and extensible microbiome data science using QIIME 2. Nature Biotechnology, 1.

Boyd, E.M., Meharg, A.A., Wright, J. and Killham, K. (1997) Assessment of toxicological interactions of benzene and its Primary degradation products (catechol and phenol) Using a Lux -modified bacterial bioassay. Environmental Toxicology and Chemistry 16(5), 849-856.

Butkovskyi, A., Bruning, H., Kools, S.A.E., Rijnaarts, H.H.M. and Wezel, A.P.V. (2017) Organic Pollutants in Shale Gas Flowback and Produced Waters: Identification, Potential Ecological Impact, and Implications for Treatment Strategies. Environmental Science & Technology 51, 4740-4750.

Callahan, B.J., McMurdie, P.J., Rosen, M.J., Han, A.W., Johnson, A.J. and Holmes, S.P. (2016) DADA2: High-resolution sample inference from Illumina amplicon data. Nat Methods 13(7), 581-583.

Campo, R. and Bella, G.D. (2019) Petrochemical slop wastewater treatment by means of aerobic granular sludge: effect of granulation process on bio-adsorption and hydrocarbons removal. Chemical Engineering Journal 378, 122083.

Capodici, M., Bella, G.D., Nicosia, S. and Torregrossa, M. (2015) Effect of chemical and biological surfactants on activated sludge of MBR system: Microscopic analysis and foam test. Bioresource Technology 177, 80-86.

Caporaso, J.G., Kuczynski, J., Stombaugh, J., Bittinger, K., Bushman, F.D., Costello, E.K., Fierer, N., Peña, A.G., Goodrich, J.K., Gordon, J.I., Huttley, G.A., Kelley, S.T., Knights, D., Koenig, J.E., Ley, R.E., Lozupone, C.A., McDonald, D., Muegge, B.D., Pirrung, M., Reeder, J., Sevinsky, J.R., Turnbaugh, P.J., Walters, W.A., Widmann, J., Yatsunenko, T., Zaneveld, J. and Knight, R. (2010) QIIME allows analysis of high-throughput community sequencing data. Nat Methods 7(5), 335-336.

Caporaso, J.G., Lauberb, C.L., Walters, W.A., Berg-Lyons, D., Lozupone, C.A., Turnbaugh, P.J., Fierer, N. and Knight, R. (2011) Global patterns of 16S rRNA diversity at a depth of millions of sequences per sample. PNAS Journal 108(1), 4516-4522.

Carrera, P., Campo, R., endez, R.M., Bella, G.D., Campos, J.L., Mosquera-Corral, A. and Rio, A.V.d. (2019a) Does the feeding strategy enhance the aerobic granular sludge stability treating saline effluents? Chemosphere 226, 865-873.

Carrera, P., Campo, R., Mendez, R., Bella, G.D., Campos, J.L., Mosquera-Corral, A. and Rio, A.V.d. (2019b) Does the feeding strategy enhance the aerobic granular sludge stability treating saline effluents? Chemosphere 226, 865-873.

Castillo-Carvajal, L.C., Sanz-Martin, J.L. and Barragan-Huerta, B.E. (2014) Biodegradation of organic pollutants in saline wastewater by halophilic microorganisms: a review. Environmental Science and Pollution Research 21(16), 9578-9588.

Cetin, E., Karakas, E., Dulekgurgen, E., Ovez, S., Kolukirik, M. and Yilmaz, G. (2018) Effects of high-concentration influent suspended solids on aerobic granulation in pilot-scale sequencing batch reactors treating real domestic wastewater. Water Research 131, 74-89.

Chen, H., Wei, Y., Liang, P., Wang, C., Hu, Y., Xie, M., Wang, Y., Xiao, B., Du, C. and Tian, H. (2020a) Performance and microbial community variations of a upflow anaerobic sludge blanket (UASB) reactor for treating monosodium glutamate wastewater: Effects of organic loading rate. Journal of Environmental Management 253, 109691.

Chen, H., YanxiaoWei, Xie, C., HongWang, Chang, S., Xiong, Y., Du, C., Xiao, B. and Yu, G. (2020b) Anaerobic treatment of glutamate-rich wastewater in a continuous UASB reactor: Effect of hydraulic retention time and methanogenic degradation pathway. Chemosphere 245, 125672.

Clark, C.E. and Veil, J.A. (2009) Produced water volumes and management practices in the United States. Argonne National Laboratory (ANL).

Consuegra, G.L., Kutschke, S., Rudolph, M. and Pollmann, K. (2020) Halophilic bacteria as potential pyrite bio-depressants in Cu-Mo bioflotation. Minerals Engineering 145, 106062.

Corsino, S.F., Campo, R., Bella, G.D., Michele Torregrossa a and Viviani, G. (2015) Cultivation of granular sludge with hypersaline oily wastewater. International Biodeterioration & Biodegradation 105, 192-202.

Corsino, S.F., Campo, R., Di Bella, G., Torregrossa, M. and Viviani, G. (2018) Aerobic granular sludge treating shipboard slop: Analysis of total petroleum hydrocarbons loading rates on performacnes and stability. Process Biochemistry 65, 164-171.

Corsino, S.F., Capodici, M., Pippo, F.D., Tandoi, V. and Torregross, M. (2019) Comparison between kinetics of autochthonous marine bacteria in activated sludge and granular sludge systems at different salinity and SRTs. Water Research 148, 425-437.
Corsino, S.F., Capodici, M., Torregrossa, M. and Viviani, G. (2017) Physical properties and Extracellular Polymeric Substances pattern of aerobic granular sludge treating hypersaline wastewater. Bioresource Technology 229, 152–159.
Cozma, P., Hlihor, R.-M., Apostol, L.C., Diaconu, M., Pogăcean, M.O. and Gavrilescu, M. (2012) Aerobic biodegradation of phenol by activated sludge in a batch reactor. Environmental Engineering and Management Journal 11(11), 2053-2058.
Cozzarelli, I.M., Skalak, K.J., Kent, D.B., Engle, M.A., Benthem, A., A.C.Mumford, Haase, K., Farag, A., Harper, D., Nagel, S.C., Iwanowicz, L.R., Orem, W.H., Akob, D.M., Jaeschke, J.B., Galloway, J., Kohler, M., Stoliker, D.L. and Jolly, G.D. (2017) Environmental signatures and effects of an oil and gas wastewater spill in the Williston Basin, North Dakota. Science of the Total Environment 579, 1781-1793.
Cui, Y.W., Zhang, H.Y., Ding, J.R. and Peng, Y.Z. (2016) The effects of salinity on nitrification using halophilic nitrifiers in a Sequencing Batch Reactor treating hypersaline wastewater. Scientific Reports 6, 24825.
Dai, C., Bin, L., Tang, B., Li, P., Huang, S., Fu, F. and Yin, Q. (2019) Promoting the granulation process of aerobic granular sludge in an integrated moving bed biofilm-membrane bioreactor under a continuous-flowing mode. Science of the Total Environment.
Deng, S., Wang, L. and Su, H. (2016) Role and influence of extracellular polymeric substances on the preparation of aerobic granular sludge. Journal of Environmental Management 173, 49-54.
Dernburg, A.F. (2012) Formaldehyde Fixation of Drosophila Tissues onto Slides for Whole-Mount FISH. Cold Spring Harbor Protocols

doi:10.1101(pdb.prot067314), 632-636.
Dijk, E.J.H.v., Pronk, M. and Loosdrecht, M.C.M.v. (2018) Controlling effluent suspended solids in the aerobic granular sludge process. Water Research 147, 50-59.
Ding, C., Zhang, X., Xiong, S., Shen, L., Yi, M., Liu, B. and Wang, Y. (2020) Organophosphonate draw solution for produced water treatment with effectively mitigated membrane fouling via forward osmosis. Journal of Membrane Science 593, 117429.
Dubois, M., Gilles, K.A., Hamilton, J.K., Rebers, P.A. and Smith, F. (1956) Colorimetric Method for Determination of Sugars and Related Substances. Analytical Chemistry 28, 350-356.
Ekici, K. (2017) Energy Saving Preventions for Aeration Process in Wastewater Treatment Plant. Ekici, K. (ed).
Elias-Samlalsingh, N. and Agard, J.B.R. (2004) Application of Toxicity Identification Evaluation Procedures For Characterizing Produced Water Using the Tropical Mysid, Metamysidopsis Insularis. Environmental Toxicology and Chemistry 23(5), 1194-1203.
Faith, D.P. (1992) Conservation evaluation and phylogenetic diversity. Biological Conservation 61, 1-10.
Fang, F., Yang, M.-M., Wang, H., Yan, P., Chen, Y.-P. and Guo, J.-S. (2018a) Effect of high salinity in wastewater on surface properties of anammox granular sludge. Chemosphere 210, 366-375.
Fang, F., Yang, M.-M., Wang, H., Yan, P., Chen, Y.-P. and Guo, J.-S. (2018b) Effect of high salinity inwastewater on surface properties of anammox granular sludge. Chemosphere 210, 366-375.
Felz, S., Al-Zuhairy, S., Aarstad, O.A., Loosdrecht, M.C.M.v. and Lin, Y.M. (2016a) Extraction of Structural Extracellular Polymeric Substances from Aerobic Granular Sludge. Journal of Visualized Experiments 115.
Felz, S., Al-Zuhairy, S., Aarstad, O.A., van Loosdrecht, M.C.M. and Lin, Y.M. (2016b) Extraction of Structural Extracellular Polymeric Substances from Aerobic Granular Sludge. Journal of Visualized Experiments 115.
Felz, S., Neu, T.R., Loosdrecht, M.C.M.v. and Lin, Y. (2020) Aerobic granular sludge contains Hyaluronic acid-like and sulfated glycosaminoglycans-like polymers. Water Research 169, 115291.

Florentino, A.P., Xu, R., Zhang, L. and Liu, Y. (2019) Anaerobic digestion of blackwater assisted by granular activated carbon: From digestion inhibition to methanogenesis enhancement. Chemosphere 233, 462-471.
Gallegos, T.J., Varela, B.A., Haines, S.S. and Engle, M.A. (2015) Hydraulic fracturing water use variability in the United States and potential environmental implications. Water Resources Research 51(7), 5839-5845.
Gao, D., Liu, L., Laing, H. and Wu, W.-M. (2011) Aerobic granular sludge: characterization, mechanism of granulation and application to wastewater treatment. Critical Reviews in Biotechnology 31(2), 137-152.
Gao, S., He, Q. and Wang, H. (2020) Research on the aerobic granular sludge under alkalinity in sequencing batch reactors: Removal efficiency, metagenomic and key microbes. Bioresource Technology 296, 122280.
Genethliou, C., Kornaros, M. and Dailianis, S. (2020) Biodegradation of olive mill wastewater phenolic compounds in a thermophilic anaerobic upflow packed bed reactor and assessment of their toxicity in digester effluents. Journal of Environmental Management 255, 109882.
Guerra, K., Dahm, K. and Dundorf, S. (2011) Oil and Gas Produced Water Management and Beneficial Use in the Western United States. U.S. Department of the Interior Bureau of Reclamation (ed), p. 129, Science & Technology Program Report No. 157, Denver, CO.
Guo, S., Vance, T.D.R., Stevens, C.A., Voets, I. and Davies, P.L. (2019) Review: RTX Adhesins are Key Bacterial Surface Megaproteins in the Formation of Biofilms. Trends in Microbiology 27(5), 453-467.
Hamed, F.A.E., Yasin, S.I.B. and Ali, M.S. (2015) The Removal of Some Metals by Natural and Modified Zeolite from Produced Water. Journal of Basic and Applied Chemistry 5(2), 16-22.
Han, K., Hong, U., Kim, Y.-W., Kwon, S. and Kim, Y. (2020) Assessing the feasibility of sequential aerobic respiration and heterotrophic denitrification of a high-strength mixture of phenol and its derivatives in the field single-well-drift test. Chemosphere 239, 124800.
Hänelt, I. and Müller, V. (2013) Molecular Mechanisms of Adaptation of the Moderately Halophilic Bacterium Halobacillis halophilus to Its Environment. Life 3(1), 234-243.
He, Q., Chen, L., Zhang, S., Wang, L., Liang, J., Xia, W., Wang, H. and Zhou, J. (2018) Simultaneous nitrification, denitrification and phosphorus removal in aerobic granular sequencing batch reactors with high aeration intensity: Impact of aeration time. Bioresource Technology 263, 214-222.
He, Q., Song, J., Zhang, W., Gao, S., Wang, H. and Yu, J. (2020a) Enhanced simultaneous nitrification, denitrification and phosphorus removal through mixed carbon source by aerobic granular sludge. journal od Hazardous Materials 382, 121043.
He, Q., Wang, H., Chen, L., Gao, S., Zhang, W., Song, J. and Yu, J. (2020b) Robustness of an aerobic granular sludge sequencing batch reactor for low strength and salinity wastewater treatment at ambient to winter temperatures. Journal of Hazardous Materials 384, 121454.
Hervé, M. (2017) RVAideMemoire: Testing and Plotting Procedures for Biostatistics. R package version 0.9-68.
Higgins, M. and Novak, J. (1997) The Effect of Cations on the Settling and Dewatering of Activated Sludges: Laboratory Results. Water Environment Research 69(2), 215-224.
Hladik, M.L., Focazio, M.J. and Engle, M. (2014) Discharges of produced waters from oil and gas extraction via wastewater treatment plants are sources of disinfection by-products to receiving streams. Science of the Total Environment 466-467, 1085-1093.
Horner, J.E., Castle, J.W. and Jr, J.H.R. (2011) A risk assessment approach to identifying constituents in oilfiel dproduced water for treatment prior to beneficial use. Ecotoxicology and Environmental Safety 74, 989-999.
Hou, X., Liu, S. and Zhang, Z. (2015) Role of extracellular polymeric substance in determining the high aggregation ability of anammox sludge. Water Research 75, 51-62.

Huang, C., Shi, Y., El-Din, M.G. and Liu, Y. (2017) Performance of flocs and biofilms in integrated fixed-film activated sludge (IFAS) systems for the treatment of oil sands process-affected water (OSPW). Chemical Engineering Journal 314, 368-377.

Huang, J.-L., Wang, H.-H., Alam, F. and Cui, Y.-W. (2019a) Granulation of halophilic sludge inoculated with estuarine sediments for saline wastewater treatment. Science of the Total Environment 682, 532-540.

Huang, J.L., Wang, H.H., Alam, F. and Cui, Y.W. (2019b) Granulation of halophilic sludge inoculated with estuarine sediments for saline wastewater treatment. Science of the Total Environment 682, 532-540.

Huang, Z., Wang, Y., Jiang, L., Xu, B., Wang, Y., Zhao, H. and Zhou, W. (2018) Mechanism and performance of a self-flocculating marine bacterium in saline wastewater treatment. Chemical Engineering Journal 334, 732-740.

Hussain, A., Dubey, S.K. and Kumar, V. (2015) Kinetic study for aerobic treatment of phenolic wastewater. Water Resources and Industry 11(C), 81-90.

Ibrahim, M.H., Moussa, D.T., El-Naas, M.H. and Nasser, M.S. (2020) A perforated electrode design for passivation reduction during the electrochemical treatment of produced water. Journal of Water Process Engineering 33, 101091.

Ikonnikova, S.A., Male, F., Scanlon, B.R., Reedy, R.C. and McDaid, G. (2017) Projecting the Water Footprint Associated with Shale Resource Production: Eagle Ford Shale Case Study. Enviromental Science & Technology 51, 14453-14461.

Ismail, S.B., de La Parra, C.J., Temmink, H. and van Lier, J.B. (2010) Extracellular polymeric substances (EPS) in upflow anaerobic sludge blanket (UASB) reactors operated under high salinity conditions. Water Research 44(6), 1909-1917.

Jesus, J., Frascari, D., Pozdniakova, T. and Danko, A.S. (2016) Kinetics of aerobic cometabolic biodegradation of chlorinated and brominated aliphatic hydrocarbons: A review. Journal of Hazardous Materials 309, 37-52.

Jimenez, S., Mic, M.M., Arnaldos, M., Medina, F. and Contreras, S. (2018) State of the art of produced water treatment

Chemosphere 192, 186-208.

Kadića, A., Chylenski, P., Hansen, M.A.T., Bengtsson, O., Eijsink, V.G.H. and Lidén, G. (2019) Oxidation-reduction potential (ORP) as a tool for process monitoring of H2O2/LPMO assisted enzymatic hydrolysis of cellulose. Process Biochemistry 86, 89-97.

Kara, F., Gurakan, G. and Sanin, F. (2008) Monovalent cations and their influence on activated sludge floc chemistry, structure, and physical characteristics. Biotechnology and Bioengineering 100(2), 231-239.

Katoh, K. and Standley, D.M. (2013) MAFFT multiple sequence alignment software version 7: improvements in performance and usability. Mol Biol Evol 30(4), 772-780.

Kembel, S.W., Cowan, P.D., Helmus, M.R., Cornwell, W.K., Morlon, H., Ackerly, D.D., Blomberg, S.P. and Webb, C.O. (2010) Picante: R tools for integrating phylogenies and ecology. Bioinformatics 26(11), 1463-1464.

Keshvari, F. and Bahram, M. (2017) Selective, sensitive and reliable colorimetric sensor for catechol detection based on anti-aggregation of unmodified gold nanoparticles utilizing boronic acid–diol reaction: optimization by experimental design methodology. Journal of the Iranian Chemical Society 14, 977-984.

Kim, K.-H. and Ihm, S.-K. (2011) Heterogeneous catalytic wet air oxidation of refractory organic pollutants in industrial wastewaters: A review. Journal of Hazardous Materials 186, 16-34.

Kondash, A. and Vengosh, A. (2015) Water Footprint of Hydraulic Fracturing. Enviromental Science & Technology 2, 276-280.

Kondash, A.J., Albright, E. and Vengosh, A. (2017) Quantity of flowback and produced waters from unconventional oil and gas exploration. Science of the Total Environment 574, 314-321.

Kong, Z., Li, L., Kurihara, R., Kubota, K. and Li, Y.-Y. (2018) Anaerobic treatment of N, N-dimethylformamide-containing wastewater by co-culturing two sources of inoculum. Water Research 139, 228-239.
Kovács, Á., Mörtl, M. and Kende, A. (2011) Development and optimization of a method for the analysis of phenols and chlorophenols from aqueous samples by gas chromatography–mass spectrometry, after solid-phase extraction and trimethylsilylation. Microchemical Journal 99, 125-131.
Lefebvre, O. and Moletta, R. (2006) Treatment of organic pollution in industrial saline waastewater: A literature review. Water Research 40, 3671-3682.
Li, H. (2013) Produced Water Quality Characterization and Prediction for Wattenberg Field, Colorado State University.
Li, L., Kong, Z., Xue, Y., Wang, T., Kato, H. and Li, Y.-Y. (2020a) A comparative long-term operation using up-flow anaerobic sludge blanket (UASB) and anaerobic membrane bioreactor (AnMBR) for the upgrading of anaerobic treatment of N, N-dimethylformamidecontaining wastewater. Science of the Total Environment 699, 134370.
Li, S., Li, D., Wang, Y., Zeng, H., Yuan, Y. and Zhang, J. (2020b) Startup and stable operation of advanced continuous flow reactor and the changes of microbial communities in aerobic granular sludge. Chemosphere 243, 125434.
Li, W., Zhenga, T., Ma, Y. and Liu, J. (2019) Current status and future prospects of sewer biofilms: Their structure, influencing factors, and substance transformations. Science of the Total Environmnet 695, 133815.
Li, X., Luo, J., Guo, G., Mackey, H.R., Hao, T. and Chen, G. (2017) Seawater-based wastewater accelerates development of aerobic granular sludge: A laboratory proof-of-concept. Water Research 115, 210-219.
Li, X.Y. and Yang, S.F. (2007) Influence of loosely bound extracellular polymeric substances (EPS) on the flocculation, sedimentation and dewaterability of activated sludge. Water Research 41, 1022-1030.
Liden, T., Santos, I.C., Hildenbrand, Z.L. and Schug, K.A. (2018) Treatment modalities for the reuse of produced waste from oil and gas development. Science of the Total Environment 643, 107-118.
Lin, Y., Kreuk, M.d., van Loosdrecht, M.C.M. and Adin, A. (2010) Characterization of alginate-like exopolysaccharides isolated from aerobic granular sludge in pilot-plant. Water Research 44, 3355-3364.
Lin, Y.M., Sharma, P.K. and Loosdrecht, M.C.M.v. (2013a) The chemical and mechanical differences between alginate-like exopolysaccharides isolated from aerobic flocculent sludge and aerobic granular sludge. Water Research 47, 57-65.
Lin, Y.M., Sharma, P.K. and van Loosdrecht, M.C.M. (2013b) The chemical and mechanical differences between alginate-like exopolysaccharides isolated from aerobic flocculent sludge and aerobic granular sludge. Water Research 47, 57-65.
Liu, J., Li, J., Xu, D. and Sellamuthu, B. (2020a) Improving aerobic sludge granulation in sequential batch reactor by natural drying: Effluent sludge recovery and feeding back into reactor. Chemosphere 242, 125159.
Liu, W., Yin, F. and Yang, D. (2020b) Granules abrasion cause deterioration of nitritation in a mainstream granular sludge reactor with high loading rate. Chemosphere 243, 125433.
Liu, Y., Ngo, H.H., Guo, W., Wang, D., Peng, L., Wei, W. and Ni, B.-J. (2020c) Impact of coexistence of sludge flocs on nitrous oxide production in a granule-based nitrification system: A model-based evaluation. Water Research 170, 115312.
Liu, Z., Lompe, K.M., Mohseni, M., Berub, P.R., Sauve, S. and Barbeau, B. (2020d) Biological ion exchange as an alternative to biological activated carbon for drinking water treatment. Water Research 168, 115148.
Long, B., Xuan, X., Yang, C., Zhang, L., Cheng, Y. and Wang, J. (2019) Stability of aerobic granular sludge in a pilot scale sequencing batch reactor enhanced by granular particle size control. Chemosphere 425, 460-469.

Loukidou, M.X. and Zouboulis, A.I. (2001) Comparison of two biological treatment processes using attached- growth biomass for sanitary landfill leachate treatment. Environmental Pollution 111(2), 273-281.
Love, M.I., Huber, W. and Anders, S. (2014) Moderated estimation of fold change and

dispersion for RNA-seq data with DESeq2. Genome Biol 15(12), 550.
Lu, H., Liu, Y.-q., Cai, J.-b., Xu, X., Xie, L.-s., Yang, Q., Li, Y.-x. and Zhu, K. (2019) Treatment of offshore oily produced water: Research and application of a novel fibrous coalescence technique. Journal of Petroleum Science and Engineering 178, 602-608.
Luo, G., Xu, J. and Meng, H. (2020) Nitrate accumulation in biofloc aquaculture systems. Aquaculture 520, 734675.
Mancini, G., Panzica, M., Fino, D., Cappello, S., Yakimov, M.M. and Luciano, A. (2017) Feasibility of treating emulsified oily and salty wastewaters through coagulation and bio-regenerated GAC filtration. Journal of Environmental Management 203, 817-824.
Mathews, M., Gotkowitz, M. and Ginder-Vogel, M. (2018) Effect of geochemical conditions on radium mobility in discrete intervals within the Midwestern Cambrian-Ordovician aquifer system. Applied Geochemistry 97, 238-246.
McMurdie, P.J. and Holmes, S. (2013) phyloseq: An R Package for Reproducible Interactive

Analysis and Graphics of Microbiome Census Data. PLoS One 8(4), e61217.
McSwain, B.S., Irvine, R.L., Hausner, M. and Wilderer, P.A. (2005) Composition and Distribution of Extracellular Polymeric Substances in Aerobic Flocs and Granular Sludge. Applied & Environmental Microbiology 71(2), 1051–1057.
Meng, F., Huang, W., Liu, D., Zhao, Y., Huang, W., Lei, Z. and Zhang, Z. (2020) Application of aerobic granules-continuous flow reactor for saline wastewater treatment: Granular stability, lipid production and symbiotic relationship between bacteria and algae. Bioresource Technology 295, 122291.
Meng, F.S., Liu, D.F., Pan, Y.W., Xi, L.M., Yang, D. and Huang, W.L. (2019) Enhanced Amount and Quality of Alginate-like Exopolysaccharides in Aerobic Granular Sludge for the Treatment of Salty Wastewater. Bioresources 14(1), 139-165.
Mohamed, S.N., Hiraman, P.A., Muthukumar, K. and Jayabalan, T. (2020) Bioelectricity production from kitchen wastewater using microbial fuel cell with photosynthetic algal cathode. Bioresource Technology 295, 122226.
Mohammad-Pajooh, E., Weichgrebe, D., Cuff, G., Tosarkani, B.M. and Rosenwinkel, K.-H. (2018) On-site treatment of flowback and produced water from shale gas hydraulic fracturing: A review and economic evaluation. Chemosphere 212, 898-914.
Nadella, M., Sharma, R. and Chellam, S. (2020) Fit-for-purpose treatment of produced water with iron and polymeric coagulant for reuse in hydraulic fracturing: Temperature effects on aggregation and high-rate sedimentation. Water Research 170, 115330.
Nagarajan, D., Kusmayadi, A., Yen, H.-W., Dong, C.-D., Lee, D.-J. and Chang, J.-S. (2019) Current advances in biological swine wastewater treatment using microalgae-based processes. Bioresource Technology 289, 121718.
Neff, J., Lee, K. and DeBlois, E.M. (2011) Produced Water: Environmental Risks and Advances in Mitigation Technologies. Kenneth Lee, J.N. (ed), Springer New York, New York.
Nie, H., Nie, M., Diwu, Z., Wang, L., Yan, H., Lin, Y., Zhang, B. and Wang, Y. (2020) Biological treatment of high salinity and low pH produced water in oilfield with immobilized cells of P. aeruginosa NY3 in a pilot-scale. Journal of Hazardous Materials 381, 121232.
Oberoi, A.S. and Philip, L. (2017a) Performance evaluation of attached biofilm reactors for the treatment of wastewater contaminated with aromatic hydrocarbons and phenolic compounds. Journal of Environmental Chemical Engineering 5, 3852-3864.

Oberoi, A.S. and Philip, L. (2017b) Variation in toxicity during the biodegradation of various heterocyclic and homocyclic aromatic hydrocarbons in single and multi-substrate systems. Ecotoxicology and Environmental Safety 135, 337-346.
Ofman, P., Struk-Sokołowska, J., Skoczko, I. and Wiater, J. (2020) Alternated biodegradation of naphthalene (NAP), acenaphthylene (ACY) and acenaphthene (ACE) in an aerobic granular sludge reactor (GSBR). Journal of Hazardous Materials 383, 121184.
Oksanen, J., Blanchet, F.G., Friendly, M., Kindt, R., Legendre, P., McGlinn, D., Minchin, P.R., O'Hara, R.B., Simpson, G.L., Solymos, P., Stevens, M.H.H., Szoecs, E. and Wagner, H. (2017) vegan: Community Ecology Package. R package version 2.4-4, https://CRAN.R-project.org/package=vegan
Orem, W., Tatu, C., Varonka, M., Lerch, H., Bates, A., Engle, M., Crosby, L. and McIntosh, J. (2014) Organic substances in produced and formation water from unconventional natural gas extraction in coal and shale. International Journal of Coal Geology 126, 20-31.
Osipi, S.R., Secchi, A.R. and Borges, C.P. (2018) Cost assessment and retro-techno-economic analysis of desalination technologies in onshore produced water treatment. Desalination 430, 107-119.
Ou, D., Li, H., Li, W., Wu, X., Wang, Y.-q. and Liu, Y.-d. (2018a) Salt-tolerance aerobic granular sludge: Formation and microbial community characteristics. Bioresource Technology 249, 132-138.
Ou, D., Li, W., Li, H., Wu, X., Li, C., Zhuge, Y. and Liu, Y.-d. (2018b) Enhancement of the removal and settling performance for aerobic granular sludge under hypersaline stress. Chemosphere 212, 400-407.
Ozaki, N., Takamura, Y., Kojima, K. and Kindaichi, T. (2015) Loading and removal of PAHs in a wastewater treatment plant in a separated sewer system. Water Research 80, 337-345.
Özsoy, G. (2006) An investigation of agricultural use potential of wastewater sludges in Turkey with respect to heavy metals and pathogens, Middle East Technical University, Ankara, Turkey.
Paredes, L., Alfonsin, C., Allegue, T., Omil, F. and Carballa, M. (2018) Integrating granular activated carbon in the post-treatment of membrane and settler effluents to improve organic micropollutants removal. Chemical Engineering Journal 345, 79-86.
Pendashteh, A.R., Abdullah, L.C., Fakhru'l-Razi, A., Madaeni, S.S., Abidin, Z.Z. and Biak, D.R.A. (2012) Evaluation of membrane bioreactor for hypersaline oily wastewater treatment. Process Safety and Environmental Protection 90, 45-55.
Pishgar, R., Dominic, J.A., Tay, J.H. and Chu, A. (2020) Pilot-scale investigation on nutrient removal characteristics of mineral-rich aerobic granular sludge: Identification of uncommon mechanisms. Water Research 168, 115151.
Pradhan, S., Fan, L., Roddick, F.A., Shahsavari, E., Ball, A.S. and Zhang, X. (2020) A comparative study of biological activated carbon based treatments on two different types of municipal reverse osmosis concentrates. Chemosphere 240, 124925.
Pramanik, B.K., Roddick, F.A. and LinhuaFan (2015) A comparative study o fbiological activated carbon, granular activated carbon and coagulation feed pre-treatmen tfo rimproving microfiltration performance in wastewater reclamation. Journal of Membrane Science 475, 147-155.
Price, M.N., Dehal, P.S. and Arkin, A.P. (2010) FastTree 2--approximately maximum-likelihood trees for large alignments. PLoS One 5(3), e9490.
Pronk, M., Bassin, J.P., Kreuk, M.K.d., Kleerebezem, R. and van Loosdrecht, M.C.M. (2014) Evaluating the main and side effects of high salinity on aerobic granular sludge. Applied Microbiology and Biotechnology 98, 1339–1348.
Pugh, S., McKenna, R., Halloum, I. and Nielsen, D.R. (2015) Engineering Escherichiacoli for renewable benzyl alcohol production. Metabolic Engineering Communications 2, 39-45.
Puyol, D., Monsalvo, V.M., Sanchis, S., Sanz, J.L., Mohedano, A.F. and Rodriguez, J.J. (2015) Comparison of bioaugmented EGSB and GAC–FBB reactors and their combination with aerobic SBR for the abatement of chlorophenols. Chemical Engineering Journal 259, 277-285.

Quast, C., Pruesse, E., Yilmaz, P., Gerken, J., Schweer, T., Yarza, P., Peplies, J. and Glockner, F.O. (2013) The SILVA ribosomal RNA gene database project: improved data processing and web-based tools. Nucleic Acids Res 41(Database issue), D590-596.

Ramos, C., Suárez-Ojeda, M.E. and Carrera, J. (2015) Long-term impact of salinity on the performance and microbial population of an aerobic granular reactor treating a high-strength aromatic wastewater. Bioresource Technology 198, 844–851.

Ranck, J.M., Bowman, R.S., Weeber, J.L., Katz, L.E. and Sullivan, E.J. (2005) BTEX Removal from Produced water Using Surfactant-Modified Zeolite. journal of environmental Engineering 131(3), 434-442.

Ren, L.-F., Chen, R., Zhang, X., Shao, J. and He, Y. (2017) Phenol biodegradation and microbial community dynamics in extractive membrane bioreactor (EMBR) for phenol-laden saline wastewater. Bioresource Technology 244, 1121-1128.

Riley, S.M., Ahoor, D.C. and Cath, T.Y. (2018) Enhanced biofiltration of O&G produced water comparing granular activated carbon and nutrients. Science of the Total Environment 640-641, 419-428.

Rogers, J.D., Ferrer, I., Tummings, S.S., Bielefeldt, A.R. and Ryan, J.N. (2017) Inhibition of Biodegradation of Hydraulic Fracturing Compounds by Glutaraldehyde: Groundwater Column and Microcosm Experiments. Enviromental Science & Technology 51, 10251-10261.

Rollemberg, S.L.d.S., Ferreira, T.J.T., Firmino, P.I.M. and Santos, A.B.d. (2020) Impact of cycle type on aerobic granular sludge formation, stability, removal mechanisms and system performance. Journal of Environmental Management 256, 109970.

Rowan, B.E.L., Engle, M.A., Kirby, C.S. and Kraemer, T.F. (2011) Radium Content of Oil- and Gas-Field Produced Waters in the Northern Appalachian Basin (USA): Summary and Discussion of Data. U.S. Department of the Interior, U.S.G.S. (ed), U.S. Geological Survey, Reston, Virginia, USGS.

Salminikhas, N., Tizaghadam, M. and Rashidi Mehrabadi, A. (2016) Treatment of saline municipal wastewater using hydrid growth system. Journal of Biological Engineering 10(9).

Sambusiti, C., Saadouni, M., Gauchou, V., Segues, B., Leca, M.A., Baldoni-Andrey, P. and Jacob, M. (2020) Influence of HRT reduction on pilot scale flat sheet submerged membrane bioreactor (sMBR) performances for Oil&Gas wastewater treatment. Journal of Membrane Science 594, 117459.

Scanlon, B.R., Reedy, R.C., Male, F. and Hove, M. (2016) Managing the Increasing Water Footprint of Hydraulic Fracturing in the Bakken Play, United States. Enviromental Science & Technology 50, 10273-10281.

Scheuner, C., Tindall, B.J., Lu, M., Nolan, M., Lapidus, A., Cheng, J.-F., Goodwin, L., Pitluck, S., Huntemann, M., Liolios, K., Pagani, I., Mavromatis, K., Ivanova, N., Pati, A., Chen, A., Palaniappan, K., Jeffries, C.D., Hauser, L., Land, M., Mwirichia, R., Rohde, M., Abt, B., Detter, J.C., Woyke, T., Eisen, J.A., Markowitz, V., Hugenholtz, P., Göker, M., Kyrpides, N.C. and Klenk, H.-P. (2014) Complete genome sequence of Planctomyces brasiliensis type strain (DSM 5305T), phylogenomic analysis and reclassification of Planctomycetes including the descriptions of Gimesia gen. nov., Planctopirus gen. nov. and Rubinisphaera gen. nov. and emended descriptions of the order Planctomycetales and the family Planctomycetaceae, pp. 1-18.

Schmidt, K., Steinberg, C.E.W., Staaks, G.B.O. and Pflugmacher, S. (2005) Influence of a Xenobiotic Mixture (PCB and TBT) Compared to Single Substances on Swimming Behavior or Reproduction of Daphnia magna. Acta Hydrochimica et Hydrobiologica 33(4), 287-300.

Shaffer, D.L., Chavez, L.H.A., Ben-Sasson, M., Castrillón, S.R.-V., Yip, N.Y. and Elimelech, M. (2013) Desalination and Reuse of High-Salinity Shale Gas Produced Water: Drivers, Technologies, and Future Directions. Enviromental Science & Technology 47, 9569-9583.

Sharghi, E.A. and Bonakdarpour, B. (2013) The study of organic removal efficiency and halophilic bacterial mixed liquor characteristics in a membrane bioreactor treating hypersaline produced water at varying organic loading rates. Bioresource Technology 149, 486–495.

Sharghi, E.A., Bonakdarpour, B. and Pakzadeh, M. (2014) Treatment of hypersaline produced water employing a moderately halophilic bacterial consortium in a membrane bioreactor: Effect of salt

concentration on organic removal performance, mixed liquor characteristics and membrane fouling. Bioresource Technology 164, 203-213.
Sharghi, E.A., Bonakdarpour, B., Roustazade, P., Amoozegarb, M.A. and Rabbanic, A.R. (2013) The biological treatment of high salinity synthetic oilfield produced water in a submerged membrane bioreactor using a halophilic bacterial consortium. Journal of Chemical Technology & Biotechnology 88(11), 2016-2026.
Shoukat, R., Khan, S.J. and Jamal, Y. (2019) Hybrid anaerobic-aerobic biological treatment for real textile wastewater. 29, 100804.
Shrestha, N., Chilkoor, G., JosephWilder, Ren, Z.J. and Gadhamshetty, V. (2018) Comparative performances of microbial capacitive deionization cell and microbial fuel cell fed with produced water from the Bakken shale. Bioelectrochemistry 121, 56-64.
Silva, D.C.d., Lucas, C.R.d.S., Juviniano, H.B.d.M., Moura, M.C.P.d.A., Neto, A.A.D. and Dantas, T.N.d.C. (2020) Novel produced water treatment using microemulsion systems to remove oil contents. Journal of Water Process Engineering 33, 101006.
Silva, N.C.G., Macedo, A.C.d., Pinheiro, Á.D.T. and Rocha, M.V.P. (2019) Phenol biodegradation by Candida tropicalis ATCC 750 immobilized on cashew apple bagasse. Journal of Environmental Chemical Engineering 7, 103076.
Singh, T., Bhatiya, A.K., Mishra, P.K. and Srivastava, N. (2020) Abatement of Environmental Pollutant Singh, P., Kumar, A. and Borthakur, A. (eds), Elsevier Inc.
Sirivedhin, T. and Dallbauman, L. (2004) Organic matrix in produced water from the Osage-Skiatook Petroleum Environmental Research site, Osage county, Oklahoma. Chemosphere 57, 463-469.
Song, X., Liu, J., Jiang, Q., Zhang, P., Shao, Y., He, W. and Feng, Y. (2019) Enhanced electron transfer and methane production from low-strength wastewater using a new granular activated carbon modified with nano-Fe3O4. Chemical Engineering Journal 374, 1344-1352.
Stringfellow, W.T., Domen, J.K., Camarillo, M.K., Sandelin, W.L. and Borglin, S. (2014) Physical, chemical, and biological characteristics of compounds used in hydraulic fracturing. Journal of Hazardous Materials 275, 37-54.
Sudmalis, D., Silva, P.D., Temmink, H., Bijmans, M.M. and Pereira, M.A. (2018) Biological treatment of produced water coupled with recovery of neutral lipids. Water Research 147, 33-42.
Taheri, E., (Hajian), M.H.K., Amin, M.M., Nikaeen, M. and Hassanzadeh, A. (2012) Treatment of saline wastewater by a sequencing batch reactor with emphasis on aerobic granule formation. Bioresource Technology 111, 21-26.
Tang, X., Pronk, W., Ding, A., Cheng, X., Wang, J., Xie, B., Li, G. and Liang, H. (2020) Coupling GAC to ultra-low-pressure filtration to modify the biofouling layer and bio-community: Flux enhancement and water quality improvement. Chemical Engineering Journal 333, 289-299.
Thomas, F., Hehemann, J.H., Rebuffet, E., Czjzek, M. and Michel, G. (2011) Environmental and gut bacteroidetes: the food connection. Frontiers in Microbiology 2, 93.
Tiedeman, K., Yeh, S., Scanlon, B.R., Teter, J. and Mishra, G.S. (2016) Recent Trends in Water Use and Production for California Oil Production. Enviromental Science & Technology 50, 7904-7912.
Tisler, S. and Zwiener, C. (2019) Aerobic and anaerobic formation and biodegradation of guanyl urea and other transformation products of metformin. Water Research 149, 130-135.
USEPA (2016) Definition and Procedure for the Determination of the Method Detection Limit, Revision 2, pp. 1-8, United States Environmental Protection Agency (EPA), Washington, DC 20460.
Veil, J. (2015) US produced water volumes and management practices in 2012. Ground Water Protection Council (ed), Veil Environmental, LLC, Oklahoma City, OK.
Villemur, R., Payette, G., Geoffroy, V., Mauffrey, F. and Martineau, C. (2019) Dynamics of a methanol-fed marine denitrifying biofilm: 2impact of environmental changes on the microbial community. PeerJ 7, e7467.
Vishniac, W. and Santer, M. (1957) The Thiobacilli. Bacteriological Reviews 21(3), 195-213.
Vyrides, I. and Stuckey, D.C. (2009) A modified method for the determination of chemical oxygen demand (COD) for samples with high salinity and low organics. Bioresource Technology 100, 979-982.

Walker, E.L., Anderson, A.M., Read, L.K. and Hogue, T.S. (2017) Water use for hydraulic fracturing of oil and gas in the South Platte River basin, Colorado. Journal of the American Water Resources Association 53(4).
Wan, C., Yang, X., Lee, D.-J., Liu, X., Sun, S. and Chen, C. (2014) Partial nitrification of wastewaters with high NaCl concentrations by aerobic granules in continuous-flow reactor. Bioresource Technology 152, 1-6.
Wang, B., Zhao, M., Guo, Y., Peng, Y. and Yuanb, Y. (2018a) Long-term partial nitritation and microbial characteristics in treating low C/N ratio domestic wastewater. Environmental Science Water Research & Technology.
Wang, D., Ji, M. and Wang, C. (2014) Degradation of organic pollutants and characteristics of activated sludge in an anaerobic/anoxic/oxic reactor treating chemical industrial wastewater. Brazilian Journal of Chemical Engineering 31(3), 703-713.
Wang, F., Zhou, L. and Zhao, J. (2018b) The performance of biocarrier containing zinc nanoparticles in biofilm reactor for treating textile wastewater. Process Biochemistry 74, 125-131.
Wang, L., Liu, X., Lee, D.-J., Tay, J.-H., Zhang, Y. and Wan, C.-L. (2018c) Recent advances on biosorption by aerobic granular sludge. journal od Hazardous Materials 357, 253-270.
Wang, W.-L., Hu, H.-Y., Liu, X., Shi, H.-X., Zhou, T.-H., Wang, C., Huo, Z.-Y. and Wu, Q.-Y. (2019) Combination of catalytic ozonation by regenerated granular activated carbon (rGAC) and biological activated carbon in the advanced treatment of textile wastewater for reclamation. Chemosphere 231, 369-377.
Wang, X., Goual, L. and Colberg, P.J.S. (2012) Characterization and treatment of dissolved organic matter from oilfield produced waters. Journal of Hazardous Materials 217-218, 164-170.
Wang, X., Yang, T., Lin, B. and Tang, Y. (2017a) Effects of salinity on the performance, microbial community, and functional proteins in an aerobic granular sludge system. Chemosphere 184, 1241-1249.
Wang, Y., Feng, M., Liu, Y., Li, Y. and Zhang, B. (2017b) Comparison of three types of anaerobic granular sludge for treating pharmaceutical wastewater. Journal of Water Reuse and Desalination in press, 1-12.
Wang, Z., van Loosdrecht, M.C.M. and Saikaly, P.E. (2017c) Gradual adaptation to salt and dissolved oxygen: Strategies to minimize adverse effect of salinity on aerobic granular sludge. Water Research 124, 702-712.
Warren, J. (2019) Toluene Removal from Produced Water by Biofilm Granular Activated Carbon System, Kansas University, ProQuest Dissertations and Theses.
Wickham, H. (2016) ggplot2: elegant graphics for data analysis, Springer.
Wu, J., Jiang, B., Feng, B., Li, L., Moideen, S.N.F., Chen, H., Mribet, C. and Li, Y.-Y. (2020a) Pre-acidification greatly improved granules physicochemical properties and operational stability of Upflow anaerobic sludge Blanket (UASB) reactor treating low-strength starch wastewater. Bioresource Technology 302, 122810.
Wu, X., Li, H., Lei, L., Ren, J., Li, W. and Liu, Y. (2020b) Tolerance to short-term saline shocks by aerobic granular sludge. Chemosphere 243, 125370.
Xu, J., Bettahalli, N.M.S., Chisca, S., Khalid, M.K., Ghaffour, N., Vilagines, R. and Nunes, S.P. (2018) Polyoxadiazole hollow fibers for produced water treatment by direct contact membrane distillation. Desalination 432, 32-39.
Xu, J., Pang, H., He, J., Nan, J., Wang, M. and Li, L. (2020) Start-up of aerobic granular biofilm at low temperature: Performance and microbial community dynamics. Science of the Total Environment 698, 134311.
Xue, W., Hao, T., Mackey, H.R., Li, X., Chan, R.C. and Chen, G. (2017) The role of sulfate in aerobic granular sludge process for emerging sulfate-laden wastewater treatment. Water Research 124, 513-520.

Yilmaz, P., Parfrey, L., Yarza, P., Gerken, J., Pruesse, E., Quast, C., Schweer, T., Peplies, J., Ludwig, W. and Glöckner, F. (2013) The SILVA and "all-species living tree project (LTP)" taxonomic frameworks. Nucleic acids research 42(D1), D643-D648.

Yin, C., Meng, F. and Chen, G.-H. (2015) Spectroscopic characterization of extracellular polymeric substances from a mixed culture dominated by ammonia-oxidizing bacteria. Water Research 68, 740-749.

Yousefi, N., Pourfadakari, S., Esmaeili, S. and Babaei, A.A. (2019) Mineralization of high saline petrochemical wastewater using Sonoelectroactivated persulfate: Degradation mechanisms and reaction kinetics. Microchemical Journal 147, 1075-1082.

Yurtsever, A., Sahinkaya, E. and Çınar, Ö. (2020) Performance and foulant characteristics of an anaerobic membrane bioreactor treating real textile wastewater. Journal of Water Process Engineering 33, 101088.

Yusoff, N., Ong, S.-A., Ho, L.-N., Wong, Y.-S., Saad, F.N.M., Khalik, W. and Lee, S.-L. (2019) Performance of the hybrid growth sequencing batch reactor (HG-SBR) for biodegradation of phenol under various toxicity conditions. Journal of Environmental Sciences 75, 64-72.

Yusoff, N.A., Ong, S.-A., Ho, L.-N., Wong, Y.-S., Saad, F.N.M., Khalik, W.F. and Lee, S.-L. (2018) Theoretical development of biofilm in hybrid growth sequencing batch reactor (HG-SBR) for degradation of phenol. Desalination and Water Treatment 107, 100-108.

Zhang, J., Zhao, R., Cao, L., Lei, Y., Liu, J., Feng, J., Fu, W., Li, X. and Li, B. (2020) High-efficiency biodegradation of chloramphenicol by enriched bacterial consortia: Kinetics study and bacterial community characterization. Journal of Hazardous Materials 384, 121344.

Zhang, T., Gregory, K., Hammack, R.W. and Vidic, R.D. (2014) Co-precipitation of Radium with Barium and Strontium Sulfate and Its Impact on the Fate of Radium during Treatment of Produced Water from Unconventional Gas Extraction. Enviromental Science & Technology 48(4596-4603).

Zhang, W., Ding, W. and Ying, a.W. (2013) Biological Activated Carbon Treatment for Removing BTEX from Groundwater. journal of environmental Engineering 139(10), 1246-1254.

Zhang, X., Chen, A., Zhang, D., Kou, S. and Lu, P. (2018) The treatment of flowback water in a sequencing batch reactor with aerobic granular sludge: Performance and microbial community structure. Chemosphere 211, 1065-1072.

Zhang, Y., Li, B., Xu, R.-X., Wang, G.-X., Zhou, Y. and Xie, B. (2016) Effects of pressurized aeration on organic degradation efficiency and bacterial community structure of activated sludge treating saline wastewater. Bioresource Technology 222, 182-189.

Zhang, Z., Du, X., Carlson, K.H., Robbins, C.A. and Tong, T. (2019) Effective treatment of shale oil and gas produced water by membrane distillation coupled with precipitative softening and walnut shell filtration. Desalination 454, 82-90.

Zhao, Y., Liu, D., Huang, W., Yang, Y., Ji, M., Nghiem, L.D., Trinh, Q.T. and Tran, N.H. (2019) Insights into biofilm carriers for biological wastewater treatment processes: Current state-of-the-art, challenges, and opportunities. Bioresource Technology 288, 121619.

Zou, L., Gusnawan, P., Zhang, G. and Yu, J. (2020) Novel Janus composite hollow fiber membrane-based direct contact membrane distillation (DCMD) process for produced water desalination. Journal of Membrane Science 597, 117756.

Zou, S., Zhang, B., Yan, N., Zhang, C., Xu, H., Zhang, Y. and Rittmann, B.E. (2018) Competition for molecular oxygen and electron donor between phenol and quinoline during their simultaneous biodegradation. Process Biochemistry in press.

Appendix A: Supplementary Information for Chapter 4

Table A1: Reactor biomass growth, COD removal and SVI as a function of salinity

	Halophile Reactor			Activated Sludge Reactor		
NaCl, g L^{-1}	MLVSS, g L^{-1}	SVI_5, mL g^{-1}	COD removal %	MLVSS, g L^{-1}	SVI_5, mL g^{-1}	COD removal %
0†	1110 ± 200	9 ± 4	76 ± 7	1420 ± 600	25 ± 13	89 ± 5
10	1190 ± 600	46 ± 16	82 ± 9	2160 ± 400	32 ± 12	92 ± 3
20	2290 ± 300	47 ± 11	91 ± 5	2150 ± 600	32 ± 16	82 ± 10
30	3280 ± 500	17 ± 7	92 ± 6	3800 ± 100	15 ± 6	90 ± 2
40	4570 ± 600	12 ± 5	80 ± 12	5250 ± 700	13 ± 5	92 ± 2
50	6100 ± 300	19 ± 4	93 ± 2	3060 ± 500	16 ± 1	87 ± 1
60	10330 ± 1000	23 ± 1	96 ± 1	2150 ± 300	16 ± 1	82 ± 3
70	8450 ± 300	20 ± 1	91 ± 2	6500 ± 200	28 ± 3	91 ± 3
80	12700 ± 100	18 ± 1	94 ± 3	6780 ± 500	20 ± 1	91 ± 4
85	12800 ± 300	23 ± 5	93 ± 1	10460 ± 2900	19 ± 3	90 ± 5

†- The first 14 days before granule formation was observed are not included in these values

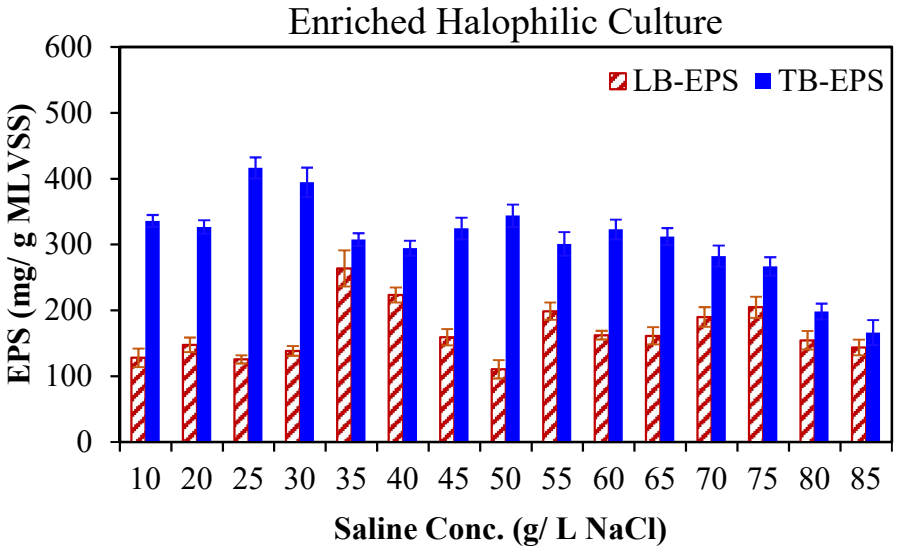

Figure A1: Loosely bound and tightly bound EPS production in the reactor inoculated with an enriched halophilic culture.

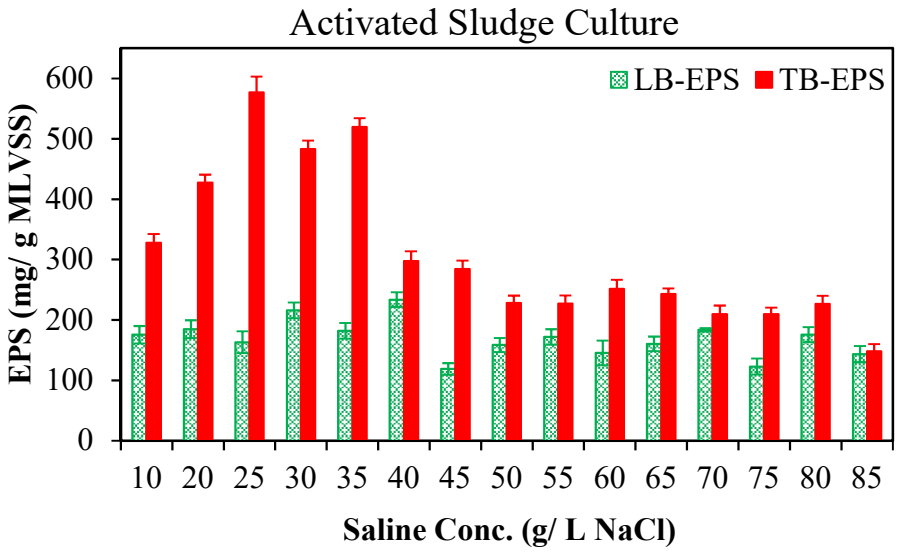

Figure A2: Loosely bound and tightly bound EPS production in the reactor inoculated with an activated sludge culture.

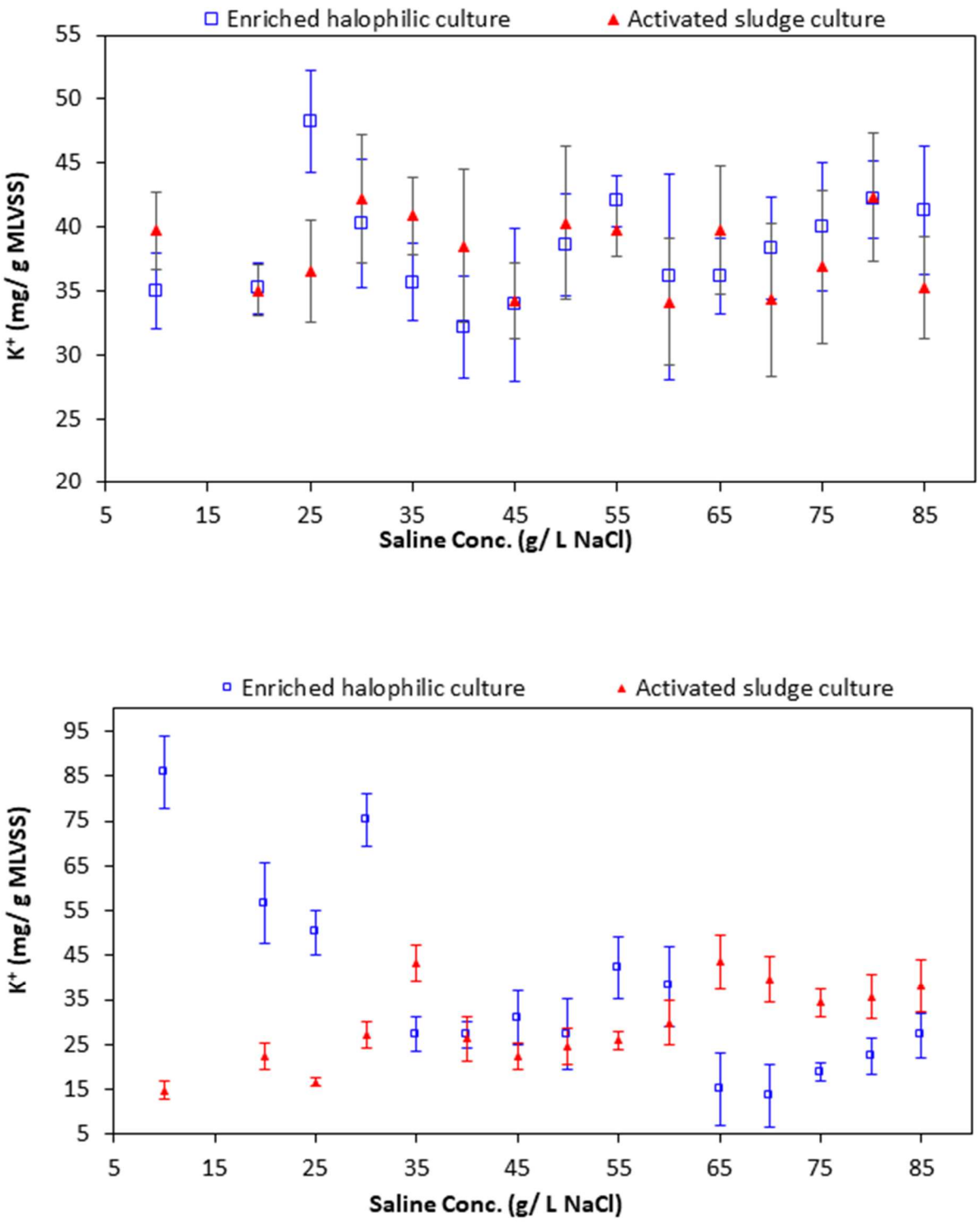

Figure A3: Potassium (K^+) concentrations in the EPS (top) and intracellular K^+ concentrations (bottom) for the enriched halophilic and activated sludge reactors.

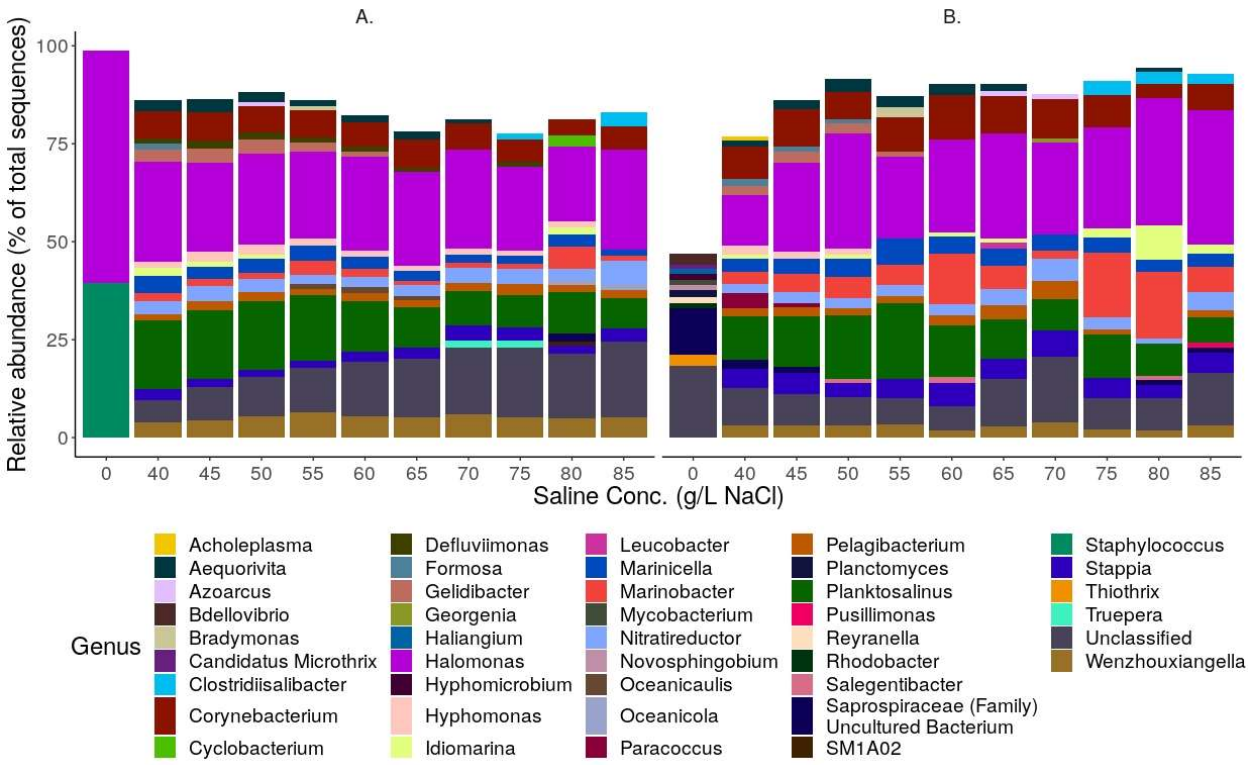

Figure A4: Stacked bar plot displaying the relative abundance of OTUs at genus level with relative abundance greater than 1% of the samples for the enriched halophilic culture treatment (A.) and activated sludge culture treatment (B.)

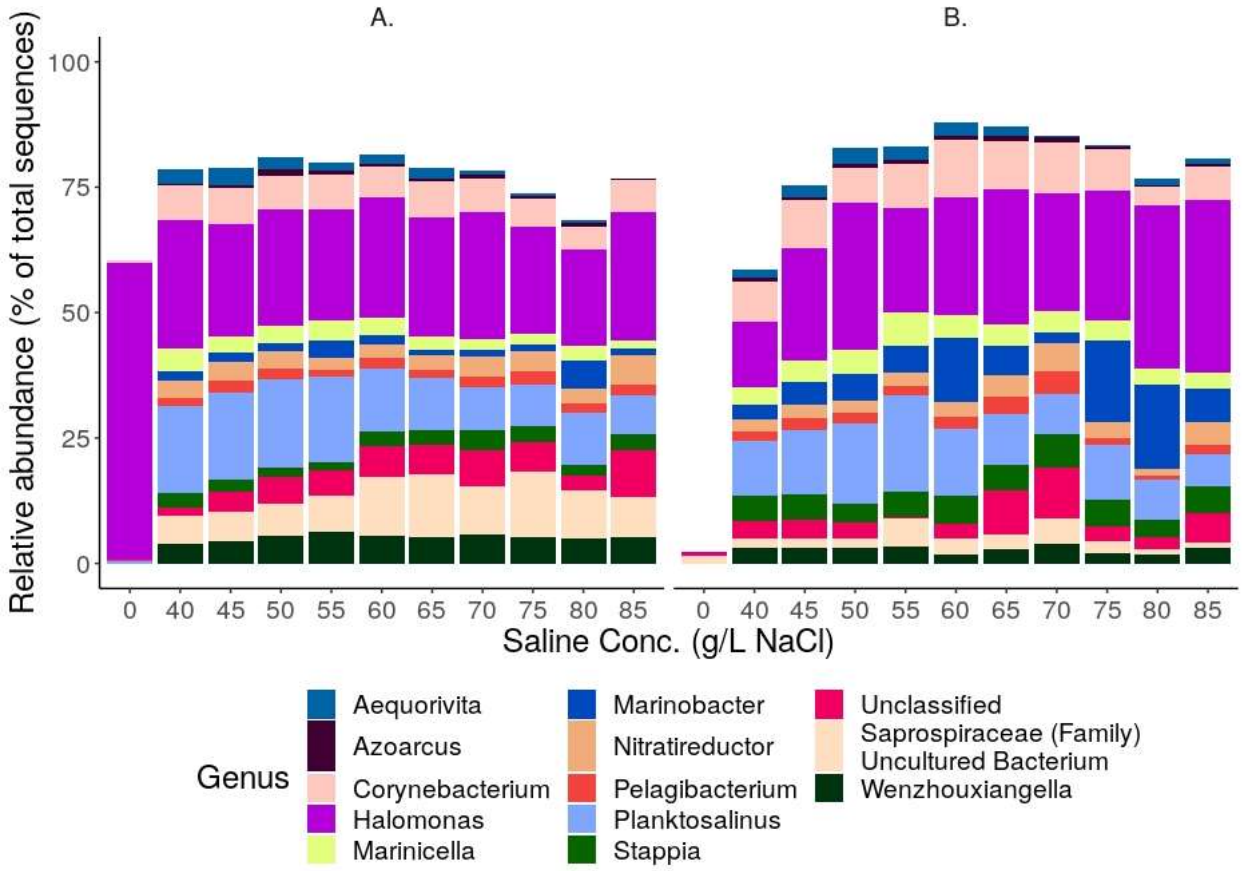

Figure A5: Stacked bar plot displaying the relative abundance of the Core microbiome, which is defined as organisms at genus level, observed in 90 % of the samples at starting conditions and from 40-85 g/L NaCl for (A) the enriched halophilic culture treatment; and (B.) the activated sludge culture treatment.

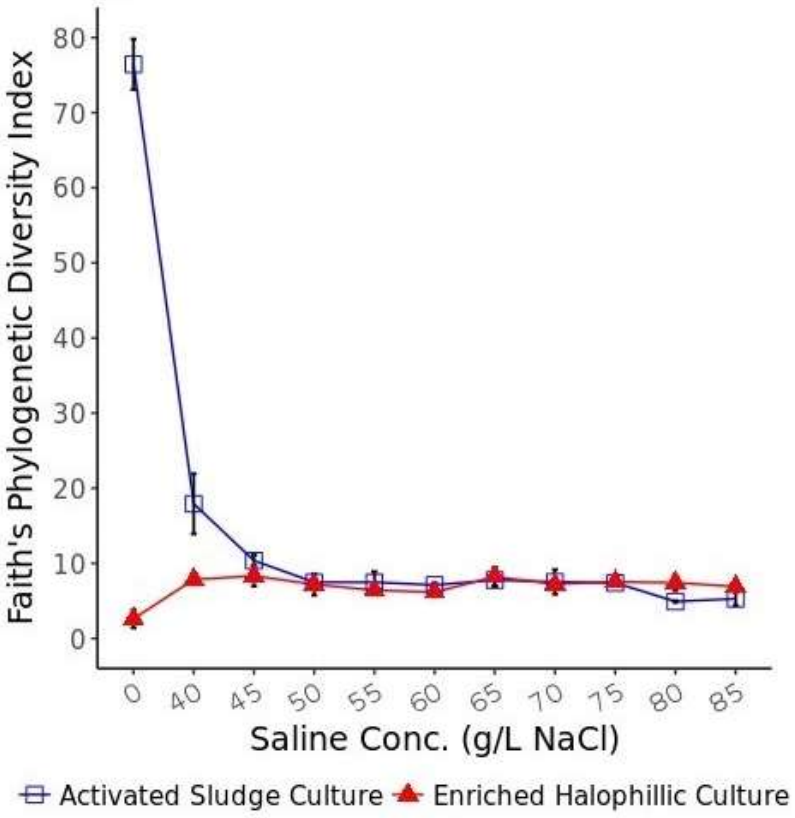

Figure A6: Faith's Phylogenetic Diversity indicating richness of microbial communities in the enriched halophilic culture treatment (Red) and activated sludge culture treatment (blue) at different saline concentrations.

Appendix B: Supplementary Information for Chapter 5

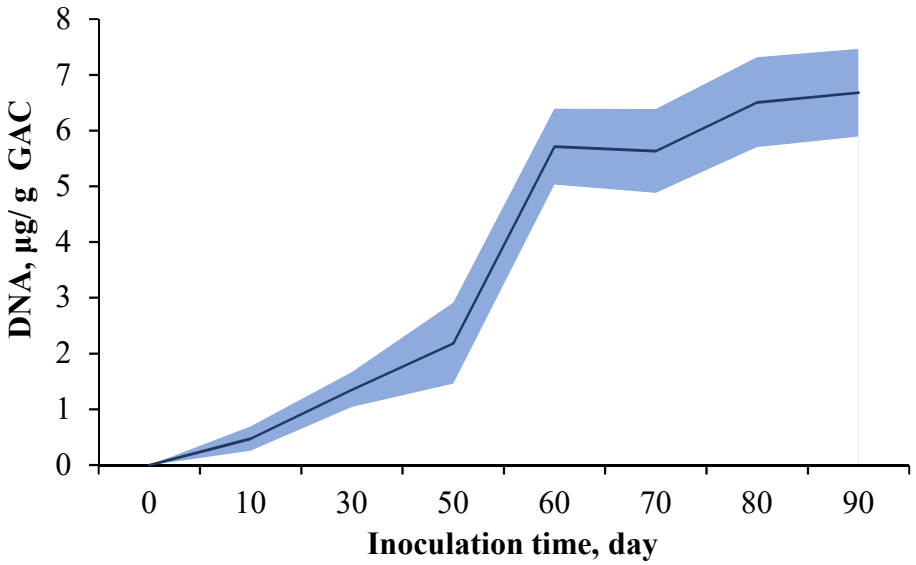

Figure B1: Quantified DNA from biofilm on GAC surface during startup period.

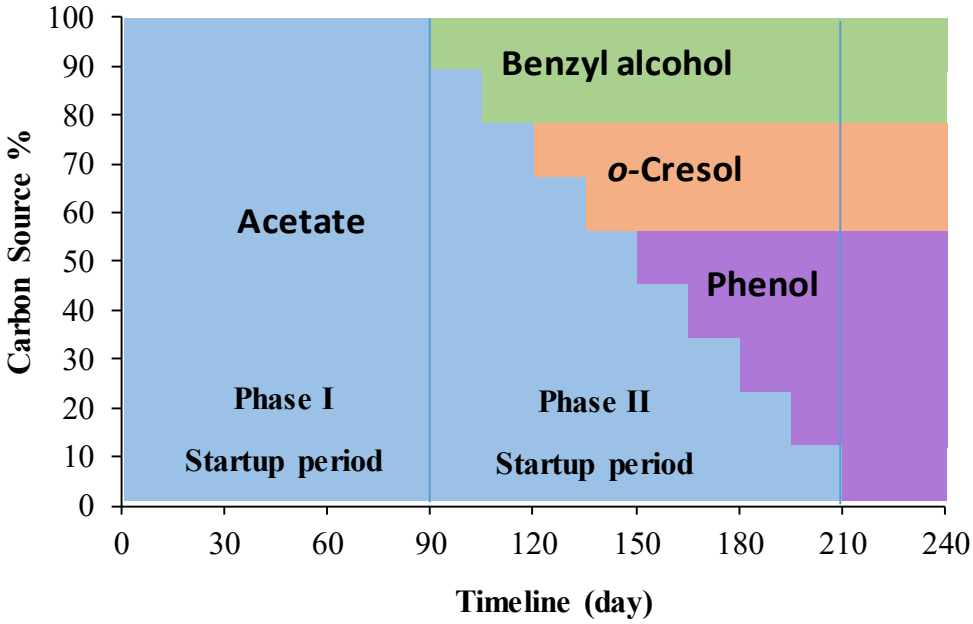

Figure B2: Carbon source during startup period and experiment operation time

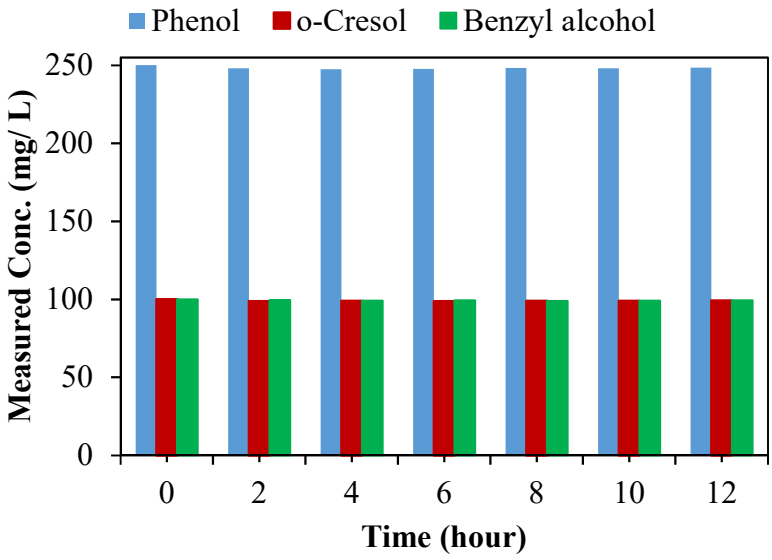

Figure B3: Aromatic compound concentrations in the batch control reactor (250 mg L^{-1} of Ph and 100 mg L^{-1} of each of BA and o-Cresol).

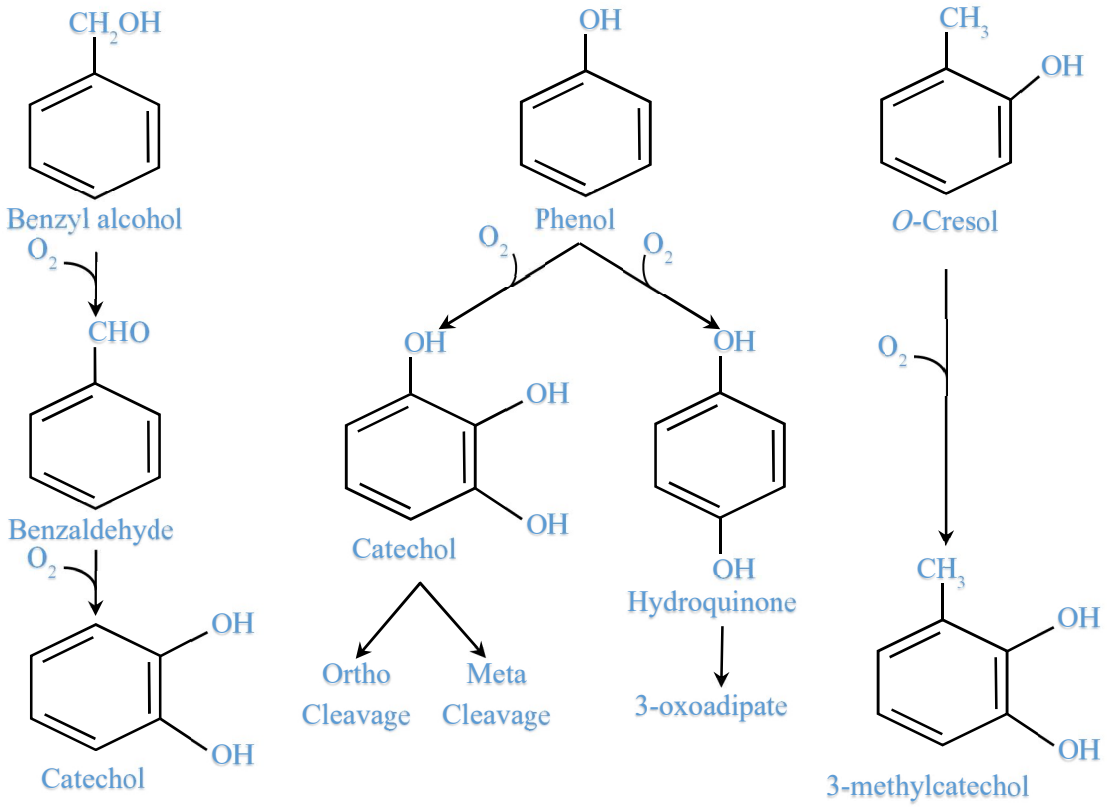

Figure B4: Benzyl alcohol, o-cresol, and phenol aerobic biodegradation pathways.

Biofilm development over time

The biofilm morphology has affected by introducing aromatic compounds to fed wastewater in both AGS and Bio-GAC systems. The biofilm texture was much less uniform in Bio-GAC biofilm by the end of phase II startup period (Figure B5 a). Big holes were observed in AGS biofilm during the same period time (Figure B5 c). Both systems, however, could establish uniform biofilm texture after 30 days of operating under hypersaline conditions and a mixture of aromatic compounds as the only carbon source. It is worth noting that the appearance of mature biofilm in Bio-GAC was smooth while it was colonized in AGS surface (Figure B5 b and d respectively). The different appearance of biofilm between AGS and Bio-GAC biofilm can be attributed to the different biogrowth in these systems as shown in Figures B8 and B9.

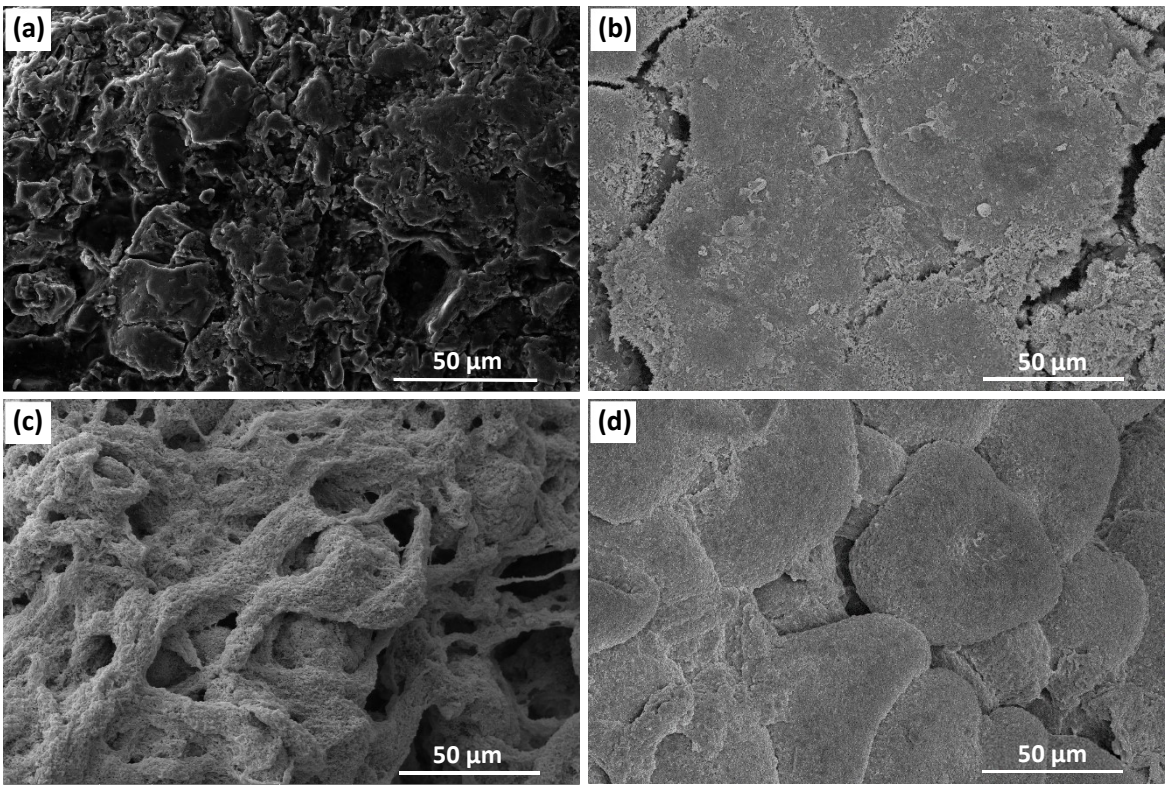

Figure B5: SEM observation showing the impact of carbon source changing on biofilm morphology. (a) and (c) biofilm of Bio-GAC and AGS at the end of startup period. (b) and (d) mature biofilm of Bio-GAC and AGS (after 240 days of operation).

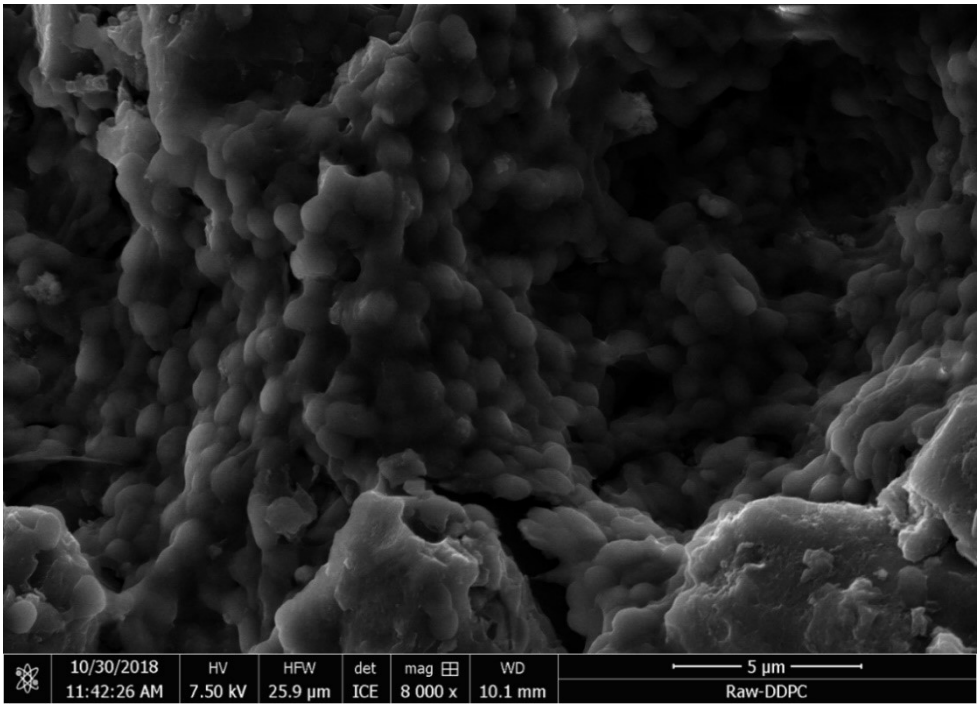

Figure B6: Developed biofilm on GAC surface during startup period.

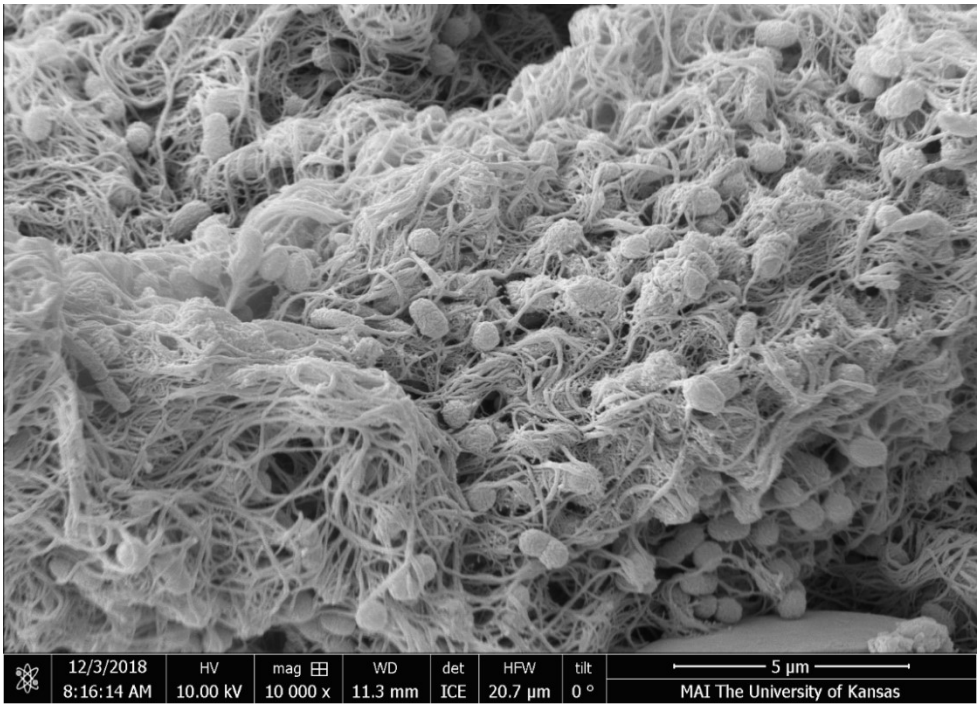

Figure B7: Developed biofilm on AGS structure during startup period.

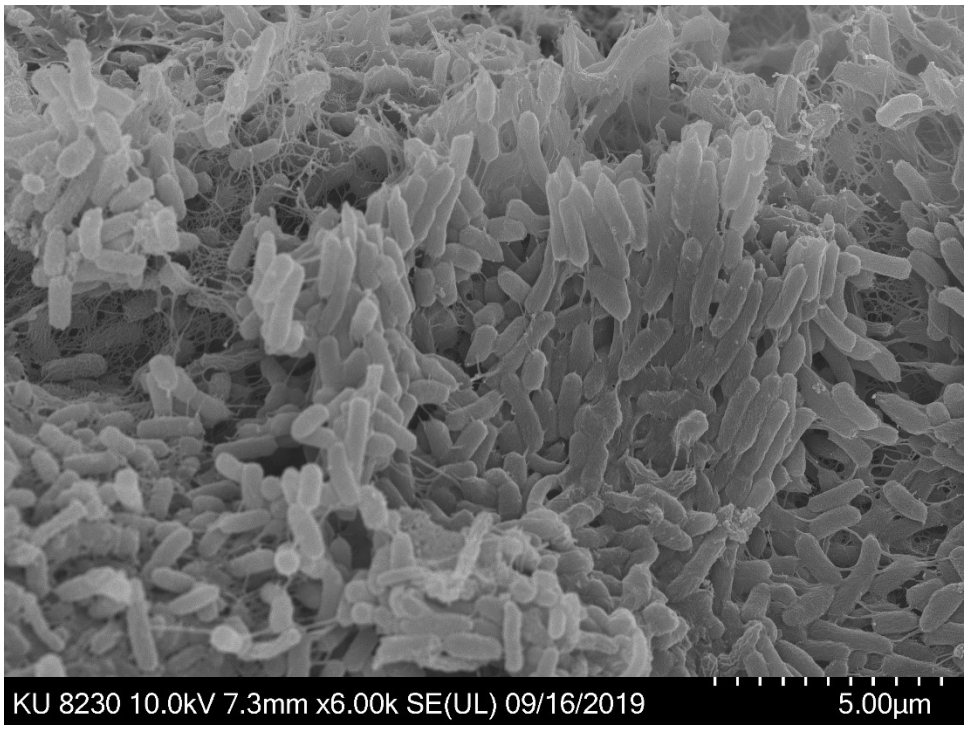

Figure B8: Mature biofilm in Bio-GAC reactor.

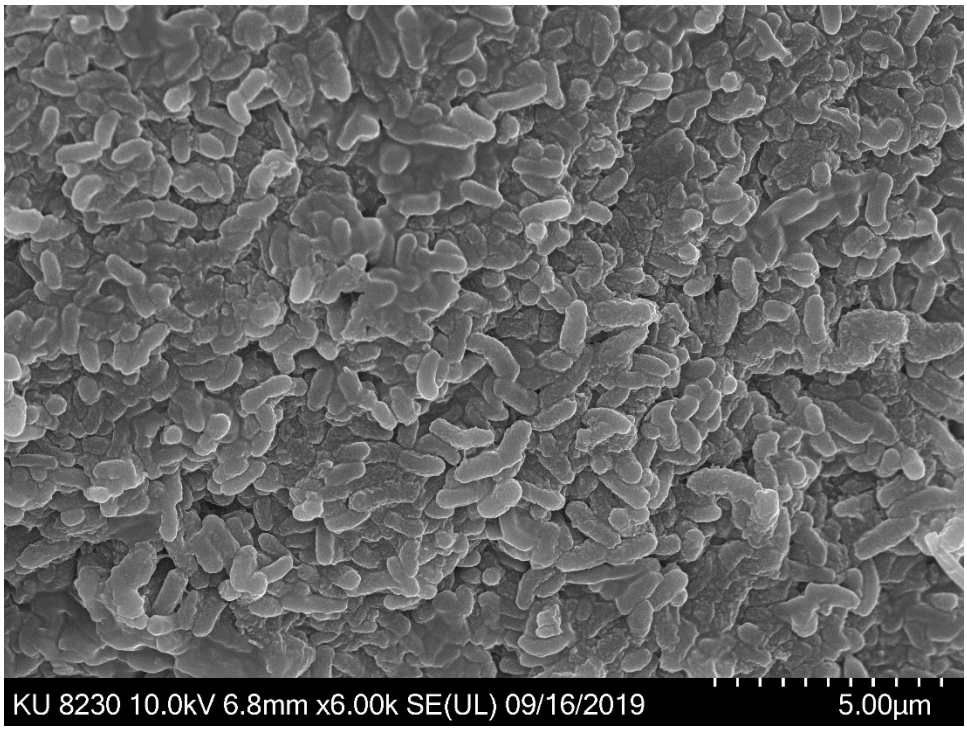

Figure B9: Mature biofilm in AGS reactor.

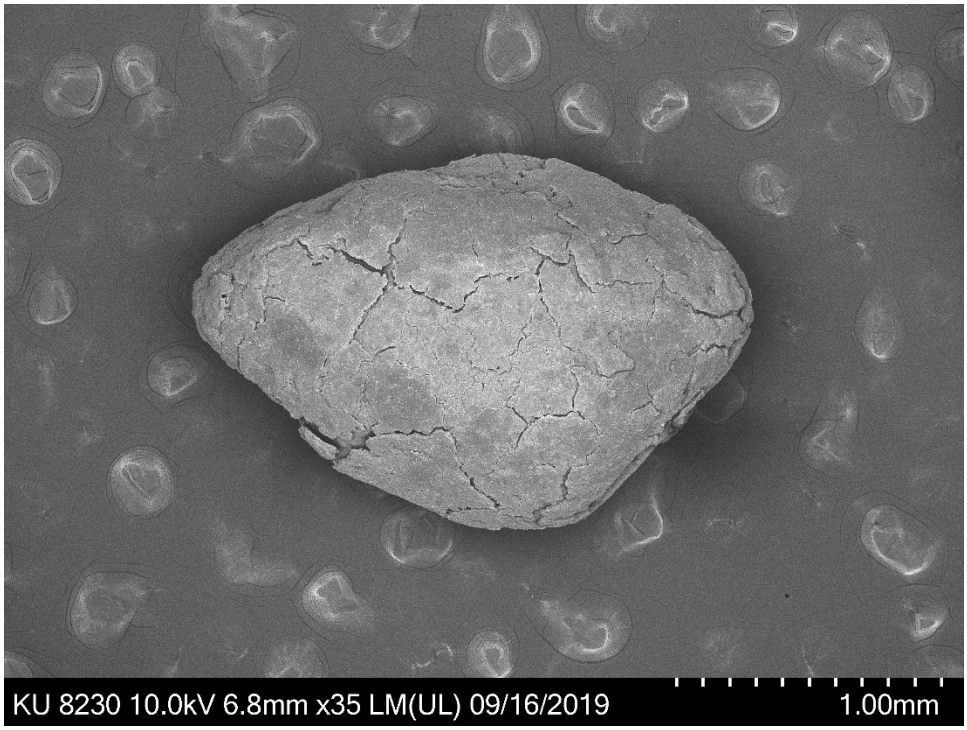

Figure B10: Developed biofilm on GAC surface consists of cocci bacterial growth only.

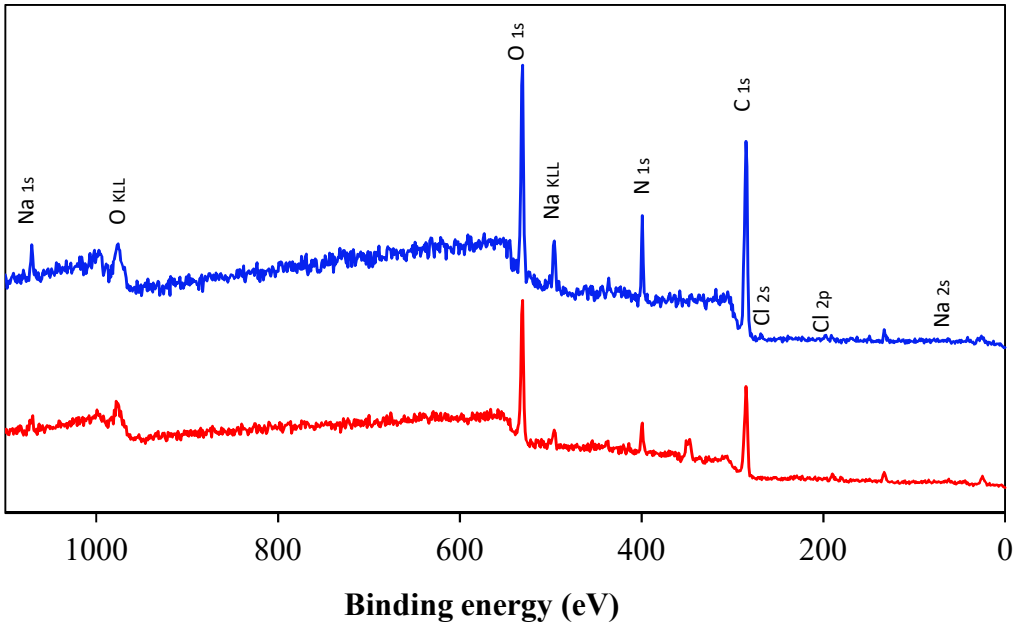

Figure B11: XPS wide survey scans for Bio-GAC samples, famine phase (top) and feast phase (bottom).

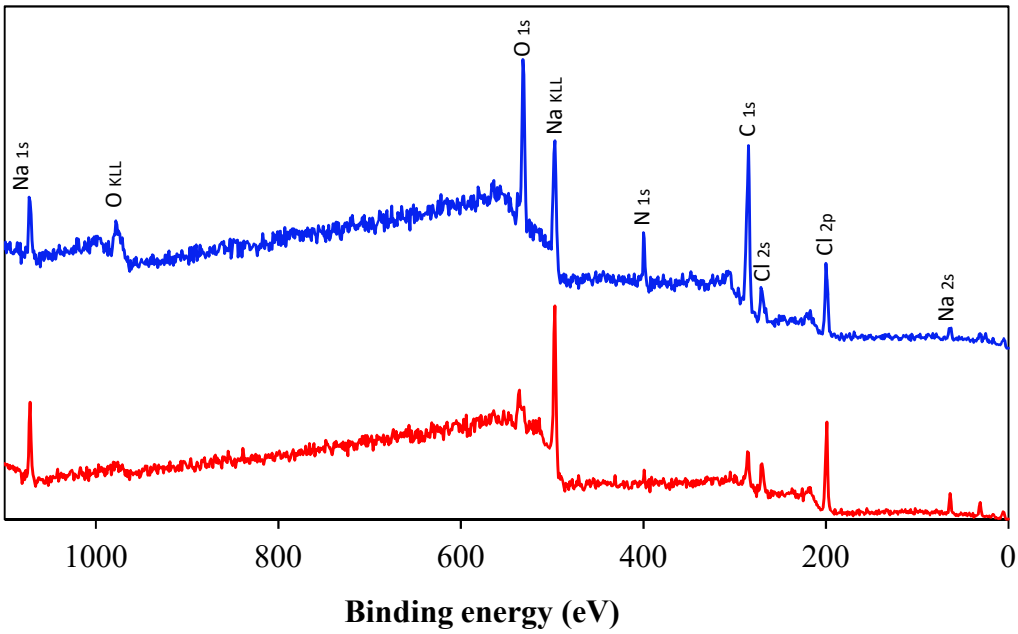

Figure B12: XPS wide survey scans for AGS samples, famine phase (top) and feast phase (bottom).

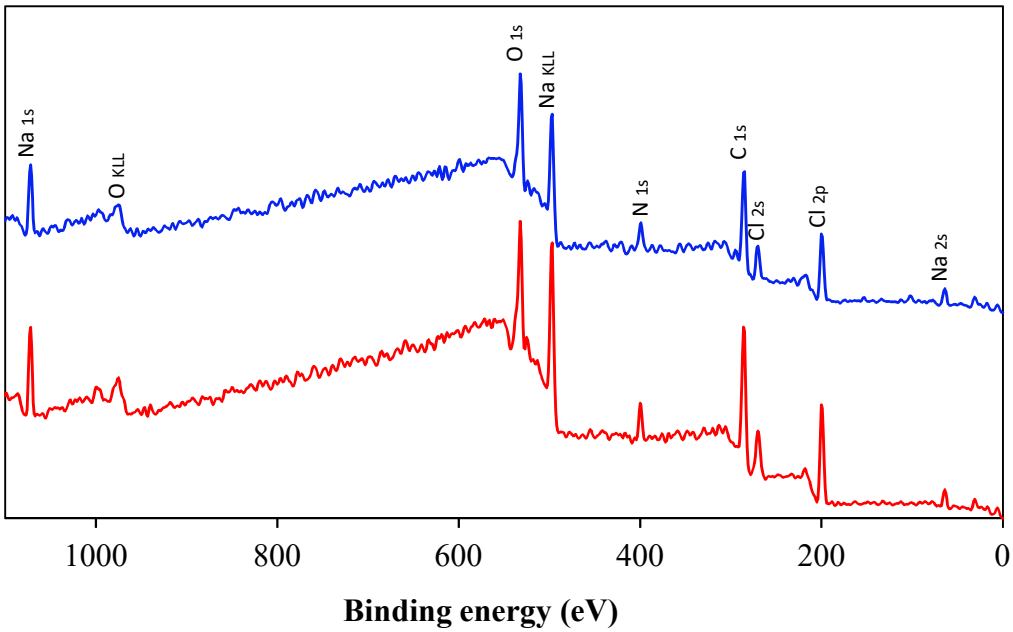

Figure B13: XPS wide survey scans for CAS samples, famine phase (top) and feast phase (bottom).

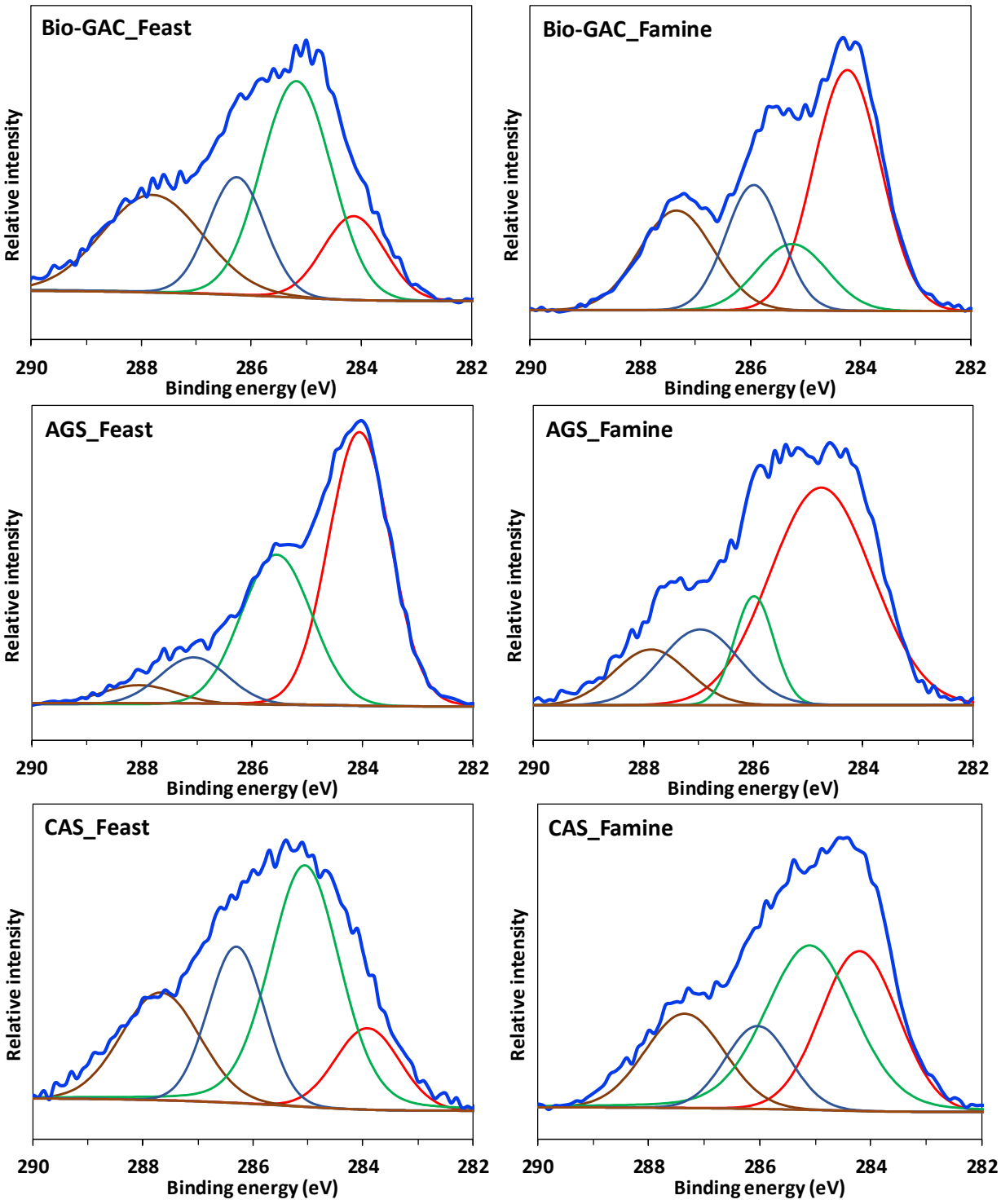

Figure B14: XPS wide survey scans of carbon atom at feast and famine phases for Bio-GAC, AGS and CAS samples. The peaks potions shifted and the area under curves changed as the operation phases switched from feast to famine.

Appendix C: Supplementary Information for Chapter 6

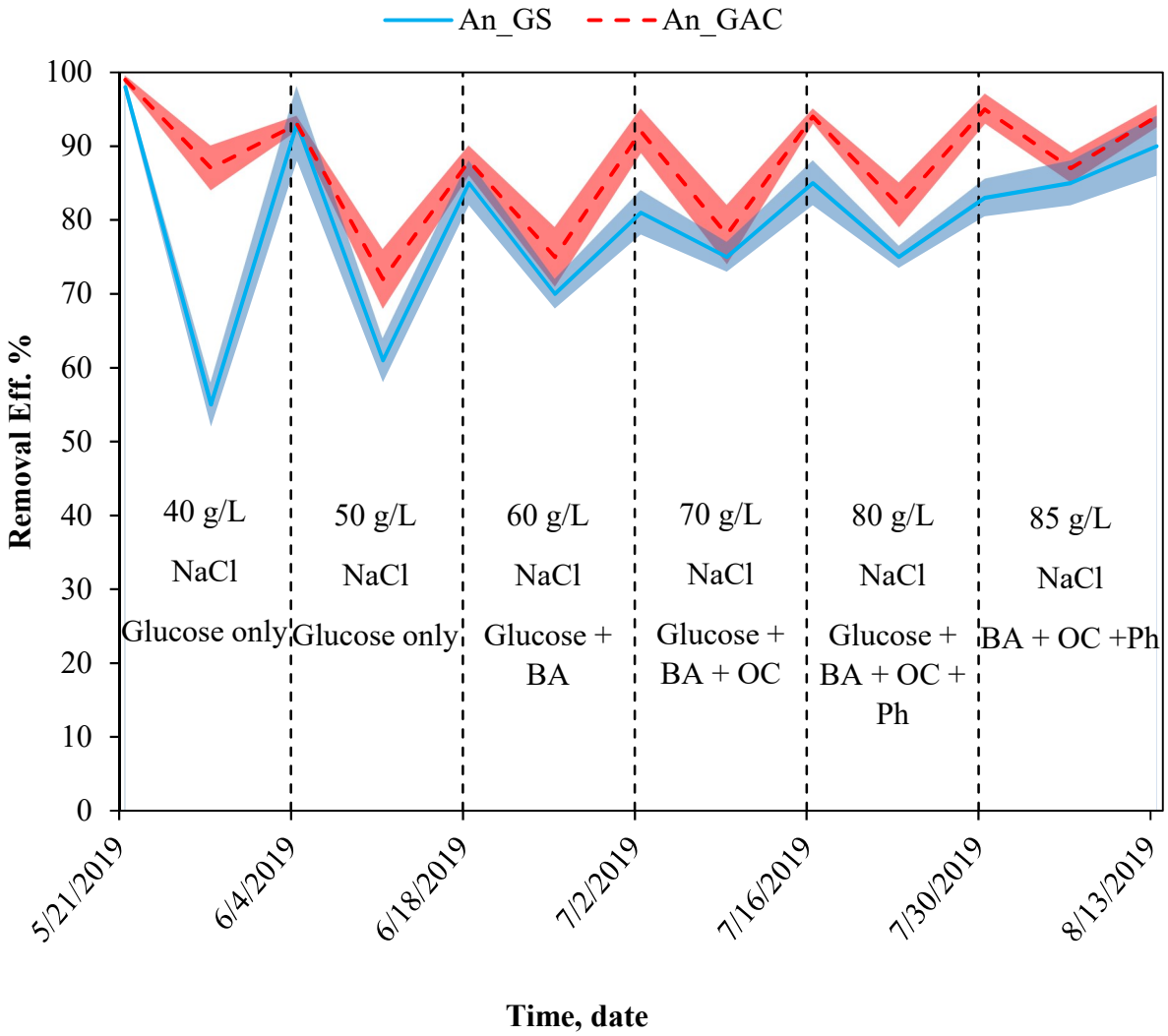

Figure C1: Carbon source and salinity adaptation period for AnGAC and UASB anaerobic reactors.

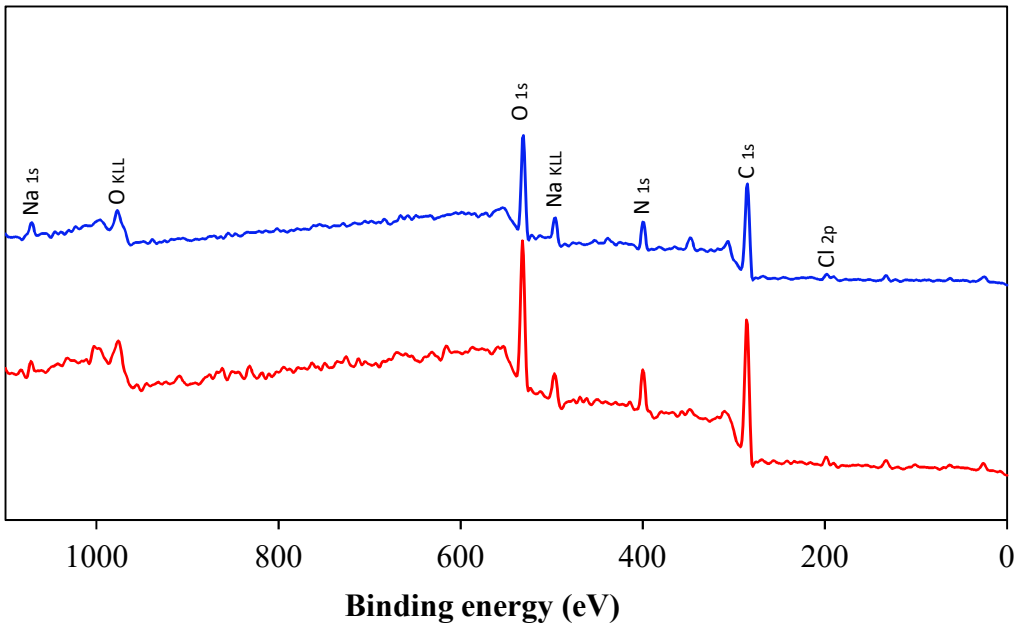

Figure C2: XPS wide survey scans for Bio-GAC samples, famine phase (top) and feast phase (bottom).

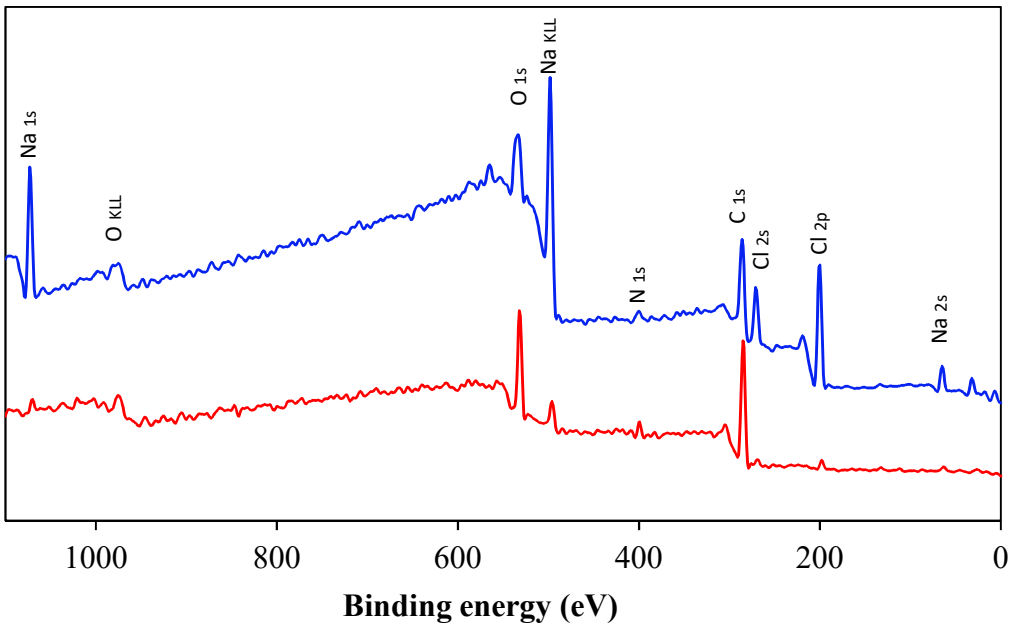

Figure C3: XPS wide survey scans for AGS samples, famine phase (top) and feast phase (bottom).

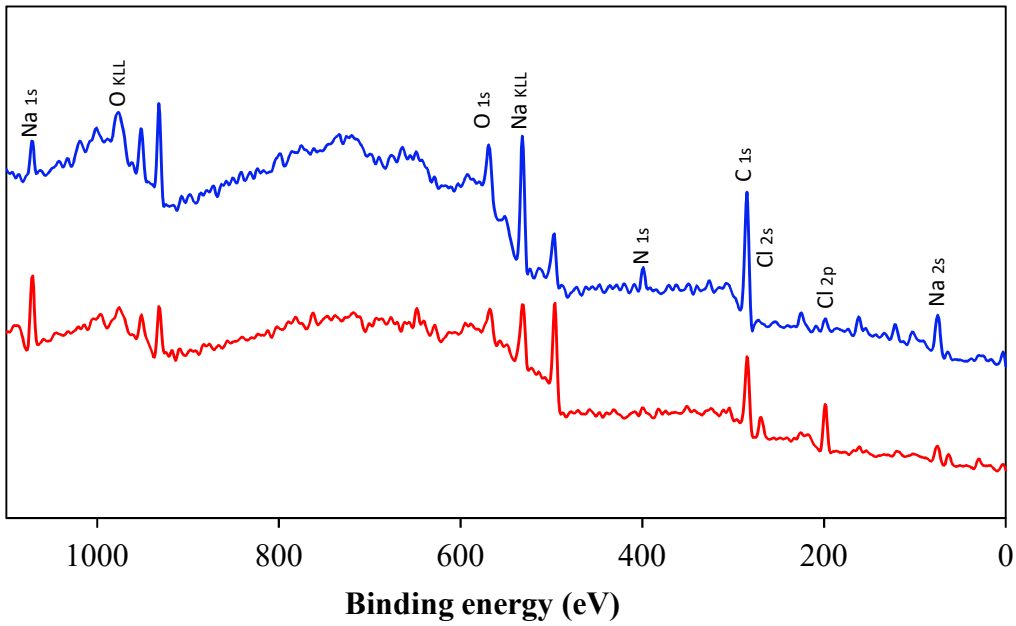

Figure C4: XPS wide survey scans for AnGAC samples, famine phase (top) and feast phase (bottom).

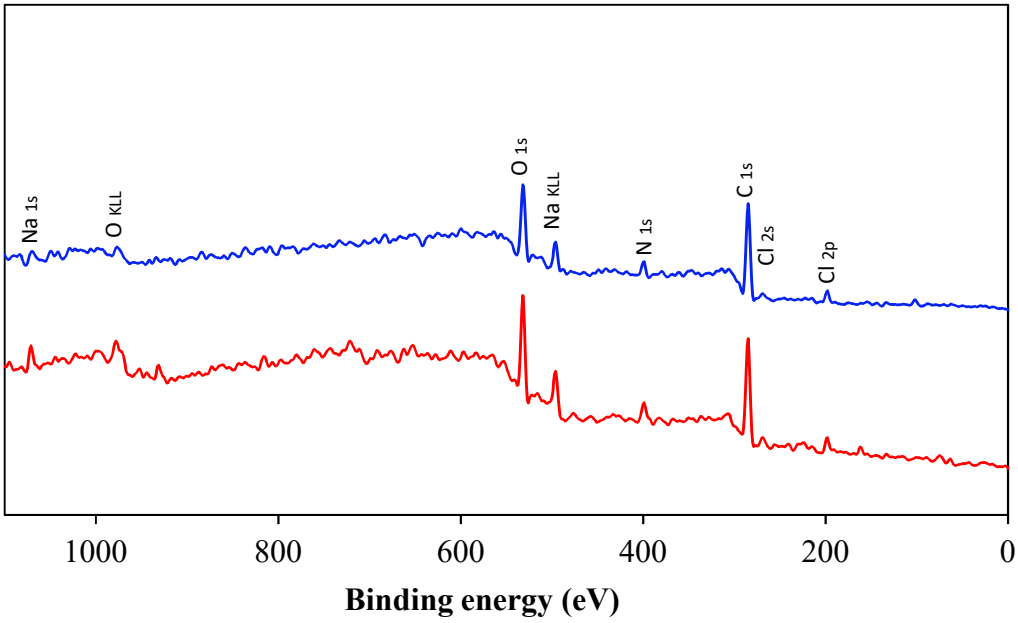

Figure C5: XPS wide survey scans for USBA samples, famine phase (top) and feast phase (bottom).

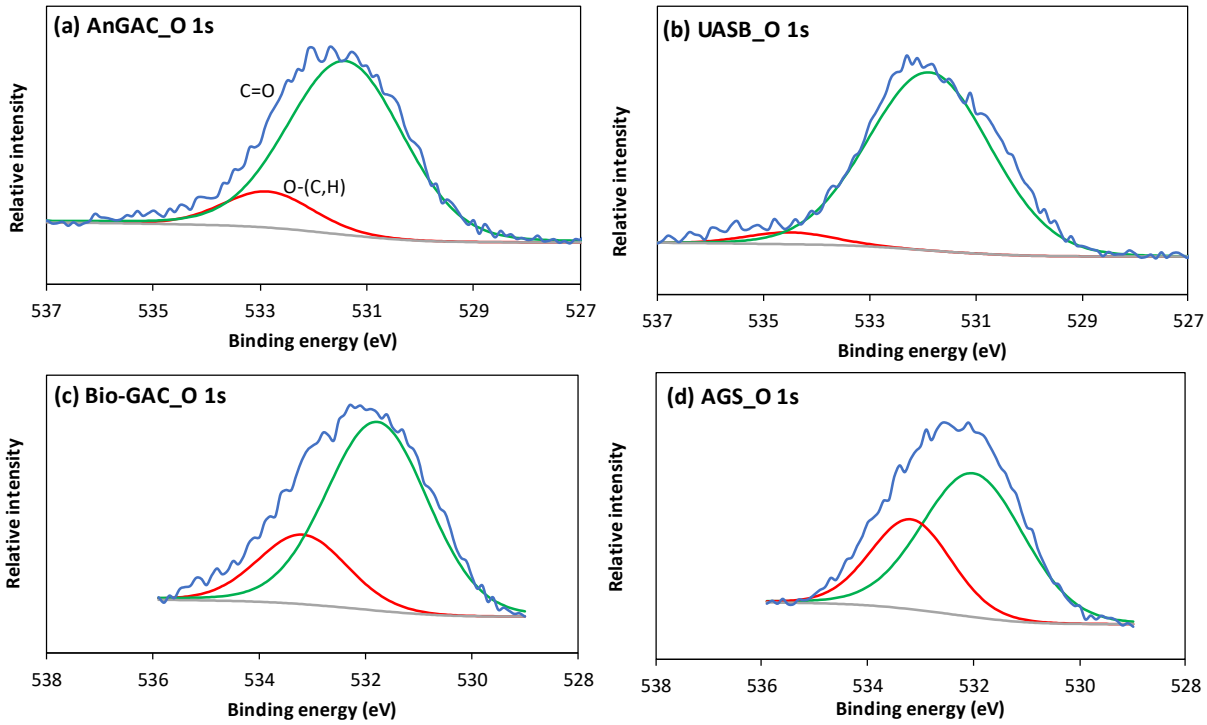

Figure C6: High-resolution O 1s spectra of (a) anaerobic biofilm integrated on GAC surface, (b) biofilm of anaerobic granular sludge, (c) aerobic biofilm integrated on GAC surface and (d) biofilm of aerobic granular sludge.

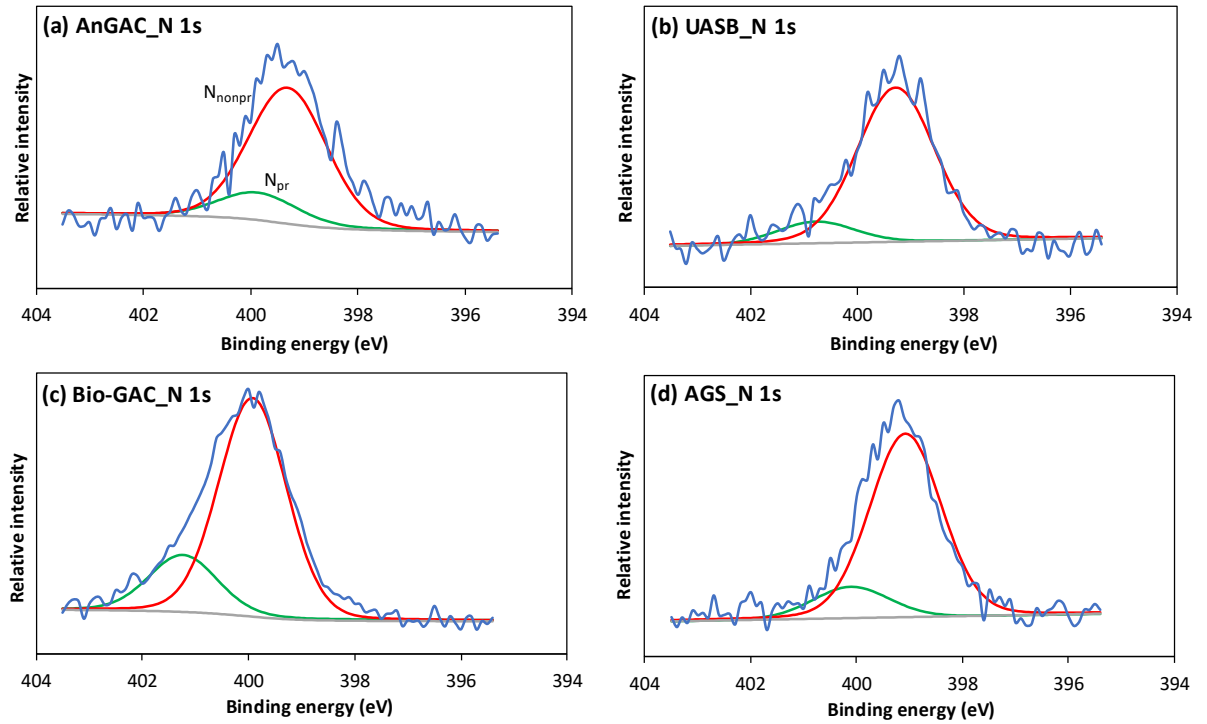

Figure C7: High-resolution N 1s spectra of (a) anaerobic biofilm integrated on GAC surface, (b) biofilm of anaerobic granular sludge, (c) aerobic biofilm integrated on GAC surface and (d) biofilm of aerobic granular sludge.

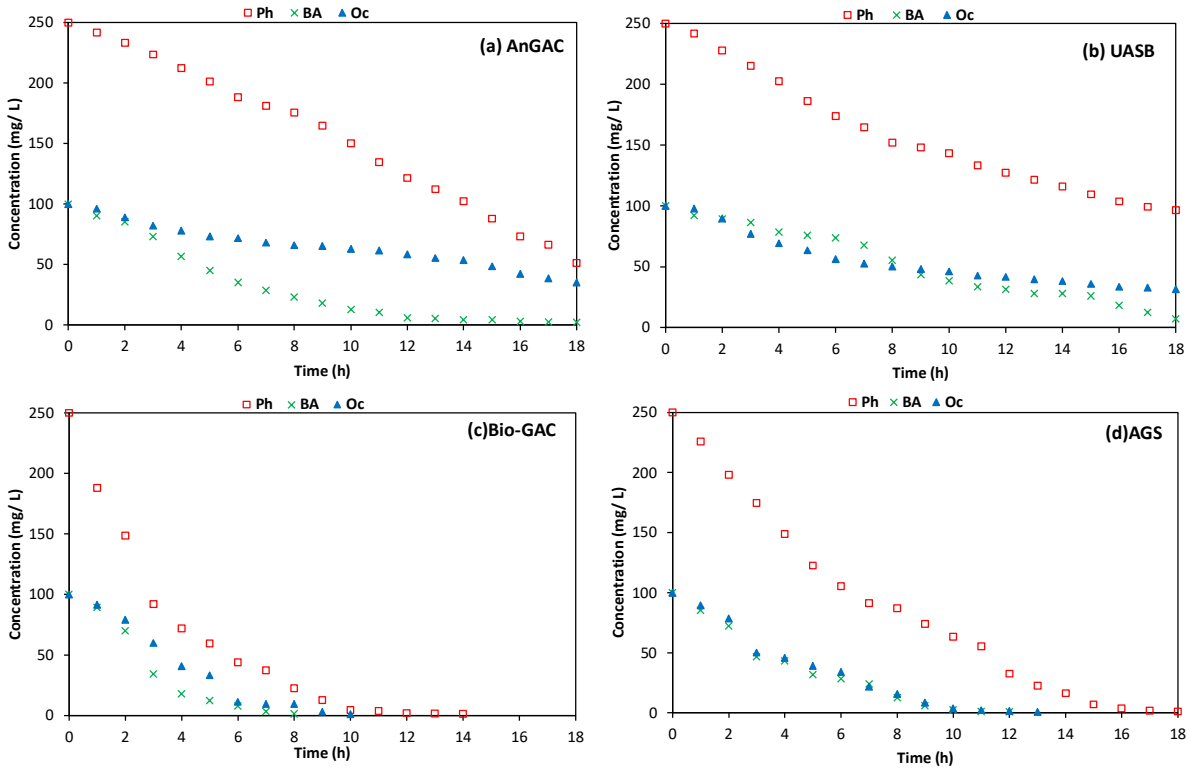

Figure C8: The residual of aromatic compounds (fed as a mixture)in anaerobic and aerobic reactors, AnGAC (a), UASB (b), Bio-GAC (c) and AGS (d).

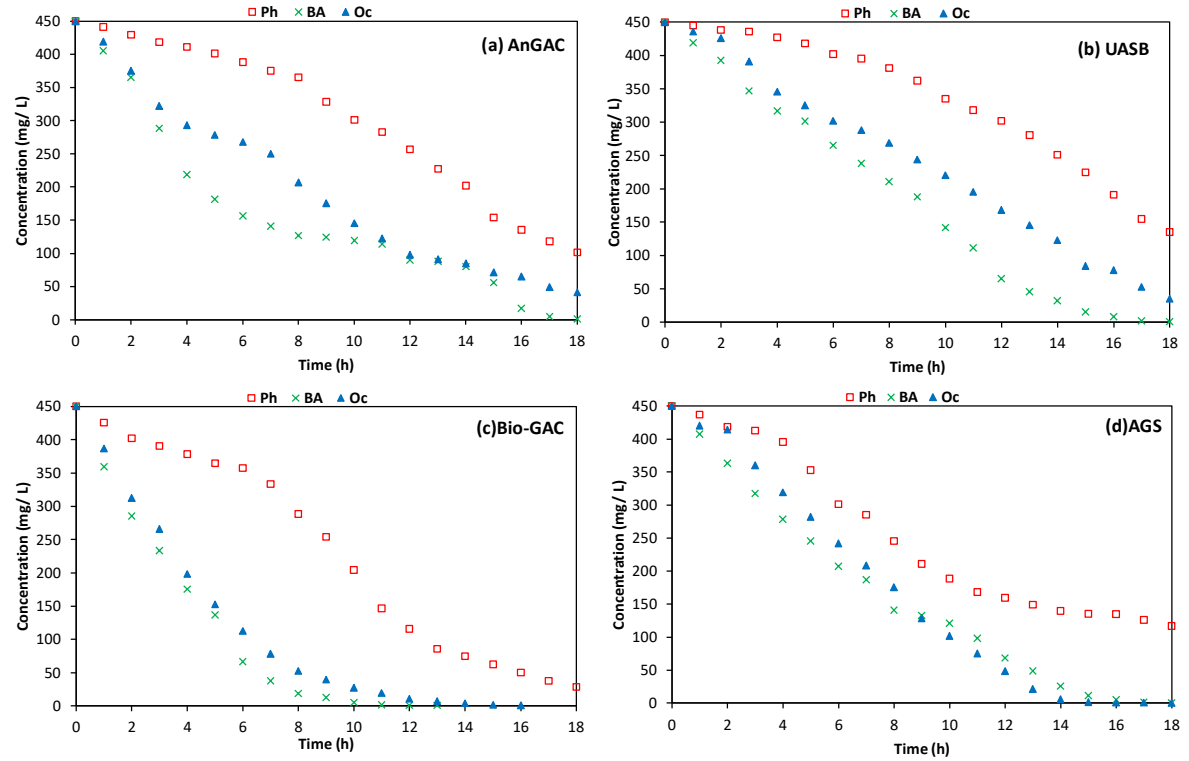

Figure C9: The residual of aromatic compounds (fed as an individual compounds) in anaerobic and aerobic reactors, AnGAC (a), UASB (b), Bio-GAC (c) and AGS 9d).

Appendix D: Agilent 7890B Gas Chromatograph (GC) Control Information

Sample Inlet: GC

Injection Source: GC ALS

Injection Location: Front

Mass Spectrometer: Enabled

Sample Prep method: None assigned to this method

GC Oven

Temperature Setpoint: On

(Initial): 40 °C

Hold Time: 1 min

Post Run: 60 °C

Program

#1 Rate: 4 °C/min

#1 Value: 120 °C

#1 Hold Time: 2 min

#2 Rate: 12 °C/min

#2 Value: 240 °C

#2 Hold Time: 1 min

Equilibration Time: 0.5 min

Max Temperature: 300 °C

Maximum Temperature Override: Disabled

Slow Fan: Disabled

Cryo: Off

ALS

Front Injector

Syringe Size: 10 µL

Injection Volume: 1 µL

Solvent A Washes (PreInj): 3

Solvent A Washes (PostInj) : 3

Solvent A Volume: 8 µL

Solvent B Washes (PreInj): 3

Solvent B Washes (PostInj): 3

Solvent B Volume: 8 µL

Sample Washes: 3

Sample Wash Volume: 8 µL

Sample Pumps: 6

Dwell Time (PreInj): 0 min

Dwell Time (PostInj): 0 min

Solvent Wash Draw Speed: 300 µL/min

Solvent Wash Dispense Speed: 3000 µL/min

Sample Wash Draw Speed: 300 µL/min

Sample Wash Dispense Speed: 3000 µL/min

Injection Dispense Speed: 6000 µL/min

Viscosity Delay: 0 sec

Sample Depth: Disabled

Injection Type: Standard

L1 Airgap: 0.2 µL

Solvent Wash Mode: A, B

Sample Overlap

Mode: Sample overlap is not enabled

ALS Errors: Pause for user interaction

Front SS Inlet He

Mode: Splitless

Heater: On 240 °C

Pressure: On 9.1473 psi

Total Flow: On 54.2 mL/min

Septum Purge Flow: On 3 mL/min

Gas Saver: On 20 After 3 min mL/min

Purge Flow to Split Vent: 50 mL/min at 2 min

Liner: Agilent 5181-3316: 900 µL (Splitless, single taper liner, deacti)

Thermal Aux 2 (MSD Transfer Line)

Temperature

Setpoint: On

(Initial) : 240 °C

Post Run: 0 °C

Column

Column #1

Flow

Setpoint: Off

(Initial) : 1.2 mL/min

Post Run: 1.2 mL/min

Agilent 19091S-433UI

HP-5ms Ultra Inert

0 °C—325 °C (350 °C): 30 m x 250 µm x 0.25 µm

Column lock: Unlocked

In: Front SS Inlet He

Out: MSD

(Initial): 40 °C

Pressure: 9.1473 psi

Flow: 1.2 mL/min

Average Velocity: 39.723 cm/sec

Holdup Time: 1.2587 min

Column Outlet Pressure: 0 psi

Signals

Signal #1: Test Plot

Description: Test Plot

Details

Save: Off

Data Rate: 50 Hz

Dual Injection Assignment: Back Sample

Signal #2: Test Plot

Description: Test Plot

Details

Save: Off

Data Rate: 50 Hz

Dual Injection Assignment: Back Sample

Signal #3: Test Plot

Description: Test Plot

Details

Save: Off

Data Rate: 50 Hz

Dual Injection Assignment: Back Sample

Signal #4: Test Plot

Description: Test Plot

Details

Save: Off

Data Rate: 50 Hz

Dual Injection Assignment: Back Sample

MS Information

-- ----------

General Information

------- ----------

Acquisistion Mode : Scan

Solvent Delay (minutes) : 5.00

Tune file : D:\MassHunter\GCMS\1\5977\ATUNE.U

EM Setting mode Gain : 1.000000

Normal or Fast Scanning : Normal Scanning

Trace Ion Detection : Off

Run Time (if MS only) : 10 minutes

[Scan Parameters]

Start Time : 5.00

Low Mass : 40.00

High Mass : 400.00

Threshold : 150

A/D Samples: : 4

[MSZones]

MS Source : 230 C maximum 250 C

MS Quad : 150 C maximum 200 C

Timed Events

----- ------

Number Events= 0

END OF MS ACQUISTION PARAMETERS

TUNE PARAMETERS for SN: US1345M203

Trace Ion Detection is OFF.

EMISSION : 34.593

ENERGY : 70.007

REPELLER : 11.194

IONFOCUS : 90.331

ENTRANCE_LE : 10.090

EMVOLTS : 1535.250

Actual EMV : 1483.1

GAIN FACTOR : 1.00

AMUGAIN : 1992.000

AMUOFFSET : 123.188

FILAMENT : 2.000

DCPOLARITY : 1.000

ENTLENSOFFS : 10.773

MASSGAIN : -185.000

MASSOFFSET : -32.000